THE ROLE OF COMMON CARDIAC COMORBIDITIES AND MITOCHONDRIAL VARIANTS AS MODIFIERS AND/OR PHENOCOPIES IN HYPERTROPHIC CARDIOMYOPATHY (HCM)

DR. MOHAMMED ABID AKHTAR
MBBS IBSC MRCP (UK)

SUPERVISORS:
PROF OLIVER RIDER
PROF MASLIZA MAHMOD
PROF HUGH WATKINS

ST PETER'S COLLEGE
RADCLIFFE DEPARTMENT OF CARDIOVASCULAR MEDICINE
UNIVERSITY OF OXFORD

THESIS SUBMITTED FOR THE DEGREE OF
MASTER OF RESEARCH IN MEDICAL SCIENCES
TRINITY TERM 2025

ACKNOWLEDGEMENTS

My sincere gratitude to everyone who has supported me throughout my clinical research fellowship and my master's thesis. This journey would not have been possible without the guidance, encouragement, and assistance of many patients.

First and foremost, I would like to thank my primary supervisor, Professor Oliver Rider, for his invaluable advice, patience and feedback. His kindness and expertise have been instrumental in the completion of this research.

I would also like to extend my gratitude to my other supervisors, Professor Hugh Watkins and Professor Masliza Mahmod, for their support, constructive feedback and suggestions. Their expertise has significantly enriched my work.

I am particularly grateful to my colleagues and friends at the Oxford Centre for Clinical Magnetic Resonance Research for their camaraderie and moral support. Special thanks to Dr. Zakariye Ashkir and Dr. Azlan Helmy Abd Samat for their assistance with data collection and analysis, and for always being there to discuss and evaluate my ideas.

Lastly, my profound gratitude goes to God to whom all gratitude belongs to, and my family for their unwavering support and encouragement throughout my academic journey. To my parents, thank you for believing in me and to my wife, thank you for being my pillar of support during the most challenging times of my research.

DECLARATION

The work presented in this thesis is my own, as are the research questions that underlie it. Excluding the references, front pages and abstracts, the word count is 16618 words.

The data for my first results chapter was prospectively obtained and is a combination of data that I acquired, and data acquired by my colleague, Dr. Zakariye Ashkir, who is currently a DPhil student in our department. I acquired and analysed my first results chapter data during the baseline assessment of patients that I recruited and enrolled in the multicentre phase II randomised clinical trial named TEMPEST, where I served as the sub-investigator and Clinical Research Fellow at the Oxford site. Professor Mahmod (Principal Investigator) and Professor Valkovic quality controlled my data analysis for my CMR and MRS data respectively. I received explicit permission from the Chief Investigator (CI) for TEMPEST, Professor Chris Miller, for using baseline data from the Oxford site for TEMPEST trial, in my thesis. Dr. Ashkir obtained his data as part of his observational study investigating the CMR differences between sarcomere positive and sarcomere negative HCM patients, for which I partly helped with recruitment and scanning. I analysed the CMR images from his study and undertook quality control analysis with ZA.

For my second results chapter, I prospectively analysed retrospective CMR images from three separate cohorts of patients with hypertension, obesity and HCM. I then performed statistical analysis on the results.

For my third, and final, results chapter, the data is a combination of prospective and retrospectively collected data. The prospective data are patients that I recruited, via our local genetics database, and scanned in our department, with the approval of our local research ethics committee. I performed the data analysis for these patients, with quality control analysis performed by colleagues, Dr. Zakariye Ashkir and Dr. Azlan Helmy Abd Samat. The retrospective data is clinical data available in the respective electronic health records of patients with the variant in question.

During this MRes, I received funding by the National Institute for Health and Care Research (NIHR) as part of my role as a Clinical Research Fellow in the TEMPEST trial.

ABBREVIATIONS

2,3-DPG	2,3 Diphosphoglycerate
^{31}P-MRS	^{31}Phosphorus Magnetic Resonance Spectroscopy
AF	Atrial Fibrillation
ANOVA	Analysis of Variance
ATP	Adenosine Triphosphate
BiVAD	Biventricular Assist Device
BMI	Body mass index
CMR	Cardiac Magnetic Resonance
CPET	Cardiopulmonary Exercise Test
CRP	C-reactive Protein
DNA	Deoxyribonucleic acid
ECG	Electrocardiogram
ECV	Extracellular Volume
ESC	European Society of Cardiology
FBC	Full Blood Count
FDG	Fluorodeoxyglucose
FID	Free Induction Decay
hs-cTnI	high-sensitivity cardiac troponin I
HCM	Hypertrophic Cardiomyopathy
HF	Heart Failure
HLA	Horizontal long axis

HR	Heart rate
ICD	Implantable Cardioverter Defibrillator
IQR	Interquartile range
LA	Left atrium
LGE	Late gadolinium enhancement
LV	Left ventricle/left ventricular
LV_DRESS	LV_Depth-Resolved Surface Coil Spectroscopy
LVEDV	Left ventricular end diastolic volume
LVEDVI	Left ventricular end diastolic volume (indexed)
LVEF	Left ventricular ejection fraction
LVESV	Left ventricular end systolic volume
LVH	Left ventricular hypertrophy
LVOT	Left ventricular outflow tract
MELAS	Mitochondrial encephalopathy, Lactic acidosis and Stroke-like episodes
MR	Magnetic Resonance
MRS	Magnetic resonance spectroscopy
mtDNA	mitochondrial DNA
mt-tRNA	mitochondrial transfer Ribonucleic Acid
NIHR	National Institute for Health Research
NSR	Normal Sinus Rhythm
NSVT	Non-Sustained Ventricular Tachycardia
NT-proBNP	N-terminal pro B-type Natriuretic Peptide
OCMR	Oxford Centre for Clinical Magnetic Resonance Research
OMGL	Oxford Medical Genetics Laboratory

OUH	Oxford University Hospital
P	Phosphorus
PCr/ATP	Phosphocreatine to adenosine triphosphate
Peak VO2	Peak Oxygen Consumption
PET CT	Positron Emission Tomography Computed Tomography
PI	Principal Investigator
PPM	Parts Per Million
RER	Respiratory Exchange Ratio
RV	Right Ventricle
RVH	Right Ventricular Hypertrophy
SA	Short Axis
SAR	Specific Absorption Rate
SCD	Sudden cardiac death
SCMR	Society of Cardiovascular Magnetic Resonance
SD	Standard deviation
SHaRe	Sarcomeric Human Cardiomyopathy Registry
SI	Signal intensity
SV	Stroke Volume
SVT	Supraventricular Tachycardia
T2DM	Type 2 Diabetes Mellitus
TIA	Transient Ischaemic Attack
TR	Repetition Time
tRNA	transfer Ribonucleic Acid
TTE	Transthoracic Echocardiography

U&Es	Urea & Electrolytes
VA	Ventricular Arrhythmias
VE	Minute Ventilation
VE/VCO_2	Minute Ventilation / Carbon Dioxide Production
VE/VO_2	Minute Ventilation / Oxygen Consumption
VLA	Vertical long axis
VO_2	Peak Oxygen Consumption

TABLE OF CONTENTS

THESIS ABSTRACT

Hypertrophic cardiomyopathy (HCM) is the most common inherited cardiac condition, typically associated with sarcomeric gene mutations. However, 40% of patients lack identifiable pathogenic variants, suggesting the role of other factors. This thesis investigates the interaction between selected genetic and non-genetic factors in HCM, focusing on the common cardiac comorbidities hypertension and obesity, and rare genetic variants known to mimic the HCM phenotype - the MT-TI:m.4300A>G mitochondrial variant. Through advanced imaging, biomarker analysis, and clinical data, this research aims to clarify the mechanisms influencing HCM phenotypes and improve diagnostic and therapeutic strategies.

CHAPTER 1: GENERAL INTRODUCTION

1.1 WHAT IS HYPERTROPHIC CARDIOMYOPATHY?

Hypertrophic cardiomyopathy (HCM) is the most common inherited cardiac condition (1, 2). It is characterised by left ventricular hypertrophy (LVH). Its prevalence in the general population ranges from 0.2% to 1.4% (3, 4). Genetic testing typically identifies pathogenic variants in the cardiac muscle's contractile unit, known as the cardiac sarcomere, inherited in an autosomal dominant manner (5).

Clinically, symptoms vary, including chest pain, shortness of breath, palpitations, dizziness and syncope, though many patients are asymptomatic and are only identified through cascade genetic screening (1, 2). Electrocardiography (ECG) abnormalities such as LVH, ST-T changes, abnormal Q waves and deep T wave inversion are common but non-specific (1, 2).

HCM is usually diagnosed by 2-dimensional (2D) transthoracic echocardiography (TTE), with a LV end-diastolic wall thickness ≥15mm or ≥13mm in patients with a pathogenic variant, excluding other causes of hypertrophy (1). Non-LVH features may include elongated mitral valve leaflets, intraventricular obstruction, systolic impairment and impaired diastolic function (6). Cardiac magnetic resonance (CMR) imaging, the gold standard modality for assessing cardiac structure and function, aids the diagnostic process in patients with poor quality TTE images, borderline HCM phenotypes, and/or phenocopies – conditions mimicking HCM but with a different genetic and pathophysiology mechanism (1, 2).

HCM carries a small but significant risk of progressive heart failure (HF) and/or sudden cardiac death (SCD), partially mitigated by primary prevention implantable cardioverter defibrillators (ICDs) in those deemed “high risk” for SCD via validated risk scores (1, 2). However, no curative therapy exists beyond cardiac transplantation for end-stage disease (1). This may be due to unresolved issues in the understanding of HCM, which I will discuss further.

1.2 THE SINGLE GENE-HYPOTHESIS

The genetic basis for HCM was first identified in 1990 with a point variant in the Myosin Heavy Chain 7 (MYH7) gene in a family with LVH and sudden cardiac death (SCD) (7). This led to the hypothesis that HCM is a monogenic disorder or "disease of the sarcomere" (8). Although some of the variants confirmed as pathogenic in HCM have also been identified in those with dilated cardiomyopathy (DCM) (9). Active variant expression also fluctuates over time – some variants key in the early development of HCM may subsequently be inactive in later stages of the disease (9). Despite advances in genetic testing, at least 40% of patients, including those with a family history of HCM, are "gene-negative" i.e. they don't have an identifiable pathogenic variant in sarcomere-related genes, raising further doubts about the monogenic model (1). HCM patients often have abnormalities in non-myocardial structures where sarcomere genes are not expressed, such as the mitral valve or coronary artery wall (10). Incomplete penetrance and variable HCM phenotypes, even among monozygotic twins, also complicate the picture (8, 11).

The identification of sarcomere-related pathogenic variants is clearly still important. Compared to genotype negative patients, sarcomere-related pathogenic variants are associated with an earlier HCM diagnosis, and higher rate of major adverse cardiac events (MACE), independent of sex and race (12, 13).

Patients with HCM likely exist on a clinical spectrum, from those with monogenic forms minimally influenced by external factors to those with common genetic traits that

predispose them to disease in the presence of modifiers, as often seen in the less investigated gene-negative HCM group (14, 15). How pathogenic and/or benign variants, epigenetic, environmental and inflammatory factors interact with one another, to what extent and when, to produce and evolve the clinical phenotype, remains unclear (particularly in “gene-negative” group) much like in DCM (10) (16) (17) (18, 19).

1.3 MODIFIERS AND PHENOCOPIES IN HCM: INTRODUCTION

1.3.1 MODIFIERS

Common genetic variants significantly impact the HCM phenotype, especially in gene-negative HCM, akin to conditions likely familial hypercholesterolaemia and Brugada syndrome (20) (21) (22) (23-25). However, data on the role of uncommon genetic and/or non-genetic or 'environmental' factors in modifying the HCM phenotype remain limited.

HCM appears to be modified by age: older patients have a higher burden of LVH and HCM related complications such as atrial fibrillation and HF (26). As older patients also have a higher burden of modifiable cardiac risk factors such as hypertension and obesity, some hypothesise that HCM may represented an exaggerated form of cardiac ageing (15, 27, 28).

Traditionally excluded from HCM prevalence studies, hypertension and obesity are now suspected as potential modifiers of the HCM phenotype, particularly in gene-negative HCM, where they occur more frequently than in the general population (3, 4). These conditions challenge the diagnostic threshold of a maximum LV wall thickness (≥15mm). For instance, hypertensive heart disease (HHD) often overlaps with HCM in wall thickness, and some patients may meet HCM criteria primarily due to these comorbidities (29). This underscores that need to delineate how much hypertrophy is attributable to HCM versus modifiable risk factors, especially since LVH due to hypertension or obesity is often reversible with appropriate treatment (30-32).

1.3.2 PHENOCOPIES

Left ventricular hypertrophy (LVH) is a very common imaging finding (33-35). It's unsurprising, therefore, that phenocopies are present in 10-15% of patients initially diagnosed with HCM (24). Examples include cardiac amyloidosis, and various mitochondrial cardiomyopathies (36) (37). While systemic features often guide clinicians to suspect phenocopies, not all phenocopies exhibit extra-cardiac manifestations, such as late onset Anderson Fabry Disease (AFD) or certain mitochondrial cardiomyopathies (38, 39) (40, 41).

Advancements in biomarker assays, genetic testing and CMR sequences have improved differentiation between HCM and phenocopies (38, 39). However, CMR techniques like T_1 mapping and late gadolinium enhancement (LGE) are not foolproof. For example, T_1 values commonly overlap between HCM, hypertensive LVH and other phenocopies, reducing their discriminatory capacity unless values are markedly abnormal (38, 39, 42, 43). Similarly, while absent LGE may favour hypertensive LVH, 50% of HCM patients lack LGE, and those with LGE do not always exhibit typical patterns of enhancement (44).

1.3.3 CHALLENGES IN MEASURING LVH

MWT, which is used to diagnose HCM, is influenced by age, sex, ethnicity and body surface area (BSA) (45, 46). Studies suggest lowering diagnostic MWT thresholds (e.g. to 10 mm in Asian females) to enhance sensitivity without compromising specificity in certain populations (36) (45-47). However, MWT alone has limitations, including inter-modality variability between TTE and CMR (48-50).

Alternatives like left ventricular mass (LVM), relative wall thickness (RWT), and septal/lateral wall thickness ratio have been proposed (6, 30, 51-55). In particular, a septal/lateral wall thickness ratio ≥1.5 was highlighted alongside a MWT ≥15mm in the original seminal paper on establishing the diagnostic criteria for HCM (56). While all these measures provide additional insights into LV geometry and phenocopy differentiation, they also face challenges in reproducibility and diagnostic accuracy (6, 30, 51-55).

1.4 HYPERTENSION: MODIFIER OR PHENOCOPY IN HCM?

Hypertension affects over one billion people globally, and is a leading cause of LVH, present in 36-41% of patients with hypertension (31, 35). The development of LVH in hypertension is driven by genetic, neurohormonal, immune, metabolic, vascular and mechanical stress mechanisms – pathways shared with HCM (22) (35) (57, 58) (57, 59, 60). With at least 25% of HCM patients having concurrent hypertension, it is reasonable to hypothesise that hypertension serves as an environmental modifier of the HCM phenotype (23, 61-63).

Some studies support this role, noting that hypertension can exacerbate LVH, increase fibrosis, and potentially worsen outcomes in patients with common sarcomeric variants, such as the MYBPC3 25-bp deletion prevalent in South Asians (15, 64). Other studies limit the influence of hypertension, concluding that it does not influence the severity or prognosis of fully developed HCM (61, 65).

As for hypertensive LVH as an HCM phenocopy, hypertensive LVH remains a common differential for gene-negative HCM (44). CMR has been explored as a tool for differentiation, but results have been inconsistent (44) (66). Measurements such as MWT ≥17mm, septum/lateral wall thickness ratio, global longitudinal strain (GLS) and tissue characterisation biomarkers, such as LGE burden or T_1 values, show promise, although their limitations should be acknowledged (29). As mentioned before, MWT is influenced by several different factors and some MWT increasing comorbidities may lead to a false positive diagnosis of HCM (45, 46). Contrary to the

traditional view that hypertensive LVH is concentric, newer CMR studies demonstrate that up to 40% of hypertensive patients exhibit eccentric or asymmetric LVH, suggesting septal/lateral wall thickness alone may be insufficient for differentiation (67-71). GLS, LGE burden or T_1 mapping are unreliable in distinguishing between HCM and hypertensive LVH when MWT exceeds 15 mm (67, 72).

Some propose repeating CMR after intensive antihypertensive therapy to observe LVH regression as a diagnostic strategy (31). However, this approach is limited by factors such as baseline LV mass, blood pressure reduction, and the type and duration of therapy (31).

This thesis seeks to clarify the dual role of hypertension as a potential modifier or HCM phenocopy, focusing on gene-negative cases. Key areas of inquiry include:

- Does hypertension influence HCM progression or severity once the phenotype is established?
- How reliably can imaging and clinical features distinguish hypertensive LVH from HCM?

Understanding these dynamics is crucial for accurate diagnosis, risk stratification and personalised treatment, particularly in patients where hypertension may modify or mimic HCM.

1.5 OBESITY: MODIFIER OR PHENOCOPY IN HCM?

In 2022, the World Health Organisation (WHO) reported that 1 in 8 people worldwide were living with obesity, if defined by a body mass index (BMI) ≥30 kg/m^2 (73). Obesity is associated with LVH, with one meta-analysis demonstrating an LVH prevalence within obesity (if defined by LVM) of 56% (74). Mechanistic contributors to LVH in obesity include haemodynamic factors, such as volume overload, and non-haemodynamic factors, such as inflammation, neurohormonal activation, and pro-hypertrophic signalling imbalances (75). Obesity may also cause LVH via LVH-causing conditions with which its associated, such as hypertension, obstructive sleep apnoea and/or diabetes mellitus (DM) (75).

Obesity is prevalent in HCM, affecting 20-40% of patients (76). A South Korean registry showed that each 1 kg/m^2 BMI increase led to a 6.3% higher risk of developing HCM (77). Even after the HCM phenotype is established, obesity appears to influence disease severity, with obese HCM patients showing a higher MWT and burden of atrial arrhythmias and myocardial fibrosis (78). However, studies on obesity's association with ventricular arrhythmias are conflicting, with many reporting a paradoxical decrease in ventricular arrhythmia burden with an increasing BMI (76).

The differentiation of obesity-associated LVH from HCM is less studied compared to hypertensive LVH. In one study of 764 patients with obesity but no hypertension, obesity was significantly associated with increased wall thickness, with every 10 kg/m^2 increment linked to a 1.0 mm and 0.8 mm increase in basal septal wall thickness in males and females, respectively (79). Notably, no patient in this cohort had a

MWT>14mm, suggesting that a MWT >14mm should prompt consideration of alternative diagnoses, such as HCM (79). Septal/wall thickness ratio, GLS and tissue characterisation including extracellular volume (ECV) haven't demonstrated a good discriminatory capacity between HCM and obesity LVH in studies thus far (75) (80) (81). Both eccentric and concentric LV remodelling has been reported in obesity (75). GLS is decreased in patients with obesity, though comparisons with obese and non-obese HCM are lacking (80). ECV has shown inconsistent results in obesity LVH (81).

The overlap between obesity and HCM raises critical diagnostic and therapeutic questions:

- How does obesity influence the HCM phenotype evolution and prognosis?
- Can imaging or clinical markers reliably distinguish obesity-associated LVH from HCM?

1.6 HYPERTENSION AND OBESITY: ADDITIVE OR SYNERGITIC EFFECT IN HCM?

When evaluating the HCM phenotype, it is important to consider the potential additive and/or synergistic effects of hypertension and obesity.

These comorbidities likely significantly interact, particularly in the development and progression of LVH (82). Antihypertensive therapies reduce LVM but this is blunted in hypertensive patients with obesity, requires substantial weight loss first before LVM can decrease, likely due to myocardial fat infiltration and the resistance of adipocytes and fibroblasts to changes in loading conditions (35) (83-86). In patients with diabetes mellitus, sodium glucose transporter 2 inhibitors (SGLT-2i) led to significantly more weight loss, and significantly lower blood pressure, epicardial fat (a source of inflammatory adipokines), and LVM (87).

In HCM, the interplay between hypertension and obesity remains unclear. The ESC EurObservational Research Program (EORP) Cardiomyopathy/Myocarditis registry found hypertension and obesity were prevalent in HCM patients. Compared to HCM patients without hypertension and obesity, patients with HCM, hypertension and obesity had an older age at presentation, worse diastolic function, more cardiac symptoms, a higher atrial fibrillation prevalence, and greater LVH and provocable LVOT gradients (78). The HCM-VAr Risk model, developed using machine learning on 700 cases, identified systolic and diastolic blood pressure, BMI and non-obstructive HCM as predictors of increased ventricular arrhythmia risk (88). This model outperformed using traditional risk factors alone in predicting SCD (88). However,

neither the EORP registry nor the HCM-Var study explored whether the effects of hypertension and obesity in HCM are synergistic or merely additive on HCM outcomes over time.

The complex interplay between hypertension, obesity and HCM raises critical questions:

- Are the effects of hypertension and obesity on HCM truly synergistic or simply additive?
- How do these combined comorbidities influence long-term outcomes in HCM patients?

1.7 MITOCHONDRIAL VARIANTS: MODIFIER OR PHENOCOPY IN HCM?

Mitochondria, critical for cellular metabolism and ATP synthesis, possess their own maternally inherited DNA (mtDNA), which can acquire variants affecting energy-dependent tissues like the heart ("mitochondrial cardiomyopathy"), brain and skeletal muscle (89). Mitochondrial cardiomyopathy frequently presents with LVH, as seen in ≈23% of patients with mitochondrial variants in a large international registry (90).

In HCM, mitochondria play a significant role in pathogenesis (91-95). Abnormal mitochondrial structure and function have been observed in both gene-positive and gene-negative HCM, with more severe dysfunction linked to sarcomeric variants and advanced LV systolic dysfunction (92, 96, 97). While data on the impact of mitochondrial variants in HCM remain limited, a small case series suggests that mtDNA variants, such as A4300G, may modify the HCM phenotype, contributing to further mitochondrial dysfunction and disease severity (98).

Most mitochondrial cardiomyopathies present as part of syndromic diseases, such as Mitochondrial encephalomyopathy, Lactic acidosis, and Stroke-like episodes (MELAS) or Leigh Syndrome, distinguishing them from HCM where systemic features are limited, if present at all (90). Most mtDNA variants are heteroplasmic, where only a subset of mtDNA is affected. However, the A4300G mtDNA variant is homoplasmic, making genotype-phenotype correlations more consistent (40) (41, 98, 99). Limited reports (which lack advanced cardiac imaging) suggest a pattern of symmetrical, non-obstructive LVH and systolic impairment, similar to mitochondrial cardiomyopathies,

but with notable differences such as the absence of extra-cardiac features leading to diagnostic overlap with HCM in A4300G mtDNA patients with LVH (41, 98, 99).

Further study of the A4300G mutation is essential to clarify if represents a unique cardiac condition, part of the non-sarcomere gene-positive HCM spectrum or a subset of mitochondrial cardiomyopathy.

1.8 HYPOTHESES AND RESEARCH AIMS

1.8.1 HYPOTHESES

i. Hypertension and obesity phenotypes both modify and are phenocopies of gene- HCM but not gene+ HCM.

ii. A4300G patients with LVH have a unique clinical, CMR and energetics profile compared to HCM and mitochondrial cardiomyopathies.

1.8.2 RESEARCH AIMS

My studies aim to assess patients with obesity, hypertension, HCM and/or the m.4300A<G mtDNA variant using blood tests, ECG, imaging and outcome data. The goal is to determine whether hypertension, obesity or the m.4300A>G can alter or mimic the HCM phenotype.

1.9 THESIS OUTLINE

Chapter 1 describes the background of my research, including any gaps in the literature and how my research plans to address them. **Chapter 2** outlines the general methods employed to answer these research questions. **Chapter 3** presents the prospectively collected serum biomarkers, CMR and ^{31}P-MRS findings of a HCM cohort at our centre. The relationship between genetic status, history of hypertension, SBP, DBP, BMI, myocardial wall thickness and LV geometry are analysed. **Chapter 4** presents the prospective CMR analysis of retrospective data from patients with hypertension and/or obesity. The relationship between SBP, DBP, BMI, myocardial wall thickness and LV geometry are analysed. **Chapter 5** presents the serum biomarkers, ECG, CMR, ^{31}P-MRS and outcome findings of patients with the A4300G mtDNA variant at our centre and compares their findings to our HCM cohort from **Chapter 3**. Finally, in **Chapter 6,** the key findings from my studies are summarised, and future research projects, in the identification of common and rare modifiers and/or phenocopies of the HCM phenotype, are discussed.

CHAPTER 2: GENERAL METHODS

2.1 ETHICS APPROVAL

All studies have local research ethics committee (REC) approval – their respective REC numbers are: 20/NW/0275 (TEMPEST), 12/LO/1979 (SARC-HCM), 06/Q1605/113 (Oxford Family Blood Pressure Study). All patients gave written informed consent, conforming to the Declaration of Helsinki (fifth revision, 2000), prior to participating in our studies.

2.2 GENERAL INCLUSION AND EXCLUSION CRITERIA

2.2.1 INCLUSION CRITERIA

Subjects were eligible for inclusion in the study if they fit the below criteria:

i) Aged between 18 and 80 years and

ii) They have one of the following conditions: hypertrophic cardiomyopathy (HCM), hypertension, obesity and/or a carrier of the A4300G mtDNA variant. The diagnostic criteria used for each of these conditions will be included in the relevant results chapter.

2.2.2 EXCLUSION CRITERIA

Subjects were excluded from the study if they had one of the below:

i) Pacemaker or implantable cardioverter defibrillator (ICD)

ii) Persistent Atrial Fibrillation

iii) Previously documented myocardial infarction or severe coronary artery disease

iv) An unstable, severe comorbidity, such as end-stage heart failure, liver or renal disease

v) Pregnancy or lactation

vi) Contraindications to MRI (including the presence of metallic implants or foreign bodies)

2.3 INVESTIGATIONS

2.3.1 CLINICAL ASSESSMENT

Heart rate, blood pressure, height and weight, clinical history, physical examination were performed, and findings recorded at each visit.

Heart rate was measured by direct palpation of the radial artery for 1 minute. Blood pressure was measured using an automated sphygmomanometer (General Electric Dinamap™ Carescape™ V100) that has been calibrated in our department (Oxford Centre for Clinical Magnetic Resonance Research and Oxford University Hospitals NHS Trust). Height was measured in centimetres to the nearest whole number. Body weight was measured in kilograms to the nearest 0.1 kilogram. Height and weight measurements were performed without shoes being worn. Clinical history and physical examination findings were undertaken as per our local protocol.

2.3.2 12-LEAD ECG

A resting 12-lead ECG was performed with a Phillips PageWriter TC30 ECG Machine and analysed using the Minnesota Code Classification system: measurements included the presence of sinus rhythm or atrial fibrillation, and the PR interval, QRS duration and QTc interval, measured in milliseconds (100).

2.3.3 24-HOUR 2-CHANNEL ECG MONITORING

Ambulatory ECG monitoring was performed using LifeSignals single-use patches. Following adequate skin preparation, the patch was applied on the left side of the chest between the sternum and the left mid-clavicular line, at the level of the second or third intercostal space (101). Patients were instructed to wear the patch for 24 hours, after which they would remove the monitor and send it to the Central Core Lab for analysis using the HE/LX analysis software (version 6.0c, Northeast Monitoring Inc.). Measurements included the number of non-sinus supraventricular or ventricular-origin heart beats per 1000 beats and the presence of non-sustained ventricular tachycardia or atrial fibrillation (including the number of episodes) (101).

2.3.4 BLOOD TESTING

Venous blood samples were taken via venepuncture for serum haemoglobin, haematocrit, urea and electrolytes, high sensitivity troponin I (hs-cTn), and iron levels. These samples were analysed in our local haematology and biochemistry unit except

for serum hs-cTn which was centrifuged and stored refrigerated (4-8°C) before being sent to Manchester University NHS Foundation Trust for analysis.

2.3.5 ^{31}PHOSPHORUS MAGNETIC RESONANCE SPECTROSCOPY

2.3.5.1 ^{31}P-MRS ACQUISITION

^{31}P cardiac MRS was also performed to estimate the phosphocreatine to ATP (PCr/ATP) ratio – a proven non-invasive surrogate marker of myocardial energetics (102, 103). Patients were scanned supine, with a dual tuned 11 cm, transmit/receive loop, radio-frequency coil placed over the heart (see **Figure 1**) (101). A set of coronal localisers confirmed the location of the coil (see **Figure 2**), and a series of inversion recovery scans were acquired at the frequency of a phenyl phosphonic acid fiducial, which is attached to the coil (101). The excitation frequency was set from -250 Hz from phosphocreatine (PCr), i.e. between ɣ- and α- adenosine triphosphate (ATP) to cover the entire ^{31}P spectrum (101). Localisation of the cardiac signal was achieved with a depth resolved surface coil spectroscopy (DRESS) sequence previously reported and validated by our group (see **Figure 2**) (102). The resulting spectrum was checked on the system to ensure an adequate signal was obtained (see **Figure 3**)

Figure 1: Dual-tuned $^{31}P/^{1}H$ surface coil from Rapid Biomedial, with four cod-liver capsules and one reference fiducial containing phenylphosphonic acid (PPA). The patient is scanned supine with both arms down by their side (*Image reproduced with permission from Dr Azlan Abds Samat).*

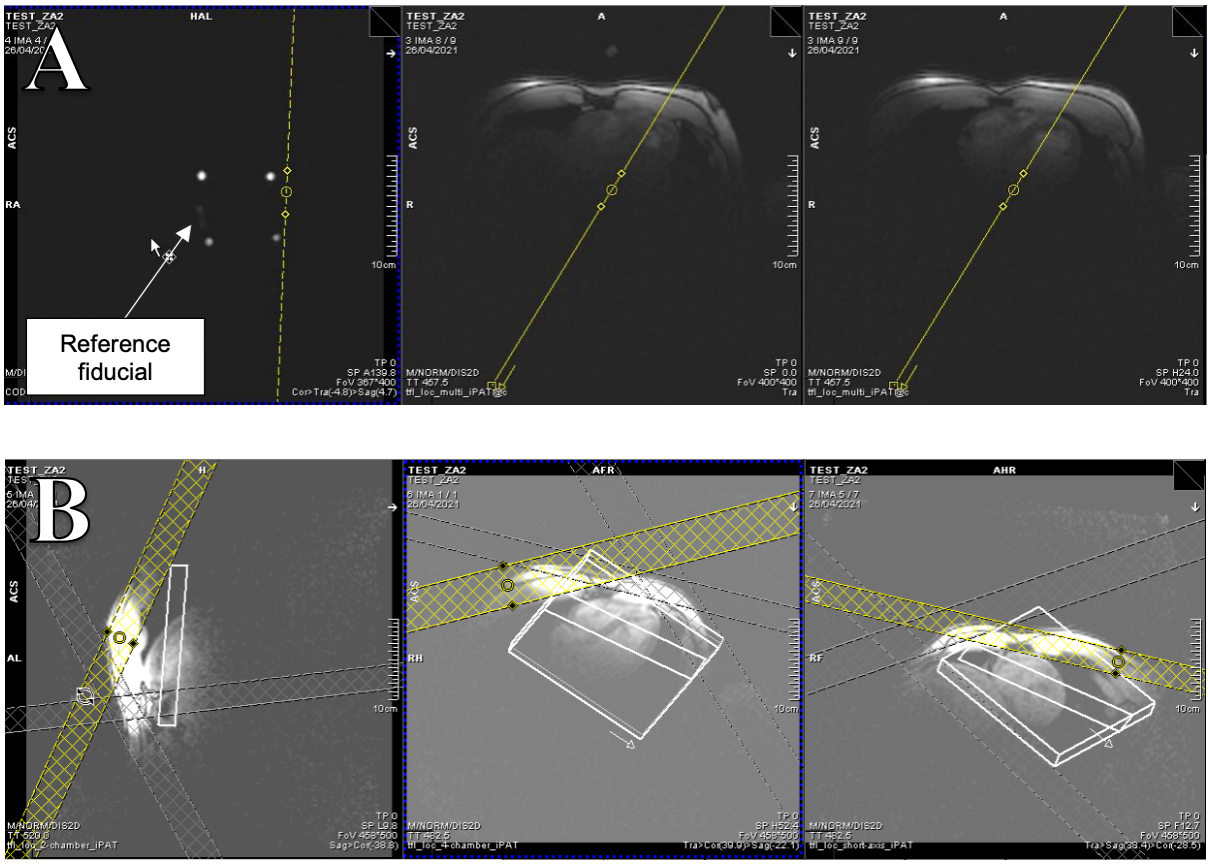

Figure 2: *Panel A* = Localiser images to ensure the coil is parallel to the chest wall and the septum is at the centre of the coil. *Panel B* = Vertical long axis, horizontal long axis, and short axis pilots to position saturation bands on to cover the muscle, but not fat, on the chest wall, as well as the liver (*Image reproduced with permission from Dr Azlan Abds Samat).*

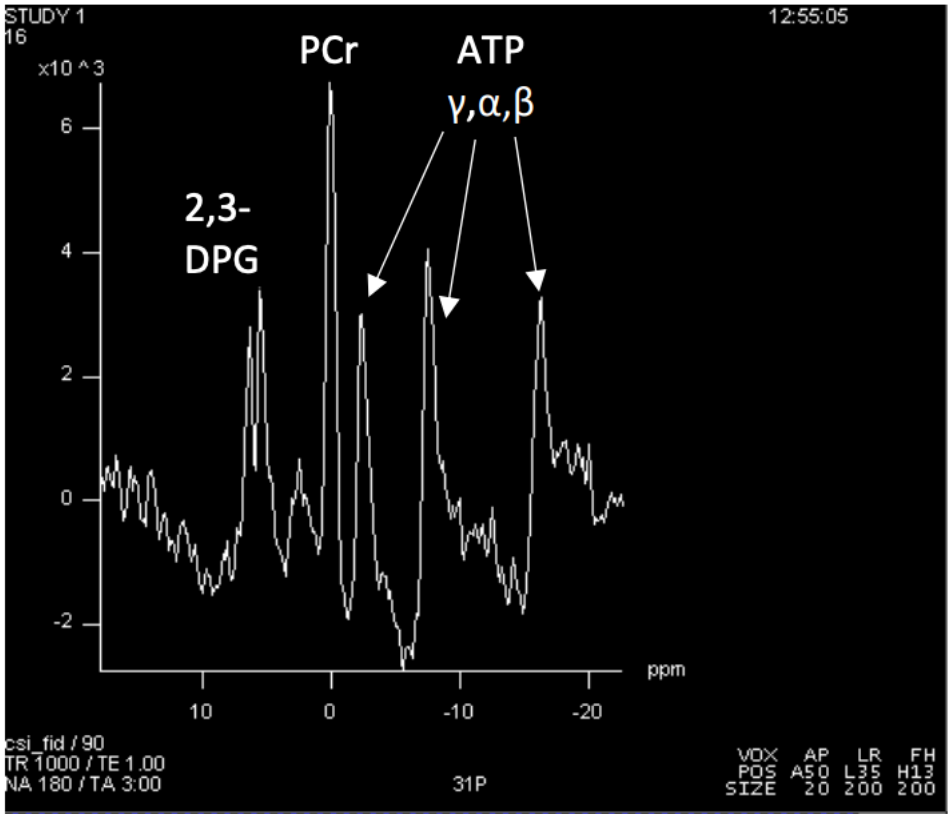

Figure 3: The resonances, separated by chemical shift in parts per million (ppm), obtained at the end of the ^{31}P-MRS that correspond to the signal intensity of α, β, and γ subunits of ATP, phosphocreatine (PCr), and 2,3-diphosphoglycerate (2,3-DPG) (*Image reproduced with permission from Dr Azlan Abds Samat).*

2.3.5.2 ^{31}P-MRS ANALYSIS

PCr/ATP ratios were quantified using MATLAB (MATLAB 2022b, The MathWorks, Inc., Natick, MA, USA). The spectrum from the DRESS slab was fitted using a custom implementation of AMARES (the Advanced Method for Accurate, Robust, and Efficient Spectral fitting) in the Oxford Spectroscopy Analysis or "OXSA" semi-automated spectroscopy postprocessing pipeline (see **Figure 4**) (104). The fitting used prior knowledge specifying 11 Lorentzian amplitudes (including α-, β-, γ-ATP, PCr, phosphodiesterase (PDE), and 2 x 2,3-diphosphoglycerate (DPG)).

The fitted amplitudes were automatically corrected for blood contamination by subtracting 30% of the average of the two 2,3-DPG signals from each ATP amplitude. The remaining PCr and ATP signals were also then automatically corrected for the effects of partial saturation using the flip angle at the centre of the voxel (calculated using Biot-Savart law and inputs about coil loading and position) and literature T_1 values. The quality of the spectra and the fit were independently assessed by a senior MRS expert (LV) in a blinded fashion (see **Figure 5**).

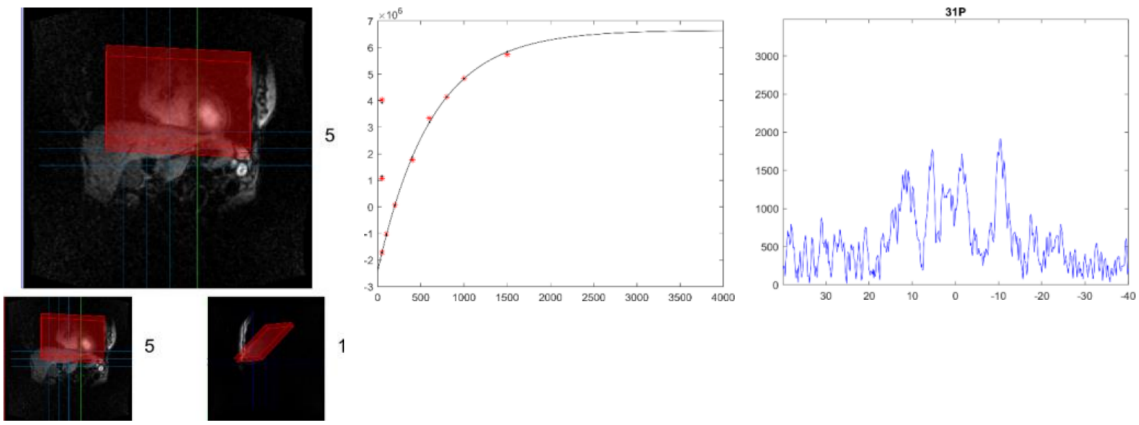

Figure 4: The custom Oxford Spectroscopy Analysis or "OXSA" semi-automated spectroscopy postprocessing pipeline to obtain the ^{31}P-MRS spectrum.

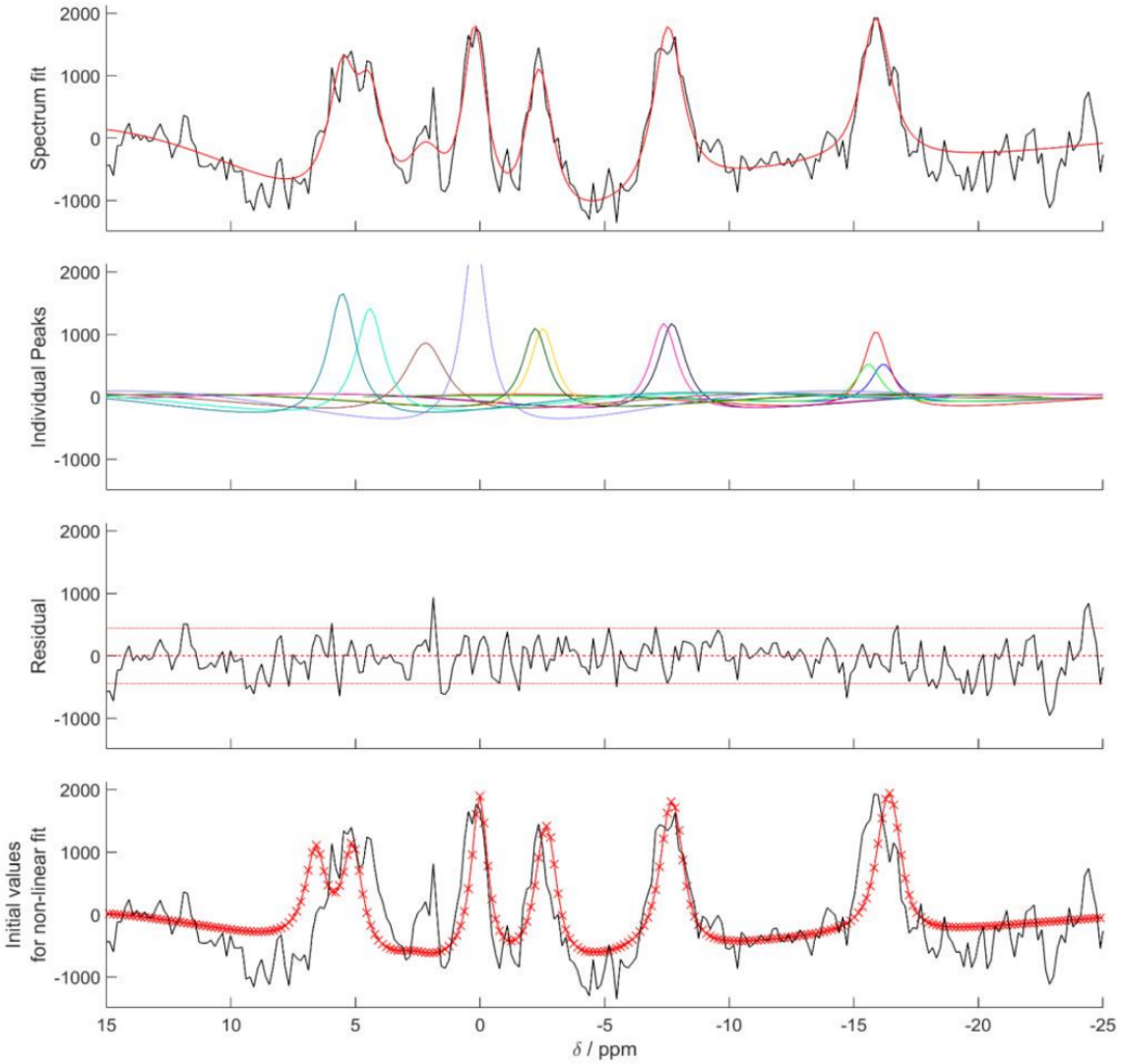

Figure 5: Fitting of the spectrum from the previous figure, factoring in prior knowledge, blood contamination and the effects of partial saturation.

2.3.6 CARDIOVASCULAR MAGNETIC RESONANCE IMAGING

CMR is the gold standard imaging modality for cardiac structure and function. Prior to the CMR, a venous blood sample for serum haematocrit (and subsequent extracellular volume analysis) was drawn and sent to our local clinical haematology laboratory where they were analysed according to standardised protocols.

Standard safety checks in line with our departmental procedures were also undertaken prior to CMR imaging, which was performed with a protocol that included:

i) cine imaging to assess cardiac biventricular volumes, function and mass

In addition, patients in **Chapter 3** and **5** underwent:

ii) pre contrast T_1 (using modified look-locker inversion recovery or MOLLI sequence on a three LV slice short-axis images) to assess diffuse fibrosis and post contrast T_1 to assess extracellular volume.

iii) late gadolinium enhancement (LGE) imaging using Gadoterate meglumine contrast (*Dotarem*; *Guerbet*, Aulnay-sous-Bois, France) given at a dose of 0.15mmol/kg, via hand injection, to assess focal fibrosis. Each bolus was followed by a 10 ml saline flush. Patients with an estimated glomerular filtration rate <30ml/min did not, however, receive contrast.

Patients in **Chapter 3** and **5** under CMR at 3 Tesla (Prisma, Siemens Healthineers, Erlangen, Germany), whereas patients in **Chapter 4** underwent CMR at 1.5 Tesla

(Siemens Healthineers, Erlangen, Germany). In **Chapters 3** and **5,** where CPET and/or ^{31}P-MRS was performed, CMR was performed before the CPET, and after ^{31}P-MRS.

All CMR images were anonymised and then analysed by myself using cvi42 (Circle Cardiovascular Imaging, Inc, Calgary, Canada) in accordance with Society for Cardiovascular Magnetic Resonance (SCMR) guidelines (105).

2.3.6.1 CINE IMAGING

2.3.6.1.1 CINE ACQUISITION

Prior to cine imaging acquisition, orthogonal, T2 True Fast Imaging with Steady State Precession (TRUEFISP), 2-, 4- and short axis chamber localisers were performed. Steady state free-precession (SSFP) breath-hold cine was then used to acquire end-expiration 4-chamber, 2-chamber, 3-chamber, LVOT long-axis (perpendicular to the 3-chamber cine), coronal LVOT, ventricular short-axis views of the LV (using 8 mm slices with no inter-slice gap) and bi-atrial short axis views of the LA (using 6 mm slices and no inter-slice gap), as shown in **Figure 6** and as previously described (106).

Scan parameters alongside a full protocol of the CMR acquisition can be found in the appendix.

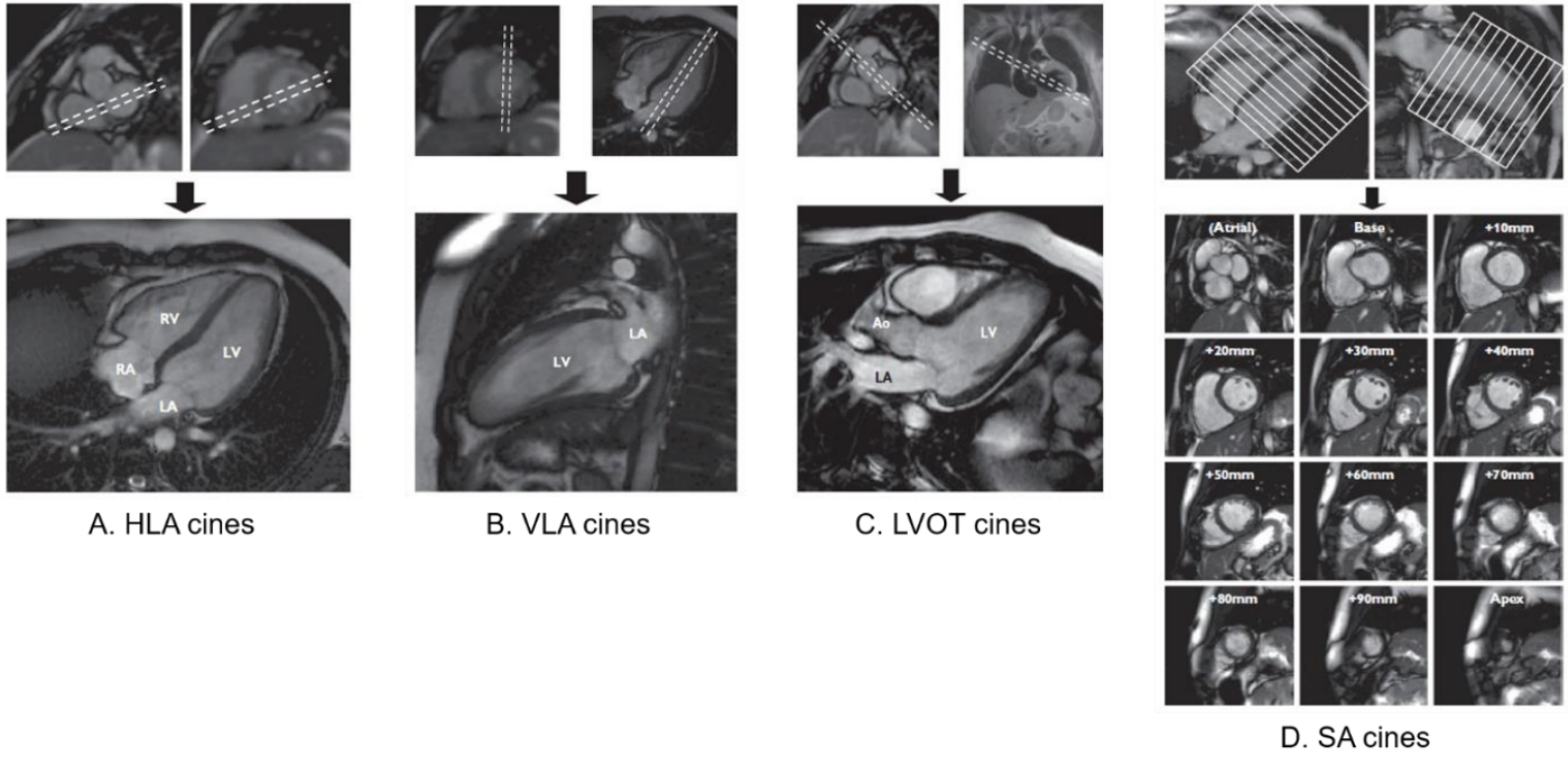

Figure 6: The horizontal long axis (HLA), vertical long axis (VLA), left ventricular outflow tract (LVOT) and short axis (SA) cine images and how they were formed from their respective pilots (with the dotted lines representing the localiser line) (*Image reproduced with permission from Dr Azlan Abds Samat).*

2.3.6.1.2 CINE ANALYSIS

Left atrial and ventricular mass, volumes and function

The epicardial and endocardial borders on the LV short axis were manually contoured at end-diastole as previously described, with the papillary muscles and trabecular tissue excluded in the endocardial border as part of volumetric and mass assessment (105). The indexed values for atrial, LV and RV end-diastolic volume (EDV), end-systolic (ESV) volume, stroke volume (SV), ejection fraction (EF) and mass were automatically generated from the cvi42 software. Left atrial anteroposterior diameter was measured in the 3-chamber view in end-systole as this method is required for the ESC SCD risk score (107). Maximal wall thickness was measured in end-diastole (as identified by closure of the mitral valve), taking care to avoid inappropriate inclusion of RV and LV trabeculations, as well as papillary structures (48).

Left ventricular qualitative assessment

The presence of systolic anterior motion of the mitral valve (SAM), significant valvular heart disease or an LV apical aneurysm were assessed on the 4-, 2- and 3- chamber views as well as the LV short axis view.

Left atrial and ventricular strain

LV strain assessment was assessed by contouring the LV, end-systolic and end-diastolic, endocardial and epicardial LV short axis, 4- and 2- chamber borders. LA strain was assessed by contouring the end-diastolic and end-systolic epicardial and endocardial borders of the LA in both the 2- and 4- chamber views, excluding the LA appendage and pulmonary veins. The post-processing software automatically

calculated the GLS, and LA (reservoir, conduit, and booster) strain values using a validated technique (105).

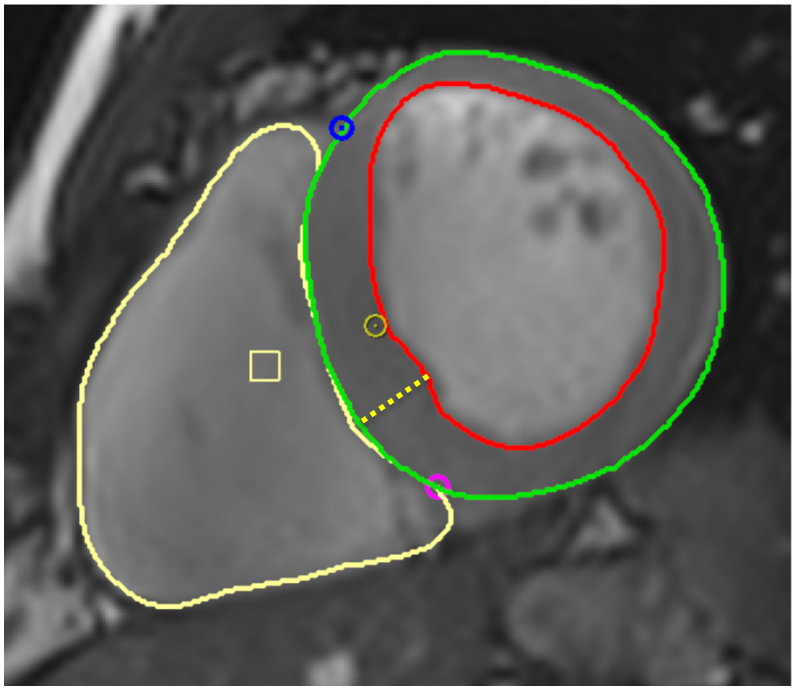

Figure 7: Endocardial (red) and epicardial (green) contours were manually drawn for each short-axis slice in the end-diastolic phase (with the same taking place for end-systole – image not shown). Maximal wall thickness (yellow dashed line) assessed manually in end-diastole, ensuring to avoid any inappropriate inclusions such as LV/RV trabeculations or papillary muscle. Myocardial mass in diastole, as well as LV/RV volumetrics and function were automatically calculated by the cvi42 software.

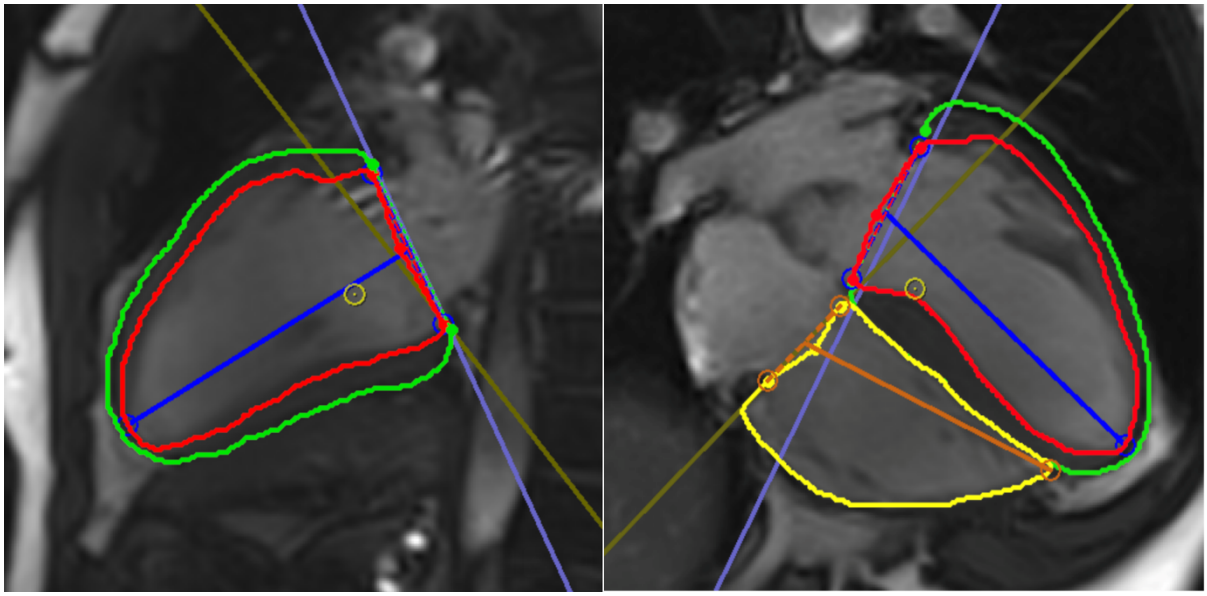

Figure 8: Endocardial (red) and epicardial (green) LV contours were manually drawn in the end-diastolic and end-systolic vertical long axis (VLA) and horizontal long axis (HLA) cine slices, with automatic calculation of the LV global longitudinal strain (GLS) via the cvi42 software.

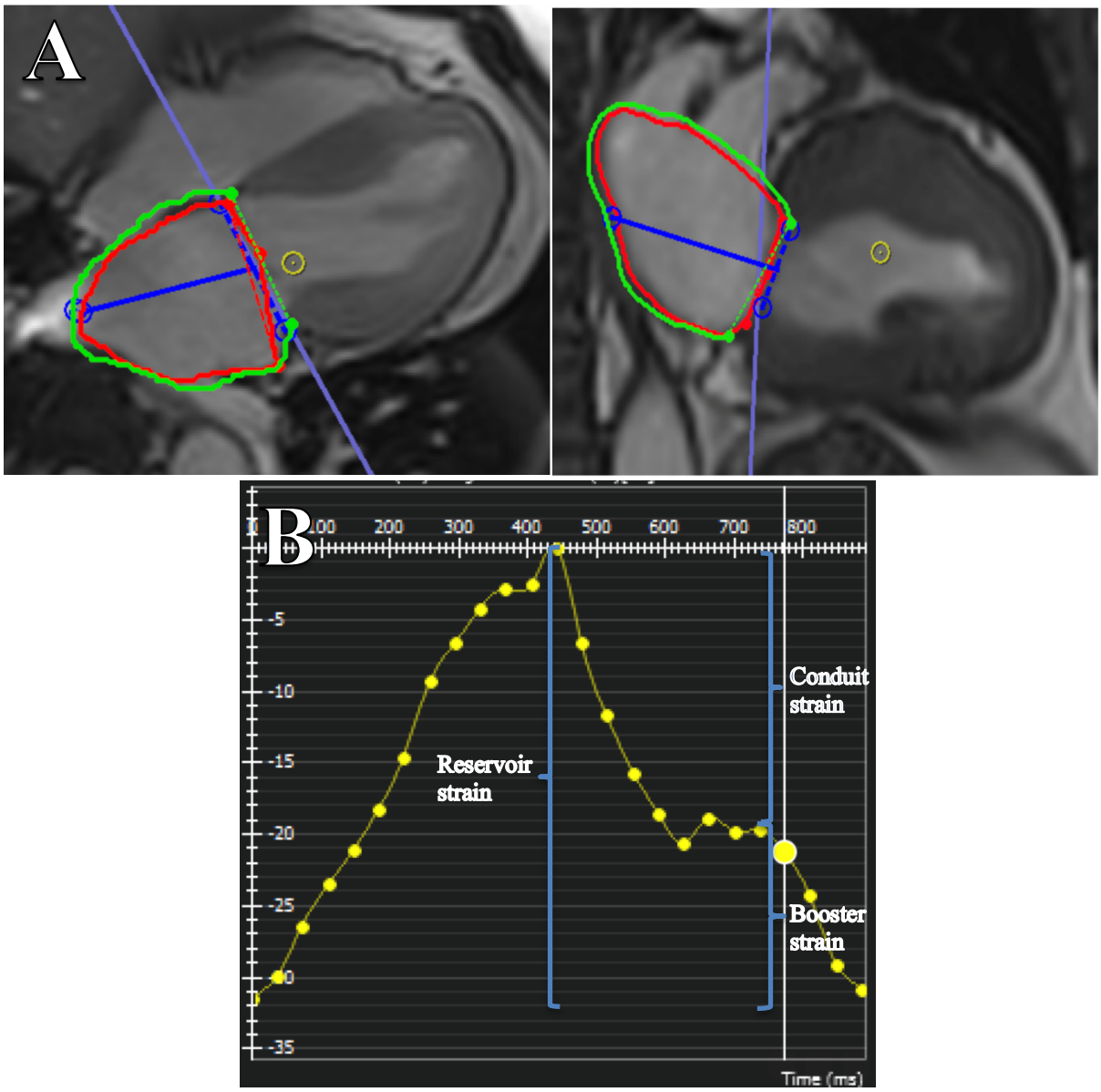

Figure 9: *Panel A* = Endocardial (red) and epicardial (green) LA contours were manually drawn in the end-diastolic and end-systolic vertical long axis (VLA) and horizontal long axis (HLA) cine slices, with automatic calculation of LA strain via the cvi42 software. *Panel B* = The values for the reservoir, conduit, and booster LA strain were manually abstracted from this graph using a validated technique (105).

2.6.2 PHASE CONTRAST IMAGING

Phase contrast imaging can be used to quantify blood flow passing through the LVOT (108). The LVOT gradient is estimated using Bernoulli's principle (108). An LVOT gradient >30mmHg indicates significant resting LVOT obstruction although TTE remains the gold standard for haemodynamic measurement, particularly as CMR underestimates flow velocity in HCM (108).

2.6.2.1 PHASE CONTRAST IMAGE ACQUISITION

A free-breathing 3-chamber phase encoded velocity map is performed, copied to the position of the 3-champer SSFP cine, with the velocity encoding (VENC) set to 2.0 m/s. This is followed by a free breathing LVOT short-axis phase-encoded velocity map, where the slice is positioned perpendicular to the LVOT long axis SSFP, at the site of the apparent highest LVOT velocity, or in the absence of an aliasing signal, at the tips of the aortic valve leaflets. The lowest possible VENC is used where aliasing is not expected to occur. In the presence of aliasing, the VENC was at least 1.0 m/s higher than that at which the aliasing occurred.

2.6.2.2 PHASE CONTRAST IMAGE ANALYSIS

The phase contrast images were analysed in cvi42 using the "2D flow" module. In the 3-chamber phase-encoded velocity-map, an area of interest was circled either just below the aortic valve, in the LVOT, or where there is aliasing in the LVOT. Background correction was performed as previously described (108). In the LVOT short-axis phase-encoded velocity-map, the flow in the aortic valve orifice was

manually circled in each slice, with background correction applied, to detect the aortic regurgitant fraction, and velocity max.

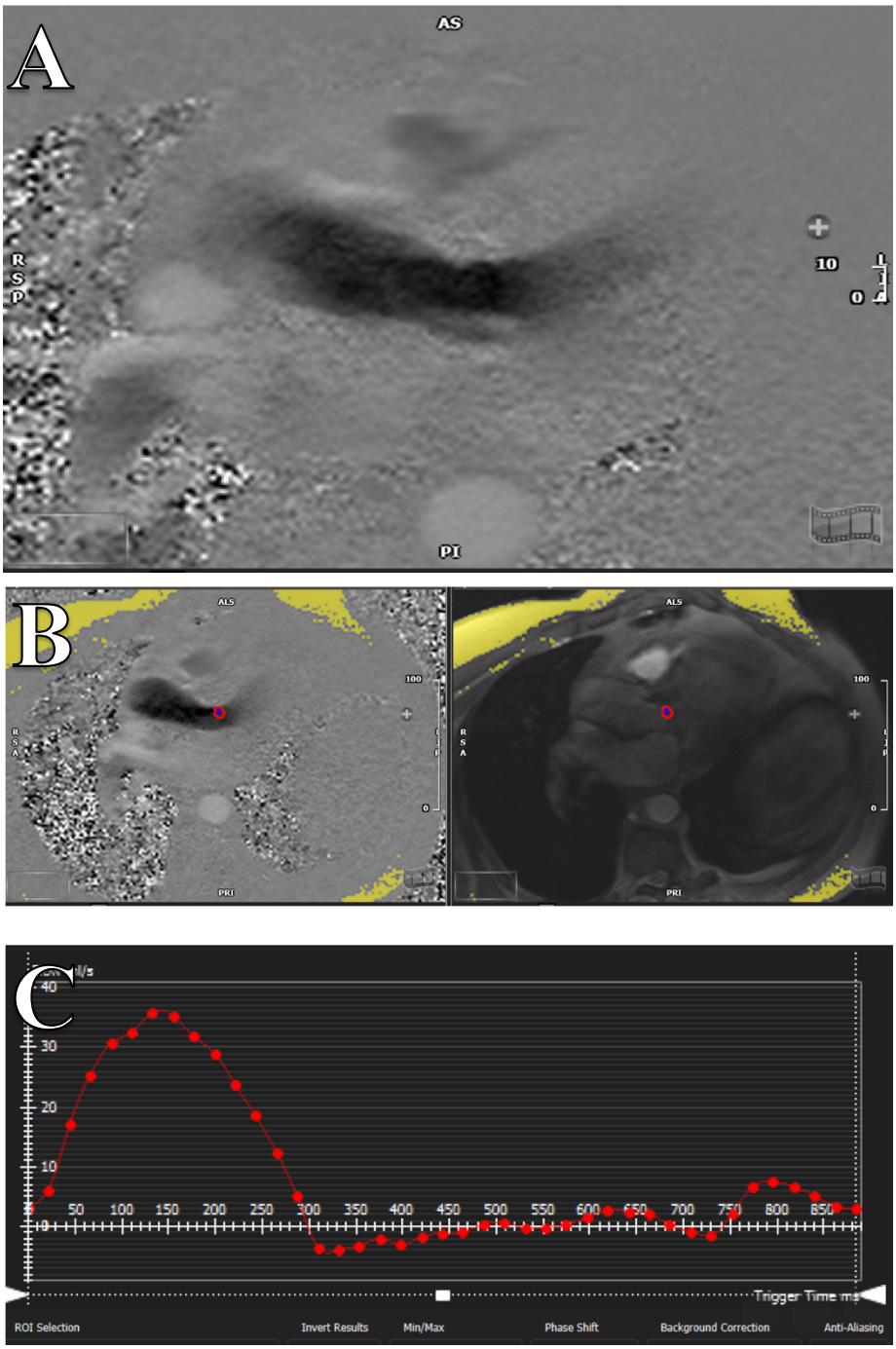

Figure 10: *Panel A* = 2D flow phase velocity map of the left ventricular outflow tract with no aliasing present (LVOT); *Panel B* = Velocity measured in the left ventricular outflow tract (LVOT) by outlining (red circle) the LV area just distal to the aortic valve in each slice of the phase velocity map, with background saturation applied; *Panel C* = the resulting flow velocity throughout the cardiac cycle.

2.6.3 LATE GADOLINIUM ENHANCEMENT (LGE)

2.6.3.1 LGE ACQUISITION

An inversion time scout was acquired six minutes after administration of the gadolinium-based contrast agent. Its position was copied from the position of mid-LV short axis SSFP cine. Using the inversion time scout, the time at which the greatest blood pool and myocardial image contrast was noted as the optimal inversion time.

The ventricular short-axis LGE imaging was then performed, with each 8 mm slice (with no inter-slice gap) copied to the positions of the ventricular short-axis SSFP cine slices, so that both images are directly comparable. Each slice was performed using a breath-hold segmented gradient echo phase sensitive inversion recovery motion corrected sequence. The inversion time was adjusted by 10 milliseconds as necessary depending on the blood pool and myocardial image contrast seen on the previous slice. Typical scan parameters were as follows: [TR/TE/TI = 3.1/1.22 ms/subject-specific ms; R = 2; flip angle = 65°; matrix = 150 x 260, field of view 425x300 mm, as previously described (108).

2.6.3.2 LGE ANALYSIS

Quantitative analysis of LGE was performed using cvi42 software. The endocardial and epicardial borders for each phase-sensitive inversion recovery (PSIR) slice were contoured, with a reference region of interest (ROI) drawn, where possible, in a myocardial area with a normal myocardial intensity signal. A signal intensity threshold at six standard deviations (6 SD) above the mean intensity of a reference region sited

was set as per the established practice of LGE assessment in patients with HCM (109). Cvi42 then automatically processed the weight of LGE in grams, as well as the percentage of the total myocardium that had a signal intensity five standard deviations above the ROI signal intensity. The LGE pattern was also visually classified for the presence of a possible myocardial infarction or myocarditis to inform the parent team of the patient for further investigation and management.

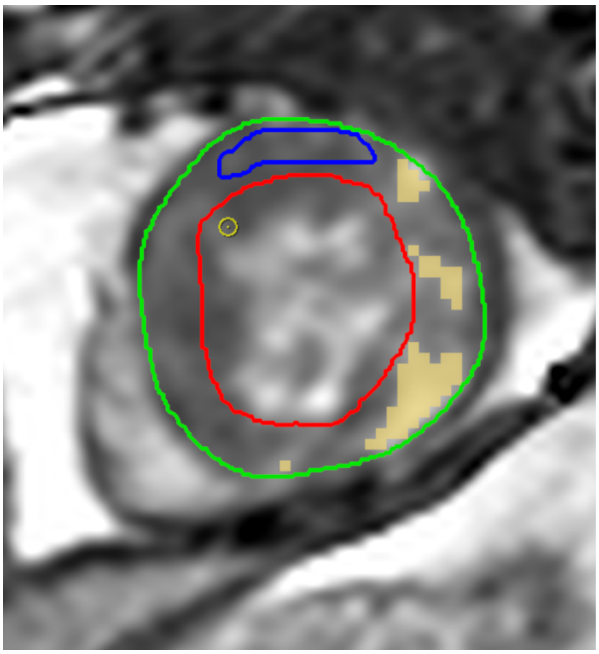

Figure 11: Endocardial and epicardial contours were manually drawn, with a reference region of interest (ROI) with normal myocardial intensity is chosen as a 'remote' region (blue contour). Focal enhancement (seen in yellow) was estimated from the extent of the enhanced myocardial pixels (defined as a signal intensity > 6 standard deviations above ROI).

2.6.4 T_1 MAPPING, T_2 MAPPING, AND EXTRACELLULAR VOLUME

2.6.4.1 MAPPING ACQUISITION

Native and post-contrast T_1 mapping was acquired using a breath-hold Siemens MOLLI sequence, as previously described (110). Two sequences were available, as part of the Siemens package, depending on whether the patient had an R-R interval greater or less than 700 milliseconds, therefore the appropriate sequence was chosen for each patient.

T_2 mapping was acquired using a breath-hold Siemens Myomaps SSFP sequence as previously described (TR/TE = 3/1.3 ms, R = 2, flip angle = 20°, Matrix = 192 x 42, field of view = 360 x 270 mm, slice thickness = 8 mm) (110). For T_1 and T_2 maps, a basal, mid, and apical ventricular short axis slice was acquired, with one slice gap in between each slice.

2.6.4.2 MAPPING AND ECV ANALYSIS

The endocardial and epicardial borders of the basal, mid and apical LV short axis slices were manually contoured for the SSFP T_1 and T_2 images in our cvi42 post processing software. The contours were conservatively drawn, staying well away from blood pool and/or fat, to avoid partial volume loss. The global T_1 value was then provided by the cvi42 software.

ECV was calculated from the Native and post-contrast T_1 maps and the serum haemotocrit obtained before scanning using the following formula: $(1-Hct)\times(\Delta R1_{myocardium}/\Delta R1_{blood})$, where Hct is the hematocrit level, and $\Delta R1$

represents the change in T_1 relaxivity (R1=1/T1) pre and post contrast T_1 (111). A raised global T_1 or T_2 value was defined as per reference ranges obtained from our local department: For T_1 values, the expected range is 1131 $\pm$ 20 ms in males and 1166 $\pm$ 20 ms in females; for T_2 values, the expected range is 39.7 $\pm$ 2 ms in males and 41.2 $\pm$ 2.0 ms in females.

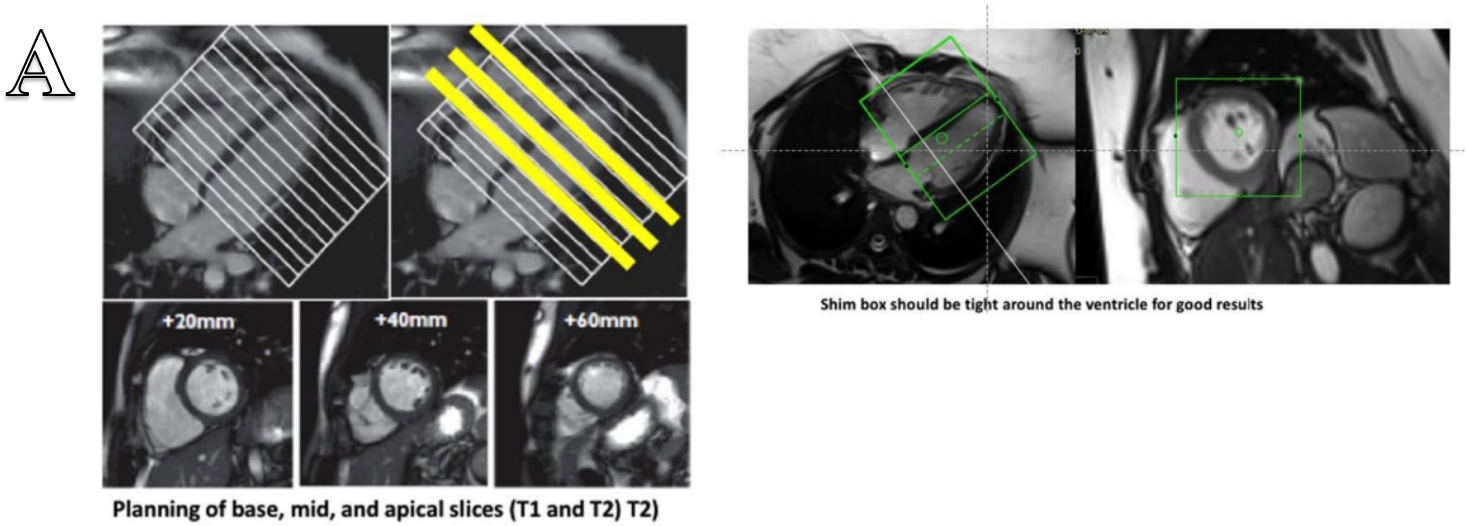

Figure 12: *Panel A* = the method by which I obtained T_1 and T_2 maps by obtaining a base, mid, and apical LV slice for each, with adequate shimming to limit artefacts. *Panel B* = the resulting contoured (endocardial and epicardial) Modified Look-Locker inversion recovery (MOLLI) map (T_1 map) with an American Heart Association 17 segment model with their respective segmental T_1 values.

2.6.5 CARDIOPULMONARY EXERCISE TESTING

2.6.5.1 CPET ACQUISITION

CPET is the gold standard for assessing a patient's exercise capacity. CPET was performed on a seated stationary cycle ergometer (Ergoline GmbH, Bitz, Germany) using an incremental protocol consisting of three minutes of unloaded cycling, followed by a 15W/min ramp aiming for a respiratory exchange ratio (RER) ≥ 1.1 Continuous respiratory gases were collected using the same metalyzer utilised in spirometry. Manual blood pressure data and peripheral oxygen saturation values was recorded at regular intervals with continuous heart rate and 12-lead ECG recording.

2.6.5.2 CPET ANALYSIS

CPET output data was automatically generated using the Metasoft studio software with the Peak VO2 calculated using the Wasserman weight algorithm (112).

2.6.6 STATISTICAL ANALYSIS

All statistical tests were performed using IBM SPSS Statistics (Version 29.0 Armonk, NY:IBM Corp).

Continuous variables are presented as mean ± SD or median (interquartile range or IQR), and categorical variables were presented as frequencies (percentages). For all statistical tests, a *p* value of >0.05 was taken as the cut-off for significance.

For discrete data, normality was assessed using the Shapiro-Wilk 2 tailed test and visual inspection of the histogram. Differences between groups were analysed using independent samples t test, Mann Whitney U-tests, or one-way analysis of variance (ANOVA) with post hoc Kruskal-Wallis test, depending on whether data were parametric or non-parametric. For independent samples t tests, the Levene's test was used to test the assumption of equal variances among subgroups and the two-sided *p* value was used. Pearson or Spearman rank correlation was used to assess correlation between two variables. The Jonckheere-Terpstra test was also performed to assess trends in ordered groups.

For categorical data, differences between groups were analysed using the chi square test or Fischer's exact test – the latter being used if the frequency in any subgroup was <5.

A partial correlation test was used to assess the strength and direction of the relationship between two variables while controlling for the effect of one or more other variables. A bivariate correlation analysis was also performed.

To assess how much predictors such as a patient's SBP, DBP or BMI contributed towards each myocardial wall thicknesses, MWT and LV geometry, a linear regression analysis was performed. For each mode, regression coefficients (β), R^2 value and p-values (via ANOVA testing) were calculated. The unstandardised regression coefficients provided the relative contribution of the independent variable e.g. SBP to the dependent variable e.g. septal wall thickness. The R^2 value indicated the proportion of variance in the dependent variable e.g. septal wall thickness explained by the independent variable e.g. SBP.

Receiver Operating Characteristic (ROC) analysis was performed to evaluate the discriminatory ability of any predictive variables. The area under the curve (AUC) was calculated to assess the diagnostic accuracy of a potential model. Sensitivity, specificity and optimal cut-off values were determined using the Youden index.

CHAPTER 3: CHARACTERISING THE HCM PHENOTYPE

3.1 ABSTRACT

Objective: Hypertrophic cardiomyopathy (HCM) is a genetic cardiac disorder characterized by asymmetric left ventricular hypertrophy (LVH) and is associated with arrhythmias, heart failure, and sudden cardiac death. This study investigates the influence of obesity, hypertension, and genetic status on myocardial structure and function in HCM patients.

Methods: We conducted a single-centre observational study including 32 HCM patients from the TEMPEST trial and 76 HCM patients from the SARC-HCM study. Systolic and diastolic blood pressure (SBP and DBP) quartiles, as well as BMI quartiles, were used to assess relationships with clinical parameters, including high-sensitivity cardiac troponin I (hs-cTnI), myocardial wall thickness, LV geometry, and arrhythmia burden.

Results: The HCM cohort (n=108) was middle-aged (56 [15] years), predominantly male (78%), with high obesity (39%) and treated hypertension (31%) rates. Most had non-obstructive HCM (90% NYHA I), increased maximal LV wall thickness (19 [8] mm) and mass (LVMI 81 [35] g/m²), reduced global longitudinal strain (-14 ± 3%), impaired myocardial energetics (PCr/ATP 1.6 [0.3]), and mild LGE burden (5 [15] g). Higher SBP correlated with concentric remodelling (decreased septal wall thickness, p=0.040; increased lateral wall thickness, p=0.006; decreased septal/lateral wall thickness ratio, p=0.016), increased LVM (p=0.013), decreased LVESV (p=0.017) and increased LVEF (p=0.003), while increasing DBP was associated with increased lateral wall thickness (p=0.012) and decreased septal/lateral (p<0.001) and anterior/inferior (p=0.011) ratios. Higher BMI was associated with an increased inferior

wall thickness (p=0.019), LVM (p<0.001), hs-cTnI (p=0.002), and decreased GLS (p=0.004). In gene-negative participants, an increasing SBP was significantly associated with a decreasing septal wall thickness (p=0.03), anterior wall thickness (p=0.01), and LVESV (p=0.003) as well as an increasing LVEF (p=0.002) and an increasing DBP was significantly associated with a decreased anterior/inferior wall thickness ratio (p=0.02) (there was no significant associations with an increasing BMI). Gene-positive participants demonstrated an increased lateral wall thickness (p=0.01) with an increasing SBP; an increasing DBP was significantly associated with an increasing LVM (p=0.04) and increasing BMI was significantly associated with a decreasing LVEF (p=0.03) and increasing LVESV (p=0.01). When just comparing the two groups, compared to gene-positive participants, gene-negative participants were older (p<0.001), had more hypertension (p<0.001), diabetes mellitus (p<0.001), and atrial fibrillation (p=0.022), higher DBP (p=0.005), a more concentric LV (p<0.001) and a thicker inferior wall (p=0.009). A ratio >1.56 moderately discriminating genotypes (AUC=0.66). Significant BMI×SBP (p=0.002) and BMI×DBP (p<0.001) interactions exacerbated septal/lateral ratio reduction.

Conclusions: This study reveals two distinct HCM pathways: (1) gene- HCM: dominated by hypertension driven concentric remodelling and (2) gene+ HCM: characterised by genetic hypertrophy and modified towards a heart failure phenotype by obesity.

The septal/lateral ratio provides a potentially clinically actionable imaging biomarker that can aid in genotype prediction where genetic testing is unavailable, monitoring

therapeutic response to BP/weight interventions and stratifying patients for targeted management.

3.2 INTRODUCTION

Hypertrophic cardiomyopathy (HCM) is a genetic condition characterized by abnormal thickening of the heart muscle, which can lead to various adverse cardiac outcomes (1, 36, 37). The clinical presentation of HCM is influenced by multiple factors, including hypertension, obesity, and genetic predispositions (1, 36, 37). Understanding how these factors interact with the disease's pathology is crucial for optimising patient management and treatment strategies.

Hypertension is known to exacerbate left ventricular hypertrophy (LVH) and adversely affect left ventricular (LV) geometry (113, 114) (115) (116). Hypertension can lead to increased myocardial wall thickness and more concentric hypertrophy, which may contribute to worsened cardiac function and increased risk of arrhythmias (113, 114) (115) (116). Similarly, obesity has emerged as a possible modifier of LVH and/or HCM, with higher body mass index (BMI) linked to greater myocardial wall thickness, higher levels of cardiac biomarkers, and increased fibrosis (35) (83, 84).

Furthermore, the role of genetic status in HCM adds an additional layer of complexity. Pathogenic sarcomeric variants in HCM can influence the disease's progression and response to environmental factors such as blood pressure and obesity, leading to different clinical presentations and outcomes (1) (8, 11) (9) (14).

This study aims to elucidate the interactions between hypertension, obesity, and genetic status in patients with HCM by analysing the effects of systolic (SBP) and

diastolic blood pressure (DBP) quartiles, body mass index (BMI), and genetic status on myocardial wall thickness, LV geometry, and clinical outcomes via the use of serum cardiac biomarkers, cardiac magnetic resonance (CMR) imaging and 31-Phosphorus magnetic resonance spectroscopy (^{31}P-MRS).

3.3 METHODS

3.3.1 PATIENTS

This is a single centre observational study. The prospectively collected data consists of 32 HCM patients that I recruited and scanned as part of a multicentre randomised control trial, TEMPEST (see Appendix I for further details), and 76 HCM patients who have been recruited by my colleague, Dr Zakariye Ashkir (ZA) as part of his observational study, SARC-HCM, where I assisted in research visits (101). All data analysis of the images, statistics and data presentation of these additional 76 patients, for this thesis, were performed by me.

The TEMPEST trial and SARC-HCM studies generally had the same inclusion and exclusion criteria. All patients with HCM, as defined by the European Society of Cardiology (ESC) guidelines, were included. Additional inclusion criteria were a minimum wall thickness of 15mm and a left ventricular ejection fraction (LVEF) >50%. Those with a history of or planned septal reduction therapy (SRT), severe coronary artery disease and/or valvular heart disease, current pregnancy or lactation or absolute contraindication to CMR were excluded from participation in either study.

“Treated hypertension” was defined as patients who were receiving at least one anti-hypertensive medication, with a history of consistent SBP/DBP recordings <140/90 mmHg and/or a label of “treated” or “controlled hypertension” in their clinical letter. Obesity was defined as a BMI >30 kg/m^2.

Patients in both studies were identified using research databases, inherited cardiac conditions (ICC) clinics and clinical magnetic resonance imaging (CMR) lists. Their recruitment took place between the 18th of October 2021 and the 21st of December 2023. The recruitment pathway for my TEMPEST cohort and the SARC-HCM study are detailed in **Figure 13.**

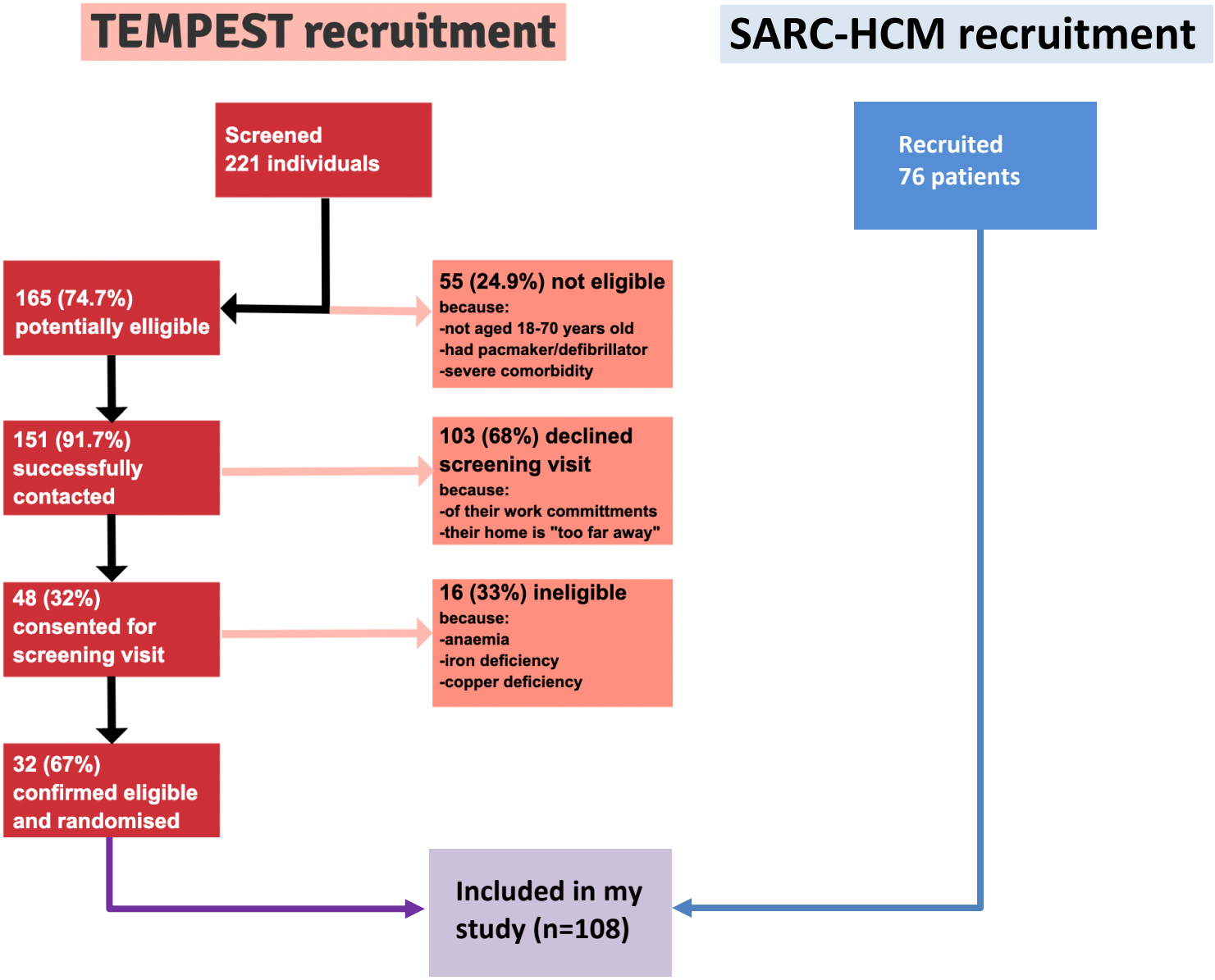

Figure 13: Amended STROBE (Strengthening The Reporting of Observational Epidemiological studies) diagram detailing recruitment process and numbers for the overall study.

3.3.2 STUDY PROTOCOL

All patients underwent a 12-lead electrocardiogram (ECG), ambulatory ECG, blood tests, CMR (3 Tesla scanner, Siemens Healthineers, Erlangen, Germany) and ^{31}P-MRS. In addition, patients recruited as part of the TEMPEST trial underwent cardiopulmonary exercise testing (CPET). The study protocol for patients from the TEMPEST trial and the SARC-HCM study are found below in **Figure 14.** Details on how these images were acquired are present in **Chapter 2**.

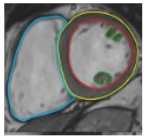

Left ventricular function
-CMR technique using Steady State Free-Precession (SSFP), breath-hold, retrospective gating cine to acquire volumetric and functional LV data.

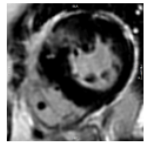

Late gadolinium enhancement (LGE) imaging
-CMR technique that uses delayed contrast enhancement to detect replacement fibrosis.

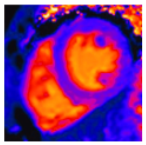

Native & post contrast Modified Look-Locker Inversion Recovery (MOLLI) T1 Mapping
-CMR technique sensitive to differences in T1 relaxation times and used to measure interstitial fibrosis and extracellular volume (ECV).

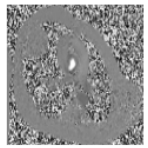

2-dimension flow imaging
-CMR technique that uses phase contrast imaging to detect intracavity obstruction.

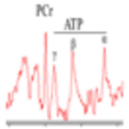

^{31}Phosphorus magnetic resonance spectroscopy
-CMR technique that is sensitive to resonant frequencies of specific cardiac molecules
-Able to detect phosphocreatine to ATP ratio (PCr/ATP ratio)

3 Tesla (Prisma, Siemens Healthineers, Erlangen, Germany)

Figure 14: Study protocol for the overall study. *Abbreviations: BP, blood pressure; CMR, cardiac magnetic resonance; ECG, electrocardiogram; HR, heart rate; LA, left atrium; LGE, late gadolinium enhancement; ^{31}P-MRS, ^{31}Phosphorus Magnetic Resonance Spectroscopy;*

3.3.3 REFERENCE RANGES

In this chapter, I used our departmental 'expected' or 'normal' reference ranges to identify which of our values were out of range (see **Table 1**). In the absence of this information, e.g. for global longitudinal strain (GLS) or MWT, I used reference ranges from the literature (see **Table 1**).

Table 1: Reference ranges for variables used.

Variable	"Normal" range		Reference
	Male	Female	
BMI (kg/m^2)	18.5 – 24.9		(117)
SBP (mmHg)	90 – 129		(118)
DBP (mmHg)	60 – 80		(118)
hs-cTnI (ng/l)	≤34	≤17	*
LVEDV (ml)	106 – 214	86 – 178	(50)
LVEDVI (ml/m^2)	50 – 108	50 – 96	(50)
LVESV (ml)	26 – 82	22 – 66	(50)
LVESVI (ml/m^2)	15 – 30	13 – 25	(50)
LVEF (%)	57 – 77		(50)
LVM (g)	92 – 176	56 – 140	(50)
LVMI (g/m^2)	49 – 85	41 – 81	(50)
GLS (%)	>-18		(119)
LGE (g) / LGEI (g/m^2)	0		(120)
RVEDV (ml)	118 – 250	77 – 201	(50)
RVEDVI (ml/m^2)	60 – 110	55 – 105	(50)
RVEF (%)	52 – 72	51 – 71	(50)
RVESV (ml)	41 – 117	24 – 84	(50)
RVESVI (ml/m2)	25 – 60	20 – 50	(50)
Rest PCr/ATP	2.1 ± 0.2		*
ESC SCD Risk score (%)	<4		(121)

*Departmental reference ranges were used. *Abbreviations: BMI, body mass index; DBP, diastolic blood pressure; ESC SCD risk score, European Society of Cardiology Sudden Cardiac Death risk score; GLS, global longitudinal strain; hs-cTnI, high sensitivity cardiac troponin I; LGE, late gadolinium enhancement; LGEI, late gadolinium enhancement index; LVEDV, left ventricular end diastolic volume; LVEDVI, left ventricular end diastolic volume index; LVEF, left ventricular ejection fraction; LVM, left ventricular mass; LVMI, left ventricular mass index; SBP, systolic blood pressure. LVESV, left ventricular end systolic volume; LVEF, left ventricular ejection fraction; PCr/ATP, phosphocreatine/adenosine triphosphate; RVEDV, right ventricular end diastolic volume; RVEDVI, right ventricular end diastolic volume index; RVEF, right ventricular ejection fraction; RVESV, right ventricular end systolic volume; RVESVI, right ventricular end systolic volume index.*

3.3.4 IMAGE ANALYSIS

Details on how the acquired images were analysed are present in **Chapter 2**.

3.3.5 STATISTICAL ANALYSIS

In this study, the Jonckheere-Terpstra (JT) test was employed to assess statistically significant trends across the various quartiles. The JT test is a non-parametric method, ideal for detecting monotonic trends in ordinal data, making it well-suited for evaluating directional patterns across different patient subgroups.

For analysing trends between categorical variables, the Chi-Square test for linear-by-linear association was used. This combination of statistical methods ensured a robust analysis of the relationships between clinical and myocardial characteristics across different HCM patient subgroups and quartiles.

In addition to these tests, simple linear regression analysis was conducted to evaluate the relationships between continuous variables such as myocardial wall thickness and SBP, DBP, or BMI. Furthermore, Receiver Operating Characteristic (ROC) analysis was used to assess the discriminative ability of certain variables, such as the septal/lateral wall thickness ratio, in distinguishing between gene-positive and gene-negative HCM patients. Further details of the evaluation of data distribution and the differences between subgroups are described in **Chapter 2.**

3.4 RESULTS

As there were no significant differences between the TEMPEST and SARC-HCM cohort, I will be presenting the results of the combined cohort. This will include the baseline demographics, followed by a per quartile SBP, DBP, and BMI analysis (including a gene positive and negative subgroup analysis).

3.4.1 OVERALL RESULTS OF THE COMBINED COHORT

Table 2 summarises the cohort characteristics (n=108): predominantly male, middle-aged, with a high prevalence of obesity and treated hypertension. The cohort demonstrated characteristic features of HCM, with preserved biventricular volumes and systolic function but significantly increased left ventricular maximal wall thickness (LV MWT) and mass/index (LVM/LVMI). Majority of cases were non-obstructive with a high-normal SBP and DBP. Reduced GLS and myocardial energetics (as measured by phosphocreatine/adenosine triphosphate ((PCr/ATP)) on ^{31}P-MRS) were observed alongside a mild burden of late gadolinium enhancement (LGE) burden. Ventricular arrhythmias were infrequent, and most patients fell into the low-risk category according to the European Society of Cardiology Sudden Cardiac Death (ESC SCD) risk scores.

Table 2: The mean/median results for the combined cohort.

	Combined cohort (n=108)
Age	56 [15]
Sex	
Male, n (%)	84 (78)
Female, n (%)	24 (22)
BMI (kg/m^2)	28 [8]
Hypertension, n (%)	33 (31)
Diabetes Mellitus, n (%)	7 (7)
Obesity, n (%)	42 (39)
Atrial Fibrillation, n (%)	6 (6)
Genotype positive, n (%)	51 (47)
Genotype negative, n (%)	56 (52)
Obstruction, n (%)	12 (11)
SAM, n (%)	5 (10)
LV apical aneurysm, n (%)	0 (0)
NYHA class I, n (%)	97 (90)
SBP (mmHg)	135 [24]
DBP (mmHg)	76 ± 9
hs-cTnI (ng/L)	13 [13]
Rest PCr/ATP	1.6 [0.3]
Septal wall thickness (mm)	17 ± 5
Lateral wall thickness (mm)	11 [7]
Anterior wall thickness (mm)	12 [6]
Inferior wall thickness (mm)	10 [4]
MLVWT (mm)	19 [8]
Septal/lateral wall thickness ratio	1.9 ± 0.6
Anterior/inferior wall thickness ratio	1.1 [0.4]
LVM (g)	163 [60]
LVMI (g/m^2)	81 [35]
LVEDV (ml)	151 ± 35
LVEDVI (ml/m^2)	75 ± 16
LVESV (ml)	35 [18]
LVESVI (ml/m^2)	17 [8]
LVEF (%)	74 ± 7
GLS (%)	-14 ± 3
LGE (g)	5 [15]
LGEI (g/m^2)	3 [8]
RVEF (%)	69 ± 8
RVEDV (ml)	152 ± 34
RVEDVI (ml/m^2)	77 [18]
RVESV (ml)	49 ± 21
RVESVI (ml/m^2)	24 ± 11
Ventricular arrhythmia, n (%)	25 (28)
ESC SCD Risk (%)	2 [0.5]

Abbreviations: BMI=body mass index, DBP=diastolic blood pressure, ESC= European Society of Cardiology, GLS=global longitudinal strain, hs-cTnI=high sensitivity cardiac troponin I, LGE=late gadolinium enhancement, LGEI=late gadolinium enhancement index, LV=left ventricle, LVEDV=left ventricular end diastolic volume, LVEDVI=left ventricular end-diastolic volume index, LVESV=left ventricular systolic volume, LVESVI=left ventricular end systolic volume index, LVEF=left ventricular ejection fraction, LVM=left ventricular mass, LVMI=left ventricular mass index, MLVWT = maximal left ventricular wall thickness, NYHA=New York heart association, PCr/ATP=phosphocreatine/adenosine triphosphate, RVEDV=right ventricular end diastolic volume, RVEDVI=right ventricular end diastolic volume index, RVEF=right ventricular ejection fraction, RVESV=right ventricular end systolic volume, RVESVI=right ventricular end systolic volume index, SBP=systolic blood pressure, SCD= sudden cardiac death risk. Data presented as mean ±SD, median [IQR] or n (%).

3.4.2 BLOOD PRESSURE AND BMI STRATIFICATION

I analysed the relationship between clinical variables and SBP and DBP quartiles. Quartile 1 represents the lowest 25% of SBPs in our cohort, while quartile 4 represents the highest 25%.

3.4.2.1 SYSTOLIC BLOOD PRESSURE TRENDS

Higher SBP quartiles had significantly greater prevalences of diabetes mellitus, obesity, and atrial fibrillation, along with a higher burden of cardiac symptoms and ventricular arrhythmias (all $p<0.001$). Higher SBP quartiles were associated with progressive concentric LV remodelling, evidenced by decreasing septal/lateral wall thickness ratios as shown in **Figure 17**. This geometric change, illustrated in **Figures 16** and **35**, was driven by opposing trends in septal and lateral wall thicknesses, accompanied by increasing LV mass and ejection fraction (**Figure 18**). **Figure 19** confirms no significant associations between SBP and myocardial fibrosis or energetics.

Table 3: Jonckheere-Terpstra Test results for trends in different parameters across systolic blood pressure (SBP) quartiles.

Category	Quartile 1	Quartile 2	Quartile 3	Quartile 4	*P* value
Age (years)	48 [18]	55 [17]	56 [13]	61 [10]	0.026
BMI (kg/m^2)	26 [7]	28 [6]	27 [6]	28 [6]	0.877
SBP (mmHg)	113 [14]	127 [3]	133 [4]	151 [20]	<0.001
DBP (mmHg)	68±7	73±12	76±8	81±9	<0.001
hs-cTnI (ng/l)	10 [18]	13 [36]	8 [10]	13 [11]	0.589
Septal wall thickness (mm)	18±5	16±4	15±6	15±5	0.040
Lateral wall thickness (mm)	9 [6]	11 [4]	13 [5]	13 [8]	0.006
Anterior wall thickness (mm)	13 [11]	12 [3]	13 [7]	10 [4]	0.232
Inferior wall thickness (mm)	10 [4]	10 [4]	10 [4]	10 [4]	0.859
MWT (mm)	20 [9]	18 [4]	18 [7]	19 [4]	0.966
LVM (g)	130 [47]	135 [64]	149 [52]	175 [44]	0.013
Septal/lateral wall thickness ratio	2 [1.2]	1.6 [0.8]	1.7 [0.6]	1.6 [1.2]	0.016
Anterior/inferior wall thickness ratio	1 [0.3]	1.1 [0.3]	1.1 [0.3]	1.1 [0.4]	0.652
LVEDV (ml)	156±29	162±30	164±31	151±37	0.657
LVESV (ml)	50 [15]	49 [18]	46 [28]	37 [23]	0.017
LVEF (%)	68±6	69±7	70±8	74±6	0.003
LVGLS (%)	-16 [3]	-16 [7]	-16 [6]	-14 [4]	0.839
LGE (g)	9 [14]	6 [14]	5 [15]	5 [14]	0.291
Rest PCr/ATP	1.7±0.3	1.7±0.3	1.5±0.4	1.5±0.4	0.104

Abbreviations: BMI=body mass index, DBP=diastolic blood pressure, LVGLS= left ventricular global longitudinal strain, hs-cTnI=high sensitivity cardiac troponin I, LGE=late gadolinium enhancement, LV=left ventricle, LVEDV=left ventricular end diastolic volume, LVESV=left ventricular systolic volume, LVEF=left ventricular ejection fraction, LVM=left ventricular mass, MWT = maximal wall thickness, PCr/ATP=phosphocreatine/adenosine triphosphate, SBP=systolic blood pressure. Data presented as mean ±SD, median [IQR] or n(%).

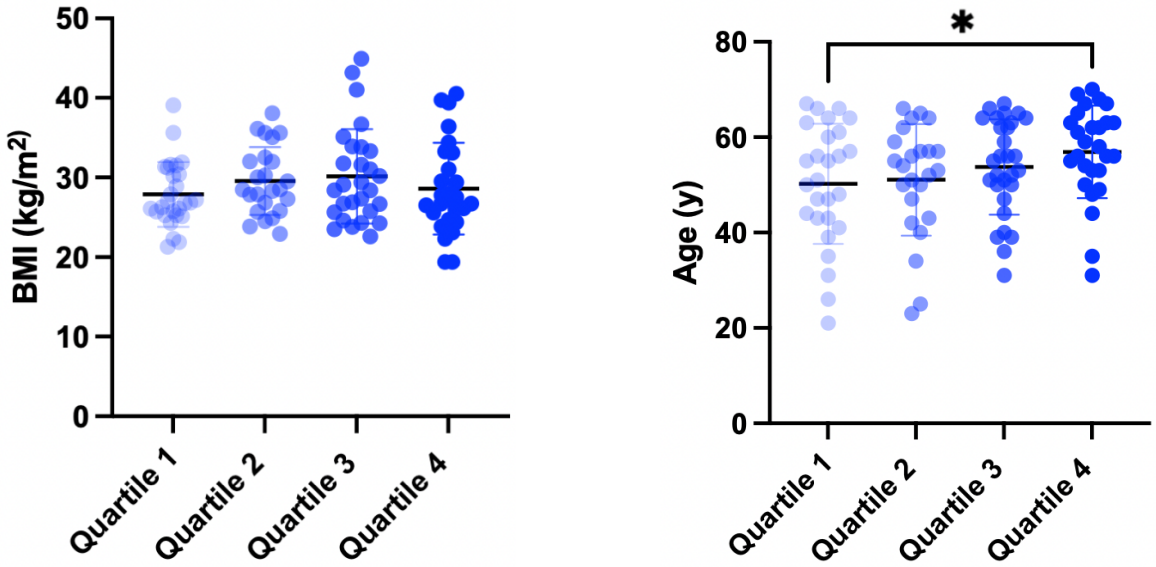

Figure 14: Differences in age and BMI per systolic blood pressure (SBP) quartiles. The Jonckheere-Terpstra Test for assessing statistically significant trends is reported: Age, *p*=0.026; BMI, *p*=0.877. ** = p<0.05, ** = p<0.01, *** = p<0.001. Abbreviations: BMI, body mass index.*

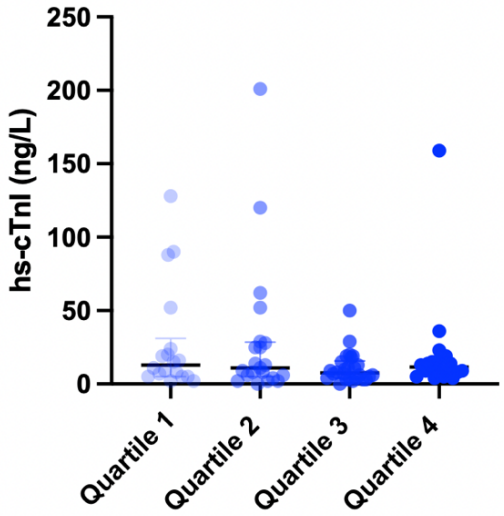

Figure 15: Differences in high sensitivity cardiac troponin I (hs-cTnI) per systolic blood pressure (SBP) quartiles. No statistically significant trend between quartiles was observed (p=0.589). *Abbreviations: hs-cTnI, high sensitivity cardiac troponin I.*

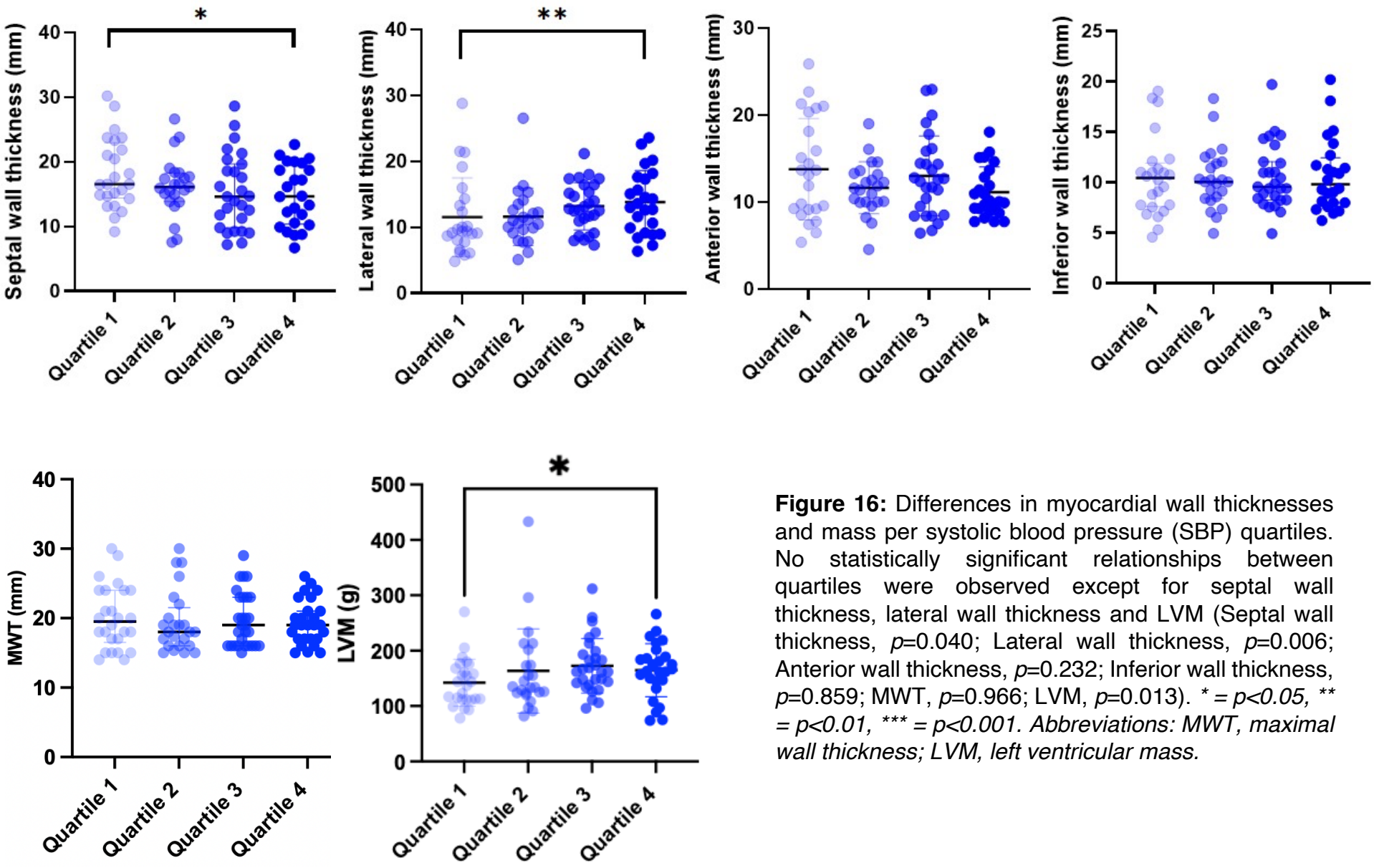

Figure 16: Differences in myocardial wall thicknesses and mass per systolic blood pressure (SBP) quartiles. No statistically significant relationships between quartiles were observed except for septal wall thickness, lateral wall thickness and LVM (Septal wall thickness, p=0.040; Lateral wall thickness, p=0.006; Anterior wall thickness, p=0.232; Inferior wall thickness, p=0.859; MWT, p=0.966; LVM, p=0.013). ** = p<0.05, ** = p<0.01, *** = p<0.001. Abbreviations: MWT, maximal wall thickness; LVM, left ventricular mass.*

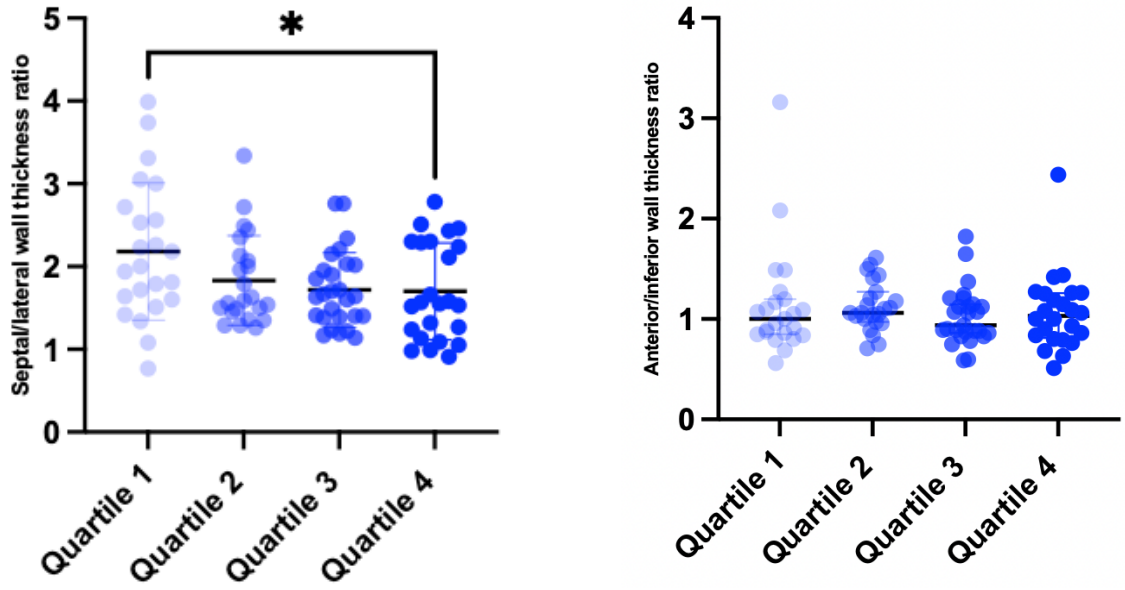

Figure 17: Differences in LV geometry per systolic blood pressure (SBP) quartiles. The Jonckheere-Terpstra Test for assessing statistically significant trends is reported: Septal/lateral wall thickness ratio, p=0.016; Anterior/inferior wall thickness ratio, p=0.652. ** = p<0.05, ** = p<0.01, *** = p<0.001.*

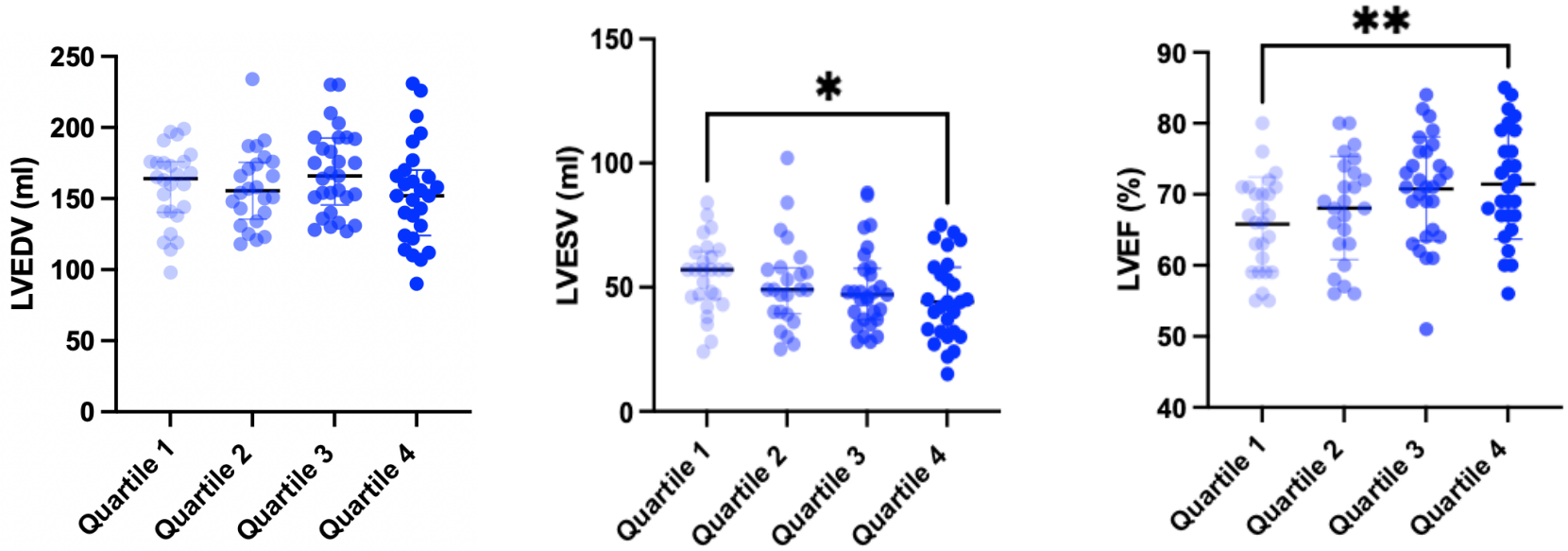

Figure 18: Differences in LV volumes and function per systolic blood pressure (SBP) quartiles. The Jonckheere-Terpstra Test for assessing statistically significant trends is reported: LVEDV, p=0.657; LVESV, p=0.017; LVEF, p=0.003. ** = p<0.05, ** = p<0.01, *** = p<0.001. Abbreviations: LVEDV, left ventricular end diastolic volume; LVESV, left ventricular end systolic volume; LVEF, left ventricular ejection fraction.*

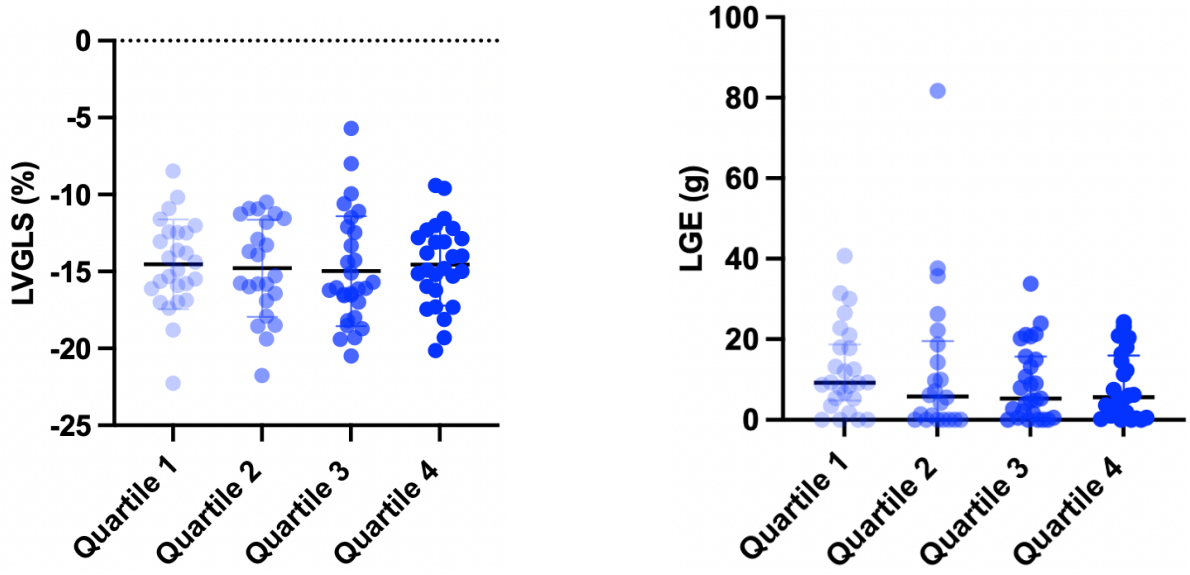

Figure 19: Differences in LV strain and fibrosis per systolic blood pressure (SBP) quartiles. No statistically significant trends were observed (LVGLS, *p*=0.839; LGE, *p*=0.291). *Abbreviations: LVGLS, left ventricular global longitudinal strain; LGE, late gadolinium enhancement.*

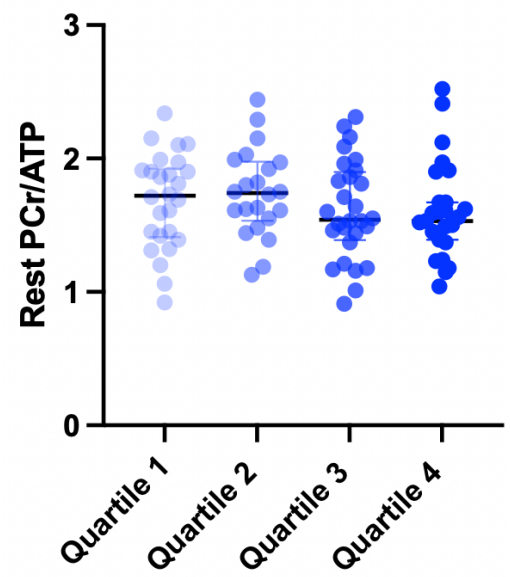

Figure 20: Differences in myocardial energetics per systolic blood pressure (SBP) quartiles. No statistically significant trend was observed (p=0.104). *Abbreviations: PCr/ATP, phosphocreatine/adenosine triphosphate.*

3.4.2.2 DIASTOLIC BLOOD PRESSURE TRENDS

Higher DBPs were significantly more likely to be male and exhibited greater prevalences of diabetes mellitus, obesity, and atrial fibrillation (all $p<0.001$). These patients showed higher rates of LVOT obstruction, SAM, cardiac symptoms, and ventricular arrhythmias (all $p<0.001$). Increasing DBP showed associations with concentric remodelling patterns, particularly through lateral wall thickening (**Figure 23**) and reduced septal/lateral wall thickness ratios (**Figure 24**). The anterior/inferior wall thickness ratio also decreased with higher DBPs (**Figure 37**), suggesting generalised geometric changes. LV mass showed particularly strong associations with higher DBPs (**Figure 25**). **Figures 21-27** demonstrate no significant associations between DBP and age, BMI, hs-cTnI level, septal, anterior, inferior and maximal myocardial wall thicknesses, LV volumes, function, fibrosis burden or myocardial energetics.

Table 4: Jonckheere-Terpstra Test results for trends in different parameters across diastolic blood pressure (DBP) quartiles.

Category	Quartile 1	Quartile 2	Quartile 3	Quartile 4	*P* value
Age (years)	52 [21]	56 [20]	54 [11]	57 [12]	0.547
BMI (kg/m^2)	27 [10]	27 [5]	28 [10]	27 [6]	0.615
SBP (mmHg)	123 [22]	128 [21]	133 [26]	135 [15]	<0.001
DBP (mmHg)	62 [5]	71 [3]	79 [4]	86 [5]	<0.001
hs-cTnI (ng/l)	11 [13]	9 [13]	12 [14]	9 [21]	0.982
Septal wall thickness (mm)	17±6	15±5	16±5	15±5	0.170
Lateral wall thickness (mm)	9 [6]	11 [7]	14 [6]	13 [7]	0.012
Anterior wall thickness (mm)	12 [6]	10 [6]	13 [7]	11 [4]	0.655
Inferior wall thickness (mm)	10 [5]	9 [3]	10 [7]	11 [3]	0.240
MWT (mm)	18 [2]	18 [9]	19 [7]	19 [4]	0.472
LVM (g)	144 [67]	129 [61]	182 [68]	163 [49]	0.002
Septal/lateral wall thickness ratio	2.2 [1.2]	2 [1]	1.6 [0.7]	1.5 [0.3]	<0.001
Anterior/inferior wall thickness ratio	1.2 [0.4]	1.1 [0.3]	1.1 [0.4]	1 [0.3]	0.011
LVEDV (ml)	172±35	146±30	153±29	165±30	0.810
LVESV (ml)	55±21	44±15	40±9	51±19	0.335
LVEF (%)	69±8	70±7	73±6	70±7	0.184
LVGLS (%)	-16 [1]	-15 [7]	-14 [5]	-15 [6]	0.816
LGE (g)	6 [13]	6 [13]	7 [15]	10 [21]	0.675
Rest PCr/ATP	1.6±0.4	1.6±0.3	1.6±0.3	1.7±0.4	0.624

Abbreviations: BMI=body mass index, DBP=diastolic blood pressure, LVGLS= left ventricular global longitudinal strain, hs-cTnI=high sensitivity cardiac troponin I, LGE=late gadolinium enhancement, LV=left ventricle, LVEDV=left ventricular end diastolic volume, LVESV=left ventricular systolic volume, LVEF=left ventricular ejection fraction, LVM=left ventricular mass, MWT = maximal wall thickness, PCr/ATP=phosphocreatine/adenosine triphosphate, SBP=systolic blood pressure. Data presented as mean ±SD, median [IQR] or n(%).

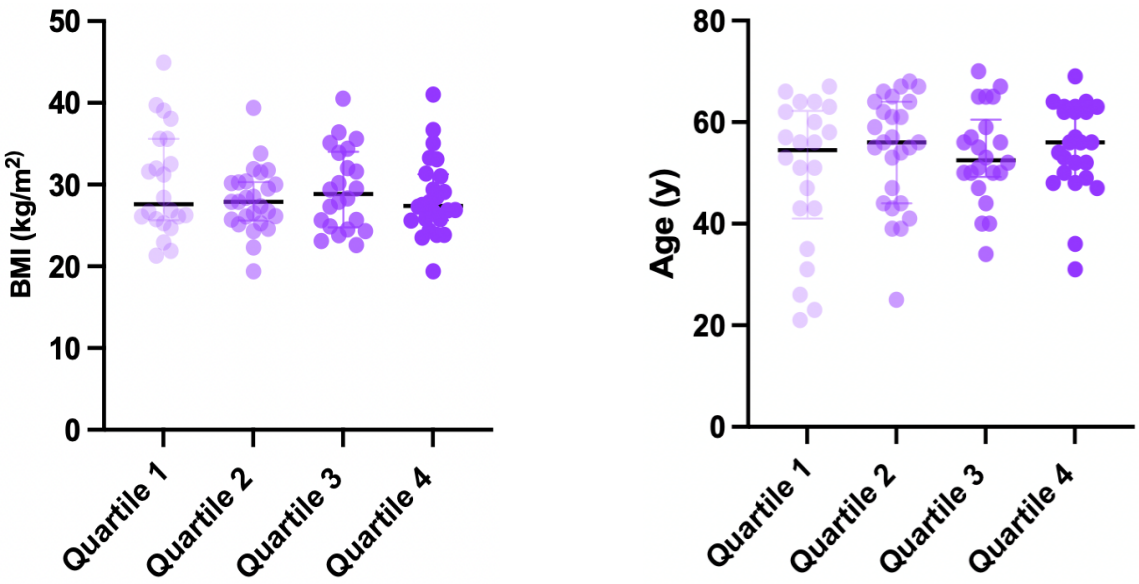

Figure 21: Differences in age and BMI per diastolic blood pressure (DBP) quartiles. No statistically significant trends were observed (Age, *p*=0.547; BMI, *p*=0.615). *Abbreviations: BMI, body mass index.*

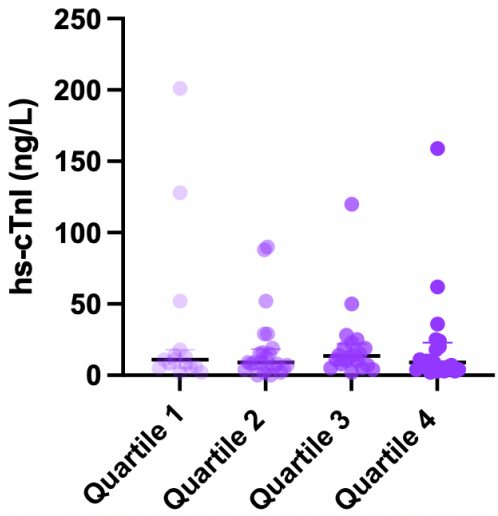

Figure 22: Differences in hs-cTnI levels per diastolic blood pressure (DBP) quartiles. No statistically significant trend was observed (p=0.982). *Abbreviations: hs-cTnI, high sensitivity cardiac troponin I.*

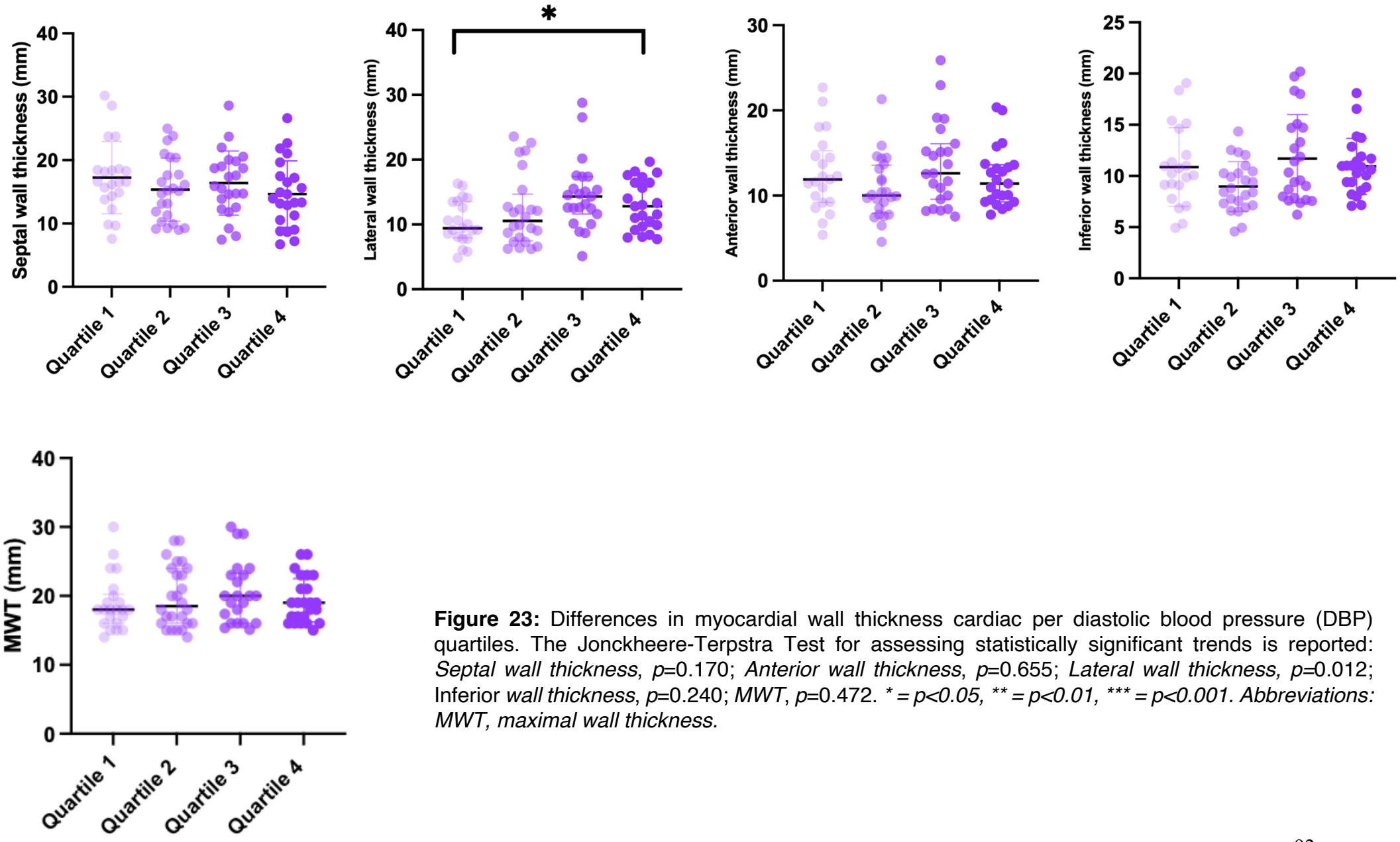

Figure 23: Differences in myocardial wall thickness cardiac per diastolic blood pressure (DBP) quartiles. The Jonckheere-Terpstra Test for assessing statistically significant trends is reported: *Septal wall thickness*, *p*=0.170; *Anterior wall thickness*, *p*=0.655; *Lateral wall thickness, p*=0.012; Inferior *wall thickness*, *p*=0.240; *MWT*, *p*=0.472. ** = p<0.05, ** = p<0.01, *** = p<0.001. Abbreviations: MWT, maximal wall thickness.*

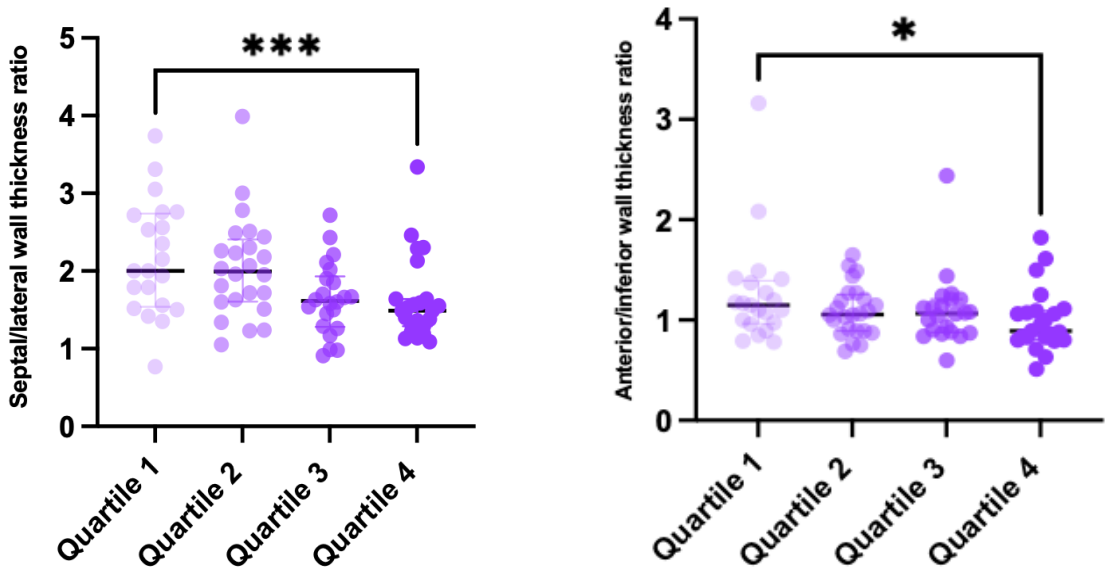

Figure 24: Differences in LV geometry per diastolic blood pressure (DBP) quartiles. The Jonckheere-Terpstra Test for assessing statistically significant trends is reported: *Septal/lateral wall thickness ratio, p*<0.001; *Anterior/inferior wall thickness ratio p*=0.011. ** = p<0.05, ** = p<0.01, *** = p<0.001.*

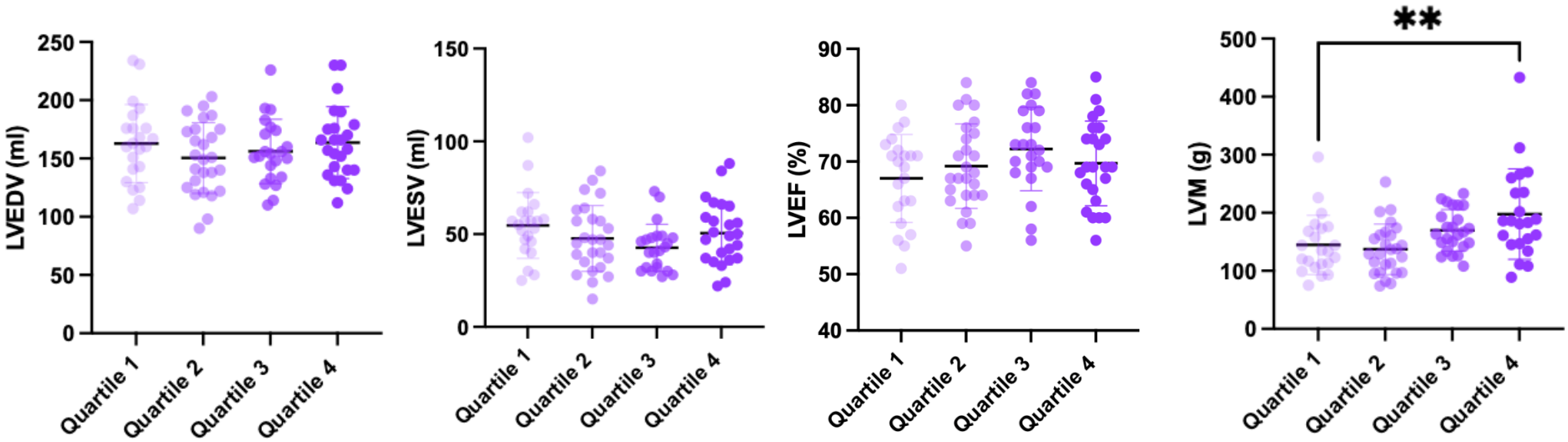

Figure 25: Differences in LV volumes, function and mass per diastolic blood pressure (DBP) quartiles. The Jonckheere-Terpstra Test for assessing statistically significant trends is reported: *LVEDV, p*=0.810; *LVESV, p*=0.335; *LVEF, p*=0.184; *LVM, p*=0.002. ** = p<0.05, ** = p<0.01, *** = p<0.001. Abbreviations: LVEDV, left ventricular end diastolic volume; LVESV, left ventricular end systolic volume; LVEF, left ventricular ejection fraction; LVM, left ventricular mass.*

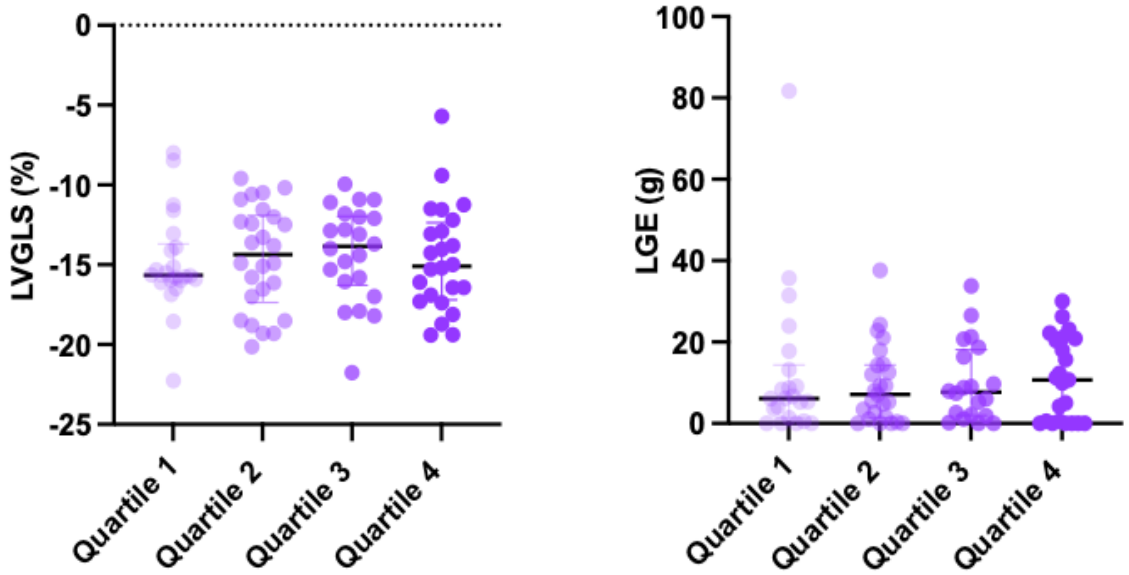

Figure 26: Differences in LV strain and fibrosis burden per diastolic blood pressure (DBP) quartiles. No statistically significant trends were observed (LVGLS, *p*=0.816; LGE, *p*=0.675). *Abbreviations: LVGLS, left ventricular global longitudinal strain; LGE, late gadolinium enhancement.*

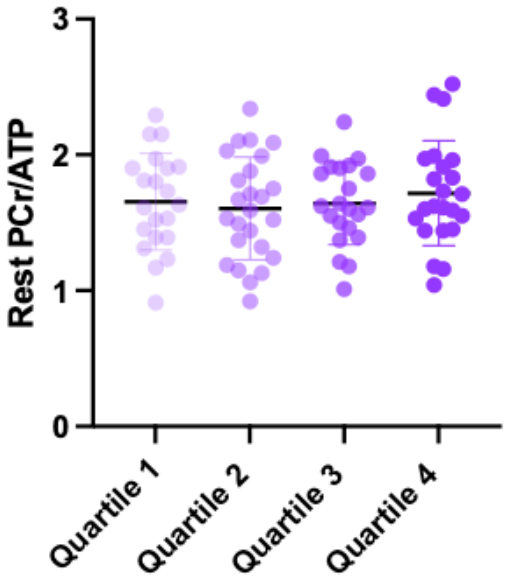

Figure 27: Differences in myocardial energetics per diastolic blood pressure (DBP) quartiles. No statistically significant trend was observed (p=0.624). *Abbreviations: PCr/ATP, phosphocreatine/adenosine triphosphate.*

3.4.2.3 BMI TRENDS

Higher BMI quartiles showed significantly greater prevalences of male sex, diabetes mellitus, atrial fibrillation, cardiac symptoms, and ventricular arrhythmias (all $p<0.001$). These patients exhibited progressive cardiac remodelling with increasing BMI, including elevated hs-cTnI levels (**Figure 29**), greater inferior wall thickness and left ventricular mass (**Figure 30**), and reduced septal/lateral wall thickness ratio (**Figure 31**) and global longitudinal strain (**Figure 32**). Notably, **Figure 28** shows BMI was not associated with age or blood pressure changes, while **Figures 30-33** confirm no significant relationships with other wall segments, ventricular volumes, ejection fraction, fibrosis burden, or myocardial energetics.

Table 5: Jonckheere-Terpstra Test results for trends in different parameters across body mass index (BMI) quartiles.

Category	Quartile 1	Quartile 2	Quartile 3	Quartile 4	*P* value
Age (years)	52 [22]	60 [12]	54 [16]	58 [14]	0.368
BMI (kg/m^2)	24 [2]	27 [1]	29 [3]	36 [6]	<0.001
SBP (mmHg)	128 [24]	131 [15]	128 [11]	133 [28]	0.801
DBP (mmHg)	75±13	74±18	75±7	75±10	0.660
hs-cTnI (ng/l)	7 [13]	8 [9]	11 [9]	20 [38]	0.002
Septal wall thickness (mm)	15±4	16±7	17±5	16±5	0.275
Lateral wall thickness (mm)	12 [9]	11 [7]	12 [4]	12 [7]	0.427
Anterior wall thickness (mm)	12 [7]	10 [4]	12 [8]	13 [5]	0.218
Inferior wall thickness (mm)	9 [3]	10 [3]	10 [3]	11 [6]	0.019
MWT (mm)	18 [5]	17 [3]	19 [8]	20 [5]	0.058
LVM (g)	125 [59]	144 [62]	157 [61]	183 [78]	<0.001
Septal/lateral wall thickness ratio	1.9 [1]	1.5 [1.2]	1.7 [0.8]	1.6 [1]	0.075
Anterior/inferior wall thickness ratio	1.1 [0.4]	1.1 [0.3]	1 [0.3]	1.1 [0.4]	0.874
LVEDV (ml)	151±27	157±24	162±31	164±44	0.106
LVESV (ml)	44±12	44±13	48±15	53±25	0.067
LVEF (%)	70±6	72±6	71±5	69±10	0.400
LVGLS (%)	-16 [4]	-16 [3]	-16 [5]	-12 [5]	0.004
LGE (g)	8 [11]	1 [11]	5 [8]	21 [20]	0.097
Rest PCr/ATP	1.7±0.3	1.7±0.8	1.6±0.3	1.6±0.4	0.367

Abbreviations: BMI=body mass index, DBP=diastolic blood pressure, LVGLS= left ventricular global longitudinal strain, hs-cTnI=high sensitivity cardiac troponin I, LGE=late gadolinium enhancement, LV=left ventricle, LVEDV=left ventricular end diastolic volume, LVESV=left ventricular systolic volume, LVEF=left ventricular ejection fraction, LVM=left ventricular mass, MWT = maximal wall thickness, PCr/ATP=phosphocreatine/adenosine triphosphate, SBP=systolic blood pressure. Data presented as mean ±SD, median [IQR] or n(%).

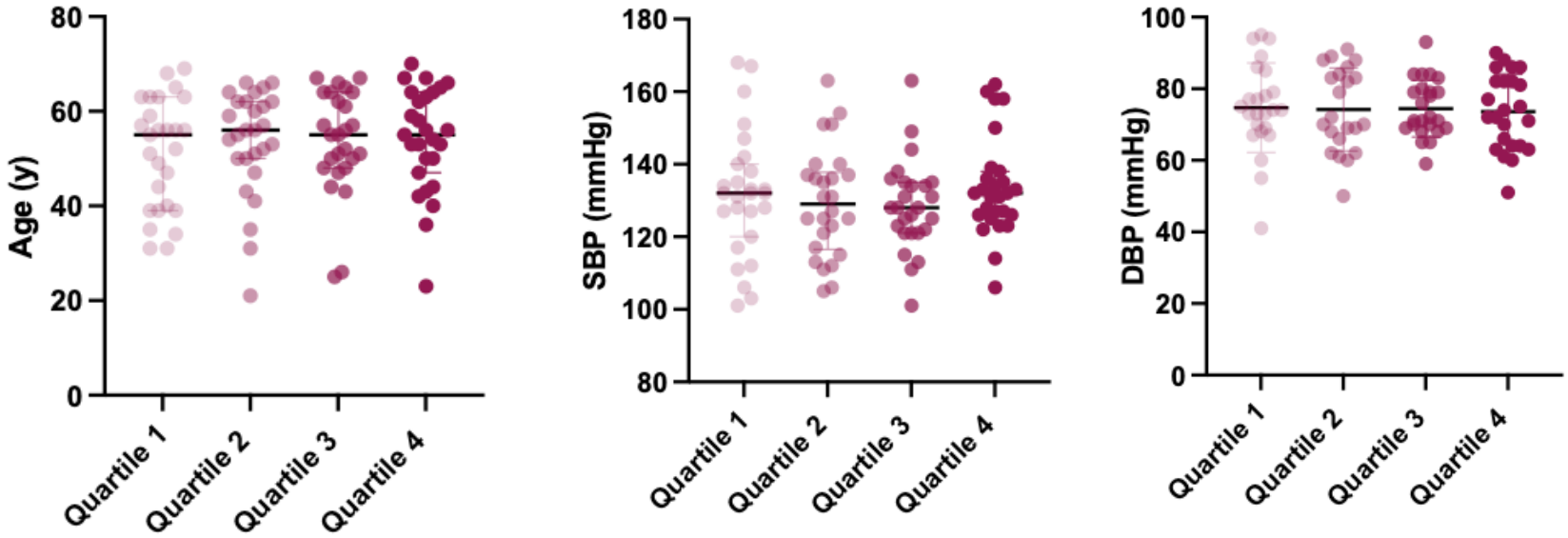

Figure 28: Differences in age, systolic blood pressure (SBP) and diastolic blood pressure (DBP) per body mass index (BMI) quartiles. No statistically significant trends were observed (Age, p=0.368; SBP, p=0.801; DBP, p=0.660). *Abbreviations: SBP, systolic blood pressure; DBP, diastolic blood pressure.*

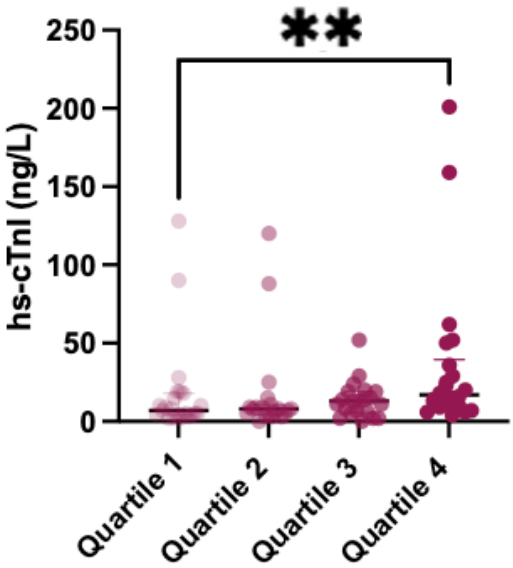

Figure 29: Differences in hs-cTnI levels per body mass index (BMI) quartiles. The Jonckheere-Terpstra Test for assessing statistically significant trends is reported (*p*=0.002). *Abbreviations: hs-cTnI, high sensitivity cardiac troponin I. * = p<0.05, ** = p<0.01, *** = p<0.001.*

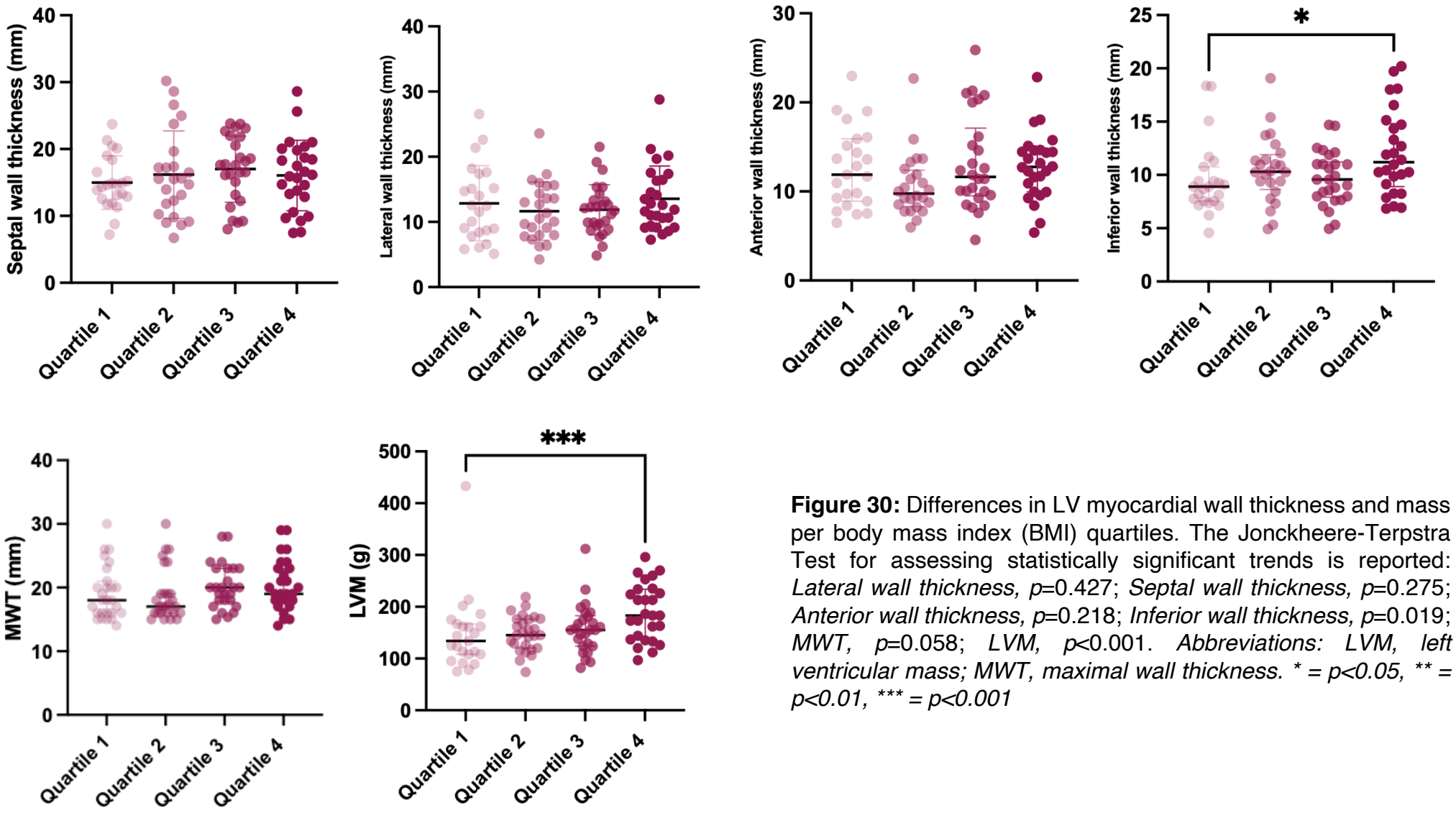

Figure 30: Differences in LV myocardial wall thickness and mass per body mass index (BMI) quartiles. The Jonckheere-Terpstra Test for assessing statistically significant trends is reported: *Lateral wall thickness, p*=0.427; *Septal wall thickness, p*=0.275; *Anterior wall thickness, p*=0.218; *Inferior wall thickness, p*=0.019; *MWT, p*=0.058; *LVM, p*<0.001. *Abbreviations: LVM, left ventricular mass; MWT, maximal wall thickness. * = p<0.05, ** = p<0.01, *** = p<0.001*

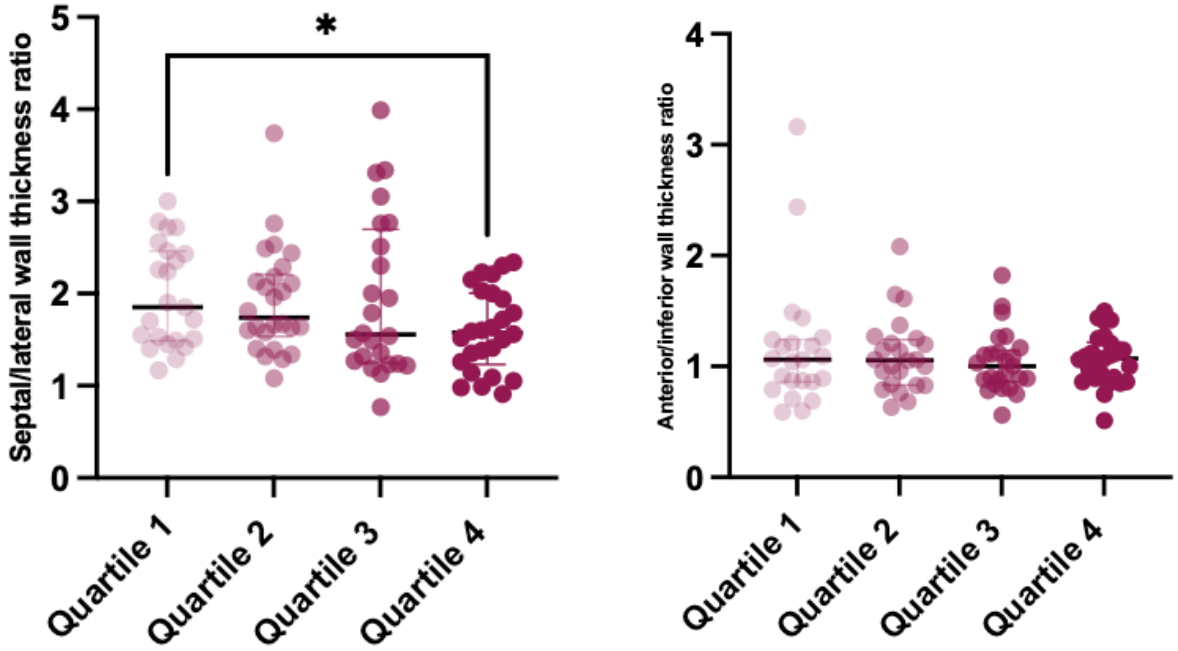

Figure 31: Differences in LV geometry per body mass index (BMI) quartiles. No statistically significant trends were observed (*Septal/lateral wall thickness* ratio, *p*=0.075; *Anterior/inferior wall thickness ratio, p*=0.874).** = p<0.05, ** = p<0.01, *** = p<0.001*.

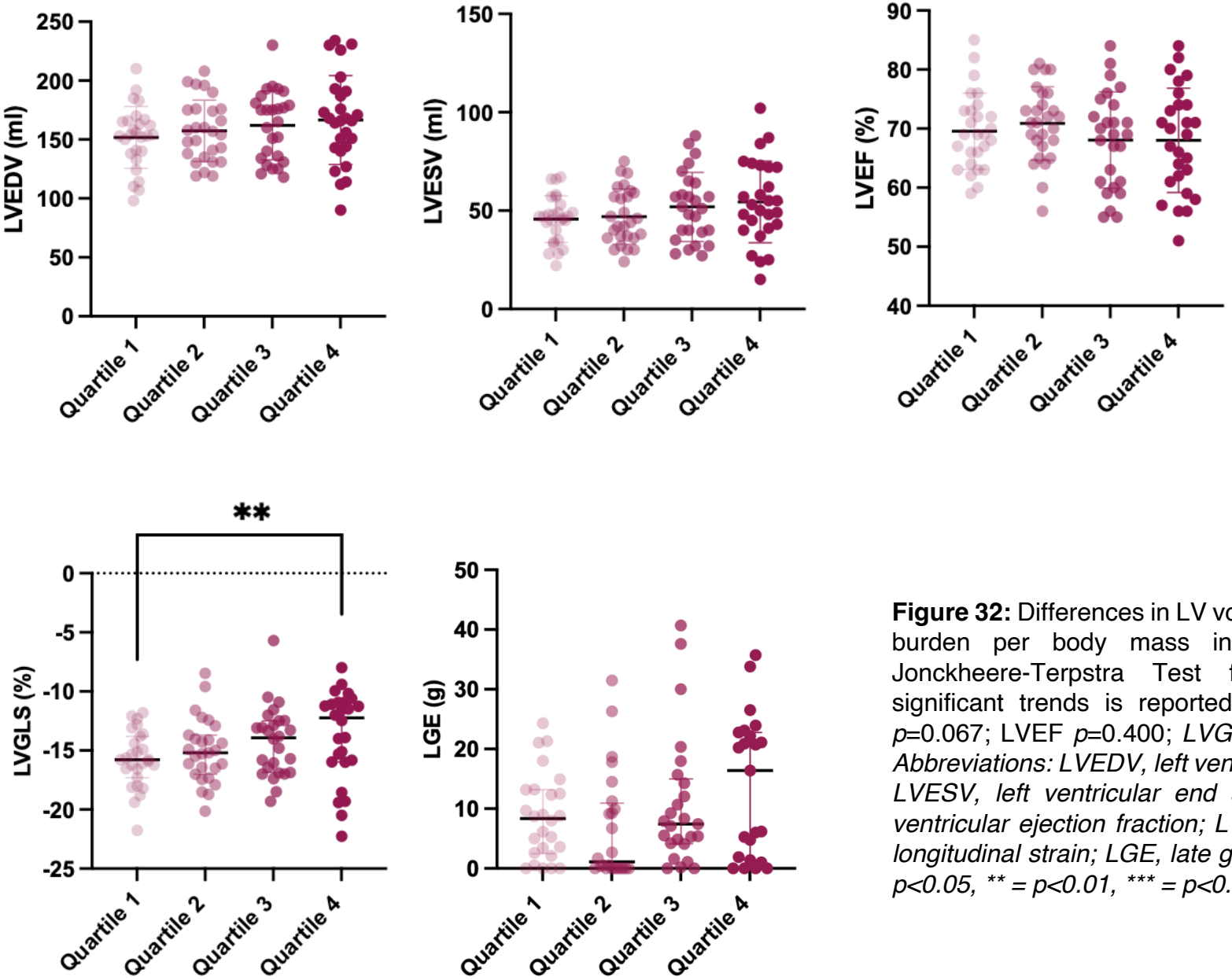

Figure 32: Differences in LV volumes, function, and fibrosis burden per body mass index (BMI) quartiles. The Jonckheere-Terpstra Test for assessing statistically significant trends is reported: *LVEDV* p=0.106; *LVESV* p=0.067; LVEF p=0.400; *LVGLS* p=0.004; *LGE* p=0.097). *Abbreviations: LVEDV, left ventricular end diastolic volume; LVESV, left ventricular end systolic volume; LVEF, left ventricular ejection fraction; LVGLS, left ventricular global longitudinal strain; LGE, late gadolinium enhancement. * = p<0.05, ** = p<0.01, *** = p<0.001.*

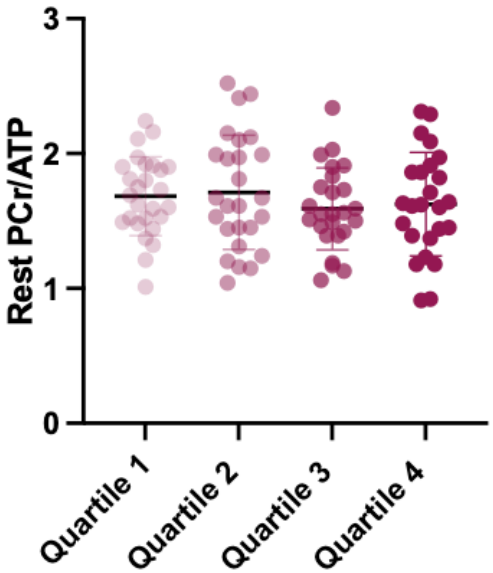

Figure 33: Differences in LV myocardial energetics per body mass index (BMI) quartiles. No statistically significant trend was observed (p=0.367). *Abbreviations: PCr/ATP, phosphocreatine/adenosine triphosphate.*

3.4.3 BLOOD PRESSURE AND BMI ASSOCIATIONS WITH VENTRICULAR GEOMETRY

To evaluate how blood pressure and body mass index influence cardiac structure, we performed linear regression analyses with myocardial wall thickness and left ventricular geometric parameters as dependent variables, and systolic blood pressure (SBP), diastolic blood pressure (DBP), or body mass index (BMI) as independent variables. As shown in **Figures 34-39**, each regression model displays the correlation coefficient (R) representing relationship strength and direction, the unstandardized beta coefficient (B) quantifying the magnitude of change in cardiac parameters per unit change in blood pressure or BMI, and the statistical significance (p-value) derived from ANOVA testing. This approach allowed us to precisely quantify how hemodynamic and metabolic factors impact specific aspects of ventricular remodelling in HCM.

3.4.3.1 THE RELATIONSHIP BETWEEN SBP AND MYOCARDIAL WALL THICKNESS AND LV GEOMETRY

Linear regression analysis revealed no significant relationship between SBP and either anterior wall thickness, inferior wall thickness or anterior/inferior wall thickness ratio (see **Figures 34** and **35**). However, there was a significant positive association between SBP and septal and lateral wall thickness as well as the septal/lateral wall thickness ratio, indicating that for every 10 mmHg increase in SBP, there was a 0.8mm decrease in septal wall thickness, a 0.9mm increase in the lateral wall thickness and a 0.1 decrease in the septal/lateral wall thickness ratio (see **Figure 35**).

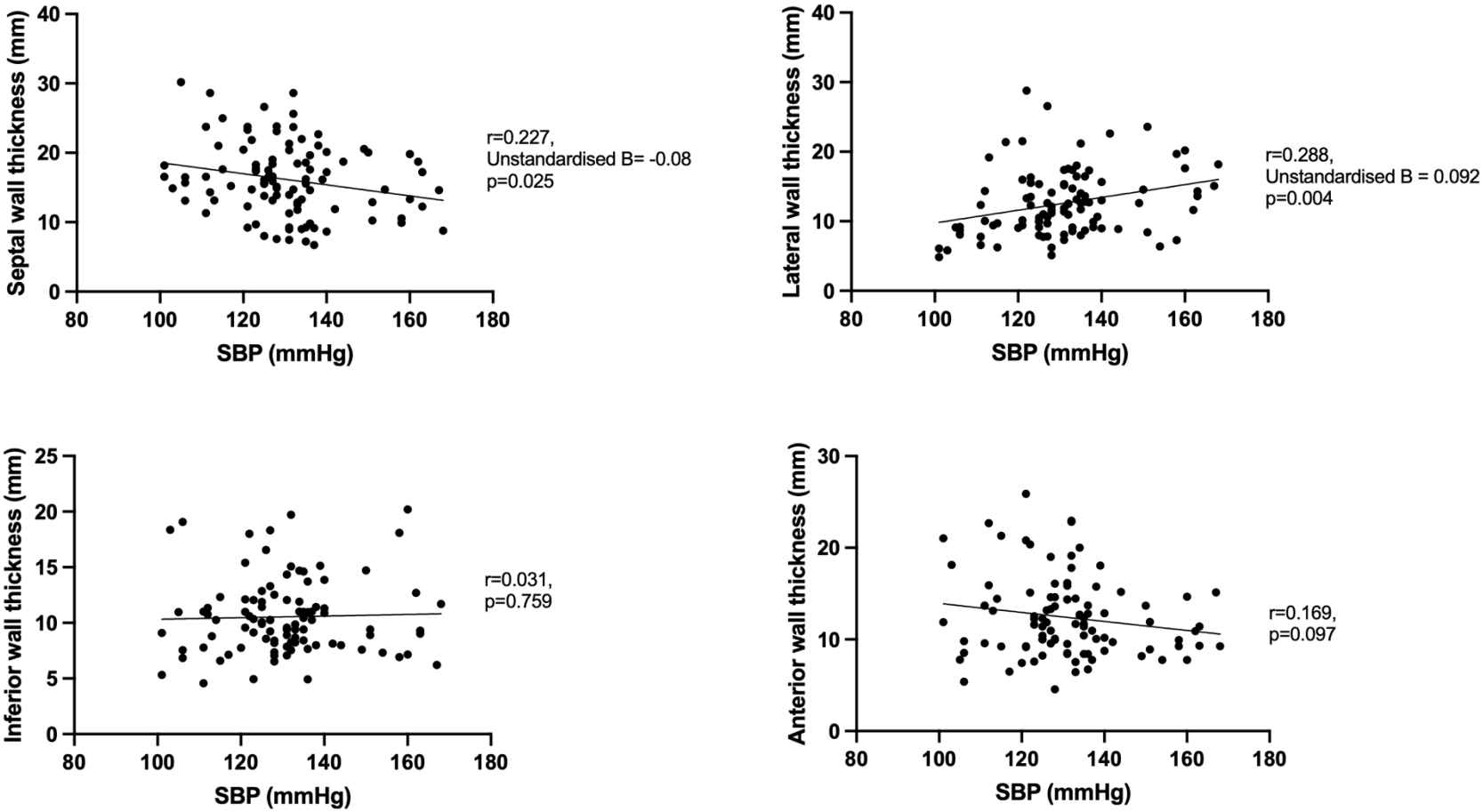

Figure 34: Linear regression analysis between SBP and myocardial wall thicknesses. The correlation (r), *p*-value and the regression coefficient or unstandardised B-, where the *p* value was <0.05, of each linear regression is included on the graph. *Abbreviations: SBP, systolic blood pressure.*

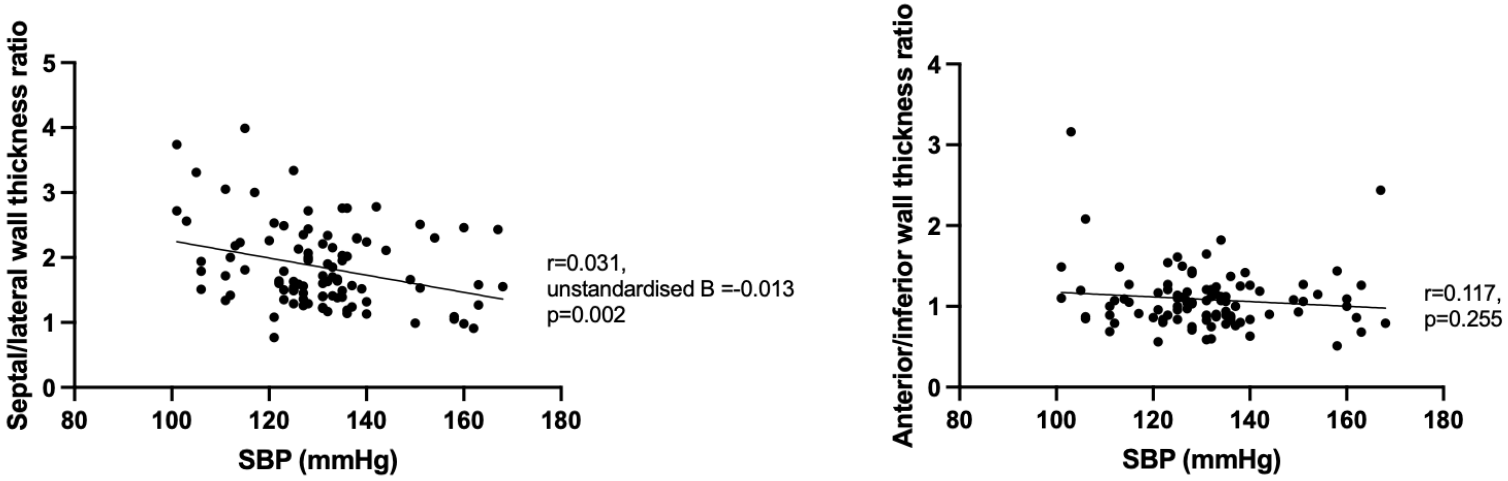

Figure 35: Linear regression analysis between SBP and myocardial wall thickness. The correlation (r), *p*-value and the regression coefficient or unstandardised B-, where the *p* value was <0.05, of each linear regression is included on the graph. *Abbreviations: SBP, systolic blood pressure.*

3.4.3.2 THE RELATIONSHIP BETWEEN DBP AND MYOCARDIAL WALL THICKNESS AND LV GEOMETRY

Linear regression analysis did not demonstrate a significant relationship between DBP and the thickness of the septal, anterior or inferior walls (see **Figure 36**). However, a significant association was found between DBP, lateral wall thickness, septal/lateral wall thickness ratio, and anterior/wall thickness ratio: for every 10 mmHg increase in DBP, there was a 0.9 mm increase in lateral wall thickness, a 0.2 decrease in septal/lateral wall thickness ratio, and a 0.1 decrease in anterior/inferior wall thickness ratio (see **Figures 36-37**).

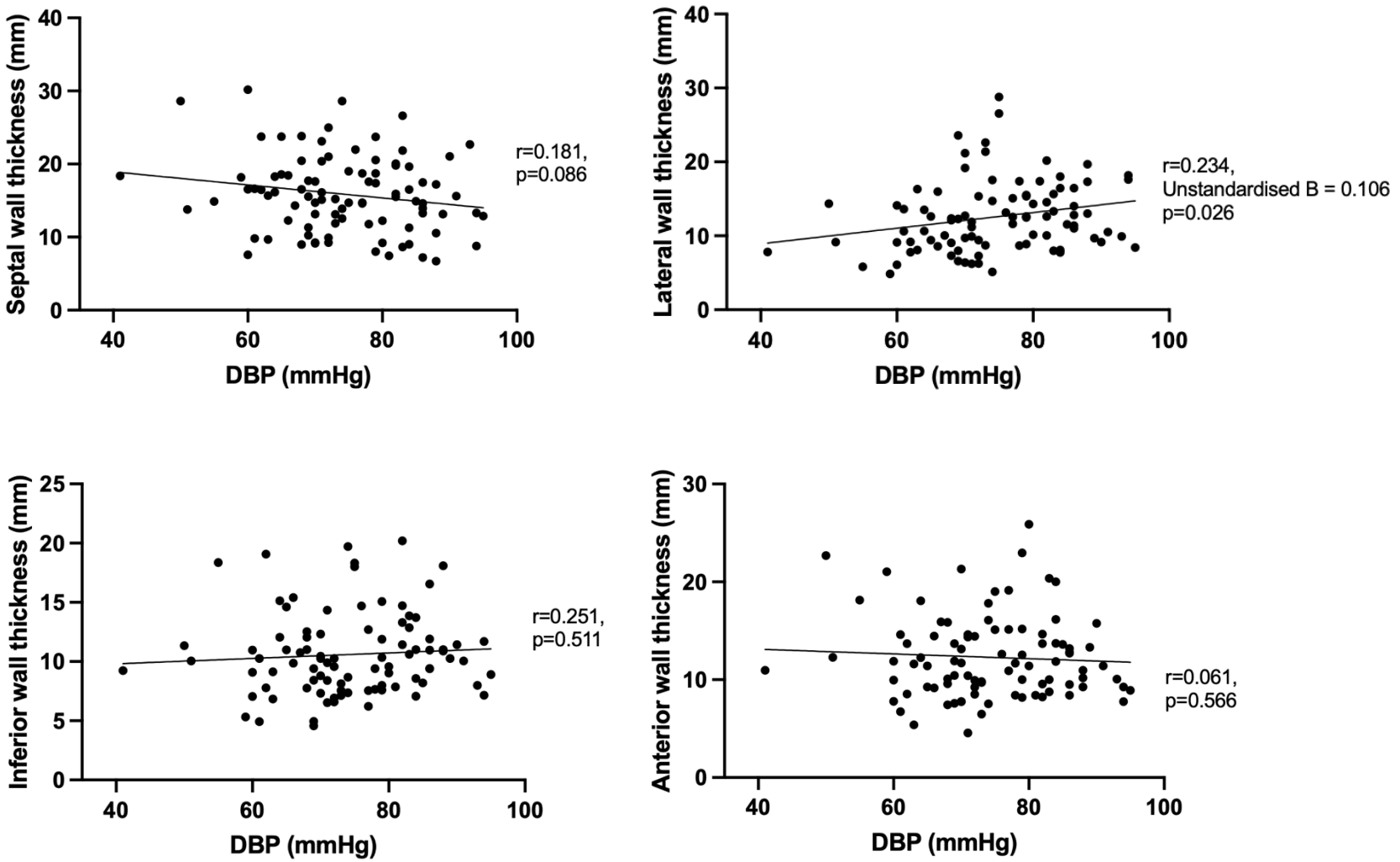

Figure 36: Linear regression analysis between DBP and myocardial wall thickness. The correlation (r), *p*-value and the regression coefficient or unstandardised B-, where the *p* value was <0.05, of each linear regression is included on the graph. *Abbreviations: DBP, diastolic blood pressure.*

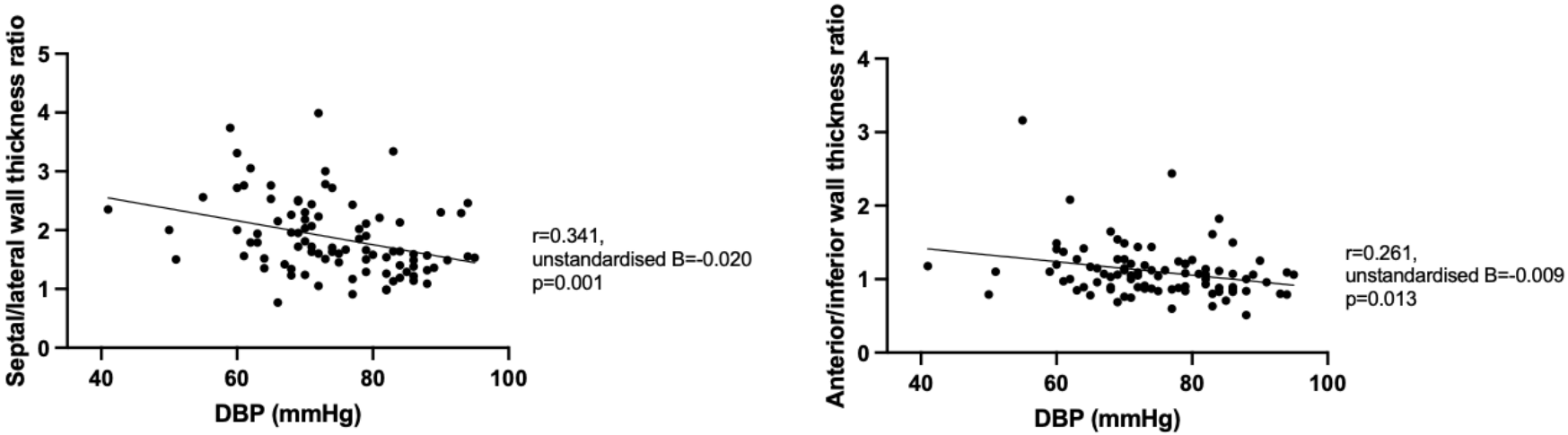

Figure 37: Linear regression analysis between DBP and LV geometry. The correlation (r), *p*-value and the regression coefficient or unstandardised B-, where the *p* value was <0.05, of each linear regression is included on the graph. *Abbreviations: DBP, diastolic blood pressure.*

3.4.3.3 THE RELATIONSHIP BETWEEN BMI, MYOCARDIAL WALL THICKNESS AND LV GEOMETRY

In the linear regression analysis, no significant associations were found between BMI and myocardial wall thickness or the anterior/inferior thickness ratio (see **Figure 38** and **39**). However, linear regression analysis between BMI and the septal/lateral wall thickness ratio demonstrated a significant relationship, suggesting that for every kg/m² increase in BMI, there is a 0.027 decrease in the septal/lateral wall thickness ratio, making the LV more concentric (see **Figure 39**).

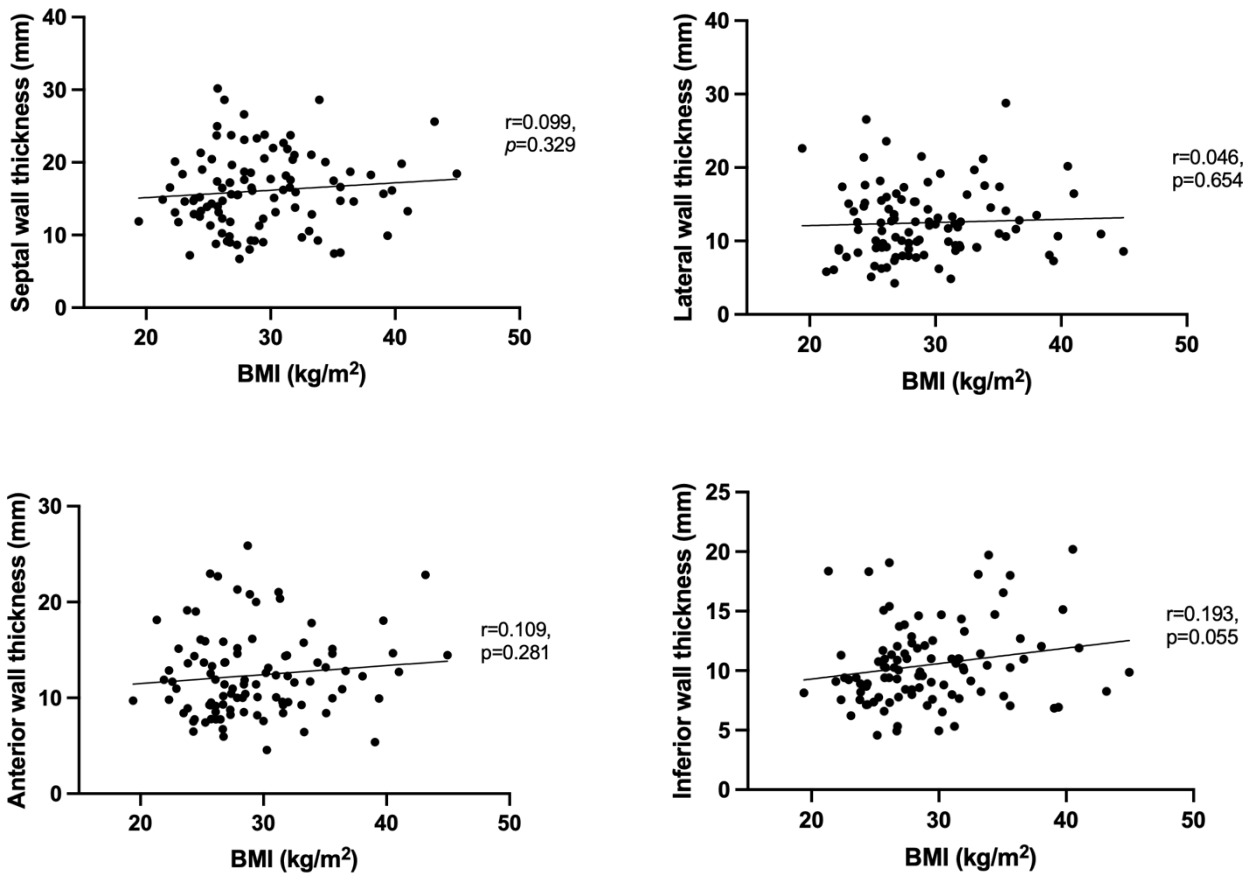

Figure 38: Linear regression analysis between BMI and myocardial wall thickness. The correlation (r), *p*-value and the regression coefficient or unstandardised B-, where the *p* value was <0.05, of each linear regression is included on the graph. *Abbreviations: BMI, body mass index.*

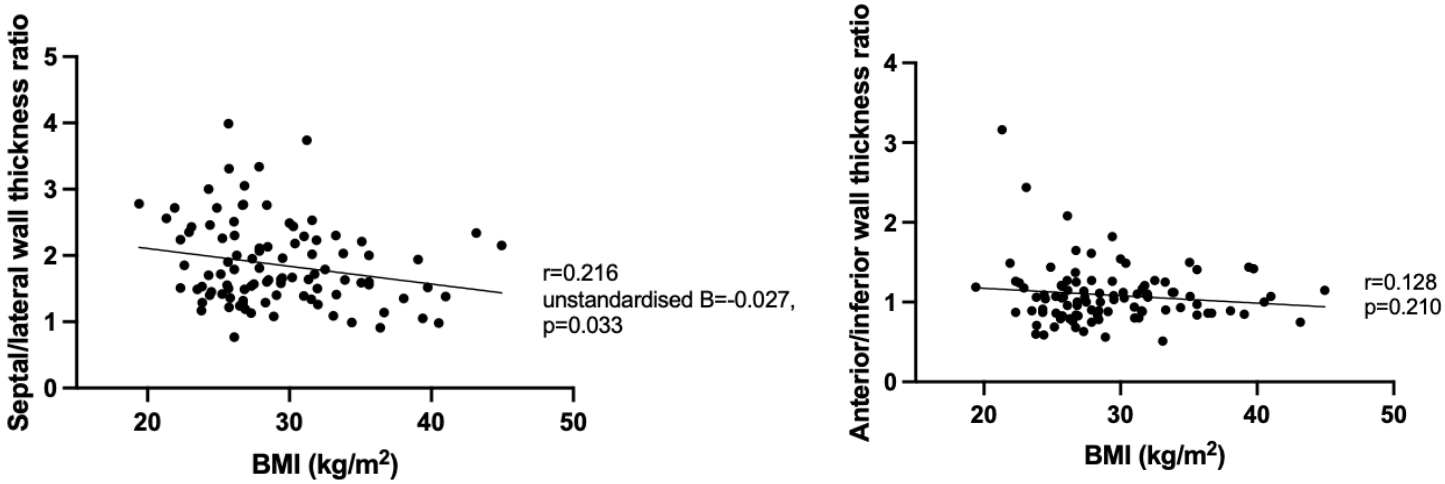

Figure 39: Linear regression analysis between BMI and LV geometry. The correlation (r), *p*-value and the regression coefficient or unstandardised B-, where the *p* value was <0.05, of each linear regression is included on the graph. *Abbreviations: BMI, body mass index.*

3.4.4 THE RELATIONSHIP BETWEEN SBP, DBP AND BMI IN OUR HCM COHORT

To investigate whether BMI and SBP have synergistic effects in combination, I performed interaction statistics using regression models. Wall thickness parameters served as the dependent variable, and SBP, BMI, DBP and their interaction terms as the independent variables.

There was no statistically significant interaction between BMI and SBP for septal wall thickness (p=0.479), anterior wall thickness (p=0.486), lateral wall thickness (p=0.252), and maximal wall thickness (p=0.743), or the anterior/inferior wall thickness ratio (p=0.296). However, a statistically significant interaction between BMI and SBP was found for inferior wall thickness (B=0.05, p=0.007) and septal/lateral wall thickness ratio (B=-0.04, p=0.002).

Similarly, there was no statistically significant interaction between BMI and DBP for septal wall thickness (p=0.133), lateral wall thickness (p=0.807), anterior wall thickness (p=0.403) or maximal wall thickness (LVMWT) (p=0.630). However, a statistically significant interaction between BMI and DBP was observed for inferior wall thickness (B=0.04, p=0.006), septal/lateral wall thickness ratio (p<0.001), and anterior/inferior wall thickness ratio (B=0.02, p=0.024).

3.4.5 THE DIFFERENCE BETWEEN GENE- VS GENE+ HCM CASES IN OUR COHORT

Table 6 and **Figure 40** summarise the differences between participants with a gene-positive (gene+) HCM patients and gene-negative (gene-) HCM patients. Compared to the gene+ group, gene-HCM patients were older, more likely to be male, and had a higher BMI, along with a greater burden of hypertension, diabetes mellitus, and atrial fibrillation. Their inferior wall thickness and DBP were also significantly higher than those of gene-positive HCM patients. Conversely, gene- HCM patients had a significantly lower MWT, septal/lateral wall thickness ratio, and anterior/inferior wall thickness ratio, indicating a more concentric LV. While gene- HCM patients had numerically higher SBP and LVMI, these differences did not reach statistical significance.

There were no significant differences between the two groups regarding other CMR parameters, resting myocardial energetics, troponin levels, or ventricular arrhythmia burden on ambulatory ECG monitoring. Both groups also had a similar, low-risk ESC SCD risk classification.

Table 6: Differences between Gene- vs gene+ HCM patient subgroups.

	Gene- (n=56)	Gene+ (n=51)	P value
Age (years)	61 [11]	51 [17]	<0.001
Sex			
Male, n (%)	48 (86)	36 (71)	0.047
Female, n (%)	8 (14)	15 (29)	
BMI (kg/m^2)	28 [6]	27 [6]	0.030
Hypertension, n (%)	26 (4)	6 (12)	<0.001
Diabetes Mellitus, n (%)	7 (13)	0 (0)	0.009
Obesity, n (%)	24 (43)	17 (33)	0.208
Atrial Fibrillation, n (%)	6 (12)	0 (0)	0.022
Obstruction, n (%)	6 (11)	6 (12)	0.552
NYHA class I, n (%)	49 (88)	47 (92)	0.725
Systolic blood pressure (mmHg)	130 ± 13	122 ± 11	0.065
Diastolic blood pressure (mmHg)	81 [18]	70 [7]	0.005
Troponin (ng/L)	6 [15]	8 [26]	0.572
Rest PCr/ATP	1.7 ± 0.4	1.8 (0.5)	0.342
Maximum LV wall thickness (mm)	18 [4]	20 [7]	0.045
Septal/lateral wall thickness ratio	1.5 [0.7]	2.1 ± 0.7	<0.001
Anterior/inferior wall thickness ratio	1 [0.4]	1.1 [0.4]	0.004
Septal wall thickness (mm)	16 ± 7	16 ± 6	0.793
Lateral wall thickness (mm)	13 ± 4	10 [7]	0.136
Anterior wall thickness (mm)	11 [4]	12 [7]	0.909
Inferior wall thickness (mm)	11 [4]	9 [3]	0.009
LV Mass index (g/m^2)	77 ± 16	62 ± 12	0.062
LVEDVI (ml/m^2)	84 ± 11	80 ± 12	0.971
LVESV (ml)	54 ± 15	51 ± 15	0.983
LV EF (%)	68 ± 5	67 ± 7	0.168
Global longitudinal strain (%)	-16 ± 3	-15 ± 3	0.199
Late gadolinium enhancement (g)	6 (14)	8 (18)	0.147
Ventricular arrhythmia, n (%)	10 (20)	15 (37)	0.071
ESC SCD Risk (%)	2 [0.2]	2.3 [0.3]	0.698

Abbreviations: BMI=body mass index, DBP=diastolic blood pressure, ESC= European Society of Cardiology, GLS=global longitudinal strain, hs-cTn=high sensitivity cardiac troponin, LGE=late gadolinium enhancement, LV=left ventricle, LVEDVI=left ventricular end-diastolic volume index, LVESV=left ventricular systolic volume, LVEF=left ventricular ejection fraction, LVMI=left ventricular mass index, MWT = maximal wall thickness, NYHA=New York heart association, PCr/ATP=phosphocreatine/adenosine triphosphate, SBP=systolic blood pressure, SCD= sudden cardiac death risk. Data presented as mean ±SD or median [IQR].

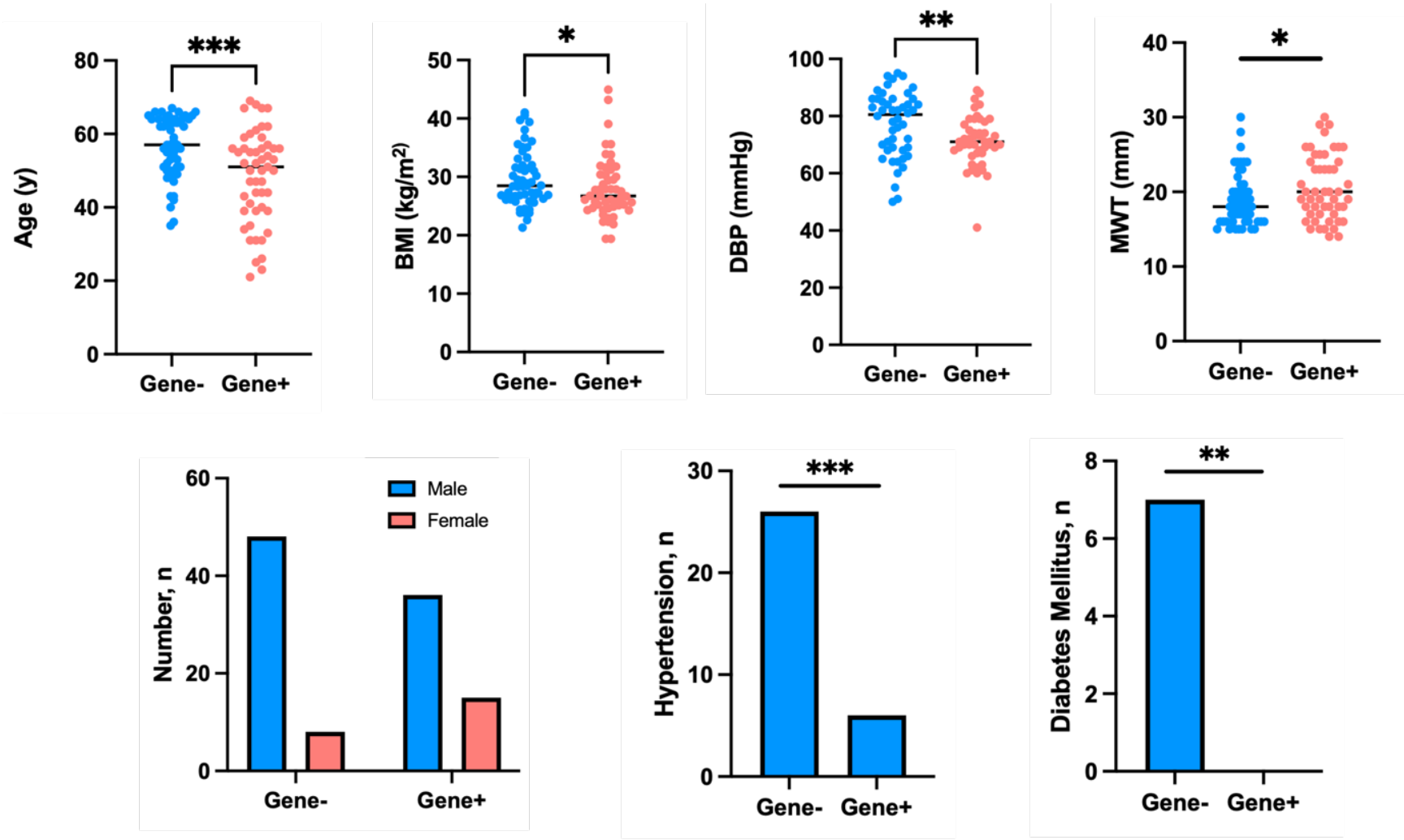

Figure 40: Significant findings in genetic subgroup analysis of our cohort. ** = p<0.05, ** = p<0.01, *** = p<0.001. Abbreviations: BMI, body mass index; DBP, diastolic blood pressure; MWT, maximal wall thickness.*

3.4.6 HCM GENETIC SUBGROUP LINEAR REGRESSION ANALYSIS BETWEEN SBP, DBP, BMI AND THE PARAMETERS IN OUR STUDY

I then performed a linear regression analysis between the various parameters in my study, including myocardial wall thickness, function and fibrosis, and SBP, DBP and BMI for the genotype positive and negative subgroups respectively.

3.4.6.1 HCM GENETIC SUBGROUP LINEAR REGRESSION FOR SBP

In the gene- HCM subgroup, the only statistically significant associations with an increasing SBP were a decreasing septal wall thickness, anterior wall thickness and LVESV and an increasing LVEF (**Figures 41** and **43**). In the gene+ HCM subgroup, an increasing SBP was associated with an increased lateral wall thickness (**Figures 41, 42** and **43**).

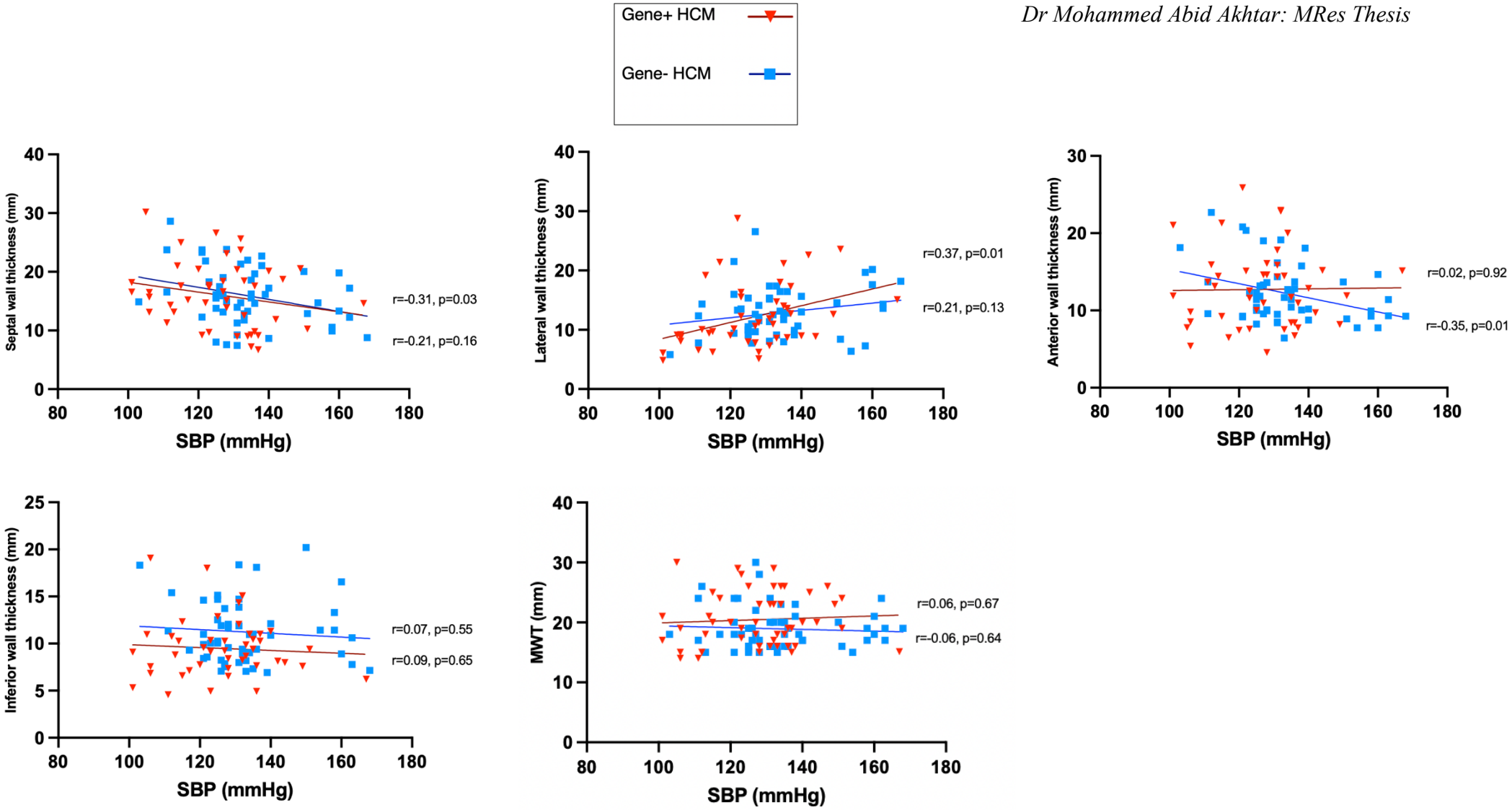

Figure 41: Linear regression analysis between SBP and myocardial wall thickness in the gene+ and gene- HCM subgroups with the correlation (r) and statistical significance (p) values included. *Abbreviations: MWT, maximal wall thickness; SBP, systolic blood pressure*.

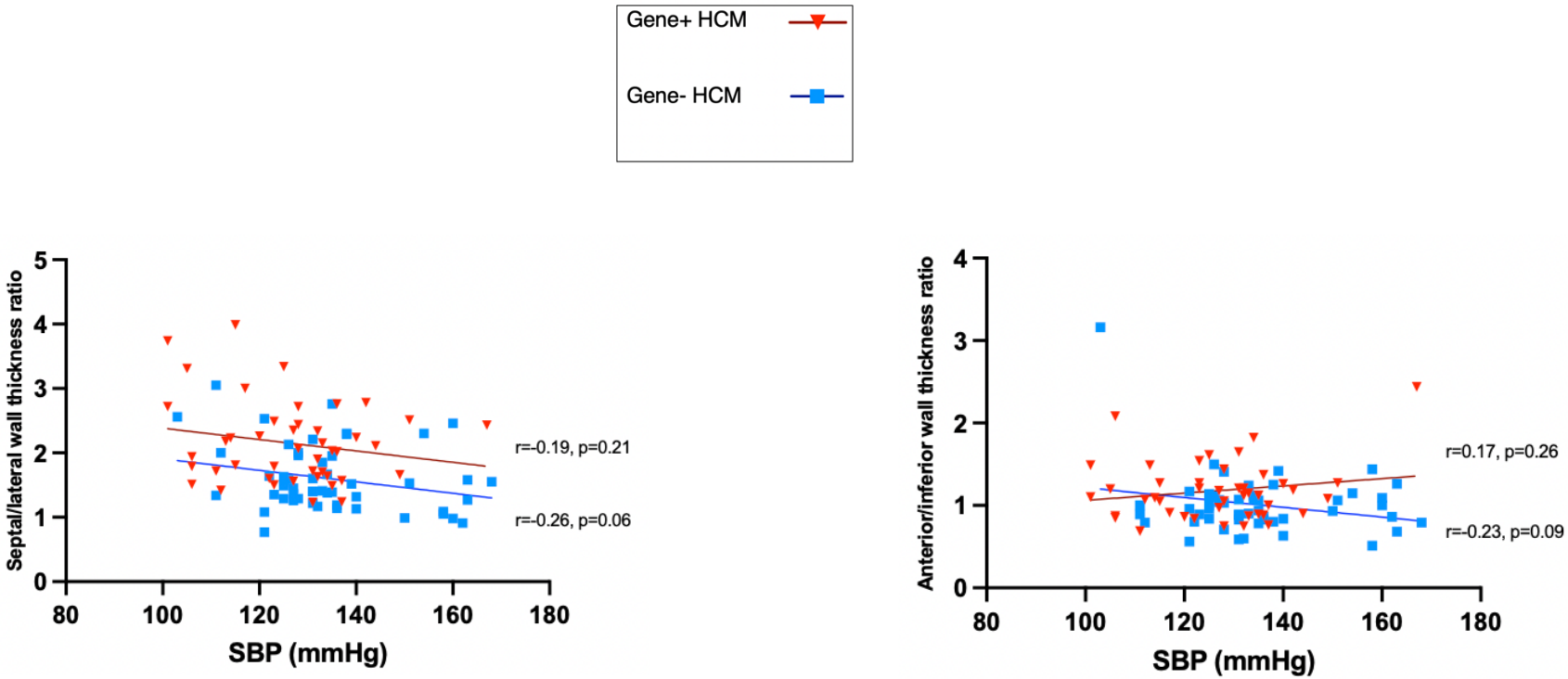

Figure 42: Linear regression analysis between SBP and LV geometry in the gene+ and gene- HCM subgroups with the correlation (r) and statistical significance (p) values included. *Abbreviations: SBP, systolic blood pressure.* represents the gene+ HCM subgroup and represents the gene- HCM subgroup.

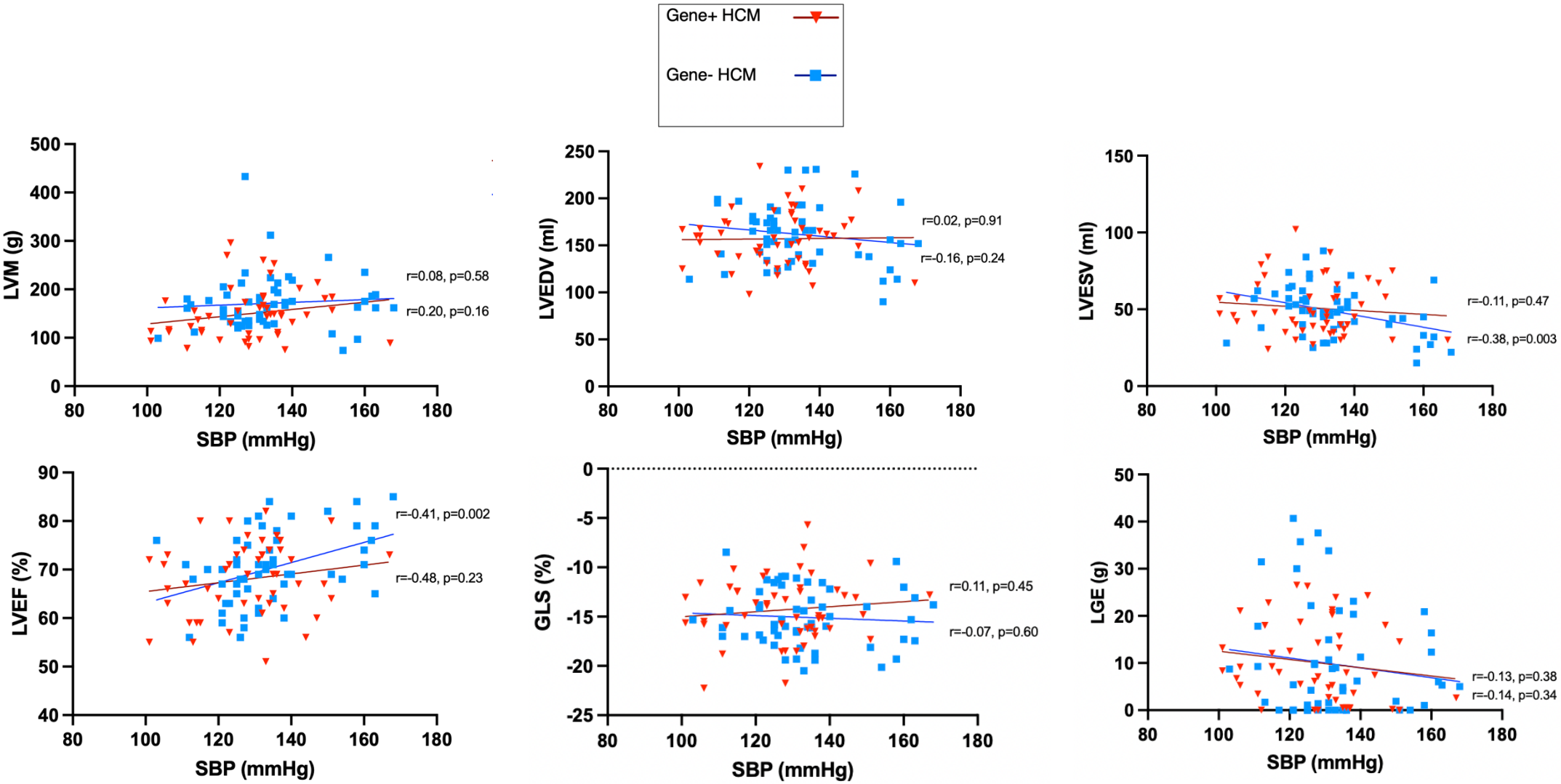

Figure 43: Linear regression analysis between SBP and LV mass, volumes, function and fibrosis in the gene+ and gene- HCM subgroups with the correlation (r) and statistical significance (p) values included. *Abbreviations: GLS, global longitudinal strain; LGE, late gadolinium enhancement; LVEDV, left ventricular end diastolic volume; LVEF, left ventricular ejection fraction; LVESV, left ventricular end systolic volume; LVM, left ventricular mass; SBP, systolic blood pressure.*

3.4.6.2 HCM GENETIC SUBGROUP LINEAR REGRESSION FOR DBP

In the gene- HCM subgroup, the only statistically significant associations with an increasing DBP were a decreasing anterior/inferior wall thickness ratio and an increasing LVM (**Figures 44** and **45**). In the gene+ HCM subgroup, there were no statistically significant associations with an increasing DBP (**Figures 44, 45** and **46**).

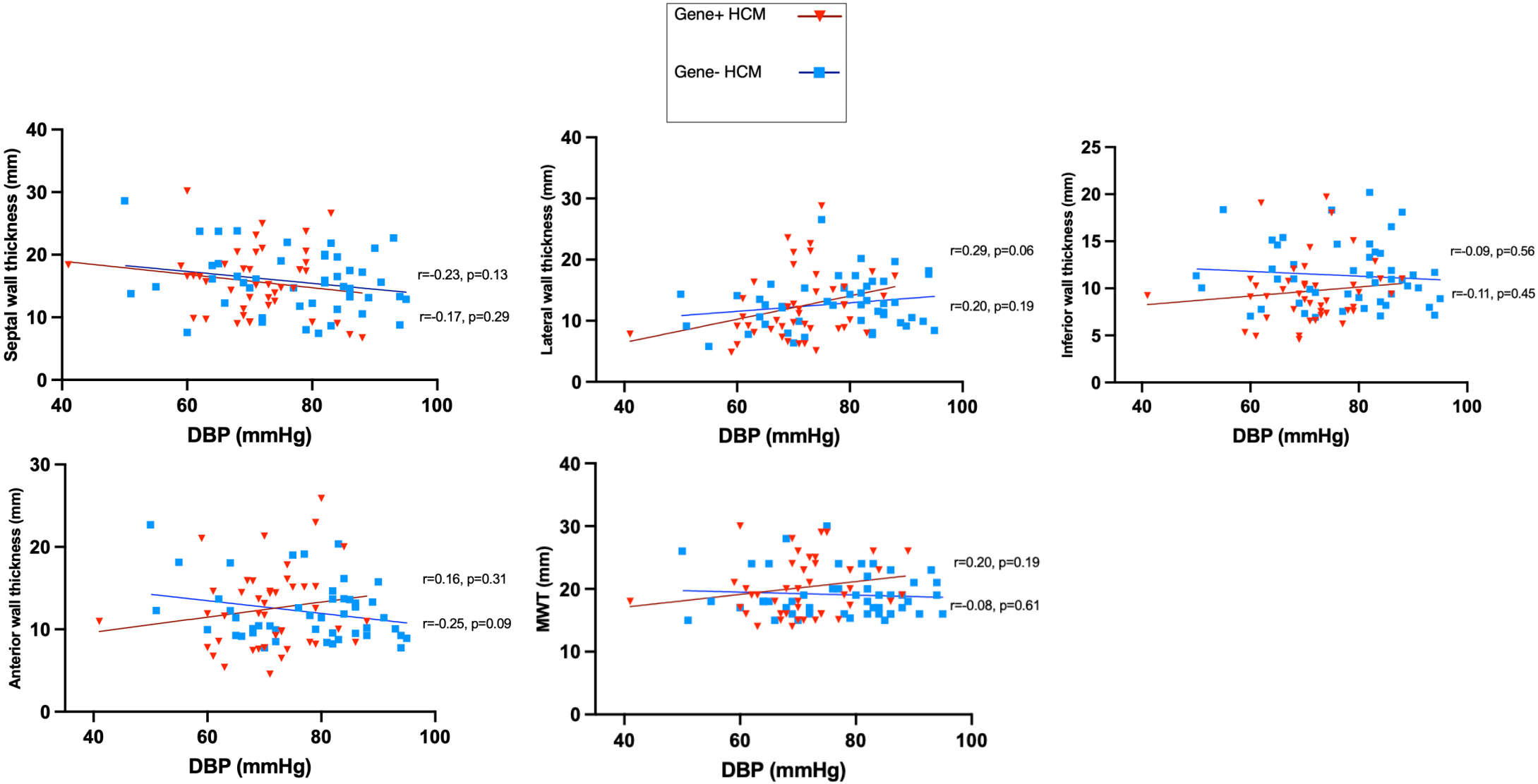

Figure 44: Linear regression analysis between DBP and myocardial wall thickness in the gene+ and gene- HCM subgroups with the correlation (r) and statistical significance (p) values included. *Abbreviations: DBP, diastolic blood pressure; MWT, maximal wall thickness.*

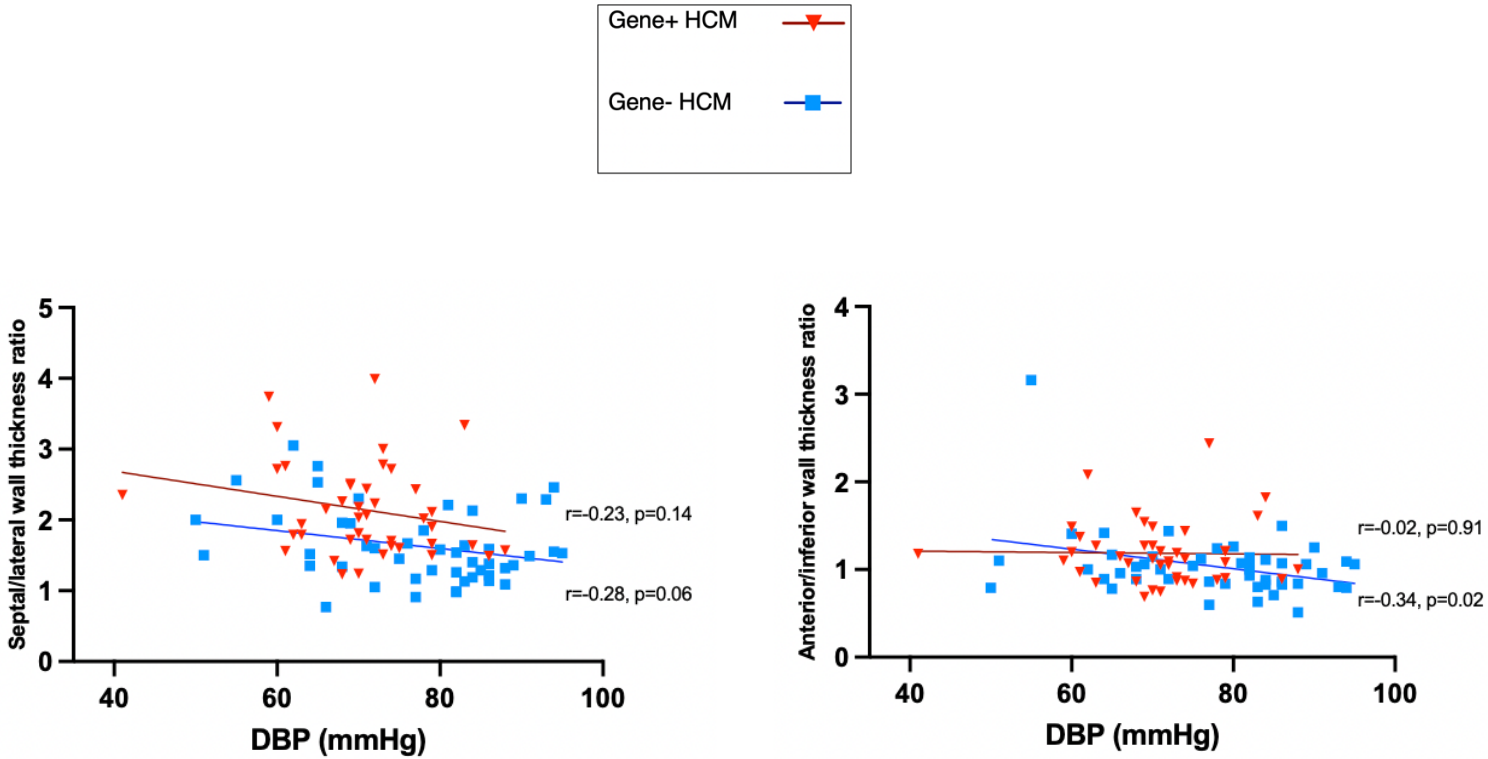

Figure 45: Linear regression analysis between DBP and LV geometry in the gene+ and gene- HCM subgroups with the correlation (r) and statistical significance (p) values included. *Abbreviations: DBP, diastolic blood pressure.*

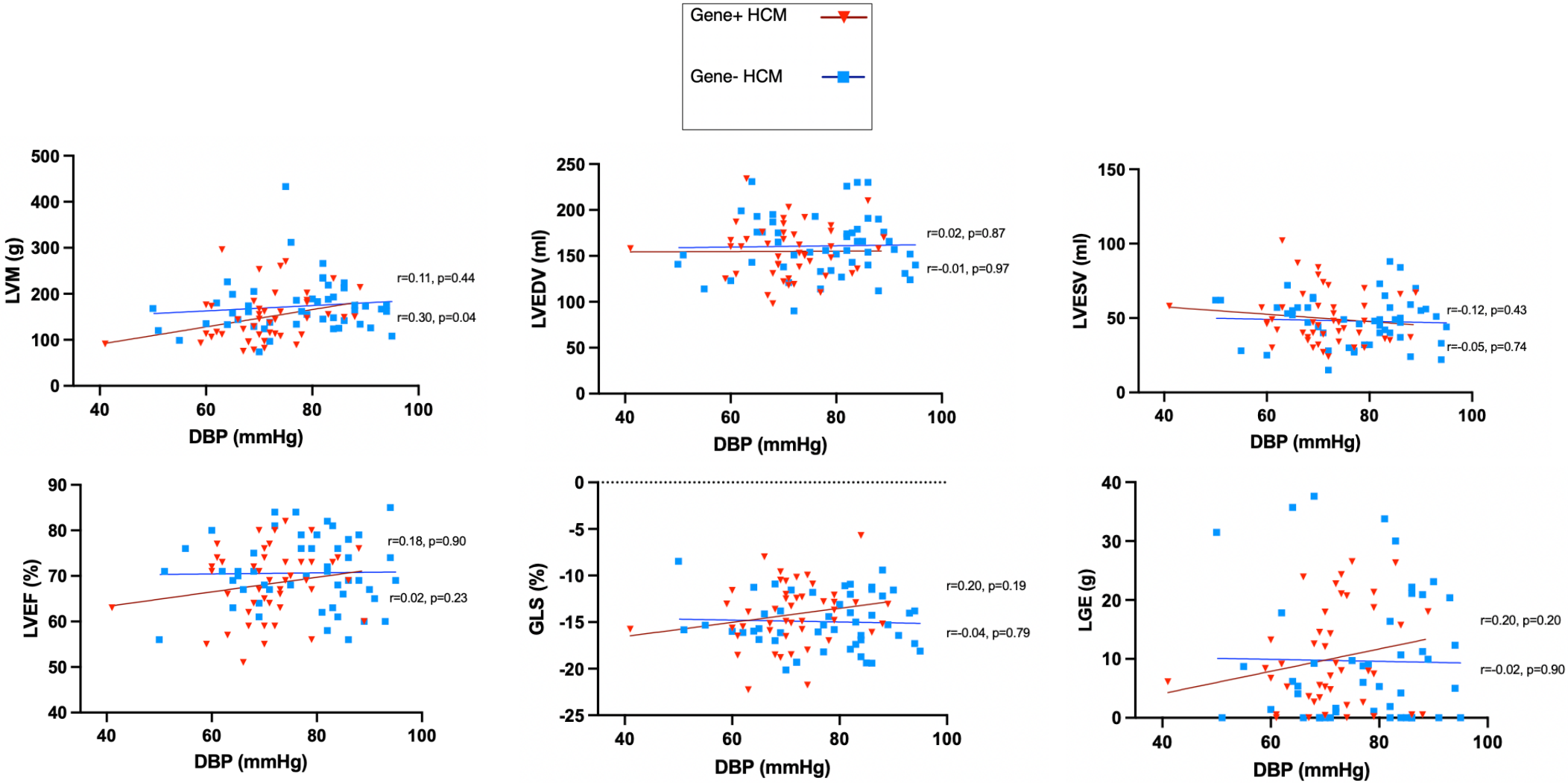

Figure 46: Linear regression analysis between DBP and LV mass, volumes, function, strain and fibrosis in the gene+ and gene- HCM subgroups with the correlation (r) and statistical significance (p) values included. *Abbreviations: DBP, diastolic blood pressure; GLS, global longitudinal strain; LGE, late gadolinium enhancement; LVEDV, left ventricular end diastolic volume; LVEF, left ventricular ejection fraction; LVESV, left ventricular end systolic volume; LVM, left ventricular mass.*

3.4.6.3 HCM GENETIC SUBGROUP LINEAR REGRESSION FOR BMI

In the gene- HCM group, there was no statistically significant trends (**Figures 47, 48** and **49**). In the gene+ HCM group, as BMI increases, there is a significant increase in LVESV and a significant decrease in LVEF (**Figures 47** and **49)**.

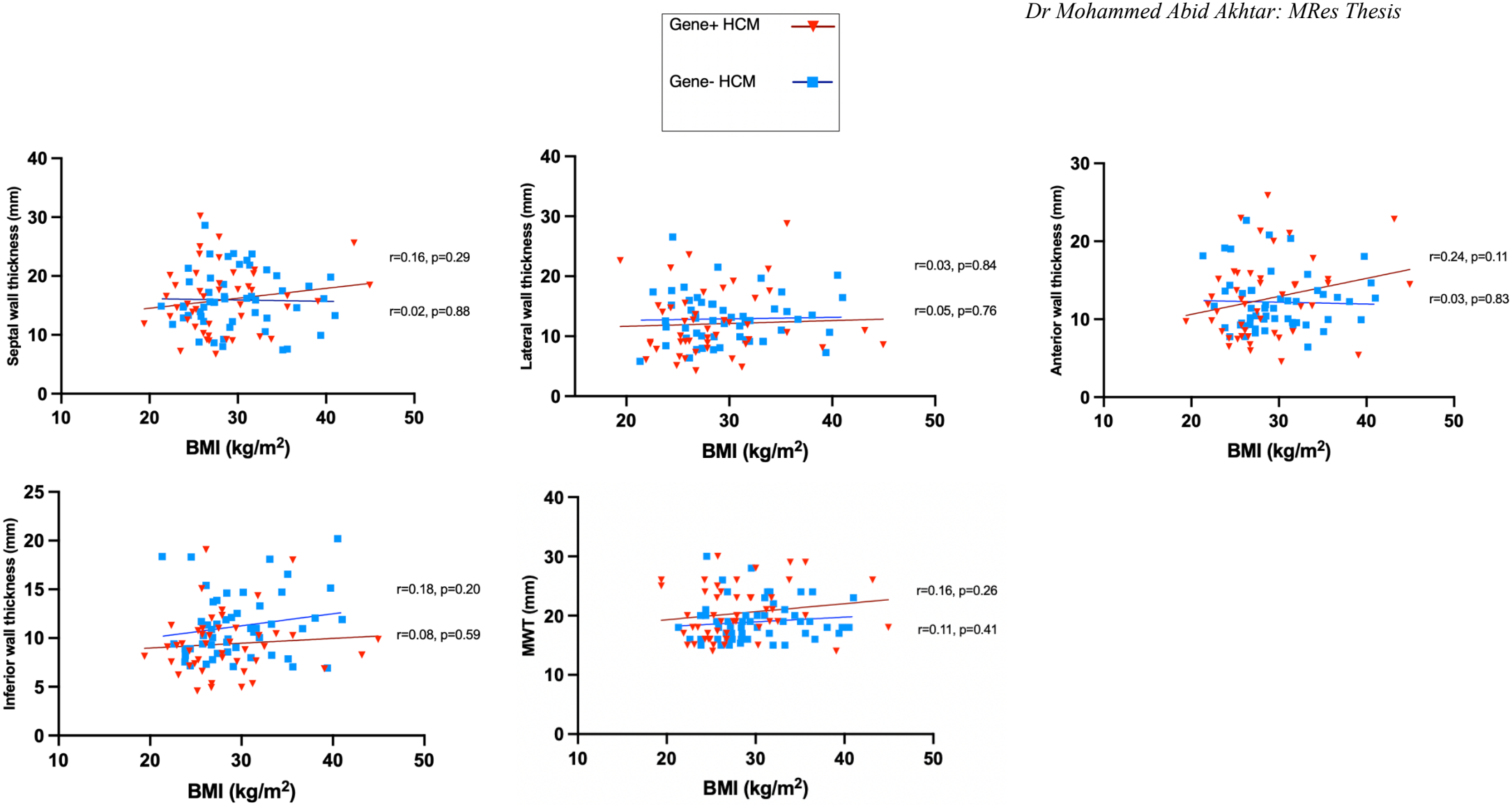

Figure 47: Linear regression analysis between BMI and myocardial wall thickness in the gene+ and gene- HCM subgroups with the correlation (r) and statistical significance (p) values included. *Abbreviations: BMI, body mass index; MWT, maximal wall thickness.*

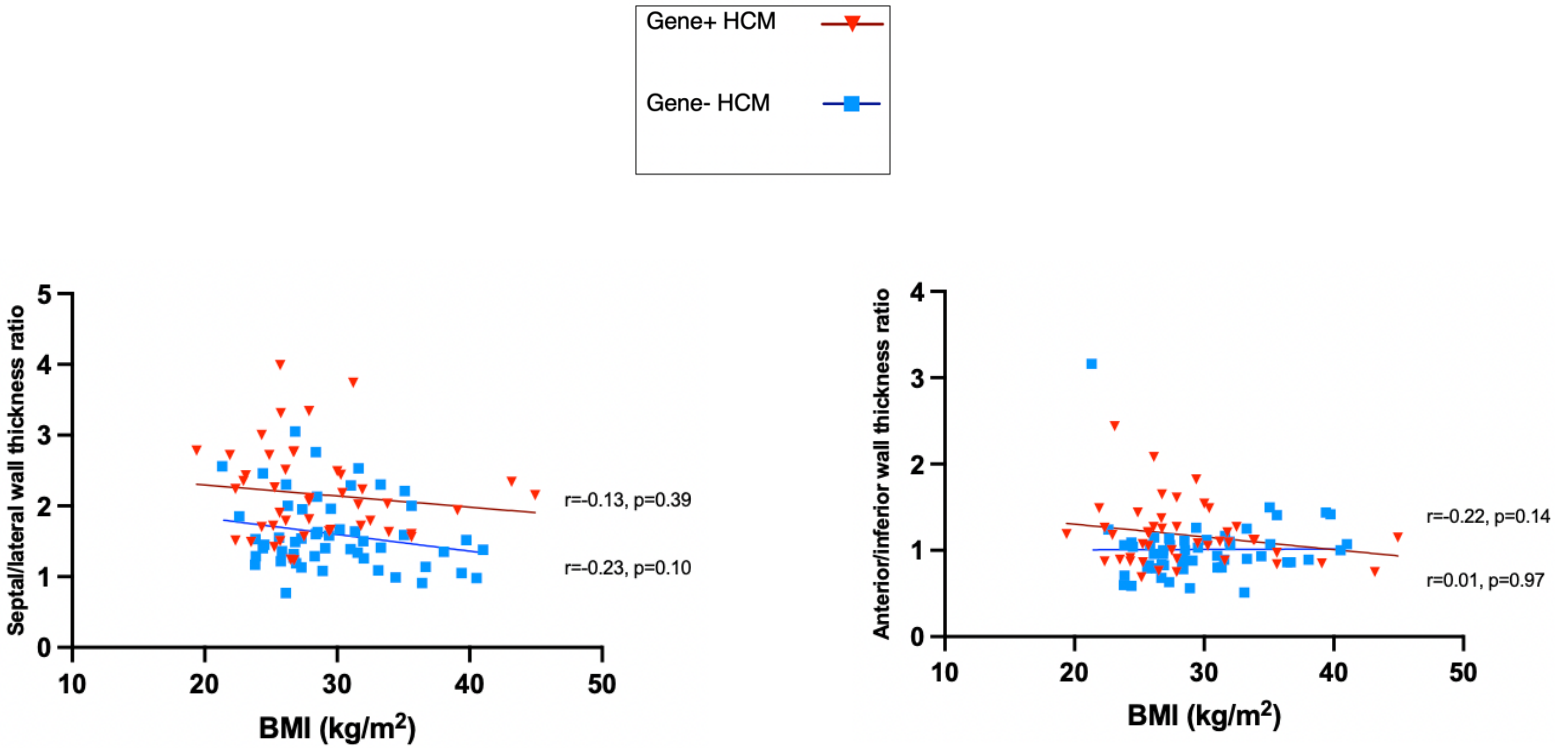

Figure 48: Linear regression analysis between BMI and LV geometry in the gene+ and gene- HCM subgroups with the correlation (r) and statistical significance (p) values included. *Abbreviations: BMI, body mass index.*

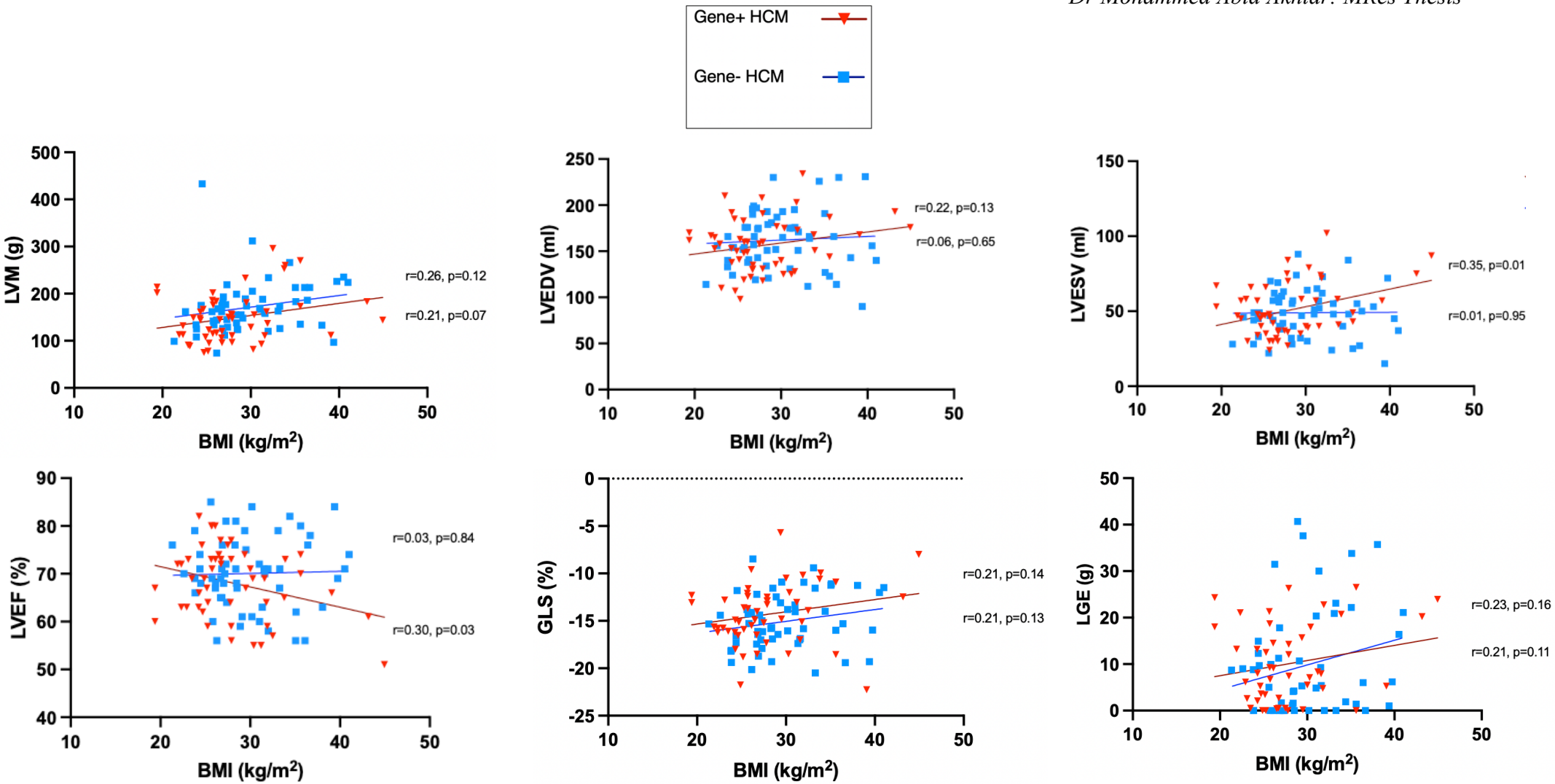

Figure 49: Linear regression analysis between BMI and LV geometry in the gene+ and gene- HCM subgroups with the correlation (r) and statistical significance (p) values included. *Abbreviations: BMI, body mass index; GLS, global longitudinal strain; LGE, late gadolinium enhancement; LVEDV, left ventricular end diastolic volume; LVEF, left ventricular ejection fraction; LVESV, left ventricular end systolic volume; LVM, left ventricular mass;*

3.4.7 SEPTAL/LATERAL WALL THICKNESS RATIO DISCRIMINATES BETWEEN GENE+ AND GENE- HCM

To explore the potential for differentiating between gene+ and gene- HCM patients using LV geometry, I conducted a Receiver Operating Characteristic (ROC) analysis to determine an optimal cutoff point for the septal/lateral wall thickness ratio that maximizes the ability to discriminate between the two groups (see **Figure 50**).

At a septal/lateral wall thickness ratio of 1.124, the sensitivity was 0.957, with a 1-specificity of 0.788, resulting in a Youden's index of 0.168. This suggests a low discriminating capability at this cutoff. However, at a higher septal/lateral wall thickness ratio of 1.56, while sensitivity dropped to 0.848, 1-specificity improved to 0.404, yielding a higher Youden's index of 0.44, along with a Gini index of 0.511 and a C-statistic of 0.66. These values suggest moderate discriminatory ability at a septal/lateral wall thickness ratio of 1.56 to identify gene+ HCM patients from gene- HCM patients.

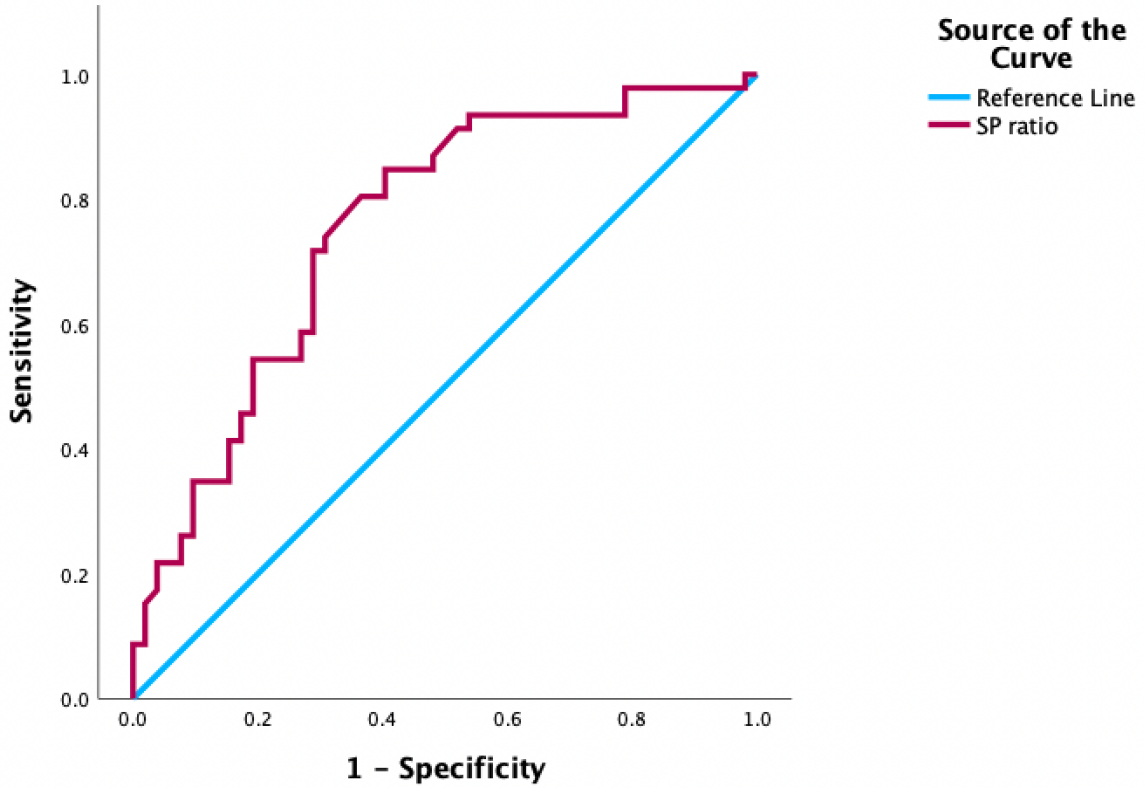

Figure 50: Receiver Operator Characteristic (ROC) analysis to differentiate gene+ HCM from gene- HCM using septal/lateral wall thickness ratio. *Abbreviations: SP ratio, septal/posterior or lateral wall thickness ratio.*

3.5 DISCUSSION

3.5.1 THE EFFECT OF SYSTOLIC BLOOD PRESSURE (SBP) AND DIASTOLIC BLOOD PRESSURE (DBP) AS MODIFIERS IN HCM

3.5.1.1 THE HCM COHORT AS A WHOLE'S RESPONSE TO INCREASING SBP AND DBP

Across the entire HCM cohort, increasing SBP and DBP was associated with a more concentric LV. In addition, an increasing SBP was associated with an increasing LV mass and systolic function, and an increasing DBP was associated with increased wall thickness.

While concentric LVH is classically linked to hypertension, its role in HCM is less studied. Our finding of obesity-associated concentric LV remodelling in HCM conflicts with prior reports (122, 123). Our finding highlights that not at all HCM patients have the typical asymmetric LVH morphology and provides a potential reason as to why this is the case (113). In addition, we report, for the first time, an association between increased DBP and increased inferior wall thickness – prior work focusing only on septal and/or anterior hypertrophy.

3.5.1.2 GENE+ AND GENE- HCM RESPONSES TO INCREASING SBP AND DBP

Interestingly, associations differed by genotype. In gene negative HCM patients, increasing DBP was associated with a more concentric LV (as assessed the anterior/inferior wall thickness ratio) and an increased LVM. Increasing SBP correlated with a decreasing septal and anterior wall thickness and LVESV, as well as an increasing LVEF.

In gene positive HCM patients, an increasing SBP was associated with an increased lateral wall thickness. There were no significant associations with an increased DBP. These findings suggest hypertension's phenotype-modifying role is stronger in gene-HCM. Lateral wall thickness with an increased SBP in gene negative HCM patients has not been reported before and may reflect atypical wall stress responses in this patient population.

3.5.2 THE EFFECT OF BMI AS A MODIFIER IN HCM

3.5.2.1 THE HCM COHORT AS A WHOLE'S RESPONSE TO INCREASING BMI

Higher BMI was associated with an increased inferior wall thickness, LVM and a more concentric LV (as assessed by the septal/lateral wall thickness ratio). Unlike blood pressure, a higher BMI also correlated with an increased hs-cTnI levels and worsening GLS.

While obesity has traditionally been associated with eccentric hypertrophy, recent data supports a link to concentric LVH (124). In our study, we observed a novel pattern of regional hypertrophy – specifically, increased inferior and anterior wall thickness in gene positive patients. Additionally, we found that obese HCM patients exhibited elevated troponin levels and worse GLS, two previously unreported associations. The higher troponin levels suggest that obesity may exacerbate myocardial injury, possibly through driving systemic inflammation (125). Meanwhile, the worse GLS indicates that BMI should be considered when interpreting strain measurements in HCM patients.

3.5.2.2 GENE+ AND GENE- HCM RESPONSES TO INCREASING BMI

In gene positive HCM patients, an increasing BMI was associated with an increasing inferior wall thickness, LVESV and decreasing LVEF. No significant trends with BMI were observed in gene negative HCM participants. Our findings suggest that obesity causes similar remodelling and contractile impairments in gene+ HCM individuals as in those with non-HCM hearts (79).

3.5.3 SYNERGY BETWEEN BMI, SBP AND DBP AND THEIR IMPACT ON MYOCARDIAL WALL THICKNESS AND LV GEOMETRY

Interaction analyses between BMI and SBP or DBP were significant for inferior wall thickness and septal/lateral wall thickness ratio. In addition, a potentially significant interaction emerged between BMI and DBP for anterior/inferior wall thickness ratio. These findings suggest regional adaptations to the combined haemodynamic and metabolic stress, possibly mediated by heterogenous receptor distributions e.g. angiotensin or insulin receptors or differential wall stress responses, as seen in some animal studies (126, 127).

3.5.4 LV GEOMETRY AS A METHOD TO DISTINGUISH BETWEEN GENE+ AND GENE- HCM

Although genetic testing has become more widely available with time, access remains limited - particularly in developing countries (128). This limitation is particularly relevant for inherited conditions such as HCM, where management strategies can differ depending on the presence of a pathogenic variant; for example, the ESC SCD risk score is only validated in sarcomeric HCM (37). To address this gap, several clinical, imaging, or combined clinical-imaging tools have been developed to predict genotype

status in patients with HCM (129-131). These tools and scores have primarily relied on descriptive phenotypic features, often derived from HCM registries, such as a positive family history, reverse septal curvature LVH, the absence of LVOT obstruction, or a high burden of LGE, which collectively suggest sarcomeric rather than non-sarcomeric HCM (113) (129-131). More recently, machine learning techniques have been applied to improve genotype prediction, showing promising results, though caution is warned due to the “black box” nature of these models (132).

Our finding of a septal/lateral wall thickness ratio cut-off of 1.56 moderately discriminated genotype status (≥1.56 would be suggestive of gene+ HCM and <1.56 would be suggestive of gene- HCM), represents a novel finding in the literature. This ratio decreased with increasing SBP, DBP, and BMI, underscoring environmental influences on the gene- concentric LV phenotype. The use of this ratio as a diagnostic tool could provide clinicians with a simple yet effective method to help assess genetic status in patients with HCM, especially in settings where genetic testing is less accessible.

3.5.5 IMPLICATIONS FOR DISEASE MANAGEMENT

The findings mandate aggressive management of hypertension and obesity in HCM. In gene- HCM, blood pressure control is critical, as SBP/DBP directly drives concentric remodelling and LV mass progression. In gene+ HCM, weight management takes priority, with obesity exacerbating myocardial injury and systolic dysfunction.

The septal/lateral ratio offers a practical imaging biomarker to identify gene- HCM patients likely to benefit from BP/weight interventions, and appropriately risk stratify patients with respect to SCD.

3.5.6 IMPLICATIONS FOR THE HYPOTHESES

Our findings support our hypothesis that hypertension and obesity serve both as phenotypic modifiers and phenocopies in gene- HCM, if we are to assume hypertensive and obesity associated LVH as being primarily mild and concentric in nature, while acting primarily as modifiers in gene+ HCM. In gene- HCM patients, the blood pressure dependent concentric remodelling demonstrates how these haemodynamic stressors can reproduce genetic hypertrophy. In gene+ HCM individuals, obesity modifies the preserved septal dominance towards a heart failure phenotype with a more dilated and impaired LV. This fundamental distinction – phenocopy versus modifiers effects – provides a mechanistic framework for understanding HCM's phenotypic spectrum and underscores the need for genotype and environmental factors-informed management strategies.

3.6 CONCLUSION

This study reveals two distinct HCM pathways: (1) gene- HCM: dominated by hypertension driven concentric remodelling and (2) gene+ HCM: characterised by genetic hypertrophy and modified towards a heart failure phenotype by obesity.

The septal/lateral ratio provides a potentially clinically actionable imaging biomarker that can aid in genotype prediction where genetic testing is unavailable, monitoring

therapeutic response to BP/weight interventions and stratifying patients for targeted management.

3.7 LIMITATIONS

Several important limitations must be acknowledged in this study. First, our analysis of diabetes mellitus was limited by low prevalence (n=7) in the cohort, though previous registry data suggest minimal phenotype differences between diabetic and non-diabetic HCM patients would likely have been found (78). Second, our cohort is predominantly white and male - reflecting both the inherent male predominance in HCM and local referral patterns. Validation in more diverse populations is required before broader generalisation of our findings. Finally, while additional parameters such as LA strain, native T1, ECV and CPET data were available for the TEMPEST sub cohort, their absence in the SARC-HCM prevented comprehensive analysis – a limitation partially mitigated by the TEMPEST subgroup analysis showing no significant differences in these variables.

CHAPTER 4: INVESTIGATION COHORTS OF HYPERTENSION AND/OR OBESITY AS HCM PHENOCOPIES

4.1 ABSTRACT

Introduction: Hypertension and obesity are prevalent conditions that significantly influence left ventricular (LV) geometry and myocardial wall thickness. These factors can modify the hypertrophic cardiomyopathy (HCM) phenotype, leading to challenges in differentiating HCM from hypertensive or obesity-induced LV hypertrophy. This study investigates the effects of systolic blood pressure (SBP), diastolic blood pressure (DBP), and body mass index (BMI) on LV structure in hypertensive, obese, and HCM populations.

Methods: This retrospective analysis utilised data from three cohorts: (1) The Hypertension Spectrum Cohort - hypertensive and normotensive patients (n=425), (2) The Metabolic Spectrum Cohort - healthy individuals with varying BMI (n=849), and (3) HCM cohort - HCM patients from an international registry (n=236). Cardiac magnetic resonance imaging (CMR) was performed to measure myocardial wall thickness, LV volumes, and function. Associations between SBP, DBP, BMI, and LV geometry were assessed using multiple linear regression and stratified analysis across quartiles for each variable.

Results: In the Hypertension Spectrum Cohort, SBP was strongly associated with septal wall thickness and asymmetric LV hypertrophy, with 9% of hypertensive patients displaying an HCM-like phenotype (MWT ≥15 mm). In the Metabolic Spectrum Cohort, obesity contributed to asymmetric LV remodelling but did not mimic HCM, with a maximum MWT of 14 mm. Asymmetric remodelling (septal/lateral wall thickness ratio ≥1.5) was observed in 9% of participants. In the HCM Cohort, BMI was associated with concentric remodelling and increased lateral wall thickness in HCM

patients, while SBP and DBP showed minimal effects, suggesting a dominant role of intrinsic pathology in HCM.

Conclusion: Hypertension, primarily driven by SBP, can mimic the HCM phenotype in some hypertensive patients, while obesity influences LV geometry differently, exacerbating concentric remodelling in HCM patients but not reaching diagnostic HCM thresholds when present in isolation. These findings underscore the need for tailored diagnostic and management strategies for hypertension and obesity in both HCM and non-HCM populations.

4.2 INTRODUCTION

Hypertension and obesity are common in hypertrophic cardiomyopathy (HCM), and as I have demonstrated in **Chapter 3, appear to** significantly modify the HCM phenotype, making the left ventricle (LV) more concentric, and increasing regional wall thickness, possibly in a synergistic fashion, with these interactions likely mediated by age and genetic status.

We have yet to validate these findings in another HCM cohort, as well as explore if hypertension and/or obesity associated LVH can mimic the HCM phenotype – particularly gene negative HCM. According to a few published studies, a maximal wall thickness (MWT) of ≥17mm in hypertension and ≥14mm in obesity means that the patient's MWT primarily is due to HCM – do we observe similar MWT thresholds in our non-HCM cohorts? (67, 79)

4.3 METHODS

4.3.1 PATIENTS

This is a retrospective analysis of data from three prospective studies:

- **Hypertension spectrum cohort** (n=425): patients with a normal ("normotensive") blood pressure and those with hypertension.
- **Metabolic spectrum cohort** (n=849): patients with and without obesity.
- **Hypertrophic Cardiomyopathy Cohort** (n=236): Hypertrophic Cardiomyopathy (HCM) patients from an international HCM registry, the Hypertrophic Cardiomyopathy Registry (HCMR).

Hypertension Spectrum Cohort

This cohort consisted of a mixed group of normotensive and hypertensive participants from phase III of the Oxford Family Blood Pressure Study - Phase III (133). 248 families (1,425 participants) were recruited between 1993 and 1996 for a genetic study of hypertension and other cardiac risk factors (133, 134). Families were selected via a proband that was diagnosed with essential or primary hypertension in the hypertension clinic at the John Radcliffe Hospital in Oxford, UK (secondary hypertension was excluded in patients using established screening) (133, 134). BP was also assessed during the participant's research visit (133, 134). All participants were or white ethnicity, and each family consisted of at least three siblings that were quantitively assessable for blood pressure (133, 134). First, second- and third-degree relatives were then recruited to form a series of extended families (133, 134). DNA testing was performed during recruitment using established methods (133, 134).

Genotyping was performing using the Illumina 660W-Quad chip that included 557,124 single nucleotide polymorphisms (SNPs) (133, 134). In 1997-2000, family members were reinvented for phenotyping using ECG and echocardiogram (133, 134). In 2007-2010, surviving members of the cohort were recruited for repeat normotensive/hypertensive status classification, using up-to-date blood pressure measurements and/or available clinic data as well as the ESC guidelines for hypertension, repeat genotyping using the latest gene panels available, and for the first time, cardiac MRI phenotyping (133). Participants were excluded from all analyses if they had atrial fibrillation or a cardiac device in situ, and any evidence of myocardial infarction, significant valvular heart disease, non-hypertensive cardiomyopathy, and/or chronic pericardial disease. In addition, normotensive participants were excluded if they had any history of cardiovascular disease or diabetes mellitus (133). All participants underwent a standard cardiomyopathy protocol CMR (with an MR aortogram) on a 1.5T MR system (Siemens, Healthineers, Germany) (133).

Metabolic Spectrum Cohort

This cohort comprises data from two observational CMR studies undertaken at our centre involving patients with varying BMIs (135, 136). The first study was undertaken in 2012, with the aim of investigating gender-specific differences in obesity associated LVH using CMR (136). The exclusion criteria were <18 years old, >80 years old, a history of cardiovascular disease, hypertension, diabetes (also excluded via a blood sample on the day of the CMR), smoking, use of prescription medications or pregnancy (136). Cine CMR at 1.5T was performed in a total of 741 subjects (obesity n=181) (136). Obesity was defined as per the World Health Organisation (WHO)

classification (i.e. BMI >30 kg/m^2) (136). The second study aimed to compare healthy controls with participants with obesity and/or hypertension with respect to LV geometry and aortic distensibility (135). All participants were between the ages of 18-80 years old (135). Healthy controls, and obesity were defined similarly to the first study and hypertension was defined similarly to the Hypertension spectrum cohort (135). All MR scans also took place on a 1.5T scanner (135). A total of 301 participants were included in this study (Healthy controls n=121; obesity n=98; hypertension n=129) (135). Of these two studies, I had access to data for a total of 849 participants.

Hypertrophic Cardiomyopathy Cohort

The HCM Cohort consists of data from the HCMR registry, an international prospective observational study. Participants underwent standard clinical evaluations, CMR (on a 3T Siemens system), and blood tests for genetic and biomarker analysis (137). Longitudinal follow-up is ongoing (137). Inclusion criteria required participants to be aged 18-65 years with an established diagnosis of HCM (MWT >15mm) without cavity dilatation, uncontrolled hypertension, a history of septal reduction therapy, myocardial infarction, severe comorbidity (e.g. diabetes mellitus with end-organ damage) or contraindication to CMR (137). A total of 2755 participants were enrolled (71% male, 17% non-white, 18% with LVOTO, 36% sarcomere positive and 50% had LGE) (113). Of this cohort, I had access to limited data of 236 participants.

Ethics

All studies were approved by the local research ethics committee in Oxford, and were in accordance with the Declaration of Helsinki, with informed written consent being obtained from each participant.

Data Overview

In total, dataset includes 1510 patients, with measurements of septal wall thickness, lateral wall thickness, the septal/lateral wall thickness ratio, sex, BMI, systolic blood pressure (SBP), and diastolic blood pressure (DBP). The CMR data (septal and lateral wall thickness) were analysed by me in accordance with the methods described in **Chapter 2**.

Statistical analysis

As described in Chapters 2 and 3.

4.4 RESULTS

4.4.1 DOES HYPERTENSION INFLUENCE LVH SEVERITY AND LV GEOMETRY IN A WAY THAT RESEMBLES HCM?

4.4.1.1 BASELINE DEMOGRAPHICS IN HYPERTENSION SPECTRUM COHORT

The Hypertension Spectrum Cohort (**Table 7**) is largely middle aged (48% male) with a high burden of cardiovascular risk factors: 50% had a history of hypertension, 33% had a SBP ≥140 mmHg on their recorded BP, and 29% were obese.

The median maximal wall thickness is high-normal, with septal hypertrophy predominating. LV volumetrics and systolic function were normal, but asymmetric remodelling was prevalent.

4.4.1.2 HTN COHORT: HOW MANY PATIENTS ARE SIMILAR TO HCM

5% (n=23) of the cohort reached MWT ≥17mm, 13% (n=55) of the cohort had a MWT ≥15mm and the maximal MWT observed in the cohort was 21mm (in the septal and/or anterior walls). Of the participants with a MWT ≥15mm, 76% (n=42) had a history of hypertension and 60% (n=33) had a septal/lateral wall thickness ratio ≥1.5. Therefore, when MWT and septal/lateral wall thickness are solely relied on, 9% (n=38) of the cohort had an imaging phenotype suggestive of HCM.

Table 7: Summary of results for Hypertension Spectrum Cohort

Category	Combined cohort (n=425)
Age	55 [16]
Sex	
Male, n (%)	205 (48)
Female, n (%)	220 (52)
BMI (kg/m^2)	28 [6]
Hypertension, n (%)	214 (50)
Diabetes Mellitus, n (%)	20 (5)
Obesity, n (%)	123 (29)
SBP (mmHg)	132 [24]
DBP (mmHg)	77 [15]
MWT (mm)	12 [4]
Septal wall thickness (mm)	12 [4]
Anterior wall thickness (mm)	9 [3]
Lateral wall thickness (mm)	9 [3]
Inferior wall thickness (mm)	10 ± 2
Septal/lateral wall thickness ratio	1.4 [0.4]
LVMI (g/m2)	64 [20]
LVEDVI (ml/m2)	71 [18]
LVESV (ml)	38 [20]
LVEF (%)	71 [9]

Abbreviations: BMI=body mass index, DBP=diastolic blood pressure, MWT=Maximal LV wall thickness, LVMI=Left Ventricular Mass Index, LVEDVI=Left Ventricular End Diastolic Volume Index, LVEF=Left Ventricular Ejection Fraction, LVESV=Left Ventricular End Systolic Volume, SBP=systolic blood pressure. Data presented as mean ±SD, median [IQR] or n(%).

4.4.1.3 HYPERTENSION SPECTRUM COHORT: SBP AND WALL THICKNESS

SBP quartile analysis via the Jonckheere-Terpstra test revealed progressive increases in wall thickness and asymmetric remodelling with increasing SBP (**Table 8, Figures 51-54**). Septal hypertrophy was most sensitive to SBP (0.4mm increase per 10mmHg SBP increase; $p<0.001$), translating to 1.2mm thickening over a 30mmHg SBP range. Higher SBP also increased anterior (0.2mm/10mmHg), inferior (0.1mm/10mmHg), MWT, LVM (0.3g/10mmHg) and septal/lateral wall thickness ratio (0.03/10mmHg; all $p<0.05$).

Table 8: Hypertension Spectrum Cohort – differences across SBP quartiles in baseline demographics, wall thickness, LV geometry, volumes and function.

Category	Quartile 1	Quartile 2	Quartile 3	Quartile 4	*P* value
Age (years)	52 [22]	57 [22]	61 [21]	69 [13]	<0.001
BMI (kg/m^2)	27 [6]	27 [6]	28 [5]	28 [5]	0.024
SBP (mmHg)	114 [7]	126 [6]	139 [8]	156 [13]	<0.001
DBP (mmHg)	71 [10]	76 [12]	81 [14]	83 [18]	<0.001
Septal wall thickness (mm)	10 [4]	11 [3]	12 [3]	13 [4]	<0.001
Lateral wall thickness (mm)	9±4	9±2	9±2	9±2	0.049
Anterior wall thickness (mm)	9 [3]	9 [3]	9 [3]	9 [4]	0.026
Inferior wall thickness (mm)	9 [4]	10 [3]	10 [3]	10 [3]	0.012
MWT (mm)	11 [4]	12 [3]	13 [3]	13 [3]	<0.001
LVM (g)	119 [43]	126 [53]	127 [51]	118 [57]	0.036
Septal/lateral wall thickness ratio	1.2 [0.4]	1.3 [0.5]	1.3 [0.4]	1.4 [0.4]	0.002
Anterior/inferior wall thickness ratio	1.0 [0.3]	1.0 [0.3]	1 [0.3]	1 [0.4]	0.764
LVEDV (ml)	130 [37]	134 [45]	137 [38]	129 [48]	0.758
LVESV (ml)	41 [19]	39 [23]	39 [16]	34 [20]	0.048
LVEF (%)	70 [9]	71 [8]	71 [9]	73 [10]	0.016

Abbreviations: BMI=body mass index, DBP=diastolic blood pressure, LVGLS= left ventricular global longitudinal strain, hs-cTnI=high sensitivity cardiac troponin I, LGE=late gadolinium enhancement, LV=left ventricle, LVEDV=left ventricular end diastolic volume, LVESV=left ventricular systolic volume, LVEF=left ventricular ejection fraction, LVM=left ventricular mass, MWT = maximal wall thickness, PCr/ATP=phosphocreatine/adenosine triphosphate, SBP=systolic blood pressure. Data presented as mean ±SD, median [IQR] or n(%).

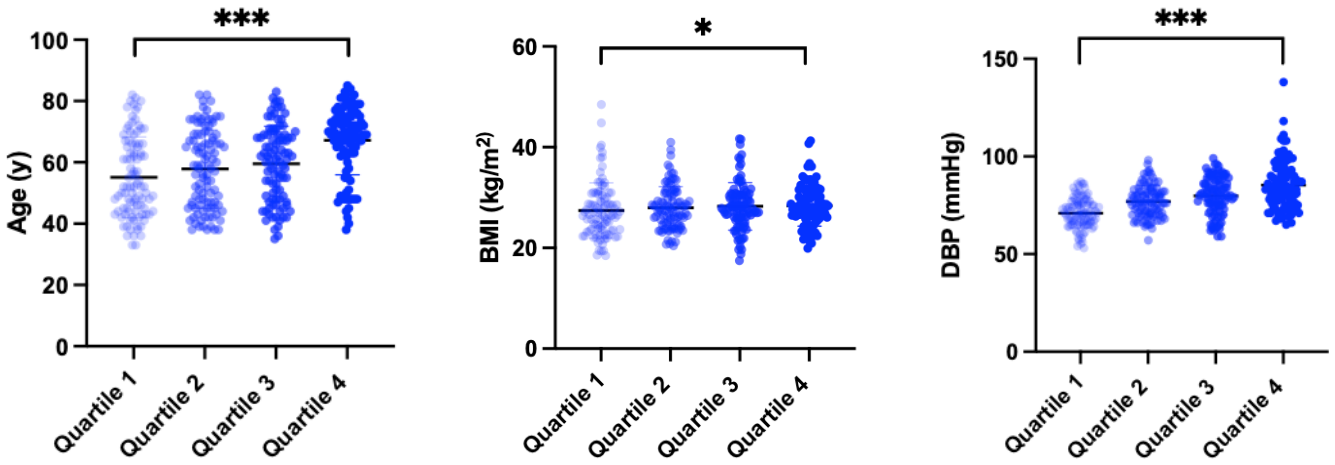

Figure 51: Differences across systolic blood pressure (SBP) quartiles in age, body mass index (BMI) and diastolic blood pressure (DBP). *Abbreviations: BMI, body mass index; DBP, diastolic blood pressure * = p<0.05, ** = p<0.01, *** = p<0.001*

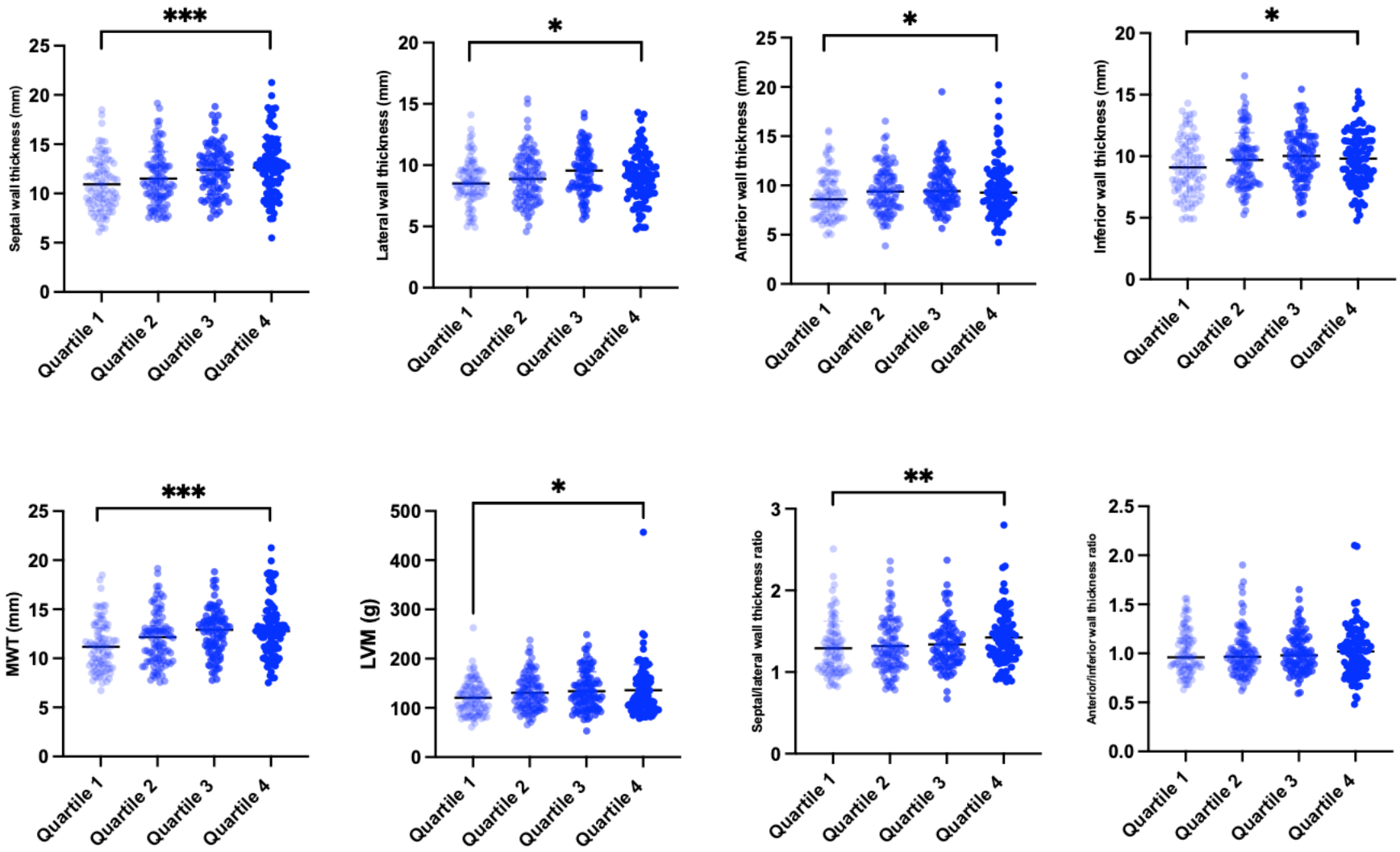

Figure 52: Differences across systolic blood pressure (SBP) quartiles in myocardial wall thicknesses, maximal wall thickness (MWT), left ventricular mass (LVM), and LV geometry. ** = p<0.05, ** = p<0.01, *** = p<0.001*

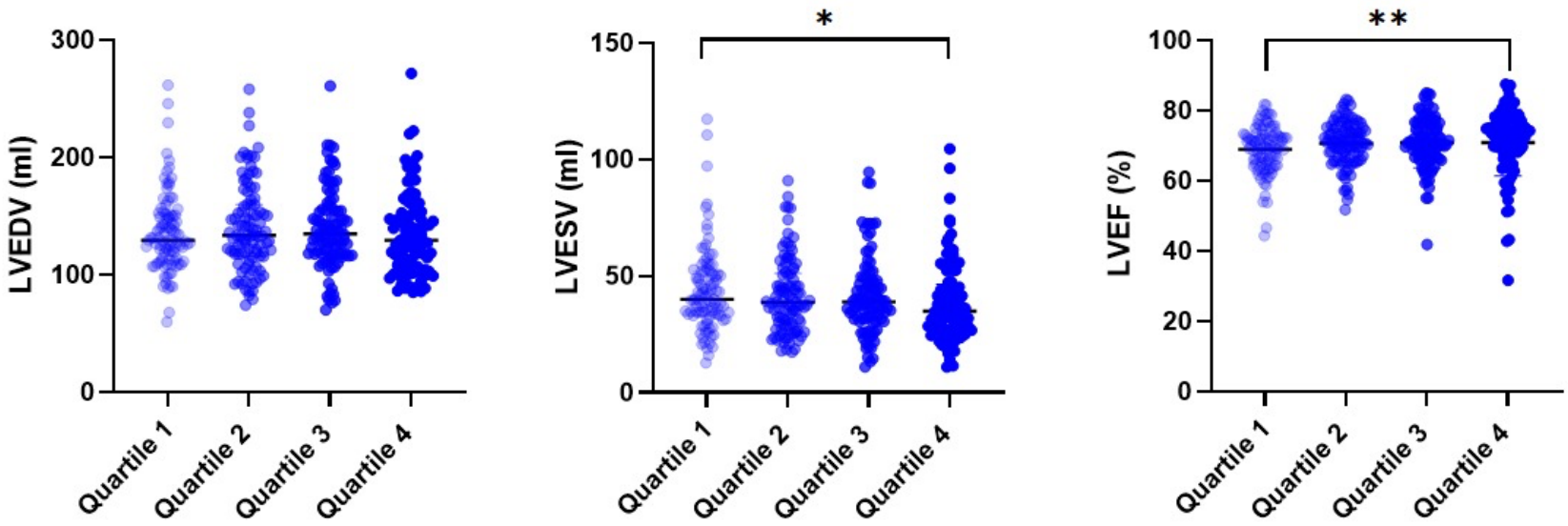

Figure 53: Differences across systolic blood pressure (SBP) quartiles in LV volumes and function. *Abbreviations: LVEDV, left ventricular end diastolic volume; LVEF, left ventricular ejection fraction; LVESV, left ventricular end systolic volume. * = p<0.05, ** = p<0.01, *** = p<0.001*

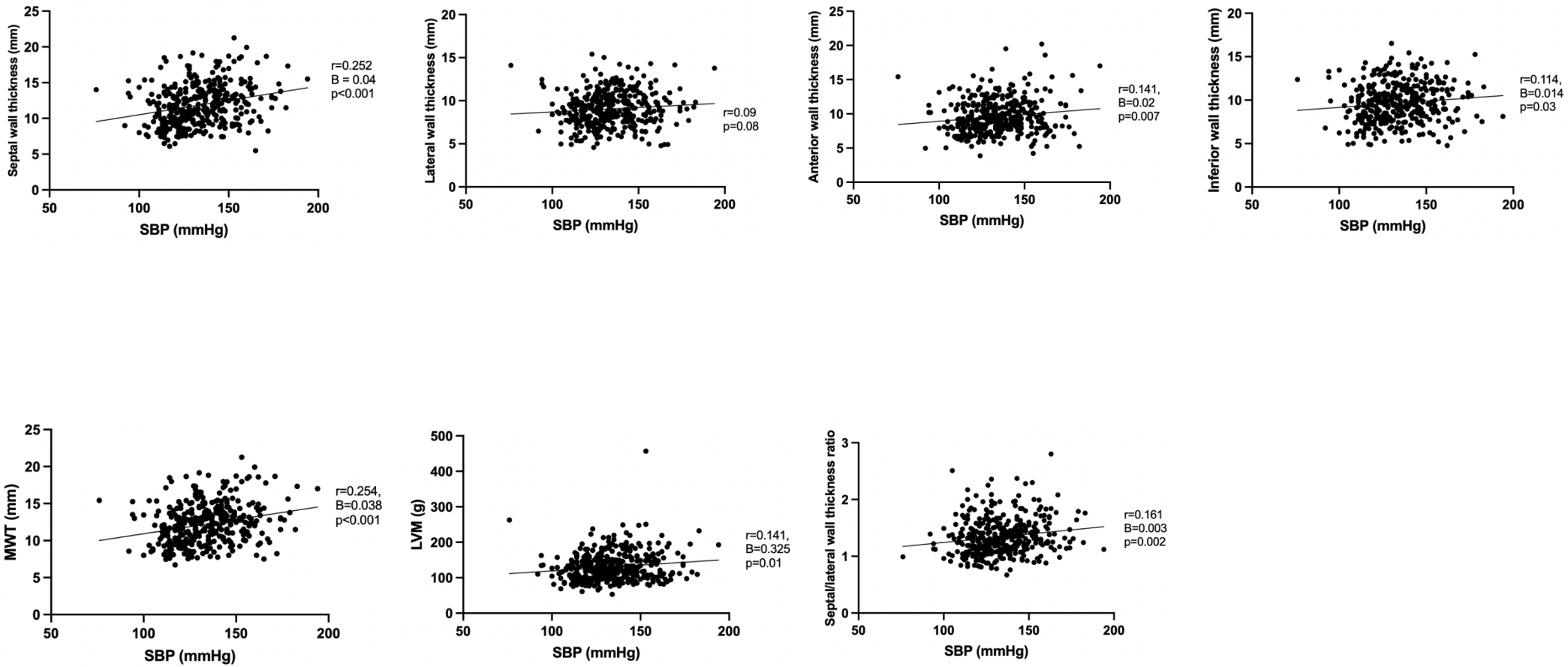

Figure 54: Linear regression analysis between systolic blood pressure (SBP) and myocardial wall thicknesses, left ventricular mass (LVM), maximal wall thickness (MWT) and LV geometry. The correlation coefficient (*r*), unstandardised B (B) and statistical significance of the model (*p*) are included on each graph.

4.4.1.4 HYPERTENSION SPECTRUM COHORT: DBP AND WALL THICKNESS

As **Table 9** and **Figures 55-58** show, across increasing DBP quartiles, all measured LV walls showed progressive thickening (all $p<0.001$): for every 10 mmHg increase in DBP, there is a 0.5 mm increase in septal wall thickness, 0.4mm increase in lateral wall thickness, 0.5mm increase in anterior wall thickness, 0.4 mm increase in inferior wall thickness, 0.5mm increase in MWT and 7g increase in LVM.

DBP elevation did not significantly alter the septal/lateral wall thickness ratio or LV systolic function – unlike SBP where wall thickening showed regional preference and affected cardiac symmetry and function.

Table 9: Hypertension Spectrum Cohort – differences across DBP quartiles in baseline demographics, wall thickness, LV geometry, volumes and function.

Category	Quartile 1	Quartile 2	Quartile 3	Quartile 4	*P* value
Age (years)	65 [27]	62 [23]	58 [24]	58 [20]	0.118
BMI (kg/m^2)	28 [7]	27 [5]	28 [6]	28 [5]	0.343
SBP (mmHg)	121 [20]	130 [23]	133 [20]	144 [22]	<0.001
DBP (mmHg)	66 [5]	74 [4]	81 [3]	91 [9]	<0.001
Septal wall thickness (mm)	11 [4]	11 [4]	12 [4]	12 [3]	0.001
Lateral wall thickness (mm)	8±2	9±2	9±2	10±2	<0.001
Anterior wall thickness (mm)	9 [3]	9 [3]	9 [4]	10 [3]	<0.001
Inferior wall thickness (mm)	9±2	10±2	10±3	10±2	<0.001
MWT (mm)	11 [4]	11 [4]	13 [4]	13 [3]	<0.001
LVM (g)	111 [38]	117 [47]	133 [58]	135 [54]	<0.001
Septal/lateral wall thickness ratio	1.4 [0.5]	1.2 [0.4]	1.3 [0.4]	1.3 [0.4]	0.483
Anterior/inferior wall thickness ratio	1.0 [0.3]	1.0 [0.3]	1.0 [0.3]	1.0 [0.3]	0.540
LVEDV (ml)	127 [40]	131 [37]	139 [52]	136 [36]	0.051
LVESV (ml)	36 [21]	43 [19]	38 [22]	39 [21]	0.192
LVEF (%)	71 [7]	70 [12]	72 [8]	70 [9]	0.440

Abbreviations: BMI=body mass index, DBP=diastolic blood pressure, LVGLS= left ventricular global longitudinal strain, hs-cTnI=high sensitivity cardiac troponin I, LGE=late gadolinium enhancement, LV=left ventricle, LVEDV=left ventricular end diastolic volume, LVESV=left ventricular systolic volume, LVEF=left ventricular ejection fraction, LVM=left ventricular mass, MWT = maximal wall thickness, PCr/ATP=phosphocreatine/adenosine triphosphate, SBP=systolic blood pressure. Data presented as mean ±SD, median [IQR] or n(%).

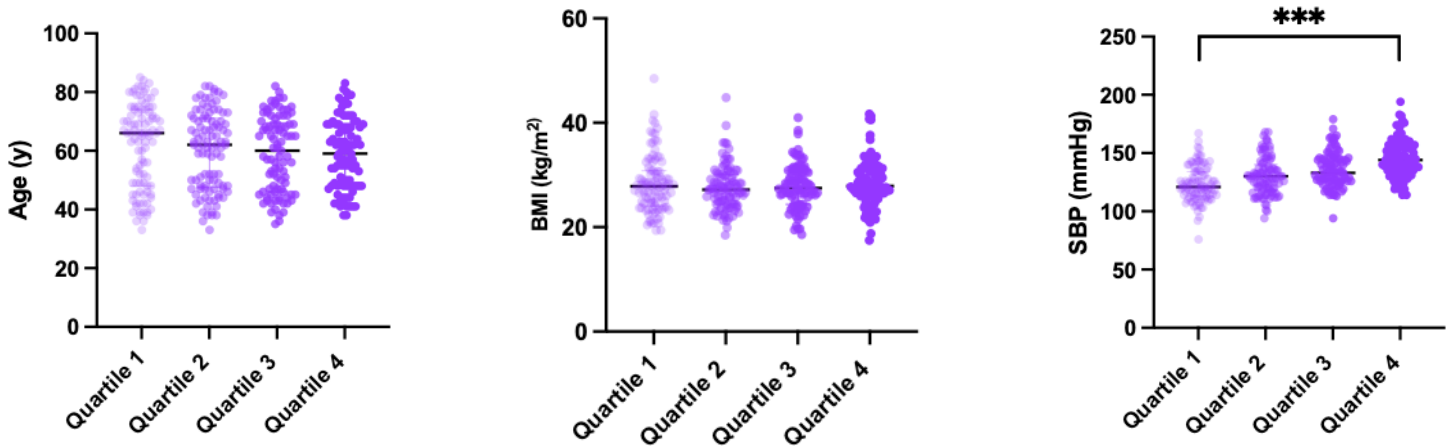

Figure 55: Differences across diastolic blood pressure (DBP) quartiles in age, systolic blood pressure (SBP) and body mass index (BMI). ** = p<0.05, ** = p<0.01, *** = p<0.001*

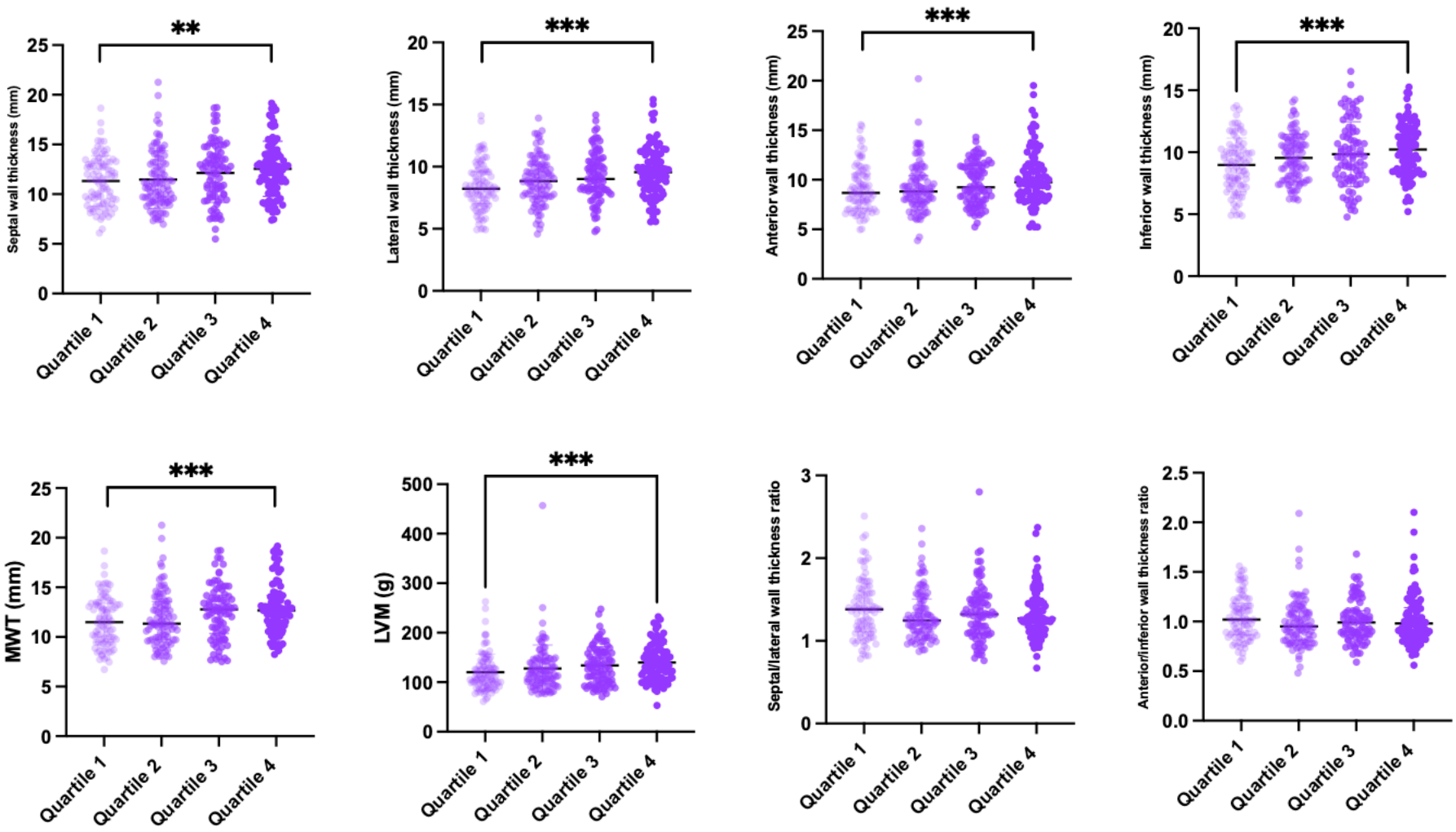

Figure 56: Differences across DBP quartiles in myocardial wall thicknesses, maximal wall thickness (MWT), left ventricular mass (LVM), maximal wall thickness (MWT) and LV geometry. ** = p<0.05, ** = p<0.01, *** = p<0.001*

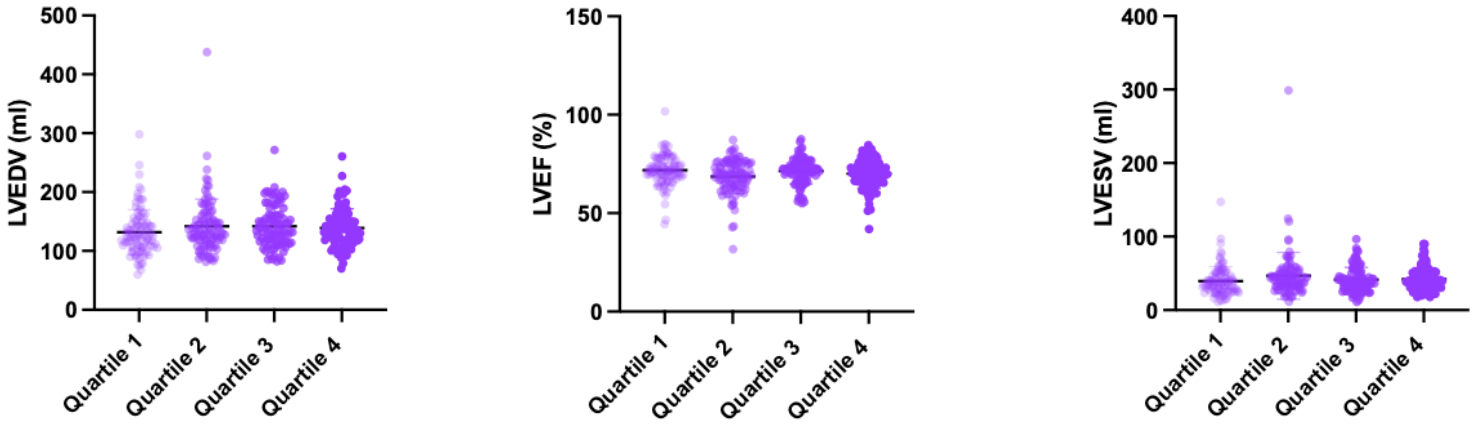

Figure 57: Differences across diastolic blood pressure (DBP) quartiles in left ventricular end diastolic volume (LVEDV), left ventricular end systolic volume (LVESV) and left ventricular ejection fraction (LVEF).

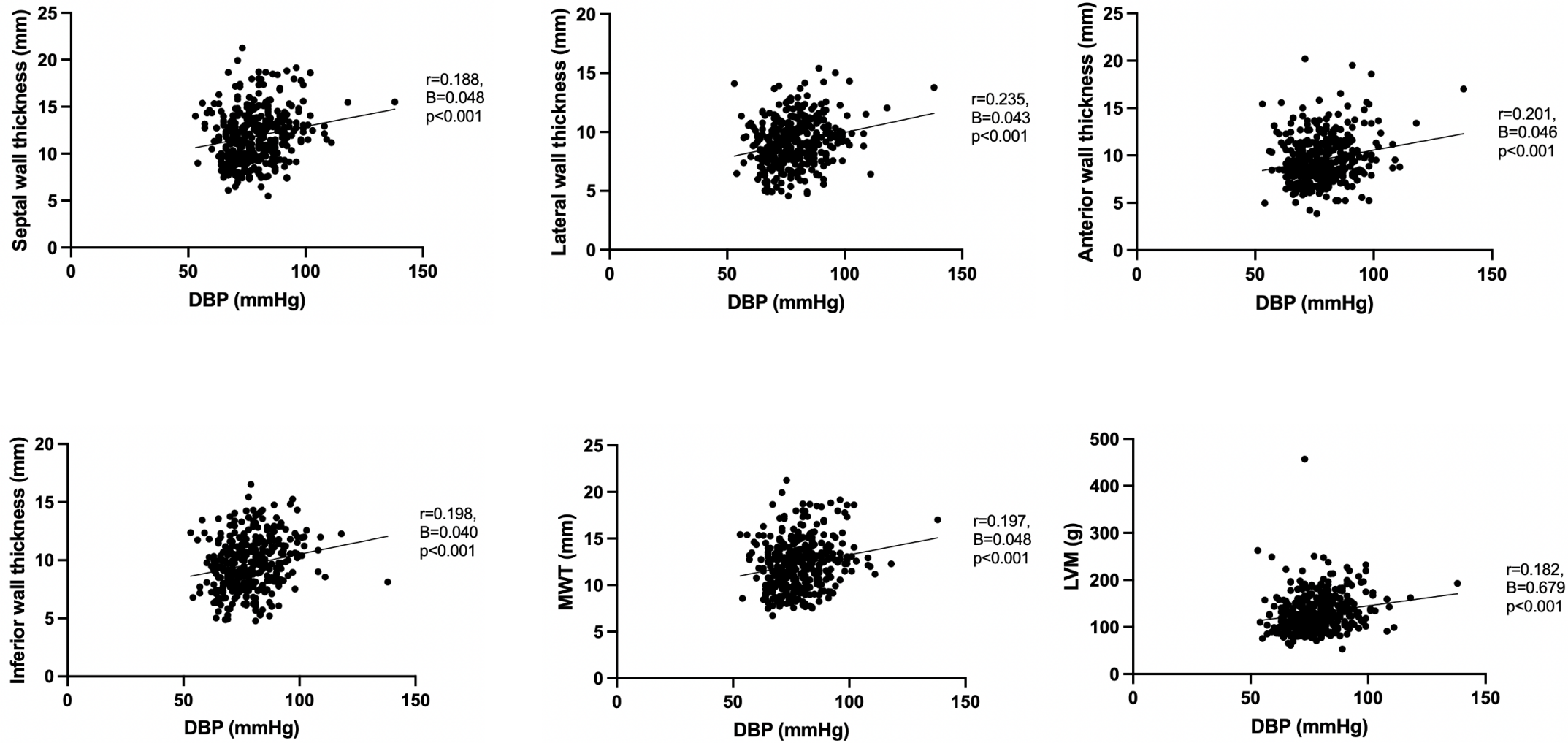

Figure 58: Linear regression analysis between diastolic blood pressure (DBP) and myocardial wall thicknesses, left ventricular mass (LVM), maximal wall thickness (MWT) and LV geometry. The correlation coefficient (*r*), unstandardised B (B) and statistical significance of the model (*p*) are included on each graph.

4.4.1.5 HYPERTENSION SPECTRUM COHORT: BMI AND WALL THICKNESS

BMI was associated with increased wall thickness (0.2mm/kg/m^2 septal wall increase, 0.08mm/kg/m^2 lateral wall increase, 0.1mm/kg/m^2 anterior wall increase, 0.1mm/kg/m^2 inferior wall increase, 0.1mm/kg/m^2 MWT increase and 2.4g/kg/m^2 LVM increase; all p<0.001), and an increased LVEDV but unlike SBP, did not affect cardiac symmetry or function (**Table 10, Figures 59-62**).

Table 10: Hypertensive Spectrum Cohort – differences across BMI quartiles in baseline demographics, wall thickness, LV geometry, volumes and function.

Category	Quartile 1	Quartile 2	Quartile 3	Quartile 4	*P* value
Age (years)	52 [21]	63 [21]	68 [24]	58 [22]	0.016
BMI (kg/m^2)	23 [2]	27 [1]	29 [1]	33 [5]	<0.001
SBP (mmHg)	126 [23]	133 [24]	135 [21]	132 [25]	0.008
DBP (mmHg)	75 [13]	79 [14]	79 [15]	78 [16]	0.265
Septal wall thickness (mm)	10 [4]	12 [4]	12 [4]	13 [4]	<0.001
Lateral wall thickness (mm)	8±2	9±2	10±2	9±2	<0.001
Anterior wall thickness (mm)	8 [3]	10 [3]	10 [3]	9 [3]	<0.001
Inferior wall thickness (mm)	9±2	10±2	10±2	10±2	<0.001
MWT (mm)	10 [3]	13 [4]	13 [3]	13 [4]	<0.001
LVM (g)	105 [35]	123 [52]	133 [46]	135 [57]	<0.001
Septal/lateral wall thickness ratio	1.2 [0.4]	1.3 [0.5]	1.3 [0.4]	1.3 [0.4]	0.087
Anterior/inferior wall thickness ratio	1.0 [0.3]	1.0 [0.3]	1.0 [0.3]	1.0 [0.3]	0.768
LVEDV (ml)	127 [35]	131 [48]	137 [47]	139 [44]	0.003
LVESV (ml)	37 [20]	38 [24]	40 [23]	40 [19]	0.254
LVEF (%)	70 [9]	71 [8]	71 [9]	72 [9]	0.090

Abbreviations: BMI=body mass index, DBP=diastolic blood pressure, LVGLS= left ventricular global longitudinal strain, hs-cTnI=high sensitivity cardiac troponin I, LGE=late gadolinium enhancement, LV=left ventricle, LVEDV=left ventricular end diastolic volume, LVESV=left ventricular systolic volume, LVEF=left ventricular ejection fraction, LVM=left ventricular mass, MWT = maximal wall thickness, PCr/ATP=phosphocreatine/adenosine triphosphate, SBP=systolic blood pressure. Data presented as mean ±SD, median [IQR] or n(%).

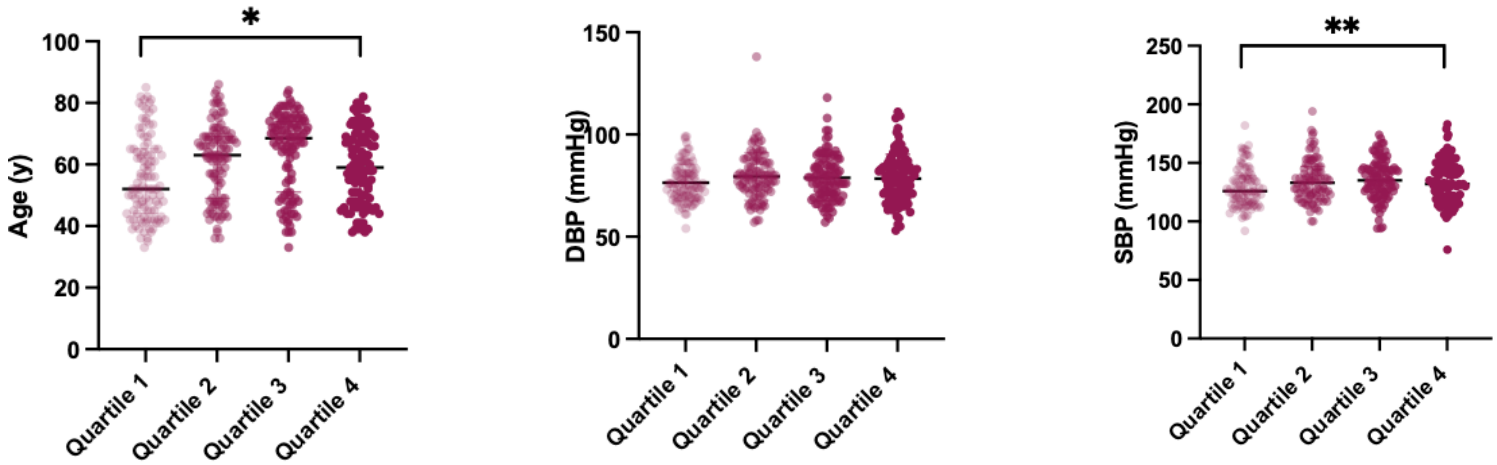

Figure 59: Differences across body mass index (BMI) quartiles in age, diastolic blood pressure (DBP) and systolic blood pressure (SBP). ** = p<0.05, ** = p<0.01, *** = p<0.001*

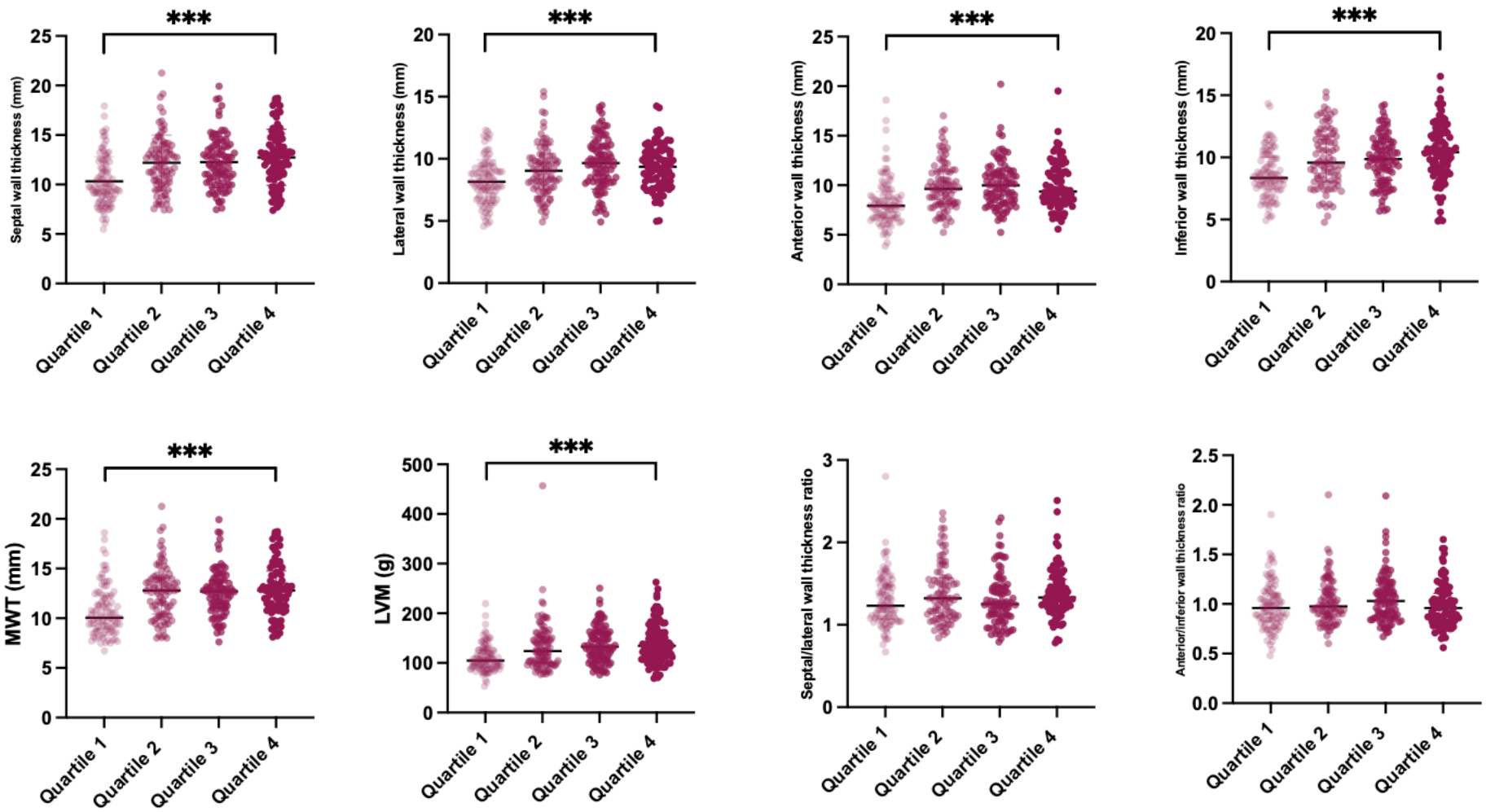

Figure 60: Differences across body mass index (BMI) quartiles in myocardial wall thicknesses, maximal wall thickness (MWT), left ventricular mass (LVM), and LV geometry. ** = p<0.05, ** = p<0.01, *** = p<0.001*

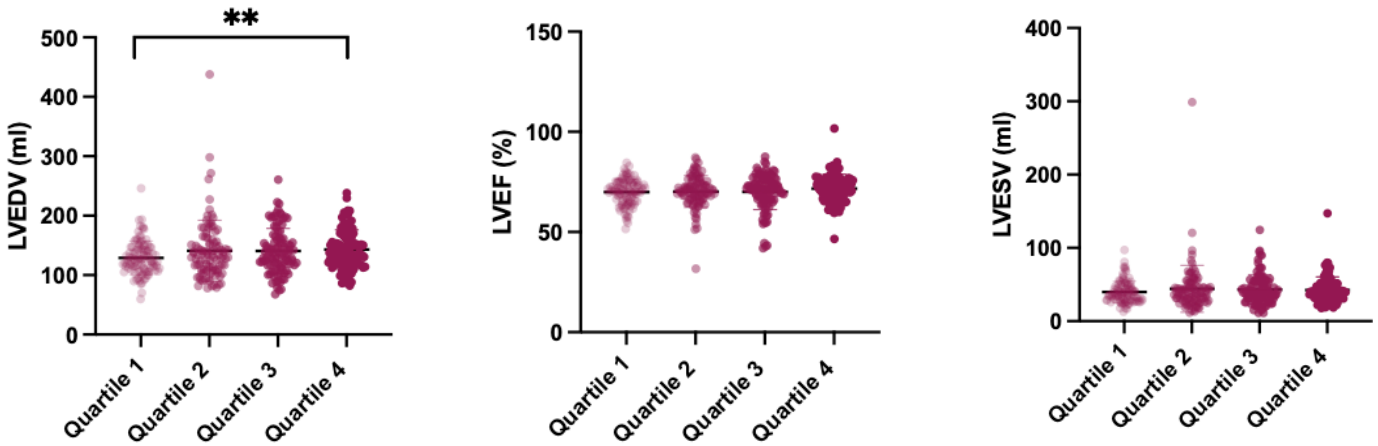

Figure 61: Differences across body mass index (BMI) quartiles in left ventricular end diastolic volume (LVEDV), left ventricular end systolic volume (LVESV) and left ventricular ejection fraction (LVEF). ** = p<0.05, ** = p<0.01, *** = p<0.001*

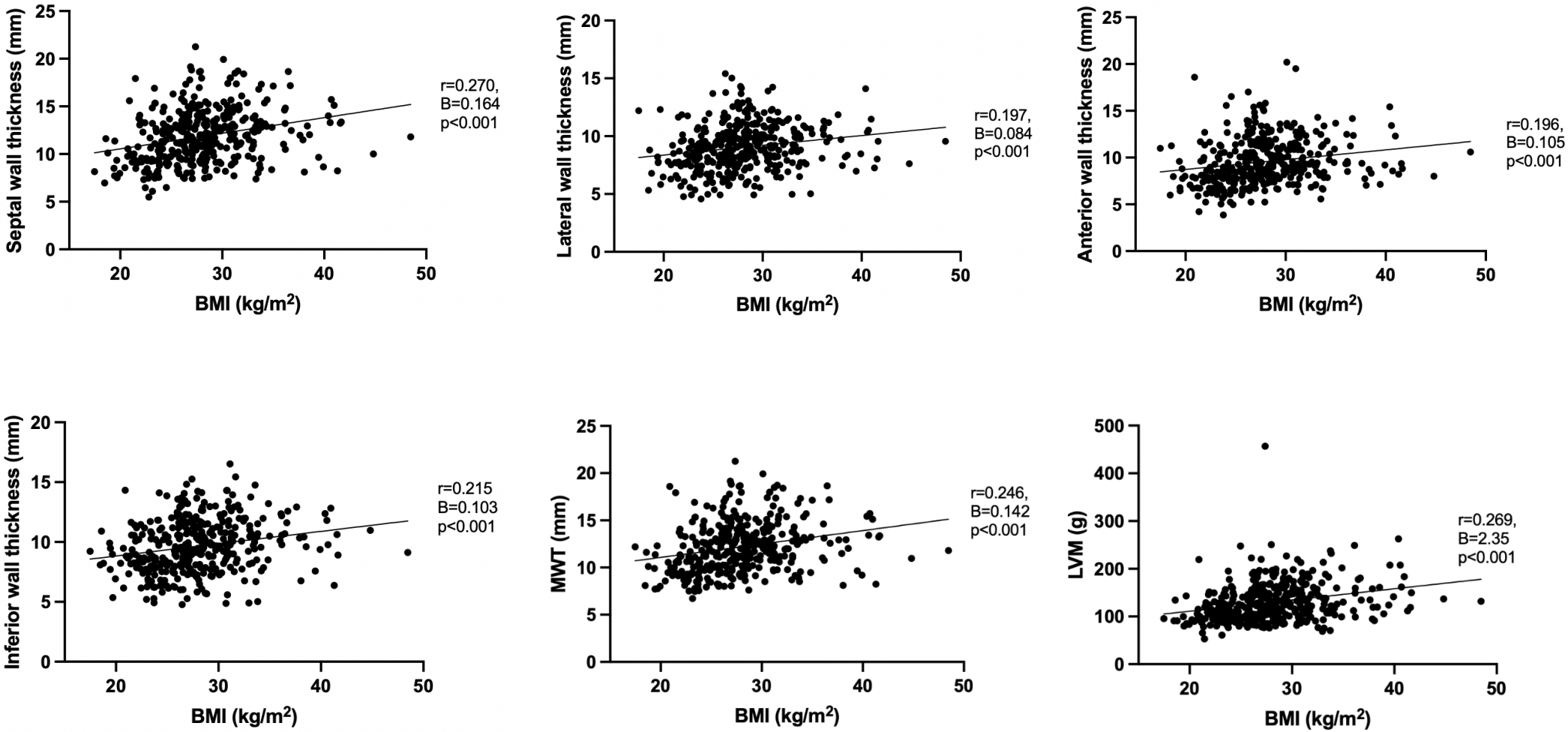

Figure 62: Linear regression analysis between body mass index (BMI) and myocardial wall thicknesses, left ventricular mass (LVM) and LV geometry. The correlation coefficient (*r*), unstandardised B (B) and statistical significance of the model (*p*) are included on each graph.

4.4.1.6 HYPERTENSION SPECTRUM COHORT: BP, BMI vs WALL THICKNESS OR LV GEOMETRY

Multiple linear regression model (**Table 11**) comparing SBP, DBP and BMI with respect to wall thickness and LV geometry demonstrated that BMI is the dominant determinant of wall thickness and LV mass, consistently being the strongest and most significant predictor across all myocardial regions. SBP and DBP had different wall thickness associations: SBP was associated with septal hypertrophy and maximal wall thickness whereas DBP is more linked to lateral and anterior wall thickening, as well as LV mass. Both SBP and DBP are associated with septal/lateral wall thickness ratio, although SBP has the stronger association. Although the above reported associations are significant, it's important that the explained variance is modest, suggesting that genetics, other haemodynamic factors and unmeasured variables also play a much larger part in explaining wall thickness and LV geometry.

Table 11: Multiple linear regression analysis between SBP, DBP and BMI and myocardial wall thicknesses and LV geometry with the values given for the coefficient of determination (R^2), adjusted coefficient of determination (Adjusted R^2), regression coefficient (B) and probability value (*p*). *Abbreviations: BMI – Body Mass Index; DBP – Diastolic Blood Pressure; SBP – Systolic Blood Pressure.*

Dependent factor	R^2	Adjusted R^2	B	*p*
Septal wall thickness	0.131	0.124		<0.001
BMI			0.152	<0.001
SBP			0.029	0.002
DBP			0.023	0.134
Lateral wall thickness	0.096	0.088		<0.001
BMI			0.085	<0.001
SBP			-0.008	0.213
DBP			0.049	<0.001
Anterior wall thickness	0.078	0.071		<0.001
BMI			0.102	<0.001
SBP			0.003	0.726
DBP			0.043	0.002
Inferior wall thickness	0.085	0.077		<0.001
BMI			0.102	<0.001
SBP			-0.002	0.781
DBP			0.042	<0.001
Maximal wall thickness	0.122	0.114		<0.001
BMI			0.131	<0.001
SBP			0.027	0.002
DBP			0.023	0.104
Left ventricular mass	0.105	0.098		<0.001
BMI			2.305	<0.001
SBP			0.075	0.573
DBP			0.618	0.004
Septal/lateral wall thickness ratio	0.050	0.042		<0.001
BMI			0.004	0.298
SBP			0.005	<0.001
DBP			-0.005	0.007

4.4.2 METABOLIC SPECTRUM COHORT: DOES OBESITY INFLUENCE LVH SEVERITY AND LV GEOMETRY IN A WAY THAT RESEMBLES HCM?

4.4.2.1 METABOLIC SPECTRUM COHORT: BASELINE DEMOGRAPHICS

This cohort (**Table 12**) compromises predominantly healthy individuals with normal-range blood pressure and an approximately balanced sex distribution. 31% (n=263) met criteria for obesity (BMI≥30 kg/m^2).

4.4.2.2 METABOLIC SPECTRUM COHORT – HEALTHY INDIVIDUALS AND THOSE WITH OBESITY: HOW DOES THIS COHORT RESEMBLE HCM?

None of the participants in this cohort have a MWT ≥15mm, however 25% (n=211) participants had a septal/lateral wall thickness ratio ≥1.3, with 77 (9%) participants have a septal/lateral wall thickness ratio ≥1.5 – a threshold more characteristic of HCM morphology.

.

Table 12: Summary of results from the Healthy Cohort.

Category	n=849
Sex	
Male, n (%)	372 (44)
Female, n (%)	477 (56)
BMI (kg/m^2)	29 [10]
SBP (mmHg)	126 [19]
DBP (mmHg)	77 ± 10
Septal wall thickness (mm)	9 [2]
Lateral wall thickness (mm)	8 ± 1
Septal/lateral wall thickness ratio	1.2 ± 0.2

Abbreviations: BMI=body mass index, DBP=diastolic blood pressure, SBP=systolic blood pressure. Data presented as mean ±SD, median [IQR] or n(%).

4.4.2.3 METABOLIC SPECTRUM COHORT: SBP TRENDS

Higher SBP significantly correlated with increasing DBP, BMI, septal and lateral wall thickness, and septal to lateral wall thickness ratio (p<0.001) (**Table 13, Figures 63-64**). Linear regression analysis demonstrated that each 10 mmHg SBP increase was associated with a 0.5 mm increase in septal wall thickness, 0.2mm increase in lateral wall thickness, and 0.04 increase in septal/lateral wall thickness ratio (see **Figure 64**).

Table 13: Differences across systolic blood pressure (SBP) quartiles in diastolic blood pressure (DBP), body mass index (BMI), LV wall thickness and geometry.

Category	Quartile 1	Quartile 2	Quartile 3	Quartile 4	*P* value
SBP (mmHg)	107 [8]	117 [4]	126 [5]	138 [8]	<0.001
DBP (mmHg)	66 [8]	73 [10]	77 [10]	82 [12]	<0.001
BMI (kg/m2)	24 [6]	25 [7]	26 [9]	29 [12]	<0.001
Septal wall thickness (mm)	8 [2]	9 [2]	9 [2]	10 [2]	<0.001
Lateral wall thickness (mm)	7 [2]	8 [2]	8 [2]	8 [2]	<0.001
Septal/lateral wall thickness ratio	1.1 [0.2]	1.1 [0.3]	1.2 [0.2]	1.2 [0.3]	<0.001

Abbreviations: BMI=body mass index, DBP=diastolic blood pressure, SBP=systolic blood pressure. Data presented as mean ±SD, median [IQR] or n(%).

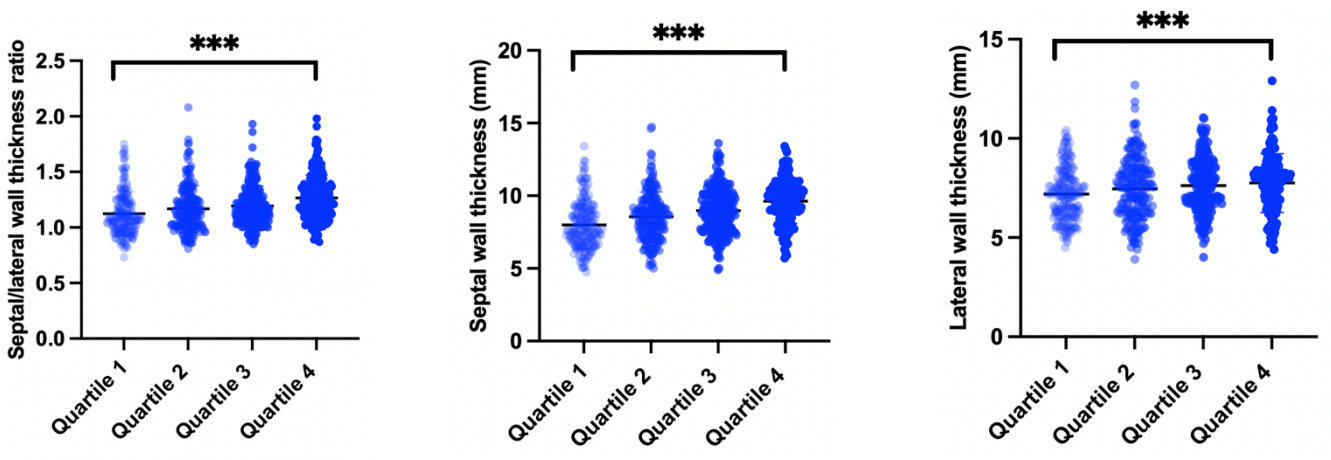

Figure 63: Differences across systolic blood pressure (SBP) quartiles in septal wall thickness, lateral wall thickness and septal/lateral wall thickness ratio. ** = p<0.05, ** = p<0.01, *** = p<0.001*

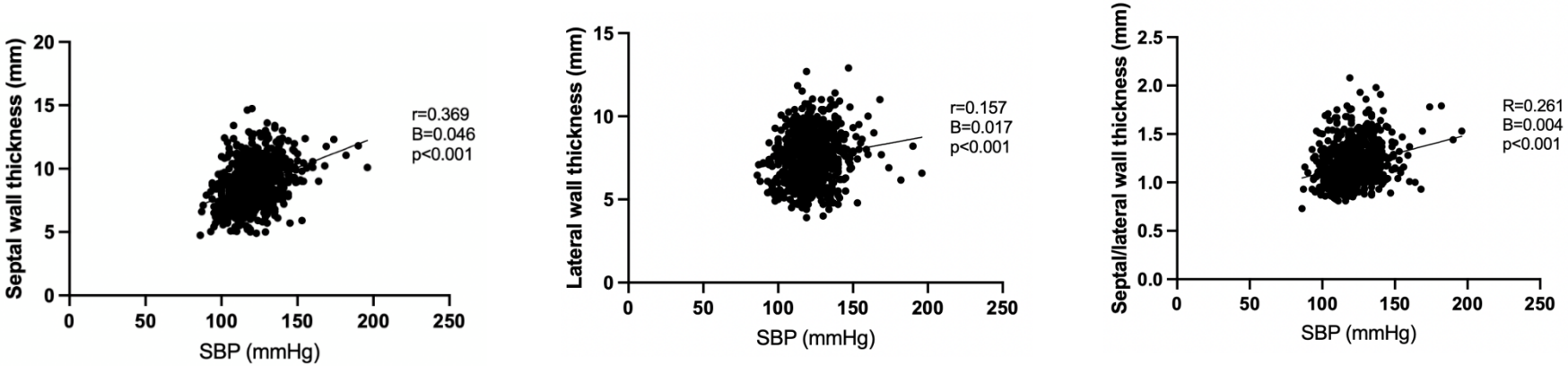

Figure 64: Linear regression analysis between systolic blood pressure (SBP) and myocardial wall thicknesses, and LV geometry. The correlation coefficient (*r*), unstandardised B (B) and statistical significance of the model (*p*) are included on each graph.

4.4.2.4 METABOLIC SPECTRUM COHORT: DBP TRENDS

Increasing DBP significantly correlated with higher SBP, BMI, septal and lateral wall thickness, and septal/lateral wall thickness ratio (all $p<0.001$) (**Table 14, Figure 65**). Each 10mmHg DBP increase was associated with a 0.6mm greater septal wall thickness, 0.2mm greater lateral wall thickness, and 0.05 increase in septal/lateral wall thickness ratio (**Figure 66**).

Table 14: Differences across diastolic blood pressure (DBP) quartiles in systolic blood pressure (SBP), body mass index (BMI), LV wall thickness and geometry.

Category	Quartile 1	Quartile 2	Quartile 3	Quartile 4	*P* value
SBP (mmHg)	110 [8]	117 [4]	126 [5]	138 [8]	<0.001
DBP (mmHg)	66 [8]	73 [10]	77 [10]	82 [12]	<0.001
BMI (kg/m2)	24 [6]	25 [8]	26 [8]	28 [10]	<0.001
Septal wall thickness (mm)	8 [2]	8 [2]	9 [2]	10 [2]	<0.001
Lateral wall thickness (mm)	7 [2]	7 [2]	8 [2]	8 [2]	<0.001
Septal/lateral wall thickness ratio	1.1 [0.2]	1.1 [0.3]	1.2 [0.3]	1.2 [0.3]	<0.001

Abbreviations: BMI=body mass index, DBP=diastolic blood pressure, SBP=systolic blood pressure. Data presented as mean ±SD, median [IQR] or n(%).

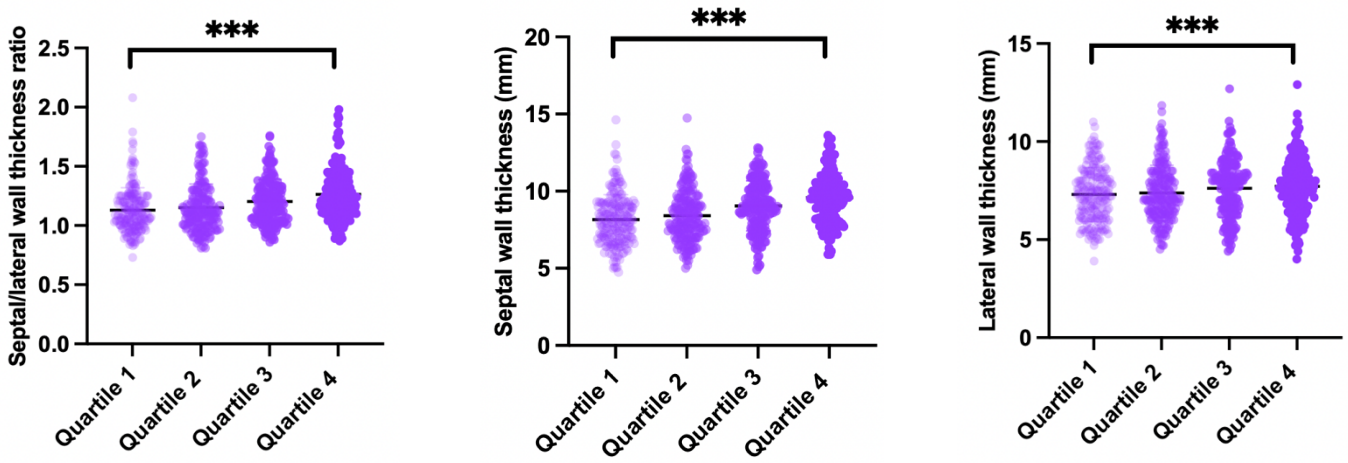

Figure 65: Differences across diastolic blood pressure (DBP) quartiles in septal wall thickness, lateral wall thickness and septal/lateral wall thickness ratio. ** = p<0.05, ** = p<0.01, *** = p<0.001*

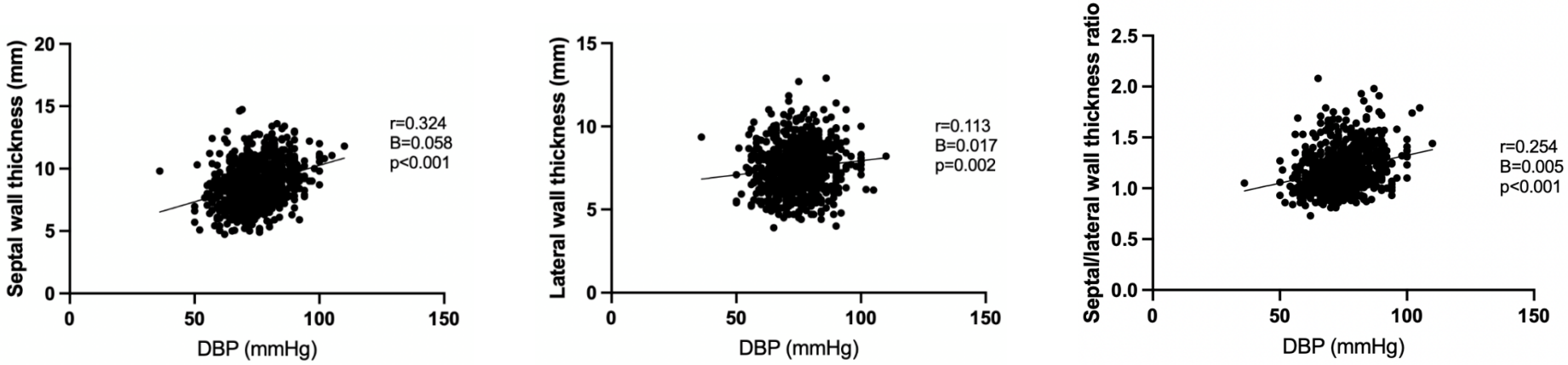

Figure 66: Linear regression analysis between diastolic blood pressure (DBP) and myocardial wall thicknesses and LV geometry. The correlation coefficient (*r*), unstandardised B (B) and statistical significance of the model (*p*) are included on each graph.

4.4.2.5 METABOLIC SPECTRUM COHORT: BMI TRENDS

With an increasing BMI, there is a significantly increasing SBP, DBP, septal and lateral wall thickness, and septal/lateral wall thickness ratio (see **Table 15** and **Figure 67**). Linear regression analysis demonstrated that for every 1 kg/m^2 increase in BMI, there is a 0.08 mm increase in septal wall thickness, 0.04mm increase in lateral wall thickness, and 0.005 increase in septal/lateral wall thickness ratio (see **Figure 68**).

Table 15: Differences across body mass index (BMI) quartiles in systolic blood pressure (SBP), diastolic blood pressure (DBP), LV wall thickness and geometry.

Category	Quartile 1	Quartile 2	Quartile 3	Quartile 4	*P* value
SBP (mmHg)	115 [13]	120 [16]	122 [17]	128 [17]	<0.001
DBP (mmHg)	71 ± 8	73 ± 8	77 ± 10	77 ± 10	<0.001
BMI (kg/m2)	21 [2]	24 [2]	28 [3]	38 [10]	<0.001
Septal wall thickness (mm)	8 [2]	9 [2]	9 [2]	9 [2]	<0.001
Lateral wall thickness (mm)	7 [2]	8 [2]	8 [2]	8 [2]	<0.001
Septal/lateral wall thickness ratio	1.1 [0.2]	1.1 [0.3]	1.2 [0.3]	1.2 [0.3]	<0.001

Abbreviations: BMI=body mass index, DBP=diastolic blood pressure, SBP=systolic blood pressure. Data presented as mean ±SD, median [IQR] or n(%).

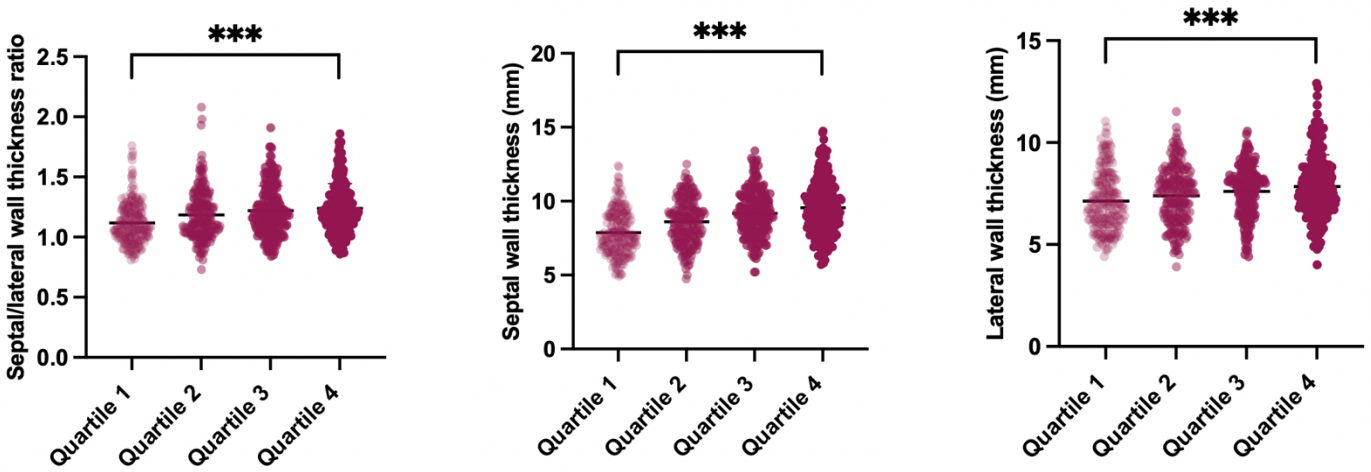

Figure 67: Differences across body mass index (BMI) quartiles in septal wall thickness, lateral wall thickness and septal/lateral wall thickness ratio. ** = p<0.05, ** = p<0.01, *** = p<0.001*

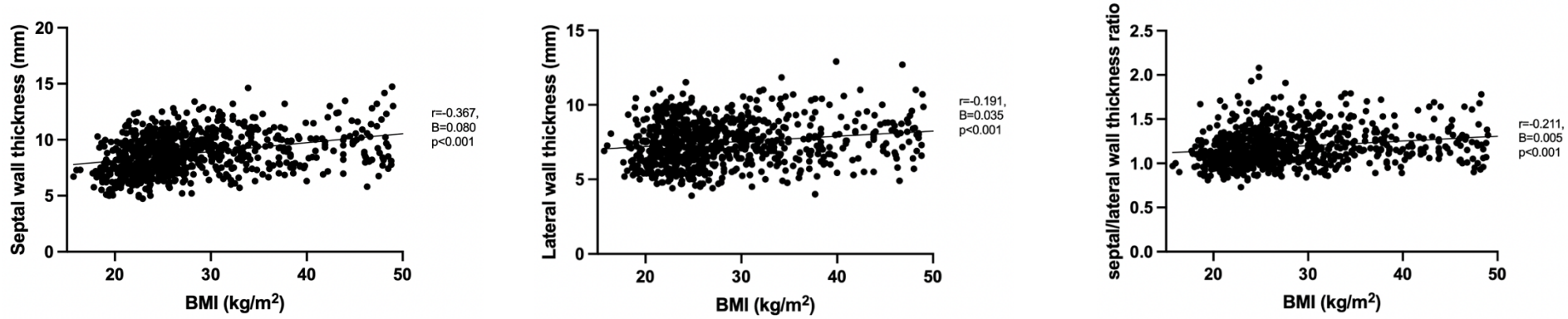

Figure 68: Linear regression analysis between BMI and myocardial wall thicknesses and LV geometry. The correlation coefficient (*r*), unstandardised B (B) and statistical significance of the model (*p*) are included on each graph.

4.4.2.6 METABOLIC SPECTRUM COHORT: BP, BMI, WALL THICKNESS AND LV GEOMETRY

In a multiple linear regression model with SBP, DBP and BMI, SBP and BMI were significantly associated with septal wall thickness, lateral wall thickness and septal/lateral wall thickness ratio, while DBP was only significantly associated with septal wall thickness and septal/lateral wall thickness ratio (see **Table 16**). Lateral wall thickness appears to be mainly influenced by BMI with SBP and DBP contributing less. The septal/lateral wall thickness ratio is moderately influenced by BMI and SBP.

Table 16: Multiple linear regression analysis between SBP, DBP and BMI and myocardial wall thicknesses and LV geometry with the values given for the coefficient of determination (R^2), adjusted coefficient of determination (Adjusted R^2), regression coefficient (B) and probability value (*p*). *Abbreviations: BMI – Body Mass Index; DBP – Diastolic Blood Pressure; SBP – Systolic Blood Pressure.*

Dependent factor	R^2	Adjusted R^2	B	*p*
Septal wall thickness				
BMI	0.101	0.098	0.057	<0.001
SBP	0.187	0.184	0.024	<0.001
DBP	0.146	0.143	0.027	<0.001
Lateral wall thickness				
BMI	0.085	0.084	0.026	<0.001
SBP	0.008	0.007	0.010	0.043
DBP	0.049	0.048	0.003	0.638
Septal wall thickness				
BMI	0.070	0.069	0.003	<0.001
SBP	0.055	0.054	0.007	0.007
DBP	0.060	0.059	0.001	0.001

4.4.3 HCM COHORT: DOES OBESITY INFLUENCE LVH SEVERITY AND LV GEOMETRY AFFECT ESTABLISHED HCM?

4.4.3.1 BASELINE DEMOGRAPHICS

The cohort has an evenly split sex, with a BMI within normal limits, and evidence of asymmetric septal hypertrophy (see **Table 17**).

Table 17: Summary of results from HCM Cohort - HCM

Category	n=236
Sex	
Male, n (%)	117 (50)
Female, n (%)	119 (50)
BMI (kg/m^2)	29 [10]
Septal wall thickness (mm)	19 ± 4
Lateral wall thickness (mm)	8 [3]
Septal/lateral wall thickness ratio	2.1 [1]

Abbreviations: BMI=body mass index. Data presented as mean ±SD, median [IQR] or n(%).

4.4.3.2 DIFFERENCE ACROSS BMI QUARTILES

With an increasing BMI, there is a significantly increasing lateral wall thickness, and septal/lateral wall thickness ratio (**Table 18, Figure 69**). Linear regression analysis demonstrated that for every 1 kg/m2 increase in BMI, there is a 0.3mm increase in lateral wall thickness, and 0.05 decrease in septal/lateral wall thickness ratio (**Figure 70**).

Table 18: Differences across BMI quartiles in LV wall thickness and geometry

Category	Quartile 1	Quartile 2	Quartile 3	Quartile 4	*P* value
BMI (kg/m2)	24 [3]	27 [2]	30 [1]	37 [6]	<0.001
Septal wall thickness (mm)	18 [8]	18 [4]	17 [5]	19 [6]	0.131
Lateral wall thickness (mm)	7 [1]	8 [3]	8 [3]	9 [4]	<0.001
Septal/lateral wall thickness ratio	2.6 [1.2]	2.3 [1.3]	2 [0.8]	1.8 [0.7]	<0.001

Abbreviations: BMI=body mass index. Data presented as mean ±SD, median [IQR] or n(%).

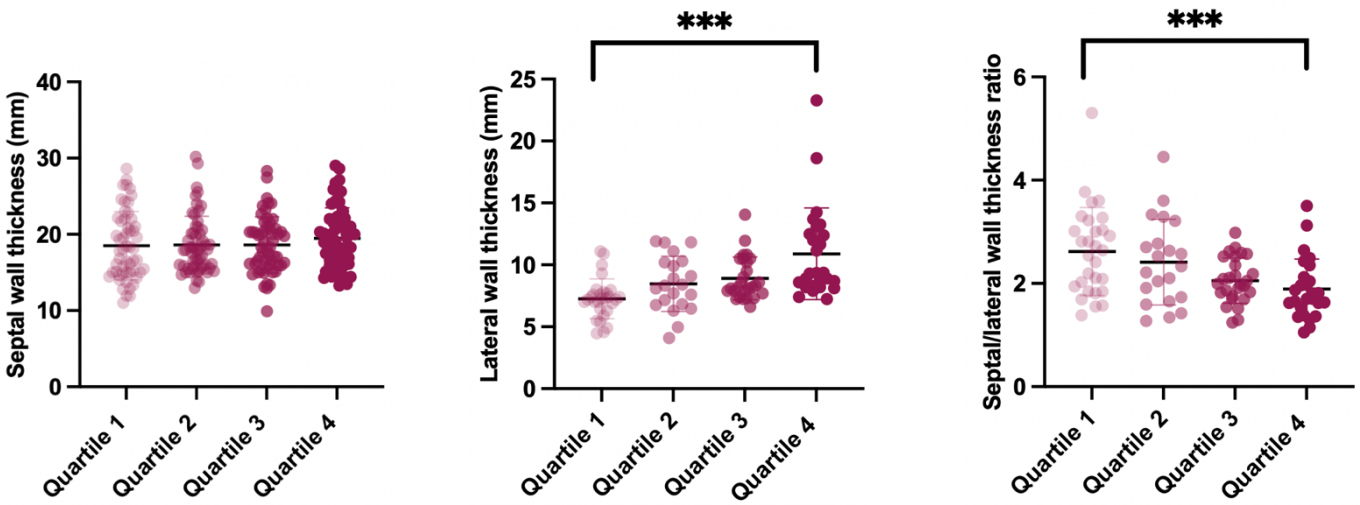

Figure 69: Differences across body mass index (BMI) quartiles in septal wall thickness, lateral wall thickness and septal/lateral wall thickness ratio. ** = p<0.05, ** = p<0.01, *** = p<0.001*

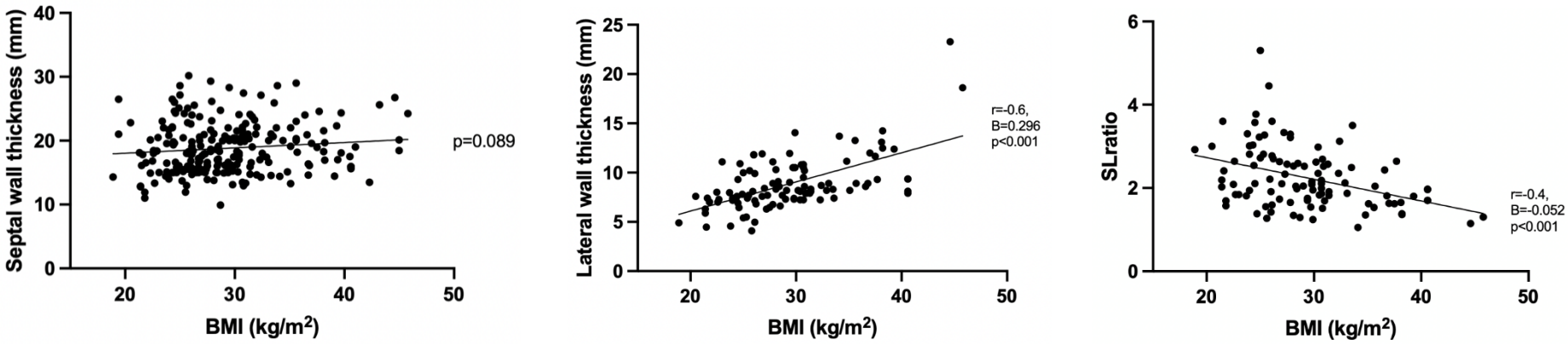

Figure 70: Linear regression analysis between body mass index (BMI) and myocardial wall thicknesses and LV geometry. The correlation coefficient (*r*), unstandardised B (B) and statistical significance of the model (*p*) are included on each graph.

4.5 DISCUSSION

Our multi-cohort analysis reveals how blood pressure and BMI differentially influence cardiac remodelling across disease states, with important implications for distinguishing true HCM from phenocopies.

4.5.1 HYPERTENSION SPECTRUM COHORT: WHEN HYPERTENSION MASQUERADES AS HCM

The Hypertension Spectrum Cohort findings reveal a spectrum of hypertensive remodelling patterns that challenge traditional diagnostic classifications. When examining isolated systolic hypertension, we observe a characteristic asymmetric septal hypertrophy pattern mirroring gene+ HCM. This pure SBP-driven remodelling explains why 9% of participants with systolic hypertension developed diagnostic HCM features (MWT ≥15mm), including 5% exceeding the previously reported 17mm threshold to distinguish between hypertensive heart disease and HCM (the maximum MWT in our cohort was 21mm). Increased SBP was also significantly associated with an increased LVEF, a characteristic feature of the hypertensive LVH phenotype.

The remodelling pattern becomes more complex when diastolic hypertension coexists. While elevated DBP is associated with increased wall thickness in all segments, it is most strongly associated with lateral wall thickening, while not significantly affecting the septal/lateral wall thickness ratio, creating an intermediate morphology that blends features of both asymmetric and concentric hypertrophy. This mixed pattern manifests as reduced septal dominance compared to isolated SBP elevation yet maintains greater asymmetry than typical concentric remodelling.

Metabolic factors introduce additional variation. BMI increases promote generalised wall thickening that further modulates the cardiac phenotype. In fact, all of three variables (SBP, DBP and BMI), BMI was the dominant determinant of wall thickness and LVM in our cohort. Interestingly, BMI was not significantly associated with septal/lateral wall thickness ratio, although there was a trend towards a more asymmetric LV.

The data from this cohort highlights the importance of recognising pure SBP-driven cases (and therefore more accurately categorising patients with hypertension into those with systolic and/or diastolic hypertension), as these patients are most likely to present with convincing HCM phenocopies requiring comprehensive evaluation. While DBP and BMI are associated with wall thickness, our data suggests that they are unlikely to present as true HCM mimics. That being said, our findings also demonstrate that SBP, DBP and BMI are modest predictors of wall thickness and/or LV geometry and ultimately, many more factors are involved that remain to be thoroughly explored.

4.5.2 METABOLIC SPECTRUM COHORT: OBESITY INDUCED REMODELLING AND DIAGNOSTIC CHALLENGES

Our Metabolic Spectrum Cohort reveals important insights into how blood pressure and BMI influence cardiac remodelling in ostensibly healthy individuals. The data demonstrate progressive increases in both septal and lateral wall thickness correlating with rising SBP, DBP, and BMI, manifesting as a reduction in septal/lateral wall thickness ratio i.e. more concentric LV.

While MWT remained below diagnostic thresholds at 14 mm, the frequent development of asymmetric remodelling patterns (seen in 18% of obese participants) presents notable clinical implications. This metabolic remodelling can create phenotypic overlap with early-stage HCM, particularly in borderline cases where mild hypertrophy (12-14 mm) accompanies asymmetric geometry. The complete absence of genotype-negative HCM phenotypes confirms that metabolic factors alone rarely produce full HCM expression, yet the observed patterns suggest obesity can mimic HCM features when combined with blood pressure elevation.

These findings underscore the importance of considering metabolic status when evaluating borderline hypertrophy, especially in family screening scenarios or populations with high obesity prevalence. The data highlight how metabolic remodelling, while typically sub diagnostic, may complicate clinical assessment and warrant comprehensive evaluation to ensure accurate classification.

4.5.3 HCM COHORT: OBESITY'S FINDINGS, BUT NOT THAT OF ELEVATED BP, VALIDATED

The HCM cohort revealed obesity's unique influence on disease expression. Each kg/m² increase correlated with increased lateral wall thickness and progressive LV concentricity, particularly in obese patients who showed 18% greater lateral wall thickness than normal-weight counterparts. This metabolic signature contrasts sharply with hypertension-driven patterns in non-HCM patients, and with obesity's associations in patients without cardiac disease in the Hypertension and Metabolic

Spectrum cohorts suggesting genetic cardiomyopathy alters the heart's response to physiological stressors. The findings position weight management as a potential modifier of HCM phenotype progression.

4.5.4 FINDINGS COMPARED WITH PREVIOUS CHAPTER

Hypertension Spectrum Cohort vs. Chapter 3

The Hypertension Spectrum Cohort's SBP-driven septal hypertrophy contrasts sharply with Chapter 3's HCM genetic subgroups. In gene-positive HCM, hypertension's impact was confined to a significant association between increased SBP and increased lateral wall thickness. Gene-negative patients showed markedly different responses: SBP paradoxically reduced septal and anterior thickness while DBP drove concentric remodelling. These findings demonstrate that hypertension appears to result in different LV wall morphologies depending on the presence or absence of a gene+/gene- HCM phenotype.

Metabolic Spectrum Cohort vs. Chapter 3

Obese participants developed mild asymmetric remodelling (max 14 mm), paralleling early HCM phenotypes. This is different to our findings in Chapter 3, where increased BMI was linked with a more concentric LV, and at the genotype level, there was no association with BMI in the gene negative subgroup, and a more dilated and impaired LV noted with an increased BMI in the gene+ subgroup. This suggests that obesity in the absence of HCM, mimics (particularly gene+) HCM but in the presence of HCM, leads to a more concentric LV with features of HF.

HCM Registry Cohort vs. Chapter 3

This cohort's response to BMI is similar to that of Chapter 3 in that both cohorts resulted in a more concentric LV in response to an increased BMI. Unlike the Chapter 3 cohort, the HCMR cohort demonstrated an increased lateral wall thickness in response to an increased BMI. This divergence may reflect the small sample size in Chapter 3, the higher metabolic comorbidities in registry populations, and/or a broader spectrum of HCM phenotypes in the HCM registry.

4.6 CONCLUSION

This chapter demonstrates that hypertension and obesity produce distinct remodelling patterns in non-HCM populations. Using the HCM registry, we validate our initial Chapter 3 finding of an increased BMI associated with a more concentric LV. Elevated systolic blood pressure causes septal-predominant hypertrophy that can mimic genetic HCM, while obesity leads to more generalised asymmetric thickening that may mimic early or borderline HCM phenotypes. These findings have important clinical implications: first, the presence of asymmetric hypertrophy alone cannot reliably distinguish between hypertensive heart disease and HCM, necessitating comprehensive evaluation including blood pressure assessment and metabolic profiling. Second, the metabolic cohort's findings highlight how obesity can independently modify cardiac geometry, potentially confounding diagnosis in borderline cases. Third, obesity appears to have an altogether different response in individuals with HCM, resulting in a more concentric LV, demonstrating how depending on an individual’s cardiac phenotype, obesity may act to modify or mimic

the HCM phenotype. Together, these results emphasise the need to consider both hemodynamic and metabolic factors when evaluating left ventricular hypertrophy, particularly in cases where the aetiology is uncertain.

4.7 LIMITATIONS

Several important limitations must be considered when interpreting these results. The retrospective design introduced significant heterogeneity, particularly in the HCM cohort where blood pressure measurements were unavailable, preventing direct comparison of hemodynamic effects across all populations. While the use of single-timepoint blood pressure readings and BMI provides clinically practical measures, these lack the precision of ambulatory monitoring or body composition analysis. The temporal gap between cohort recruitments, with more recent HCM registry data compared to older reference populations, may introduce confounding due to evolving diagnostic technologies. Finally, the predominantly white, male composition of the cohorts, while reflective of HCM epidemiology, may limit generalisability to more diverse populations. These limitations highlight the need for future prospective studies with standardized metabolic profiling across more representative populations.

CHAPTER 5: CHARACTERISING THE A4300G CARDIOMYOPATHY

5.1 ABSTRACT

Background: Mitochondrial DNA (mtDNA) variants, such as MT-TL1.3243A>G, are well-known to cause distinct mitochondrial syndromes including a mitochondrial cardiomyopathy. The MT-TI.4300A>G variant however remains understudied, leaving its phenotype ambiguous – uncertain as to whether it represents mitochondrial cardiomyopathy, or a subgroup of sarcomere-negative hypertrophic cardiomyopathy (HCM) given the reported absence of extra-cardiac features. This study aims to determine the prevalence and comprehensively characterise the phenotype of the m.4300A>G variant.

Methods: DNA sequencing of two internal HCM registries was undertaken to establish variant prevalence. Clinical and imaging data for individuals with the m.4300A>G were analysed. Eligible individuals underwent clinical history-taking, electrocardiogram (ECG), serum cardiac and mitochondrial biomarker assessment, cardiac magnetic resonance (CMR), ^{31}Phosphorus-magnetic resonance spectroscopy (^{31}P-MRS) and cardiopulmonary exercise testing (CPET).

Results: *Prevalence:* The prevalence of the m.4300A>G variant was 1-2 per 1000 genotype negative HCM. *Baseline demographics:* We identified 38 individuals, belonging to 6 separate families, with the variant. Our cohort was white, middle-aged, predominantly female with a normal BMI. Most patients had minimal cardiac symptoms, with a high prevalence of LVH (55%), predominantly among males, and a low prevalence of cardiac risk factors or extra-cardiac mitochondrial disease manifestations. *ECG:* Resting 12-lead ECG abnormalities were common in those with LVH, including lateral lead Q waves and T wave inversions. *Serum biomarkers:*

Elevated serum troponin and NT-pro BNP levels correlated with the presence of LVH. *CMR* revealed symmetrical, non-obstructive LVH, with significant lateral wall fibrosis and elevated T_1 and T_2. *^{31}P-MRS* demonstrated impaired myocardial energetics across the cohort. CPET was normal in all patients. *Outcomes:* LV systolic impairment was common (55%). Cardiac mortality was also high, particularly due to sudden cardiac death (SCD), though ventricular arrhythmias were not seen.

Conclusion: The m.4300A>G is a rare but significant contributor to the genotype-negative HCM population, presenting with a distinct phenotype. Individuals with the m.4300A>G cardiomyopathy demonstrate significantly raised troponin levels, a typical ECG and fibrosis pattern involving the lateral wall, frequent LV systolic dysfunction, a high mortality rate and very few, mild, extra-cardiac manifestations. These characteristic features suggest that m.4300A>G cardiomyopathy is a distinct condition, with important differences from sarcomeric HCM, and other mitochondrial diseases, and a potentially unrecognised role of inflammation in its pathogenesis and pathogenicity.

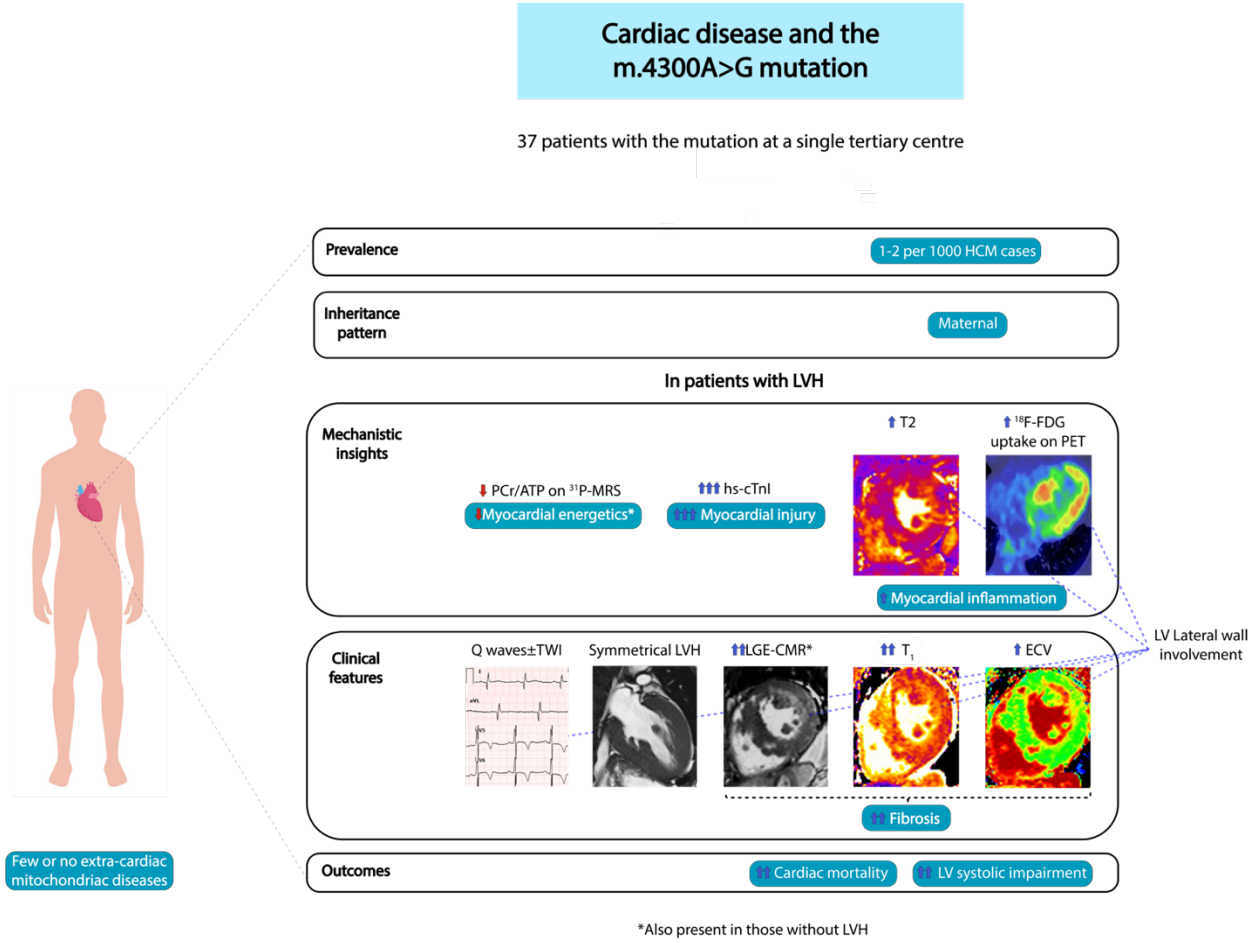

Figure 71: *Abbreviations: ECV, Extracellular volume hs-cTnI, high sensitivity cardiac troponin I; HCM, hypertrophic cardiomyopathy; LGE-CMR, Late Gadolinium Enhancement-Cardiac Magnetic Resonance; LV, Left ventricular; LVH, left ventricular hypertrophy; mtDNA, mitochondrial DNA; PCr/ATP, Phosphocreatine/Adenosine Triphosphate; PET, Positron Emission Tomography; TWI, T wave inversion; 18F-FDG, 18Fluorodeoxyglucose; 31P-MRS, 31Phosphorus-Magnetic Resonance Spectroscopy*

5.2 INTRODUCTION

Mitochondria are essential intracellular structures where cellular energy production in the form of adenosine triphosphate (ATP) synthesis takes place (89). Mitochondria possess their own genome, called mitochondrial DNA (mtDNA), which is only transmitted maternally (89). mtDNA variants, which occur in 1 in 4300 individuals (138), can disrupt ATP synthesis, resulting in dysfunction and/or death of the mitochondria, and subsequently, the host cell (89). The resulting 'mitochondrial disease' can affect any organ within the human body, although it most commonly affects those with the greatest energy requirements, such as the heart, where mitochondrial disease is labelled as a 'mitochondrial cardiomyopathy (89).

There are many knowns about mitochondrial cardiomyopathies, particularly those that are secondary to mtDNA variants. The commonest mtDNA variant, MT-TL1:m.3243A>G, a point variant in the mitochondrially encoded transfer ribonucleic acid (tRNA) leucine gene, is largely representative of mtDNA variants in general (40). The MT-TL1:m.3243A>G variant is heteroplasmic i.e. affected mtDNA levels can vary from person to person, and in the same individual, from organ to organ (40). In the 40-50% of patients with the TL1:m.3243A>G variant that develop a cardiomyopathy, there is a relatively consistent pattern of symmetrical, non-obstructive, moderate left ventricular hypertrophy (LVH), moderate to severe left ventricular systolic impairment, and significant extra-cardiac mitochondrial disease manifestations, such as encephalomyopathy and skeletal myopathy (40).

In comparison, much less is known about the MT-TI:m.4300A>G variant, which is due to a point variant in the mitochondrial tRNA isoleucine gene(99). Its prevalence, for example, remains unclear (99). The largest international registry of patients with genetically confirmed mitochondrial syndromes (n=600) reported only 2 cases of patients with the MT-TI:m.4300A>G variant (90). This mitochondrial variant seems much more common in HCM populations however, where it is often labelled as non-sarcomeric HCM due to its reported lack of extra-cardiac mitochondrial disease manifestations, which is unusual for a mitochondrial cardiomyopathy (3). This is supported by two studies in which 0.6-2% of previously "genotype negative" HCM patients were found to have the MT-TI:m.4300A>G variant on whole genome sequencing (139, 140). Similar to other mitochondrial cardiomyopathies, this variant is associated with a symmetrical, non-obstructive LVH pattern with a high LV systolic impairment burden, as reported in largely TTE-based, singleton or small pedigree studies (41, 98, 99).

To establish the prevalence of the m.4300A>G variant and clarify if its phenotype is more similar to HCM or that of other mitochondrial cardiomyopathies, we performed a single-centre comprehensive characterisation of individuals with this variant encompassing serum cardiac biomarkers, CMR, ^{31}Phosphorus Magnetic Resonance (^{31}P-MRS), cardiopulmonary exercise testing (CPET) and ambulatory ECG monitoring findings.

5.3 METHODS

5.3.1 GENETIC ANALYSIS TO ESTABLISH M.4300A>G PREVALENCE

Individuals with the m.4300A>G variant were identified from two large internal HCM registries at our centre, Hypertrophic Cardiomyopathy Registry (HCMR) and the National Institute for Health and Care Research (NIHR) BioResource for Rare Disease (BRRD) (23, 113, 141). Individuals from these registries had previously provided informed consent for their blood samples to undergo genomic sequencing at our United Kingdom Accreditation Service (UKAS)-accredited clinical diagnostics laboratory, the Oxford Medical Genetics Laboratory (OMGL). Non-sarcomeric genotype ('genotype negative') status was confirmed in these registries using a minimum of 13 HCM-related genes (23, 113, 141). Variants associated with other HCM phenocopies such as Danon's disease were excluded from the study. Genes of interest were selected based on established panels, and their locations were identified using a genome database (141). Variants in these genes were extracted and analysed using bioinformatics tools to determine their impact and frequency (141). The analysis included counting rare variants, checking their coverage and performing statistical tests such as Fisher's exact test and odds (141). Variant classification was undertaken following clinical guidelines, ensuring a robust analysis of the frequency of the m.4300A>G variant in our genotype-negative HCM populations(141).

5.3.2 STUDY POPULATION FOR M.4300A>G VARIANT PHENOTYPING

Comprehensive clinical information of individuals with the m.4300A>G variant was extracted from electronic medical records using prior consent obtained during their genetic testing. These included details of relevant clinical symptoms and signs, blood results, electrocardiogram (ECG) and cardiac investigations. All individuals with a minimum left ventricular wall thickness ≥ 13mm based on transthoracic echocardiogram (TTE), CMR or postmortem examination were identified and labelled as LVH+ in accordance with the European Society of Cardiology's (ESC) guidelines for the diagnosis of HCM (142). Individuals aged 18 to 80 years old and without an absolute contraindication to CMR were invited for a single research visit at the University of Oxford Centre for Clinical Magnetic Resonance Research (OCMR) and Oxford Cardiovascular Clinical Research Facility (CCRF) located in the John Radcliffe Hospital in Oxford, UK. Written informed consent was obtained from all individuals. The study was performed under an existing ethics approval by the National Research Ethics Committee (REC ref 12/LO/1979).

5.3.3 INVESTIGATIONS

5.3.3.1 ANTHROMORPHIC, BIOCHEMICAL AND CLINICAL ASSESSMENT AND ANALYSIS

Clinical observations (including height, weight, heart rate and blood pressure), physical examination findings and resting 12-lead ECG were recorded for each participant. Clinical history and records were reviewed for evidence of symptomatic or asymptomatic multiorgan involvement, using the Newcastle Mitochondrial Disease Adult Scale (NMDAS). Blood samples were taken for high sensitivity troponin I (hs-

cTnI) to assess myocardial injury, B-type natriuretic peptide (NT-proBNP) to assess cardiac strain, creatine kinase (CK) and lactate to assess skeletal involvement, and C-reactive protein (CRP) to assess systemic inflammation. 24-hour ambulatory ECG monitoring was performed using wearable biosensors (LifeSignals, Milpitas, USA). The resting 12-lead ECG was analysed for abnormalities using the Minnesota Code Classification system(100). 24-hour ambulatory ECG was analysed using HE/LX analysis software (version 6.0c, Northeast Monitoring Inc). General outcome data was obtained from participants attending a research visit, and, through them, their relatives. Outcome data consisted of whether an individual was deceased or alive, the cause of death if they were deceased, the presence of cardiac disease (particularly heart failure and conduction disease) and/or extra-cardiac manifestations associated with mitochondrial disease.

5.3.3.2 CMR AND ^{31}P CARDIAC MRS PROTOCOL

Please see Chapter 2 for the imaging protocol.

5.3.3.3 CMR AND ^{31}P-MRS POST-PROCESSING

Please see Chapter 2 for the imaging post-processing.

5.3.3.4 SPIROMETRY AND CARDIOPULMONARY EXERCISE TEST (CPET) PROTOCOL AND ANALYSIS

CPET was performed on a seated stationary cycle ergometer (Ergoline GmbH, Bitz, Germany) using an incremental protocol consisting of three minutes of unloaded cycling, followed by a 15W/min ramp aiming for a respiratory exchange ratio (RER) ≥ 1.1. Continuous respiratory gases were collected using the same metalyzer utilised in

spirometry. Output data was automatically generated using the Metasoft studio software with the Peak VO2 calculated using the Wasserman weight algorithm (112). A cut off of >50 for the ventilatory equivalents for oxygen (VE/VO2) was used to diagnose skeletal myopathy (143).

5.3.3.5 STATISTICAL ANALYSIS

All statistical analyses were performed using SPSS Version 27.0 (IBM, Armonk, NY, USA). Normality was determined using the Shapiro-Wilk 2 tailed test. Parametric continuous variables were presented using mean ± standard deviation, and non-parametric continuous variables using median (interquartile range). Categorical data were described using frequency and percentages. Differences between cohorts were evaluated using the independent Student's t test, Mann-Whitney U-test, ANOVA or Kruskal-Wallis Test as appropriate.

5.4 RESULTS

5.4.1 M.4300A>G VARIANT PREVALENCE

Our genetic analysis demonstrated a frequency of 1-2 individuals with the m.4300A>G variant per 1000 genotype negative HCM cases.

5.4.2 STUDY POPULATION CHARACTERISTICS

Baseline population characteristics are summarised in **Table 19.** A total of 38 individuals with the m.4300A>G variant, belonging to 6 separate families, were included in our study (see **Table 20; Appendix IV Figure 1**). Our cohort was primarily white, middle-aged, with an overall female sex preponderance, though the majority of patients with LVH were male. The cohort generally had a normal BMI, and minimal symptoms from a cardiac perspective, despite more than half of the participants demonstrating evidence of LVH. Only five patients had evidence of extra-cardiac mitochondrial disease manifestations (unilateral deafness, migraines, and non-insulin dependent diabetes mellitus), but these were all mild in nature. Concomitant cardiovascular comorbidities such as hypertension were uncommon in our cohort.

Table 19: m.4300A>G cohort baseline characteristics

	A4300G n=38
Age, yrs	44 (22-57)
Female, n (%)	20 (54)
White ethnicity, n (%)	38 (100)
BMI, (kg/m2)	26 (24-30)
Hypertension, n (%)	2 (5)
Coronary Artery Disease, n (%)	0 (0)
Extra-cardiac manifestations	
Diabetes Mellitus, n (%)	4 (11)
Leber Hereditary Optic Neuropathy, n (%)	2 (5)
Chronic progressive external ophthalmoplegia, n (%)	0 (0)
Congenital deafness, n (%)	1 (3)
Migraines, n (%)	1 (3)
Epilepsy, n (%)	0 (0)
Gastrointestinal dysmotility	0 (0)
Respiratory muscle weakness*	0 (0)
Myopathy	0 (0)
Renal failure	0 (0)
Hepatic steatosis	0 (0)
NYHA functional class I, n (%)	27 (71)
Syncope, n (%)	0 (0)
Conduction disease, n (%)	0 (0)
Left ventricular hypertrophy, n (%)	21 (55)
Atrial fibrillation, n (%)	7 (18)
Ventricular arrhythmias, n (%)	0 (0)

Data are expressed as median (interquartile range) or n (%). BMI, Body Mass Index; NYHA, New York Heart Association.

Table 20: Summary of m.4300A>G variant family pedigrees with clinical details

Case	Baseline Pedigree	Proband Age	Family members with the variant ± cardiomyopathy
1	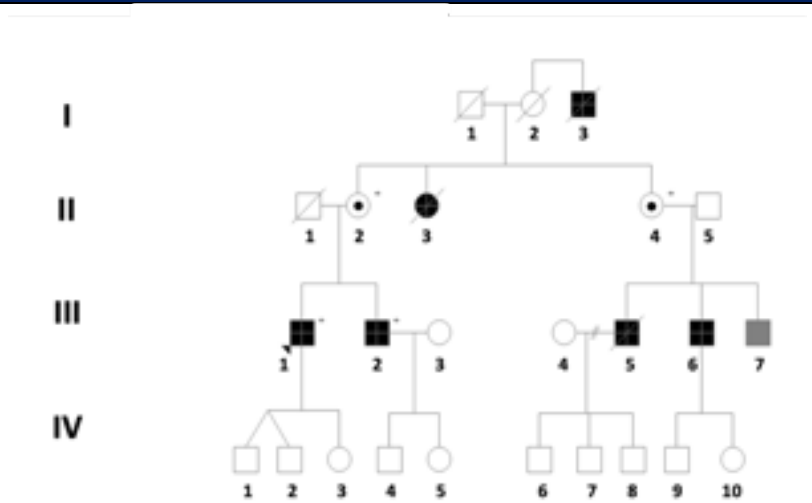	At cardiomyopathy diagnosis: 49 y At last follow-up: 56 y	I-3: LVH+: Deceased (SCD): 30 y II-2: A4300G LVH-: Alive II-3: A4300G LVH+: Deceased (HF): 22 y II-4: A4300G LVH-: Alive **III-1: A4300G LVH+ (ICD): Alive** III-2: A4300G LVH+: Alive III-5: A4300G LVH+: Deceased (SCD): 49 y III-6: A4300G LVH+ (ICD): Alive III-7: A4300G LVH±: Alive
2		At cardiomyopathy diagnosis/death: 0-1 y	III-1: A4300G LVH+ (ICD): Alive: 76 y III-3: A4300G LVH-: Alive: 67 y IV-2: A4300G LVH+: Alive: 38 y IV-4: A4300G LVH-: Alive IV-7: A4300G LVH-: Alive V-1: No A4300G (via MRT), dilated LV: Alive: 2 **V-2: A4300G LVH+: Deceased (SCD): 2 y** V-3: A4300G LVH+: Alive: 23 y V-4: A4300G LVH+: Deceased (HF): 1 y

3	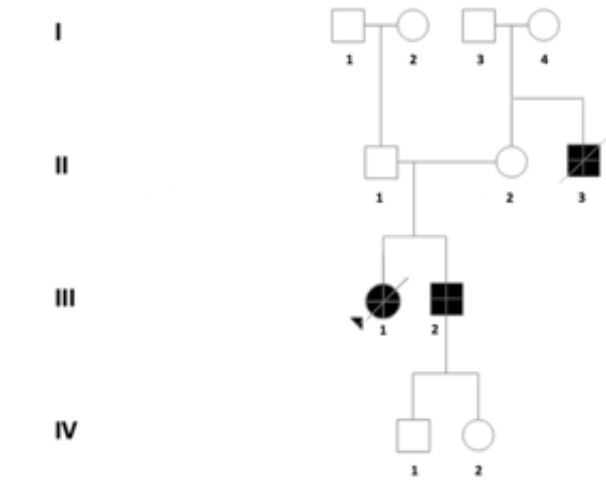	At cardiomyopathy diagnosis/death: 50 y	II-3: LVH+: Deceased (SCD): 60 y **III-1: A4300G LVH+: Deceased: 50 y** III-2: A4300G LVH+ (ICD): Alive: 61 y
4	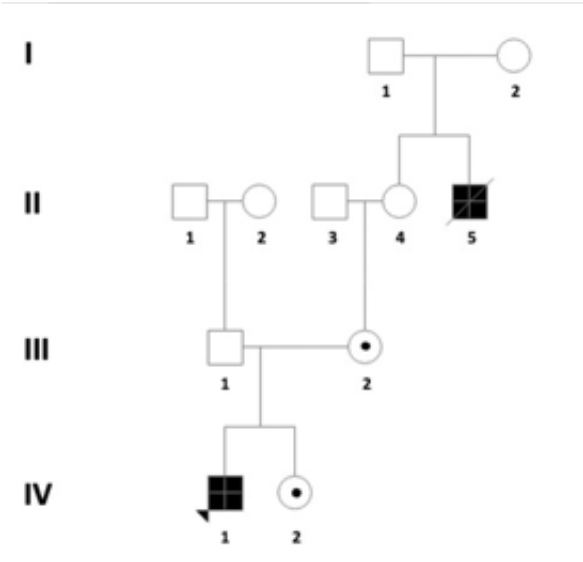	At cardiomyopathy diagnosis: 11 y At last follow-up: 19 y	II-5: LVH+, HF: Deceased (unknown): 80 y III-2: A4300G LVH-: Alive: 48 y **IV-1: A4300G LVH+ (OCTx): Alive: 19 y** IV-2: A4300G LVH-: Alive: 17 y

5	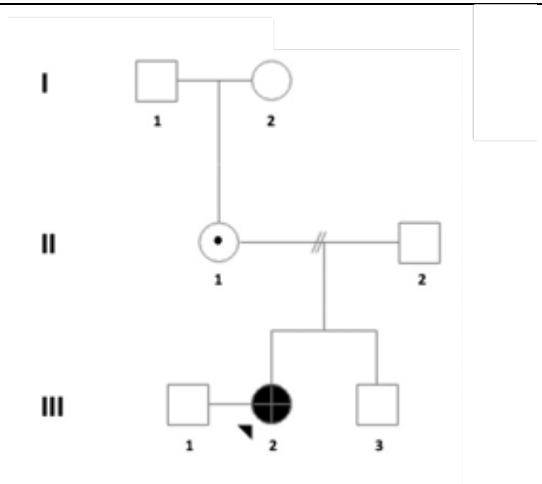	At cardiomyopathy diagnosis: 35 y At last follow-up: 43 y	II-1: A4300G LVH-: Alive: 70 y **III-2: A4300G LVH+ (ICD): Alive: 43 y**
6	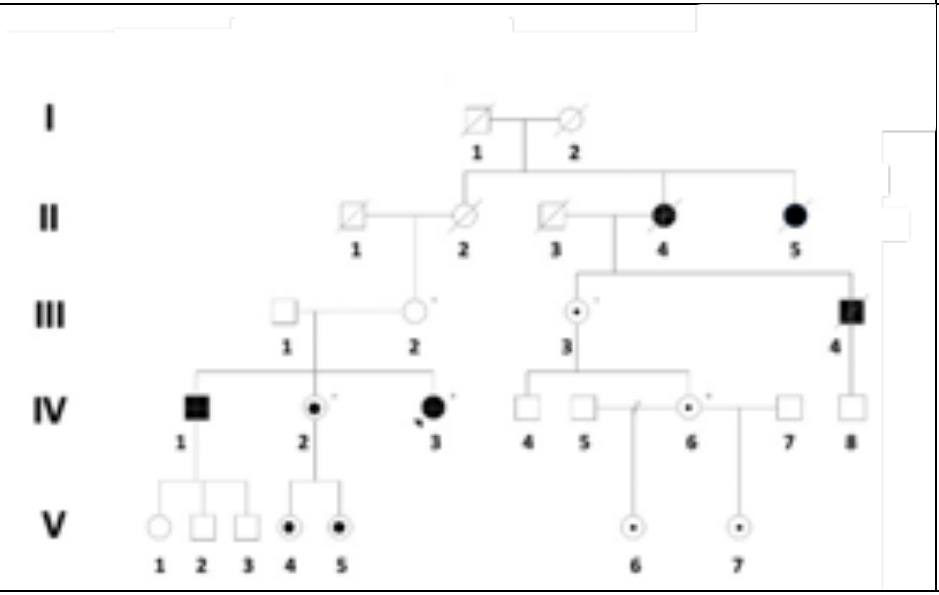	At cardiomyopathy diagnosis: 43 y At last follow-up: 52 y	II-4: LVH+: Deceased (SCD): 80 y II-5: LVH+: Deceased (SCD): 2 y III-3: A4300G LVH-: Alive: 81 y III-4: A4300G LVH+: Deceased (SCD): 39 y IV-1: A4300G LVH+ (ICD): Alive: 57 y IV-2: A4300G LVH-: Alive: 55 y **IV-3: A4300G LVH+: Alive: 52 y** IV-6: A4300G LVH-: Alive: 56 y V-4: A4300G LVH-: Alive: 26 y V-5: A4300G LVH-: Alive: 23 y V-6: A4300G LVH-: Alive: 15 y V-7: A4300G LVH-: Alive: 39 y

■ / ● indicates carrier of the m.4300A>G variant with left ventricular hypertrophy (LVH) on cardiac imaging. ⊡ / ⦿ with a black dot indicates carrier of the m.4300A>G variant without LVH on cardiac imaging. Probands are highlighted in bold. *Abbreviations: ICD, Implantable cardioverter defibrillator; LVH, Left ventricular hypertrophy; LVH+, left ventricular hypertrophy; LVH-, prehypertrophic; OCTx, Orthotopic cardiac transplant; SCD, Sudden cardiac death*

5.4.3 RESTING 12-LEAD AND AMBULATORY ECG MONITORING

All resting 12-lead ECG traces demonstrated normal sinus rhythm. All individuals in the LVH- group had a normal ECG except for one individual who had pathological Q waves in their lateral leads. Conversely, in the LVH+ group 89% had an abnormal ECG. These abnormalities included left ventricular hypertrophy by voltage criteria (33%), fractionated QRS complexes in the inferior/lateral leads (44%), poor R wave progression (22%), pathological Q waves and/or symmetrical T wave inversions in the lateral leads (89%) and ST segment elevation in lead III (11%). There was no evidence of advanced atrioventricular (AV) block, arrhythmia, bundle branch block, or a prolonged QTc interval on ambulatory ECG monitoring in individuals with or without LVH.

5.4.4 SERUM BIOMARKERS

Serum cardiac biomarker data was available in 9 individuals. In those with LVH (n=7), both hs-cTnI and NT-pro BNP levels were significantly raised. Those without LVH had normal hs-cTnI and NT-pro BNP levels. Serum mitochondrial disease biomarkers were available in 15 cases, all of whom had a normal serum CK, Lactate and CRP level.

5.4.5 CMR

The CMR results are summarised in **Table 21.** When compared to published reference ranges, participants with LVH had a non-dilated LV, with a mildly increased MWT, high-normal LV indexed mass, and mild to severe systolic impairment. Regional wall

motion abnormalities were not common, and where present, only affected the lateral wall. LA function was mildly reduced including peak, conduit, and booster strain. The RV was non-dilated with preserved function in all cases. Significantly increased intramural myocardial LGE, T_1, and ECV was present, and primarily, but not exclusively, affected the lateral wall (see **Figure 72**). A similar, but milder, pattern of myocardial fibrosis was also seen in participants without LVH, who had significantly elevated T1 and ECV values, and, in one case, intramural LGE in the lateral wall (see **Figure 74**).

Specific features associated with HCM such as reverse septal LVH pattern, myocardial crypts, systemic anterior motion of the mitral valve (SAM) and apical aneurysm were not present in any case, irrespective of whether they had LVH.

Table 21: CMR parameters in individuals with A4300G LVH+

CMR parameters	A4300G LVH+ (n=9)	Normal range (50, 144-147)*
Maximal wall thickness, mm	16 ± 2	4-12
LV Mass indexed, g	85 (58-99)	30-85
LV end diastolic volume indexed, ml	85 (73-108)	53-99
LV Ejection Fraction, %	51 (39-65)	57-79
RV end diastolic volume indexed, ml	80 (72-84)	51-109
RV ejection fraction, %	63 (59-67)	52-74
LA area (cm^2)	27 (22-33)	13-32
LAEF, %	53 (33-62)	59±3
LV GLS, -%	16 (9-17)	16±2
LA strain peak, %	25 (18-34)	39±9
LA strain conduit, %	14 (7-19)	25±8
LA strain booster, %	10 (6-20)	14±4
LV ECV, %	30 (16-42)	25±4
LV Native T_1 (ms)	1240 (1079-1345)	1150±21
LV LGE% mass	31 (6-39)	-

Data are expressed as mean ± standard deviation, median (interquartile range). *Reference range for men and women (references provided in brackets). *Abbreviations: ECV = Extracellular volume; GLS = Global longitudinal strain; LGE = Late gadolinium enhancement; LV = left ventricular; LA=left atrial; LAEF = Left atrial ejection fraction; RV=Right ventricle.*

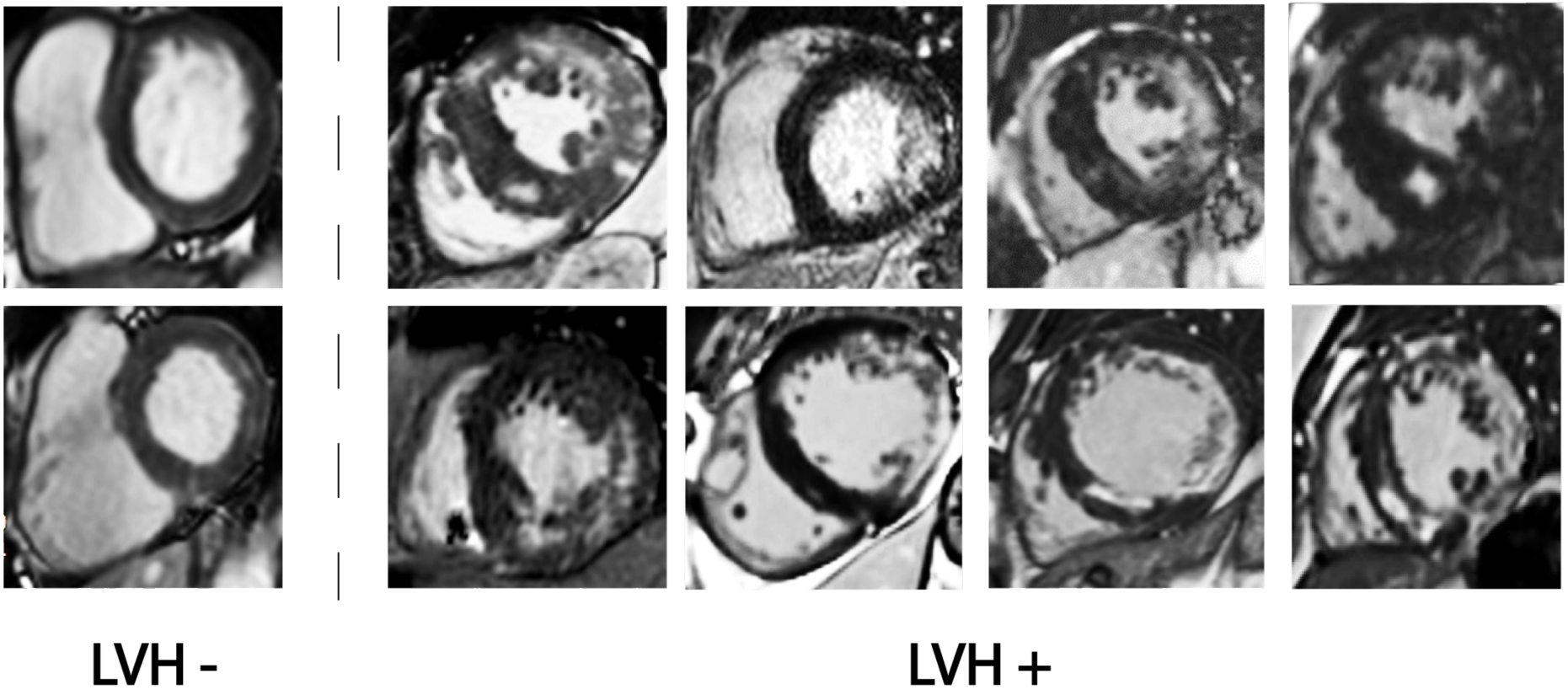

Figure 72: LV Short axis CMR slices from ten individuals in our cohort with left ventricular hypertrophy (LVH+) on the right-hand side and without (LVH-) on the left-hand side.

5.4.6 ^{31}P-MRS

In total seven m.4300A>G carriers underwent ^{31}P-MRS. They demonstrated a significantly reduced resting PCr/ATP ratio when compared to age- and BMI- matched healthy control data within our department (m.4300A>G 1.42 ± 0.21 vs Controls 2.07 ± 0.24, *p<0.001*) – see **Figure 73.**

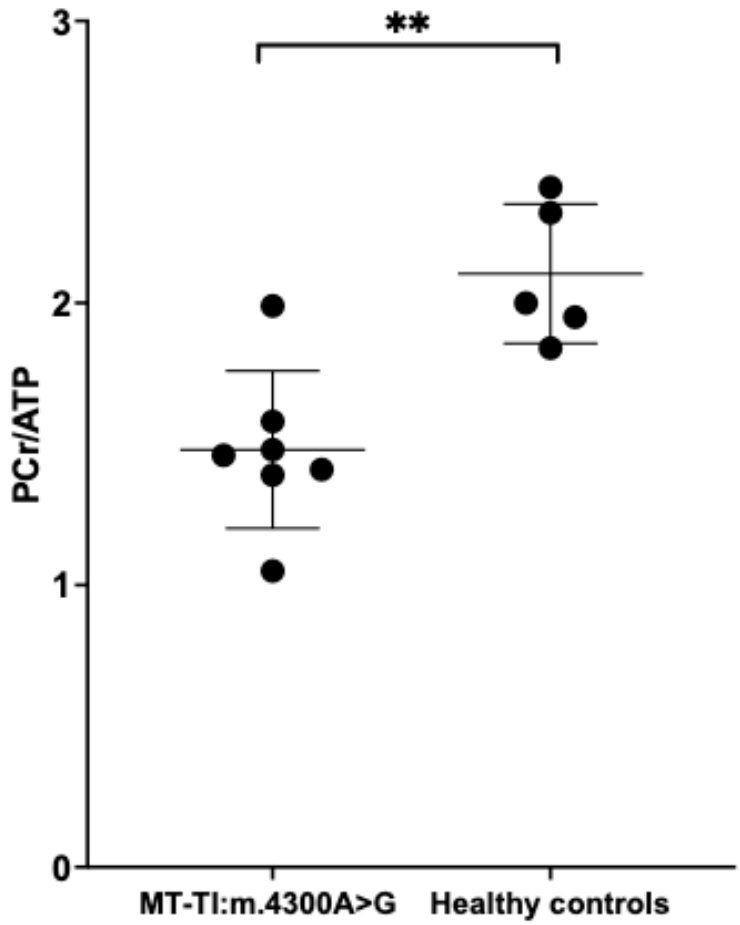

Figure 73: Rest phosphocreatine/adenosine triphosphate ratio (PCr/ATP), obtained from ^{31}Phosphorus-magnetic resonance spectroscopy (31P-MRS) in individuals with the m.4300A>G variant (irrespective of LVH status) compared to healthy control data from our centre.

5.4.7 ^{18}F-FDG PET-CT

Two individuals underwent ^{18}Fluorodeoxyglucose Positron Emission Tomography with Computed Tomography (^{18}F-FDG PET-CT) for investigation of raised serum troponin levels (>1000 ng/l). These individuals demonstrated significant uptake in their lateral wall, which corresponded to lateral wall abnormalities identified on T1, T2 and LGE CMR (one example is demonstrated in **Figure 74**).

5.4.8 CPET

All individuals, irrespective of the presence of LVH, had a normal spirometry, a peak oxygen consumption (VO_2)≥80% predicted, a peak ventilatory equivalent of oxygen VE/VO2<50, and a peak respiratory exchange ratio (RER)≥1.1. There were no inappropriate heart rate or blood pressure responses to exercise, nor were there any significant ECG changes during CPET.

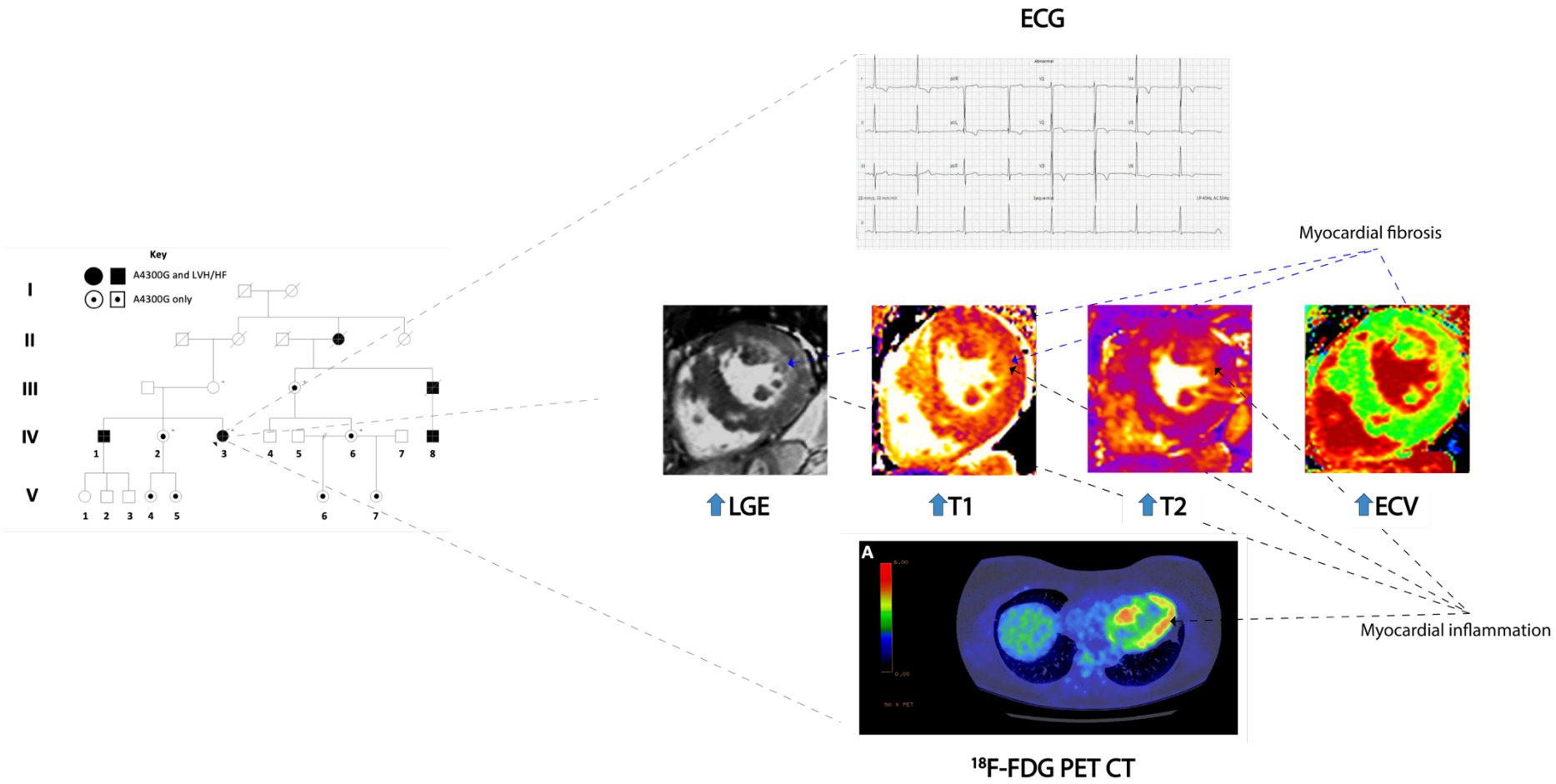

Figure 74: Pedigree 6 proband results demonstrating lateral lead abnormalities on ECG that reflect myocardial inflammation and myocardial fibrosis involving the lateral wall on CMR and ^{18}F-FDG PET-CT imaging. *Abbreviations: ECG, electrocardiogram; ECV, extracellular volume; LGE, late gadolinium enhancement; ^{18}F-FDG PET CT, ^{18}Fluorodeoxyglucose Positron Emission Tomography Computed Tomography.*

The proband is a 50-year-old female with right sided hearing loss. She had an incidental diagnosis of “HCM” with the m.4300A>G variant after cardiomegaly was noted on her chest X-ray following a hospital admission with a pneumonia. She currently has no cardiorespiratory symptoms. Her ECG is grossly abnormal as demonstrated and blood tests revealed a persistently raised troponin I (1334 ng/l). T1 mapping was raised with a global value of 1354 ± 68 ms (peak value of 1478 ms in the region of maximal hypertrophy and fibrosis; the normal range in our centre is 1166 ± 20 ms). T2 mapping revealed a global value of 46 ± 3 ms (with a peak value of 54 ms in the mid-apical anterior wall; the normal range in our centre is 43-50 ms). Global extracellular volume (ECV) was also raised at 31%. Her ^{18}F-FDG PET-CT demonstrated significant uptake in the interventricular septum and lateral wall.

5.4.9 OUTCOMES

Table 22 summarises the outcomes from our cohort. There were two non-cardiac deaths in our cohort, which were due to ovarian cancer and end-stage chronic pulmonary obstructive airways disease (COPD). Cardiac mortality was seen in 48% of those with LVH, with the majority of deaths attributed to sudden cardiac death (SCD). Interestingly, although heart failure was a relatively common diagnosis in our cohort (29%), leading to the implantation of primary prevention implantable cardioverter defibrillators (ICDs) - very few of the deceased patients had a prior diagnosis of heart failure, nor was there a record of an ICD discharge in our cohort. Similarly, ambulatory monitoring did not reveal episodes of non-sustained or sustained ventricular arrhythmias. Atrial fibrillation, however, was reasonably common in our cohort, and somewhat unexpectedly, it was more prevalent in those without LVH than in those with LVH. Among those with LVH and heart failure, only one patient required advanced heart failure therapy, ultimately undergoing cardiac transplantation after being hospitalized with cardiogenic shock.

Table 22: Clinical outcomes from our cohort

Clinical outcomes	All A4300G (n=38)	A4300G LVH- (n=17)	A4300G LVH+ (n=21)
Cardiac death, n (%)	10 (26%)	0	10 (48%)
Sudden cardiac death, n (%)	7 (18%)	-	7 (33%)
Death due to HF, n (%)	3 (8%)	-	3 (14%)
Heart Failure, n (%)	11 (29%)	0	11 (52%)
Cardiac transplantation, n (%)	1 (3%)	-	1 (5%)
Sustained ventricular arrhythmia, n (%)	0	0	0
ICD implantation, n (%)	6 (22%)	0	6 (29%)
Atrial Fibrillation, n (%)	7 (18%)	5 (29%)	2 (10%)

Abbreviations: A4300G LVH-, prehypertrophic A4300G patients; A4300G LVH+, A4300G patients with LVH; HF, heart failure; ICD, implantable cardioverter defibrillator

5.5 DISCUSSION

Our study establishes the prevalence of the m.4300A>G variant in the genotype negative HCM population, and comprehensively characterises its associated cardiac disease phenotype. We confirm previously noted features, such as the maternal inheritance pattern, a non-obstructive and symmetrical LVH pattern, and the absence of extra-cardiac mitochondrial disease manifestations. In addition, we highlight novel aspects, including lateral Q waves and/or T wave inversions on ECG, a distinct pattern of lateral myocardial wall fibrosis, significant biomarker and imaging evidence of myocardial injury and inflammation, impaired myocardial energetics on ^{31}P-MRS and a high frequency of SCD and heart failure occurring across a wide age range.

5.5.1 IS M.4300A>G A COMMON OR RARE VARIANT?

Our study resolves the discrepancies regarding the prevalence of the m.4300A>G variant. While a smaller study found the variant in 1 of 58 genotype-negative HCM patients, our larger study shows a much lower prevalence (139). This finding aligns with an international registry of patients with mitochondrial syndromes, where we initially speculated that the low prevalence of m.4300A>G variant was due to the registry's focus on patients with mitochondrial syndromes and m.4300A>G's cardiac specific presentation (90). By identifying m.4300A>G as a rare variant in the HCM population, our study helps to further characterise the sarcomere-negative HCM population (148-152).

5.5.2 CLINICAL DEMOGRAPHICS

Our cohort corroborates the clinically noted similarities between m.4300A>G LVH and sarcomeric HCM: a majority male population in those with LVH, minimal symptoms and a high prevalence of LVH (153). Compared to the general population, cardiac risk factors, including hypertension, are reported to occur at a higher frequency in individuals with mitochondrial disease (154) and sarcomeric HCM (93), but this was not the case in our cohort, suggesting that there is a tighter relationship between the m.4300A>G and the cardiac phenotype observed. The tissue specificity of the m.4300A>G variant is supported by the low levels of extra-cardiac mitochondrial manifestations in our cohort, as well as the presence of normal serum mitochondrial disease biomarkers and CPET parameters such as a peak VE/VO2<50, making it more similar to HCM than other mitochondrial variants (143).

5.5.3 LATERAL WALL ECG AND CMR ABNORMALITIES

The presence of lateral lead Q waves and T wave inversions exclusively in m.4300A>G with LVH along with a normal ECG in those without LVH, suggests that the ECG could be a potential screening tool for detecting LVH in m.4300A>G patients, and may point towards the absence of a sarcomeric variant. This is because the lateral lead ECG pattern is rare in sarcomeric HCM or other mtDNA variants and ECG abnormalities are common in prehypertrophic patients with sarcomeric variants (21, 22)(155-157). Interestingly, advanced conduction disease which is typically associated with cardiomyopathies that most closely resemble mitochondrial cardiomyopathies, was not present in any of our cases (158). Atrial fibrillation was also surprisingly common in our m.4300A>G patients without LVH, which has not been

reported in sarcomeric positive phenotype negative cases or other mitochondrial variants – this may reflect a more aggressive underlying pathophysiology in m.4300A>G in comparison to other cardiomyopathies, or may just be a limitation of the small numbers in our study (159, 160).

CMR imaging is not included in the NMDAS assessment of patients with mitochondrial disease, and yet revealed many abnormalities that would have otherwise been missed in TTE-based assessments. In our cohort, CMR revealed symmetrical, non-obstructive LVH and a high burden of intramural lateral wall fibrosis. This is not typically seen in sarcomeric HCM but has been reported in a small (n=3) CMR case series of m.4300A>G patients, other mitochondrial cardiomyopathies, Anderson-Fabry disease, Becker's muscular dystrophy, myocarditis, hypertension and/or valvular heart disease (113, 156, 161-165). In these conditions, lateral wall involvement may result from greater mitochondrial dysfunction and increased reactive oxygen species (ROS) production, as it endures more mechanical stress than other myocardial walls, and in the case of myocarditis the lateral wall involvement may be explained by its direct contact with the pericardium, which is often the first structure to be affected by inflammation (161, 162, 166). The frequency and burden of LGE in our cohort is much higher than previously noted in individuals with other mitochondrial variants (33%), or HCM individuals (156, 167, 168). The extent of LGE may be associated with the degree of acute inflammation in our individuals, and similar to cardiac sarcoidosis may help delineate who will benefit from immunomodulatory therapy, if this is felt to be appropriate (169, 170). In m.4300A>G patients without LVH, T_1 and ECV values were elevated, a finding also observed in sarcomere positive patients without LVH, although the appearance of lateral wall LGE in a m.4300A>G

patient without LVH in our cohort, has not been reported thus far in HCM or mitochondrial variants (159, 160).

5.5.4 POOR OUTCOMES: LV SYSTOLIC DYSFUNCTION AND SUDDEN DEATH

Levels of impaired GLS and systolic function in our cohort are similar to a small case series of individuals with the m.3243A>G variant but are much greater than seen in mitochondrial variants as a whole (7%), or HCM (5%) (90, 156, 171). Significant LV systolic dysfunction appears to be more common after the third decade of life in our cohort, possibly due to the age-dependent pathogenicity associated with mitochondrial variants (172). The cardiac mortality in our cohort is much higher than seen in previous m.4300A>G variant reports or in HCM (90, 156, 171). Moreover the m.4300A>G variant in our cohort showed a much stronger association with death in infancy than seen in HCM (156, 167, 168). However similar to “end-stage” HCM individuals (i.e. an LVEF <50%) (173, 174), ventricular arrhythmias and advanced heart failure therapies were not common in our cohort.

5.5.5 MECHANISTIC INSIGHTS: MYOCARDIAL ENERGETICS, INJURY AND/OR INFLAMMATION

Troponin levels in our cohort were significantly higher than seen in HCM and other mitochondrial cardiomyopathies, even though the degree of LVH and fibrosis are similar between these groups and there was no significant burden of coronary disease in our cohort (175-177). Our troponin levels are comparable to those seen in inflammatory cardiomyopathies, suggesting an underlying inflammatory process (178). This is supported by raised T_2 levels, the presence of LGE in the lateral wall (as seen in my myocarditis), and significant uptake on ^{18}F-FDG PET CT. These findings

are also seen in inflammatory cardiomyopathies such as AFD, Becker muscular dystrophy and cardiac sarcoidosis (162, 179, 180). In one of our cases, serial ^{18}F-FDG PET CT and CMR demonstrated significantly increased uptake prior to the development of florid LGE in the lateral wall, as has been seen HCM, where increased FDG was reported as closely correlated to troponin levels, and was attributed to myocardial inflammation, and abnormal myocardial metabolism (181-183).

The significantly reduced rest PCr/ATP in our cohort, irrespective of the presence of LVH, is similar to HCM (184-186). PCr/ATP is also reduced in individuals with other mtDNA variants without LVH, including the A3243G mtDNA variant (187, 188). Impaired energetics is an attractive explanation for the mechanism of the m.4300A>G cardiomyopathy. Campbell et al have hypothesised that reduced ATP production leads to mitochondrial fusion, and that the abnormally enlarged and dysfunctional mitochondria disrupt normal sarcomere structure and impair myocardial contractility (189). Dysfunctional mitochondrial metabolism also causes increased ROS release which itself causes myocardial inflammation and fibrosis (189).

5.5.6 HCM OR A MITOCHONDRIAL CARDIOMYOPATHY?

The m.4300A>G cardiomyopathy shares some features with HCM, such as a high LVH penetrance, but it also exhibits unique aspects, like early cardiac mortality and lateral wall abnormalities on ECG and CMR. Similarly, while there are overlaps with other mitochondrial cardiomyopathies, such as the LVH and LGE pattern, the absence of significant extra-cardiac mitochondrial disease appears unique to the m.4300A>G variant. As a disease entity, the m.4300A>G variant appears to lie somewhere in between HCM and other mitochondrial cardiomyopathies (see **Table 23**).

Table 23: Comparison of m.4300A>G associated cardiomyopathy with sarcomeric HCM and mitochondrial cardiomyopathies

	Mitochondrial variants (177, 190)	A3243G mtDNA variant (90, 159)	A4300G mtDNA variant (41, 98, 99)	Sarcomeric variants (27, 113)
Prevalence	1 in 4300	1 in 6250	**1-2 in 1000 Gene-HCM**	1 in 200
% mtDNA affected	Variable	Variable	All	-
ECG	Conduction disease	-	**Lateral lead Q waves, TWI, LVH**	LVH Q waves, TWI, STE
LVH prevalence	24%	30-40%	**54%**	50%
LVH pattern	Symmetrical	Symmetrical	Symmetrical	Asymmetric (90%)
LVOTO	Nil	Nil	Nil	66%
LV systolic dysfunction	6.6%	30-40%	**63%**	5-15%
LGE	Intramural/ Subepicardial Lateral wall	Subepicardial LGE	**Intramural Lateral wall**	Patchy
Cardiac death	3% per year	8-9% per year	**10% per year**	1-6% per year
Cardiac risk factors	HTN	HTN	**None**	HTN, T2DM
Extra-cardiac disease	83%	60-70%	**Few or none**	-

5.5.7 CLINICAL IMPLICATIONS

Clinicians should have a high index of suspicion for the m.4300A>G variant in patients with LVH, especially those displaying the key findings from our study, as this variant is not common, and therefore underdiagnosed and not routinely tested for. Early intervention with established heart failure therapies, along with tailored ICD criteria, could help mitigate the morbidity and mortality of m.4300A>G associated cardiomyopathy. Consideration of novel treatments, such as mitochondria stabilisers, mitochondrial replacement therapy and even immunomodulator therapies, may be warranted, particularly if inflammation is confirmed as a key factor in m.4300A>G's pathophysiology (90, 191, 192).

5.5.8 LIMITATIONS

Previous studies have demonstrated mitochondrial variants, including m.4300A>G, being present in sarcomeric HCM, therefore we should ideally have assessed m.4300A>G in this population too. As our study consisted of prospective and retrospectively collected data, there is a risk of survivorship and selection bias. We attempted to limit the latter by including not only patients with the m.4300A>G variant, but their relatives too. The limitations of post-mortem analysis, which informed many of our cause-of-death determinations, made it difficult to rule out heart failure in SCD cases, particularly when cardiac chambers were not dilated – a finding not always indicative of the absence of heart failure. Our suspicion of an underlying inflammatory process would need to be further investigated with a comprehensive multiomics profile using myocardial samples from individuals with LVH.

5.5.9 CONCLUSION

Individuals with the m.4300A>G cardiomyopathy demonstrate significantly raised troponin levels, a typical ECG/FDG-PET and fibrosis pattern involving the lateral wall, frequent LV systolic dysfunction, a high mortality rate and little to no extra-cardiac manifestations. These characteristic features suggest that m.4300A>G cardiomyopathy is a distinct condition, with important differences from sarcomeric HCM, and other mitochondrial diseases, and point towards the potential role of inflammation in its pathogenesis and pathogenicity.

CHAPTER 6: CONCLUSION AND FUTURE WORK

6.1 CONCLUSION

This thesis demonstrates distinct pathways by which hemodynamic, metabolic, and genetic factors shape cardiac remodelling in hypertrophic cardiomyopathy, with three main findings.

First, in the overall HCM cohort, hypertension and obesity modified LV geometry and function in different ways. Hypertension produced more concentric remodelling while amplifying hyperdynamic features (higher LVEF, smaller cavity), whereas obesity contributed to concentric hypertrophy with novel inferior wall involvement, along with expected obesity-related traits such as greater myocardial injury and impaired longitudinal strain. When stratified by genotype, these effects were attenuated: hypertension primarily affected gene-negative HCM, while obesity drove gene-positive HCM toward a dilated, heart failure–like phenotype.

Second, in non-HCM cohorts, systolic hypertension alone reproduced an HCM-like phenotype with asymmetric LVH beyond diagnostic thresholds, whereas obesity alone produced only a borderline HCM phenotype. However, across hypertensive and metabolic cohorts, obesity emerged as the strongest independent determinant of wall thickness, above and beyond blood pressure.

Third, the MT-TI:m.4300A>G variant represents a high-risk mitochondrial subtype, with a distinctive fibrosis pattern, absence of systemic mitochondrial disease, and a

high frequency of heart failure and cardiac death, supporting its role as an HCM phenocopy.

Together, these findings refine clinical understanding in three ways: (i) comorbidity management should be tailored by genotype, with aggressive blood pressure control in gene-negative HCM and weight reduction in gene-positive HCM (a strategy made more feasible by GLP-1 agonists); (ii) hypertensive and obesity-related heart disease remain important differentials when evaluating borderline or mild HCM; and (iii) the poor prognosis of MT-TI carriers highlights the need for distinct surveillance strategies. Collectively, this work supports a precision medicine framework, integrating genetics and comorbidities to guide risk-factor management and identify mitochondrial phenocopies for early intervention.

6.2 VALIDATION AND EXPANSION OF FINDINGS

The primary focus of future work will be two-fold. Firstly, we aim to validate our findings through a large, prospective study that includes diverse cohorts of patients with hypertension, obesity, and an additional cohort of patients with diabetes mellitus. This expansion will enhance the robustness of our results and allow for a more comprehensive understanding of the interplay between these conditions. I also intend to validate my findings from our HCM patients by personally analysing data from the HCMR registry.

6.3 LIFESTYLE INTERVENTION STUDIES

Secondly, we plan to undertake a pilot study followed by a randomised control trial (RCT) to determine the effects of lifestyle interventions on myocardial wall thickness. The interventions will include weight loss, aggressive blood pressure control, and optimisation of blood glucose levels/HbA1c. Each type of intervention will be tested in separate trials.

6.4 WEIGHT LOSS INTERVENTIONS

Weight loss trials using a Very Low Energy Diet (VLED) have already demonstrated benefits in conditions such as diabetes and obesity (193). VLED has an excellent safety profile with mild side effects that resolve after the diet is completed and a very low risk of electrolyte derangement (193). Our centre has already initiated a trial with heart failure patients (both HFrEF and HFpEF) and has ethics approval for a trial with patients with LVH. A recent case series showed that HCM patients who lost weight through diet and lifestyle changes or bariatric surgery had a significantly decreased mean LV mass and wall thickness, alongside significant weight loss and improved NYHA status (194).

By conducting a similar trial with a proven, safe, accessible, and reproducible method of weight loss (i.e., VLED) in a larger cohort of HCM patients, we aim to demonstrate a highly effective way of reducing wall thickness in HCM patients. This could prove to be more effective than current medications like mavacamten and safer than septal reduction therapies, particularly since BMI has a strong association with septal wall thickness.

Reducing wall thickness would not only alleviate symptoms in HCM patients but could also potentially reclassify some patients into a lower ESC SCD risk category. Additionally, a lower burden of LGE is likely due to decreased wall thickness and a higher BMI's association with increased LGE. A lifestyle intervention could offer a cheaper, more accessible, and safer treatment for HCM patients compared to new medications.

6.5 WEIGHT LOSS AND DIET INTERVENTIONS

Diet interventions offer an attractive option for weight loss in HCM, especially since many overweight HCM patients are limited in their exercise capacity due to symptoms or left ventricular outflow tract obstruction. While antihypertensive medications may cause LVH regression, they do not fully reverse the hypertensive heart disease phenotype, with some patients experiencing worsening LV diastology despite a decrease in LVM (195).

6.6 MACHINE LEARNING AND DATA ANALYSIS

Future work also consists of utilising machine learning to measure wall thickness, cardiac function, analyse data clusters and their overlaps. Principal component analysis (PCA) and K-means clustering will be used to identify patterns and similarities within each cohort that were previously unknown to us.

APPENDICES

APPENDIX I – TEMPEST INCLUSION AND EXCLUSION CRITERIA

Inclusion and exclusion criteria for the HCM patients enrolled into the TEMPEST trial:

Table 1: Inclusion and exclusion criteria for the TEMPEST trial (101)

Inclusion criteria
Written informed consent.
Age 18-70 inclusive
HCM as defined by the European Society of Cardiology guidelines as: "a wall thickness ≥15 mm, on the most recent CMR (or Transthoracic Echocardiogram in the absence of a CMR) in one or more LV myocardial segments that is not explained solely by loading conditions".
New York Heart Association class I, II or III at the most recent clinical assessment performed prior to the baseline visit.
Exclusion criteria
Previous or planned septal reduction therapy.
Previously documented myocardial infarction or severe coronary artery disease.
Uncontrolled hypertension (systolic blood pressure of >180mmHg or a diastolic blood pressure of > 100mmHg at Visit 1.
Known LV EF < 50%, as measured on the most recent CMR scan (preferably) or echocardiogram performed prior to the baseline visit.

Previously documented persistent atrial fibrillation.
Anaemia, defined as haemoglobin below the local site normal reference range, at Visit 1.
Iron deficiency, defined as serum iron below the local site normal reference range, at Visit 1.
Copper deficiency, defined as serum copper below the normal reference range, at Visit 1.
Pacemaker or implantable cardioverter defibrillator.
Known severe valvular heart disease, as demonstrated on the most recent heart imaging.
Previously documented other cardiomyopathic cause of myocardial hypertrophy
History of hypersensitivity to any of the components of the investigational medicinal product
Known contraindication to MRI scanning.
Pregnancy, lactation or planning pregnancy
Any medical condition, which in the opinion of the Investigator, may place the patient at higher risk from his/her participation in the study, or is likely to prevent the patient from complying with the requirements of the study or completing the study.

APPENDIX II – PROTOCOLS

CMR protocol

1. Orthogonal localiser to adjust the heart to isocentre.

2. Axial bright-blood TrueFISP localiser: 20 or more single-shot axial slices to cover the thorax from just above aortic arch to just below left ventricular apex. Acquisition generally split over 2- 3 breath-holds.

3. Localisers to derive the cardiac planes as per local procedure e.g., 2-chamber localiser, 4- chamber localiser, short-axis localiser.

4. 4-chamber steady state free-precession (SSFP) breath-hold cine. Ideally retrospective gating.

5. 2-chamber SSFP breath-hold cine. Ideally retrospective gating.

6. 3-chamber SSFP breath-hold cine. Ideally retrospective gating. (The order in which the 4-, 2-, and 3-chamber cines are acquired can be adjusted in line with local preference).

7. LVOT long-axis (i.e. perpendicular to the 3-chamber cine) SSFP breath-hold cine. Ideally retrospective gating.

8. Ventricular short-axis SSFP breath-hold cine stack. Ideally retrospective gating. 8mm slices. No inter-slice gap. Check each slice for artefact and repeat as necessary. Check to ensure the base and apex of the left ventricle are fully covered.

9. Basal, mid and apical -ventricular short-axis T_1 mapping. Basal slice position: Copy to the position of the most basal short-axis cine slice that does not contain any LVOT at end-diastole i.e. there should be a „complete ring" of myocardium visible. Mid slice position: Copy to the position of the short-axis cine slice that is two slices more apical

than the short-axis slice chosen as the basal slice. Apical slice position. Copy to the position of the short-axis cine slice that is two slices more apical than the short-axis slice chosen as the mid slice. Sequence: A Modified Look-Locker Inversion Recovery (MOLLI) sequence should ideally be used. Breath-hold. Patients should undergo the same T_1 mapping sequence at baseline (visit 2) and at the end of the trial (visit 6).

10. 3-chamber phase-encoded velocity mapping. Copy to the position of the 3-chamber SSFP cine. Set the velocity encoding (VENC) to 2.0 m/s. Free breathing.

11. LVOT short-axis phase-encoded velocity mapping. Position the slice perpendicular to the LVOT using the 3-chamber and LVOT long-axis SSFP cines as reference. Use the 3-chamber phase-encoded velocity mapping to position the slice at the site of the apparent highest LVOT blood flow velocity. Set an appropriate VENC i.e. the lowest possible where aliasing is not expected to occur. A VENC of 2.0 m/s is the minimum that should be used, but, if an elevated LVOT blood flow velocity is expected based on the appearances of the cines, a higher VENC should be used e.g. 3.0 m/s. If aliasing occurs at the chosen VENC, the acquisition should be repeated using a VENC that is at least 1.0 m/s higher than that at which the aliasing occurred. Free breathing.

12. Gadolinium-based contrast agent administration. The method of injection (power injector or by hand) should be as per local policy. A single scout left ventricular short-axis image should be acquired immediately following contrast injection and should be labelled as “Contrast injection end”. (This will allow verification of the timing of injection).

13. Atrial short-axis SSFP breath-hold cine stack. Ideally retrospective gating. 6mm slices. No inter-slice gap. Check each slice for artefact and repeat as necessary.

14. Inversion time scout. Acquire 6 minutes after gadolinium-based contrast agent administration. Copy to the position of the 4-chamber SSFP cine or a short-axis SSFP cine.

15. Ventricular short-axis late gadolinium enhancement imaging. Copy to the positions of the ventricular short-axis SSFP cine slices (so that the late gadolinium enhancement and cine images are directly comparable). 8mm slices. No inter-slice gap. Sequence: Breath-hold segmented gradient echo phase sensitive inversion recovery; motion correct if available. Start with the optimal inversion time as per the inversion time scout, and subsequently adjust as necessary.

16. Basal, mid and apical-ventricular short-axis T_1 mapping. Repeat the basal and mid-ventricular short-axis T_1 mapping using the same slice positions and sequence as were used before contrast agent administration. Begin the acquisition 15 minutes after contrast agent administration (start the timer when the contrast agent syringe is empty).

CPET (cycle ergometer)

A maximal CPET is to be defined as that with a respiratory exchange ratio (RER) of >1.10. Prior to starting the CPET, usual safety checks should be performed in line with local procedures

1. Patients should have standard spirometry prior to the exercise portion of the study. This should include forced expiratory volume in 1 second (FEV1), forced vital capacity (FVC) and flow volume loop analysis.

2. Patients should be set up on the bike ensuring the correct ride height and handlebar position.

3. Patients should have continuous ECG monitoring applied.

4. Patients should have their mask fitted and checked for leaks prior to commencement of the test.

5. Breath by breath gas exchange analysis and continuous ECG monitoring must be performed throughout the test. Heart rate, peak heart rate and percentage predicted heart should be calculated. VCO2 (litres/min), work rate (watts), heart rate and respiratory exchange ratio (RER) should be averaged every 10 seconds.

6. BP should be recorded at rest, warm up and every 3 minutes during the exercise phase and into the recovery phase until the BP has normalised and the patient has recovered. 7. Rest and warm up phases should last for 3 minutes.

8. A 15W Ramp protocol should be used.

9. Patients should be encouraged to continue the exercise phase for as long as possible aiming for an RER of >1.10.

10. Sites should record the reason for cessation of the exercise phase e.g. breathlessness, leg pain, chest pain.

APPENDIX III – KEY DEFINITIONS

Table 1: Key definitions

Characteristic	Our definition
Left ventricular hypertrophy (LVH)	LV maximal wall thickness of ≥13 mm in genotype positive patients [1].
Sudden cardiac death	Sudden, unexpected death, with a cardiac cause identified either ante- or postmortem [1l]
Pathological Q wave	25% of the height of the partner R wave, Q wave >3mm in depth and/or >0.04s in duration in at least two leads except aVR [33]
LVH by voltage criteria	S wave depth in V1 + tallest R wave height in V5-V6 > 35 mm [5]
Conduction disease	The presence of any degree of atrioventricular block, bundle branch block, left anterior or left posterior fascicular block on a 12-lead ECG
Extra-cardiac mitochondrial disease manifestations	Any one of the following: dysphagia, respiratory failure, diabetes mellitus, retinopathy, chronic progressive external ophthalmoplegia (CPEO), epilepsy, intestinal dysmotility, migraines, myopathy, peripheral neuropathy, sensorineural hearing loss, and stroke-like episodes [19]

Sustained Ventricular Arrhythmias	≥3 consecutive beats with a rate >100 beats per minute, originating from the ventricles, lasting for at least 30 seconds or requiring an intervention for termination [1]
(Clinical) Atrial Fibrillation	Irregularly irregular R-R intervals, absence of distinct repeating P waves and irregular atrial activations, documented for a minimum of 30 seconds on a single lead, or an entire 12-lead ECG [1]
LV systolic dysfunction	Left ventricular ejection fraction (LVEF) categories: Severely abnormal <30%; moderately abnormal, 30-40%; mildly abnormal, 41-56%; reference, 57-77%; hyperdynamic, □78% [Petersen et al]
Raised troponin I level	>14ng/l (as per our local laboratory)

APPENDIX IV – RECRUITMENT PROCESS FOR CHAPTER 5

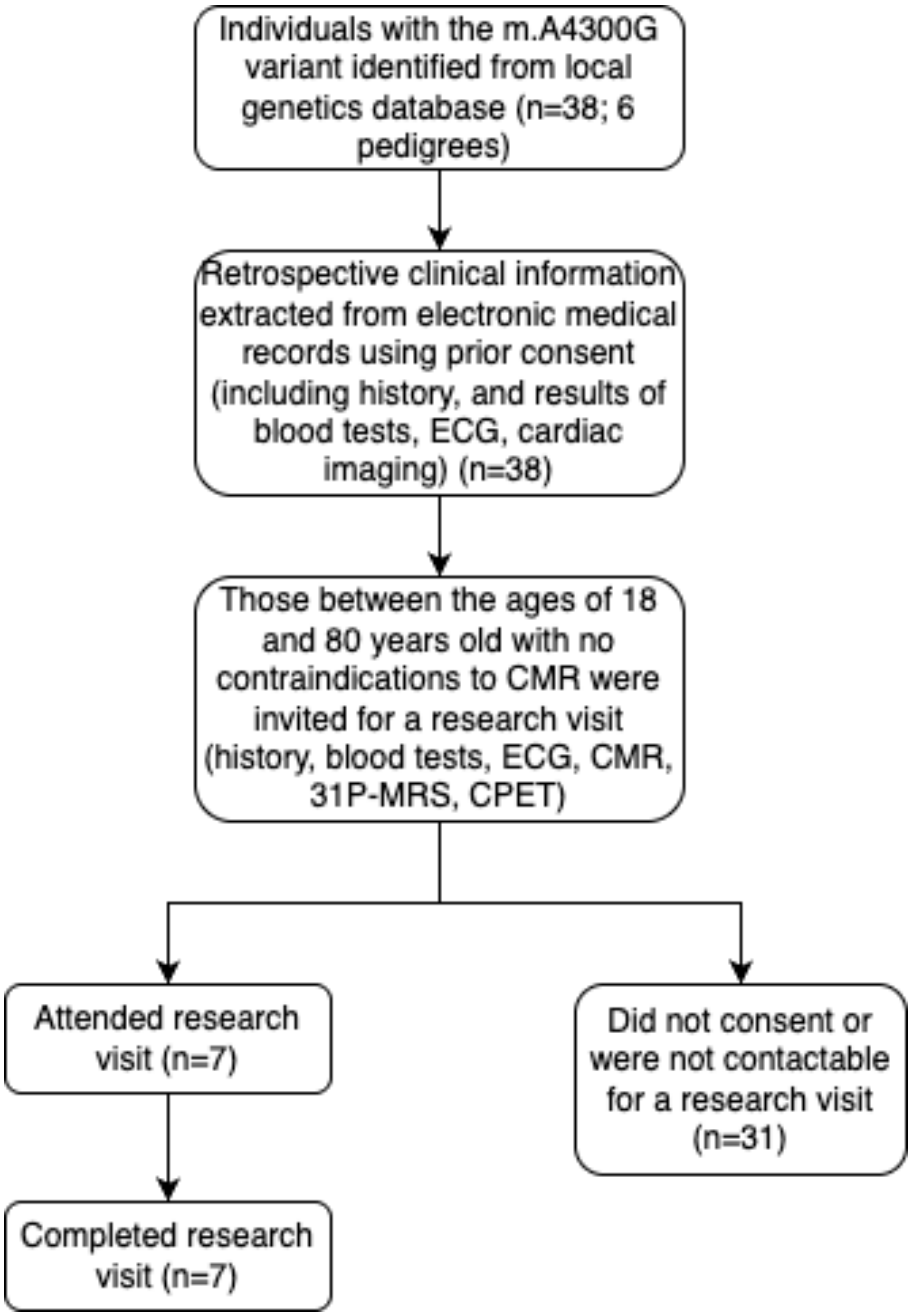

Figure 1: Recruitment process for Chapter 5 / A4300G mtDNA study based on the CONSORT 2010 flowchart conventions (*Abbreviations: CMR, cardiac MRI; CPET, cardiopulmonary exercise testing; ECG, electrocardiogram; 31P-MRS, 31-Phosphorus Magnetic Resonance Spectroscopy)*

ACKNOWLEDGEMENTS

I thank the following patients for their guidance and support:

Professor Oliver Rider

Professor Masliza Mahmod

Professor Hugh Watkins

Professor Ladislav Valkovic

Professor Stefan Neubauer

Professor Chris Miller

Dr Zakariye Ashkir

Dr Azlan Abd Samat

Liliana Rodriguez

REFERENCES

1. Ommen SR, Mital S, Burke MA, Day SM, Deswal A, Elliott P, et al. 2020 AHA/ACC guideline for the diagnosis and treatment of patients with hypertrophic cardiomyopathy: executive summary: a report of the American College of Cardiology/American Heart Association Joint Committee on Clinical Practice Guidelines. Journal of the American College of Cardiology. 2020;76(25):3022-55.
2. Elliott PM, Anastasakis A, Borger MA, Borggrefe M, Cecchi F, Charron P, et al. 2014 ESC guidelines on diagnosis and management of hypertrophic cardiomyopathy. Russian Journal of Cardiology. 2015(5):7-57.
3. McKenna WJ, Judge DP. Epidemiology of the inherited cardiomyopathies. Nat Rev Cardiol. 2021;18(1):22-36.
4. Massera D, McClelland RL, Ambale-Venkatesh B, Gomes AS, Hundley WG, Kawel-Boehm N, et al. Prevalence of Unexplained Left Ventricular Hypertrophy by Cardiac Magnetic Resonance Imaging in MESA. J Am Heart Assoc. 2019;8(8):e012250.
5. Frey N, Luedde M, Katus HA. Mechanisms of disease: hypertrophic cardiomyopathy. Nat Rev Cardiol. 2011;9(2):91-100.
6. Mandeş L, Roşca M, Ciupercă D, Popescu BA. The role of echocardiography for diagnosis and prognostic stratification in hypertrophic cardiomyopathy. J Echocardiogr. 2020;18(3):137-48.
7. Solomon SD, Jarcho J, McKenna W, Geisterfer-Lowrance A, Germain R, Salerni R, et al. Familial hypertrophic cardiomyopathy is a genetically heterogeneous disease. The Journal of clinical investigation. 1990;86(3):993-9.
8. Chumakova OS, Baulina NM. Advanced searching for hypertrophic cardiomyopathy heritability in real practice tomorrow. Frontiers in Cardiovascular Medicine. 2023;10.
9. Pasipoularides A. Challenges and Controversies in Hypertrophic Cardiomyopathy: Clinical, Genomic and Basic Science Perspectives. Revista Española de Cardiología (English Edition). 2018;71(3):132-8.
10. Younger J, Lo A, McCormack L, McGaughran J, Prasad S, Atherton JJ. Hypertrophic Cardiomyopathy: Challenging the Status Quo? Heart Lung Circ. 2020;29(4):556-65.
11. Bombace S, My I, Francone M, Monti L. Tumoral Phenocopies of Hypertrophic Cardiomyopathy: The Role of Cardiac Magnetic Resonance. J Clin Med. 2021;10(8).
12. Olivotto I, Girolami F, Ackerman MJ, Nistri S, Bos JM, Zachara E, et al., editors. Myofilament protein gene mutation screening and outcome of patients with hypertrophic cardiomyopathy. Mayo Clinic Proceedings; 2008: Elsevier.
13. Ho CY, Day SM, Ashley EA, Michels M, Pereira AC, Jacoby D, et al. Genotype and lifetime burden of disease in hypertrophic cardiomyopathy: insights from the Sarcomeric Human Cardiomyopathy Registry (SHaRe). Circulation. 2018;138(14):1387-98.
14. Maron BJ, Maron MS, Maron BA, Loscalzo J. Moving Beyond the Sarcomere to Explain Heterogeneity in Hypertrophic Cardiomyopathy: JACC Review Topic of the Week. J Am Coll Cardiol. 2019;73(15):1978-86.

15. Finocchiaro G, Magavern E, Sinagra G, Ashley E, Papadakis M, Tome-Esteban M, et al. Impact of Demographic Features, Lifestyle, and Comorbidities on the Clinical Expression of Hypertrophic Cardiomyopathy. J Am Heart Assoc. 2017;6(12).
16. Lillo R, Graziani F, Franceschi F, Iannaccone G, Massetti M, Olivotto I, et al. Inflammation across the spectrum of hypertrophic cardiac phenotypes. Heart Fail Rev. 2023;28(5):1065-75.
17. Ashrafian H, Redwood C, Blair E, Watkins H. Hypertrophic cardiomyopathy:a paradigm for myocardial energy depletion. Trends Genet. 2003;19(5):263-8.
18. Yokoyama T, Nakano M, Bednarczyk JL, McIntyre BW, Entman M, Mann DL. Tumor necrosis factor-alpha provokes a hypertrophic growth response in adult cardiac myocytes. Circulation. 1997;95(5):1247-52.
19. Li YY, McTiernan CF, Feldman AM. Proinflammatory cytokines regulate tissue inhibitors of metalloproteinases and disintegrin metalloproteinase in cardiac cells. Cardiovasc Res. 1999;42(1):162-72.
20. Talmud PJ, Shah S, Whittall R, Futema M, Howard P, Cooper JA, et al. Use of low-density lipoprotein cholesterol gene score to distinguish patients with polygenic and monogenic familial hypercholesterolaemia: a case-control study. Lancet. 2013;381(9874):1293-301.
21. Bezzina CR, Barc J, Mizusawa Y, Remme CA, Gourraud JB, Simonet F, et al. Common variants at SCN5A-SCN10A and HEY2 are associated with Brugada syndrome, a rare disease with high risk of sudden cardiac death. Nat Genet. 2013;45(9):1044-9.
22. Aung N, Vargas JD, Yang C, Cabrera CP, Warren HR, Fung K, et al. Genome-Wide Analysis of Left Ventricular Image-Derived Phenotypes Identifies Fourteen Loci Associated With Cardiac Morphogenesis and Heart Failure Development. Circulation. 2019;140(16):1318-30.
23. Harper AR, Goel A, Grace C, Thomson KL, Petersen SE, Xu X, et al. Common genetic variants and modifiable risk factors underpin hypertrophic cardiomyopathy susceptibility and expressivity. Nat Genet. 2021;53(2):135-42.
24. Marian AJ, Braunwald E. Hypertrophic Cardiomyopathy: Genetics, Pathogenesis, Clinical Manifestations, Diagnosis, and Therapy. Circ Res. 2017;121(7):749-70.
25. Maron BJ, Maron MS, Semsarian C. Double or compound sarcomere mutations in hypertrophic cardiomyopathy: a potential link to sudden death in the absence of conventional risk factors. Heart Rhythm. 2012;9(1):57-63.
26. Charron P, Dubourg O, Desnos M, Isnard R, Hagege A, Millaire A, et al. Diagnostic value of electrocardiography and echocardiography for familial hypertrophic cardiomyopathy in a genotyped adult population. Circulation. 1997;96(1):214-9.
27. Ho CY, Day SM, Ashley EA, Michels M, Pereira AC, Jacoby D, et al. Genotype and Lifetime Burden of Disease in Hypertrophic Cardiomyopathy: Insights from the Sarcomeric Human Cardiomyopathy Registry (SHaRe). Circulation. 2018;138(14):1387-98.
28. Olivotto I, Marchionni N. No heart is an island: hypertrophic cardiomyopathy, diabetes, and the test of time. Eur Heart J. 2019;40(21):1678-80.
29. Sipola P, Magga J, Husso M, Jääskeläinen P, Peuhkurinen K, Kuusisto J. Cardiac MRI assessed left ventricular hypertrophy in differentiating hypertensive heart

disease from hypertrophic cardiomyopathy attributable to a sarcomeric gene mutation. Eur Radiol. 2011;21(7):1383-9.
30. Licordari R, Trimarchi G, Teresi L, Restelli D, Lofrumento F, Perna A, et al. Cardiac Magnetic Resonance in HCM Phenocopies: From Diagnosis to Risk Stratification and Therapeutic Management. J Clin Med. 2023;12(10).
31. Williams B, Mancia G, Spiering W, Agabiti Rosei E, Azizi M, Burnier M, et al. 2018 ESC/ESH Guidelines for the management of arterial hypertension. Eur Heart J. 2018;39(33):3021-104.
32. Cianciulli TF, Morita LA, Saccheri MC, Zylberman M. Hypothyroid cardiomyopathy: A reversible phenocopy of hypertrophic cardiomyopathy. Echocardiography. 2021;38(9):1673-7.
33. Cuspidi C, Sala C, Negri F, Mancia G, Morganti A. Prevalence of left-ventricular hypertrophy in hypertension: an updated review of echocardiographic studies. J Hum Hypertens. 2012;26(6):343-9.
34. Gerdts E, Izzo R, Mancusi C, Losi MA, Manzi MV, Canciello G, et al. Left ventricular hypertrophy offsets the sex difference in cardiovascular risk (the Campania Salute Network). International Journal of Cardiology. 2018;258:257-61.
35. daSilva-deAbreu A, Alhafez BA, Lavie CJ, Milani RV, Ventura HO. Interactions of hypertension, obesity, left ventricular hypertrophy, and heart failure. Curr Opin Cardiol. 2021;36(4):453-60.
36. Elliott PM, Anastasakis A, Borger MA, Borggrefe M, Cecchi F, Charron P, et al. 2014 ESC Guidelines on diagnosis and management of hypertrophic cardiomyopathy: the Task Force for the Diagnosis and Management of Hypertrophic Cardiomyopathy of the European Society of Cardiology (ESC). Eur Heart J. 2014;35(39):2733-79.
37. Arbelo E, Protonotarios A, Gimeno JR, Arbustini E, Barriales-Villa R, Basso C, et al. 2023 ESC Guidelines for the management of cardiomyopathies. Eur Heart J. 2023;44(37):3503-626.
38. Umer M, Kalra DK. Cardiac MRI in Fabry disease. Front Cardiovasc Med. 2022;9:1075639.
39. Stankowski K, Figliozzi S, Battaglia V, Catapano F, Francone M, Monti L. Fabry Disease: More than a Phenocopy of Hypertrophic Cardiomyopathy. Journal of Clinical Medicine. 2023;12(22):7061.
40. Di Toro A, Urtis M, Narula N, Giuliani L, Grasso M, Pasotti M, et al. Impediments to Heart Transplantation in Adults With MELAS(MT-TL1:m.3243A>G) Cardiomyopathy. J Am Coll Cardiol. 2022;80(15):1431-43.
41. Taylor RW, Giordano C, Davidson MM, d'Amati G, Bain H, Hayes CM, et al. A homoplasmic mitochondrial transfer ribonucleic acid mutation as a cause of maternally inherited hypertrophic cardiomyopathy. J Am Coll Cardiol. 2003;41(10):1786-96.
42. Sado DM, White SK, Piechnik SK, Banypersad SM, Treibel T, Captur G, et al. Identification and assessment of Anderson-Fabry disease by cardiovascular magnetic resonance noncontrast myocardial T1 mapping. Circ Cardiovasc Imaging. 2013;6(3):392-8.
43. Haaf P, Garg P, Messroghli DR, Broadbent DA, Greenwood JP, Plein S. Cardiac T1 Mapping and Extracellular Volume (ECV) in clinical practice: a comprehensive review. Journal of Cardiovascular Magnetic Resonance. 2016;18(1):89.
44. Hinojar R, Varma N, Child N, Goodman B, Jabbour A, Yu CY, et al. T1 Mapping in Discrimination of Hypertrophic Phenotypes: Hypertensive Heart Disease and

Hypertrophic Cardiomyopathy: Findings From the International T1 Multicenter Cardiovascular Magnetic Resonance Study. Circ Cardiovasc Imaging. 2015;8(12).
45. Hunain S, Rhodri D, Joao A, Rebecca H, Luis L, Jessica A, et al. 3 Beyond 15mm: towards a new personalised, AI measured definition of hypertrophic cardiomyopathy using an age, sex, and body surface area -adjusted approach. Heart. 2023;109(Suppl 1):A3-A4.
46. Augusto JB, Davies RH, Bhuva AN, Knott KD, Seraphim A, Alfarih M, et al. Diagnosis and risk stratification in hypertrophic cardiomyopathy using machine learning wall thickness measurement: a comparison with human test-retest performance. Lancet Digit Health. 2021;3(1):e20-e8.
47. Le TT, Huang B, Pua CJ, Tornekar V, Schumacher-Maurer A, Toh DF, et al. Lowering the Recommended Maximal Wall Thickness Threshold Improves Diagnostic Sensitivity in Asians With Hypertrophic Cardiomyopathy. JACC Asia. 2021;1(2):218-26.
48. Hindieh W, Weissler-Snir A, Hammer H, Adler A, Rakowski H, Chan RH. Discrepant Measurements of Maximal Left Ventricular Wall Thickness Between Cardiac Magnetic Resonance Imaging and Echocardiography in Patients With Hypertrophic Cardiomyopathy. Circ Cardiovasc Imaging. 2017;10(8).
49. Norrish G, Ding T, Field E, Cervi E, Ziółkowska L, Olivotto I, et al. Relationship Between Maximal Left Ventricular Wall Thickness and Sudden Cardiac Death in Childhood Onset Hypertrophic Cardiomyopathy. Circ Arrhythm Electrophysiol. 2022;15(5):e010075.
50. Kawel-Boehm N, Hetzel SJ, Ambale-Venkatesh B, Captur G, Francois CJ, Jerosch-Herold M, et al. Reference ranges ("normal values") for cardiovascular magnetic resonance (CMR) in adults and children: 2020 update. J Cardiovasc Magn Reson. 2020;22(1):87.
51. Olivotto I, Maron MS, Autore C, Lesser JR, Rega L, Casolo G, et al. Assessment and significance of left ventricular mass by cardiovascular magnetic resonance in hypertrophic cardiomyopathy. J Am Coll Cardiol. 2008;52(7):559-66.
52. Henein MY, Pilebro B, Lindqvist P. Disease progression in cardiac morphology and function in heart failure: ATTR cardiac amyloidosis versus hypertensive left ventricular hypertrophy. Heart Vessels. 2022;37(9):1562-9.
53. Kansal MM, Lester SJ, Surapaneni P, Sengupta PP, Appleton CP, Ommen SR, et al. Usefulness of two-dimensional and speckle tracking echocardiography in "Gray Zone" left ventricular hypertrophy to differentiate professional football player's heart from hypertrophic cardiomyopathy. Am J Cardiol. 2011;108(9):1322-6.
54. Noureldin RA, Liu S, Nacif MS, Judge DP, Halushka MK, Abraham TP, et al. The diagnosis of hypertrophic cardiomyopathy by cardiovascular magnetic resonance. J Cardiovasc Magn Reson. 2012;14(1):17.
55. Marciniak M, Gilbert A, Loncaric F, Fernandes JF, Bijnens B, Sitges M, et al. Septal curvature as a robust and reproducible marker for basal septal hypertrophy. J Hypertens. 2021;39(7):1421-8.
56. Henry WL, Clark CE, Epstein SE. Asymmetric septal hypertrophy. Echocardiographic identification of the pathognomonic anatomic abnormality of IHSS. Circulation. 1973;47(2):225-33.
57. Tini G, Autore C, Musumeci B. The Many Faces of Arterial Hypertension in Hypertrophic Cardiomyopathy and Its Phenocopies: Bystander, Consequence, Modifier. High Blood Press Cardiovasc Prev. 2021;28(4):327-9.

58. Del Pinto R, Ferri C. The role of Immunity in Fabry Disease and Hypertension: A Review of a Novel Common Pathway. High Blood Press Cardiovasc Prev. 2020;27(6):539-46.
59. Aistrup GL, Gupta DK, Kelly JE, O'Toole MJ, Nahhas A, Chirayil N, et al. Inhibition of the late sodium current slows t-tubule disruption during the progression of hypertensive heart disease in the rat. Am J Physiol Heart Circ Physiol. 2013;305(7):H1068-79.
60. Coppini R, Ferrantini C, Yao L, Fan P, Del Lungo M, Stillitano F, et al. Late sodium current inhibition reverses electromechanical dysfunction in human hypertrophic cardiomyopathy. Circulation. 2013;127(5):575-84.
61. Pérez-Sánchez I, Romero-Puche AJ, García-Molina Sáez E, Sabater-Molina M, López-Ayala JM, Muñoz-Esparza C, et al. Factors Influencing the Phenotypic Expression of Hypertrophic Cardiomyopathy in Genetic Carriers. Revista Española de Cardiología (English Edition). 2018;71(3):146-54.
62. Brown DW, Giles WH, Croft JB. Left ventricular hypertrophy as a predictor of coronary heart disease mortality and the effect of hypertension. American Heart Journal. 2000;140(6):848-56.
63. Claes GRF, van Tienen FHJ, Lindsey P, Krapels IPC, Helderman-van den Enden ATJM, Hoos MB, et al. Hypertrophic remodelling in cardiac regulatory myosin light chain (MYL2) founder mutation carriers. European Heart Journal. 2015;37(23):1815-22.
64. Dhandapany PS, Sadayappan S, Xue Y, Powell GT, Rani DS, Nallari P, et al. A common MYBPC3 (cardiac myosin binding protein C) variant associated with cardiomyopathies in South Asia. Nat Genet. 2009;41(2):187-91.
65. Luo Q, Chen J, Zhang T, Tang X, Yu B. Retrospective analysis of clinical phenotype and prognosis of hypertrophic cardiomyopathy complicated with hypertension. Sci Rep. 2020;10(1):349.
66. Wu LM, Wu R, Ou YR, Chen BH, Yao QY, Lu Q, et al. Fibrosis quantification in Hypertensive Heart Disease with LVH and Non-LVH: Findings from T1 mapping and Contrast-free Cardiac Diffusion-weighted imaging. Sci Rep. 2017;7(1):559.
67. Neisius U, Myerson L, Fahmy AS, Nakamori S, El-Rewaidy H, Joshi G, et al. Cardiovascular magnetic resonance feature tracking strain analysis for discrimination between hypertensive heart disease and hypertrophic cardiomyopathy. PLoS One. 2019;14(8):e0221061.
68. Puntmann VO, Jahnke C, Gebker R, Schnackenburg B, Fox KF, Fleck E, Paetsch I. Usefulness of magnetic resonance imaging to distinguish hypertensive and hypertrophic cardiomyopathy. Am J Cardiol. 2010;106(7):1016-22.
69. Kato TS, Noda A, Izawa H, Yamada A, Obata K, Nagata K, et al. Discrimination of nonobstructive hypertrophic cardiomyopathy from hypertensive left ventricular hypertrophy on the basis of strain rate imaging by tissue Doppler ultrasonography. Circulation. 2004;110(25):3808-14.
70. Petersen SE, Selvanayagam JB, Francis JM, Myerson SG, Wiesmann F, Robson MD, et al. Differentiation of athlete's heart from pathological forms of cardiac hypertrophy by means of geometric indices derived from cardiovascular magnetic resonance. J Cardiovasc Magn Reson. 2005;7(3):551-8.
71. Wagner S, Auffermann W, Buser P, Semelka RC, Higgins CB. Functional description of the left ventricle in patients with volume overload, pressure overload,

and myocardial disease using cine magnetic resonance imaging. Am J Card Imaging. 1991;5(2):87-97.
72. Rodrigues JC, Rohan S, Ghosh Dastidar A, Harries I, Lawton CB, Ratcliffe LE, et al. Hypertensive heart disease versus hypertrophic cardiomyopathy: multi-parametric cardiovascular magnetic resonance discriminators when end-diastolic wall thickness ≥ 15 mm. Eur Radiol. 2017;27(3):1125-35.
73. Zaromytidou M, Savvatis K. The weight of obesity in hypertrophic cardiomyopathy. Clin Med (Lond). 2023;23(4):357-63.
74. Cuspidi C, Rescaldani M, Sala C, Grassi G. Left-ventricular hypertrophy and obesity: a systematic review and meta-analysis of echocardiographic studies. J Hypertens. 2014;32(1):16-25.
75. Murdolo G, Angeli F, Reboldi G, Di Giacomo L, Aita A, Bartolini C, Vedecchia P. Left ventricular hypertrophy and obesity: only a matter of fat? High Blood Press Cardiovasc Prev. 2015;22(1):29-41.
76. Fumagalli C, Maurizi N, Day SM, Ashley EA, Michels M, Colan SD, et al. Association of Obesity With Adverse Long-term Outcomes in Hypertrophic Cardiomyopathy. JAMA Cardiol. 2020;5(1):65-72.
77. Park JB, Kim DH, Lee H, Hwang IC, Yoon YE, Park HE, et al. Obesity and metabolic health status are determinants for the clinical expression of hypertrophic cardiomyopathy. Eur J Prev Cardiol. 2020;27(17):1849-57.
78. Lopes LR, Losi MA, Sheikh N, Laroche C, Charron P, Gimeno J, et al. Association between common cardiovascular risk factors and clinical phenotype in patients with hypertrophic cardiomyopathy from the European Society of Cardiology (ESC) EurObservational Research Programme (EORP) Cardiomyopathy/Myocarditis registry. Eur Heart J Qual Care Clin Outcomes. 2022;9(1):42-53.
79. Lewis AJM, Rayner JJ, Abdesselam I, Neubauer S, Rider OJ. Obesity in the absence of comorbidities is not related to clinically meaningful left ventricular hypertrophy. Int J Cardiovasc Imaging. 2021;37(7):2277-81.
80. He J, Yang W, Wu W, Sun X, Li S, Yin G, et al. Clinical features, myocardial strain and tissue characteristics of heart failure with preserved ejection fraction in patients with obesity: A prospective cohort study. EClinicalMedicine. 2023;55:101723.
81. Lertlaksameewilai P, Songsangjinda T, Kaolawanich Y, Yindeengam A, Krittayaphong R. Extracellular volume and left ventricular hypertrophy by cardiac magnetic resonance are independent predictors of cardiovascular outcome in obesity. Sci Rep. 2022;12(1):18758.
82. Olivotto I, Cecchi F, Poggesi C, Yacoub MH. Patterns of disease progression in hypertrophic cardiomyopathy: an individualized approach to clinical staging. Circ Heart Fail. 2012;5(4):535-46.
83. Lv J, Liu Y, Yan Y, Sun D, Fan L, Guo Y, et al. Relationship Between Left Ventricular Hypertrophy and Diabetes Is Likely Bidirectional: A Temporality Analysis. J Am Heart Assoc. 2023;12(6):e028219.
84. Jordan J, Yumuk V, Schlaich M, Nilsson PM, Zahorska-Markiewicz B, Grassi G, et al. Joint statement of the European Association for the Study of Obesity and the European Society of Hypertension: obesity and difficult to treat arterial hypertension. Journal of hypertension. 2012;30(6):1047-55.
85. Tadic M, Cuspidi C, Marwick TH. Phenotyping the hypertensive heart. Eur Heart J. 2022;43(38):3794-810.

86. Borlaug BA. The pathophysiology of heart failure with preserved ejection fraction. Nat Rev Cardiol. 2014;11(9):507-15.
87. Wang Y, Zhong Y, Zhang Z, Yang S, Zhang Q, Chu B, Hu X. Effect of sodium-glucose cotransporter protein-2 inhibitors on left ventricular hypertrophy in patients with type 2 diabetes: A systematic review and meta-analysis. Front Endocrinol (Lausanne). 2022;13:1088820.
88. Bhattacharya M, Lu DY, Kudchadkar SM, Greenland GV, Lingamaneni P, Corona-Villalobos CP, et al. Identifying Ventricular Arrhythmias and Their Predictors by Applying Machine Learning Methods to Electronic Health Records in Patients With Hypertrophic Cardiomyopathy (HCM-VAr-Risk Model). Am J Cardiol. 2019;123(10):1681-9.
89. Braunwald E. Mitochondrial cardiomyopathy: a fertile field for research. European Heart Journal. 2023;44(26):2361-2.
90. Savvatis K, Vissing CR, Klouvi L, Florian A, Rahman M, Béhin A, et al. Cardiac Outcomes in Adults With Mitochondrial Diseases. J Am Coll Cardiol. 2022;80(15):1421-30.
91. Wijnker PJM, Sequeira V, Kuster DWD, Velden JV. Hypertrophic Cardiomyopathy: A Vicious Cycle Triggered by Sarcomere Mutations and Secondary Disease Hits. Antioxid Redox Signal. 2019;31(4):318-58.
92. Unno K, Isobe S, Izawa H, Cheng XW, Kobayashi M, Hirashiki A, et al. Relation of functional and morphological changes in mitochondria to myocardial contractile and relaxation reserves in asymptomatic to mildly symptomatic patients with hypertrophic cardiomyopathy. Eur Heart J. 2009;30(15):1853-62.
93. Neubauer S. The failing heart--an engine out of fuel. N Engl J Med. 2007;356(11):1140-51.
94. Sordahl LA, McCollum WB, Wood WG, Schwartz A. Mitochondria and sarcoplasmic reticulum function in cardiac hypertrophy and failure. Am J Physiol. 1973;224(3):497-502.
95. Wallace DC. Mitochondrial diseases in man and mouse. Science. 1999;283(5407):1482-8.
96. Nollet EE, Duursma I, Rozenbaum A, Eggelbusch M, Wüst RCI, Schoonvelde SAC, et al. Mitochondrial dysfunction in human hypertrophic cardiomyopathy is linked to cardiomyocyte architecture disruption and corrected by improving NADH-driven mitochondrial respiration. Eur Heart J. 2023;44(13):1170-85.
97. Ranjbarvaziri S, Kooiker KB, Ellenberger M, Fajardo G, Zhao M, Vander Roest AS, et al. Altered Cardiac Energetics and Mitochondrial Dysfunction in Hypertrophic Cardiomyopathy. Circulation. 2021;144(21):1714-31.
98. Arbustini E, Fasani R, Morbini P, Diegoli M, Grasso M, Dal Bello B, et al. Coexistence of mitochondrial DNA and beta myosin heavy chain mutations in hypertrophic cardiomyopathy with late congestive heart failure. Heart. 1998;80(6):548-58.
99. Casali C, d'Amati G, Bernucci P, DeBiase L, Autore C, Santorelli FM, et al. Maternally inherited cardiomyopathy: clinical and molecular characterization of a large kindred harboring the A4300G point mutation in mitochondrial deoxyribonucleic acid. J Am Coll Cardiol. 1999;33(6):1584-9.
100. Blackburn H. Classification of the electrocardiogram for population studies: Minnesota Code. J Electrocardiol. 1969;2(3):305-10.

101. Farrant J, Dodd S, Vaughan C, Reid A, Schmitt M, Garratt C, et al. Rationale and design of a randomised trial of trientine in patients with hypertrophic cardiomyopathy. Heart. 2023.
102. Jane Ellis MH, Marco Spartera, William Watson, Christopher T. Rodgers, and Ladislav Valkovic. Comparison of human cardiac 31P-MRS on 3 T Trio and Prisma scanners. ISMRM Annual Meeting2019.
103. Valkovič L, Clarke WT, Schmid AI, Raman B, Ellis J, Watkins H, et al. Measuring inorganic phosphate and intracellular pH in the healthy and hypertrophic cardiomyopathy hearts by in vivo 7T (31)P-cardiovascular magnetic resonance spectroscopy. J Cardiovasc Magn Reson. 2019;21(1):19.
104. Purvis LAB, Clarke WT, Biasiolli L, Valkovič L, Robson MD, Rodgers CT. OXSA: An open-source magnetic resonance spectroscopy analysis toolbox in MATLAB. PLoS One. 2017;12(9):e0185356.
105. Schulz-Menger J, Bluemke DA, Bremerich J, Flamm SD, Fogel MA, Friedrich MG, et al. Standardized image interpretation and post-processing in cardiovascular magnetic resonance - 2020 update. Journal of Cardiovascular Magnetic Resonance. 2020;22(1):19.
106. Kramer CM, Barkhausen J, Bucciarelli-Ducci C, Flamm SD, Kim RJ, Nagel E. Standardized cardiovascular magnetic resonance imaging (CMR) protocols: 2020 update. Journal of Cardiovascular Magnetic Resonance. 2020;22(1):17.
107. Mills H, Espersen K, Jurlander R, Iversen K, Bundgaard H, Raja AA. Prevention of sudden cardiac death in hypertrophic cardiomyopathy: Risk assessment using left atrial diameter predicted from left atrial volume. Clin Cardiol. 2020;43(6):581-6.
108. Amano Y, Kitamura M, Takano H, Yanagisawa F, Tachi M, Suzuki Y, et al. Cardiac MR Imaging of Hypertrophic Cardiomyopathy: Techniques, Findings, and Clinical Relevance. Magn Reson Med Sci. 2018;17(2):120-31.
109. Raman B, Ariga R, Spartera M, Sivalokanathan S, Chan K, Dass S, et al. Progression of myocardial fibrosis in hypertrophic cardiomyopathy: mechanisms and clinical implications. Eur Heart J Cardiovasc Imaging. 2019;20(2):157-67.
110. Messroghli DR, Radjenovic A, Kozerke S, Higgins DM, Sivananthan MU, Ridgway JP. Modified Look-Locker inversion recovery (MOLLI) for high-resolution T1 mapping of the heart. Magn Reson Med. 2004;52(1):141-6.
111. Ghemrawi M, Tejero NF, Duncan G, McCord B. Pyrosequencing: Current forensic methodology and future applications-a review. Electrophoresis. 2023;44(1-2):298-312.
112. Glaab T, Taube C. Practical guide to cardiopulmonary exercise testing in adults. Respir Res. 2022;23(1):9.
113. Neubauer S, Kolm P, Ho CY, Kwong RY, Desai MY, Dolman SF, et al. Distinct Subgroups in Hypertrophic Cardiomyopathy in the NHLBI HCM Registry. J Am Coll Cardiol. 2019;74(19):2333-45.
114. Ho CY, Day SM, Ashley EA, Michels M, Pereira AC, Jacoby D, et al. Genotype and Lifetime Burden of Disease in Hypertrophic Cardiomyopathy. Circulation. 2018;138(14):1387-98.
115. Vullaganti S, Levine J, Raiker N, Syed AA, Collins JD, Carr JC, et al. Fibrosis in Hypertrophic Cardiomyopathy Patients With and Without Sarcomere Gene Mutations. Heart Lung Circ. 2021;30(10):1496-501.

116. Magrì D, Mastromarino V, Gallo G, Zachara E, Re F, Agostoni P, et al. Risk Stratification in Hypertrophic Cardiomyopathy. Insights from Genetic Analysis and Cardiopulmonary Exercise Testing. J Clin Med. 2020;9(6).
117. Ng CD. Stratification of BMI categories among older adults within and across countries. Public Health Nutr. 2020;23(2):254-63.
118. Unger T, Borghi C, Charchar F, Khan NA, Poulter NR, Prabhakaran D, et al. 2020 International Society of Hypertension Global Hypertension Practice Guidelines. Hypertension. 2020;75(6):1334-57.
119. Guzzardi DG, White JA, Labib D, Dykstra S, Flewitt J, Feuchter P, et al. Normative healthy reference values for global and segmental 3D principal and geometry dependent strain from cine cardiac magnetic resonance imaging. Int J Cardiovasc Imaging. 2023;39(1):115-34.
120. Holtackers RJ, Emrich T, Botnar RM, Kooi ME, Wildberger JE, Kreitner KF. Late Gadolinium Enhancement Cardiac Magnetic Resonance Imaging: From Basic Concepts to Emerging Methods. Rofo. 2022;194(5):491-504.
121. O'Mahony C, Akhtar MM, Anastasiou Z, Guttmann OP, Vriesendorp PA, Michels M, et al. Effectiveness of the 2014 European Society of Cardiology guideline on sudden cardiac death in hypertrophic cardiomyopathy: a systematic review and meta-analysis. Heart. 2019;105(8):623-31.
122. Rayner JJ, Abdesselam I, d'Arcy J, Myerson SG, Neubauer S, Watkins H, et al. Obesity-related ventricular remodelling is exacerbated in dilated and hypertrophic cardiomyopathy. Cardiovasc Diagn Ther. 2020;10(3):559-67.
123. Yildiz M, Oktay AA, Stewart MH, Milani RV, Ventura HO, Lavie CJ. Left ventricular hypertrophy and hypertension. Prog Cardiovasc Dis. 2020;63(1):10-21.
124. de Simone G, Izzo R, De Luca N, Gerdts E. Left ventricular geometry in obesity: Is it what we expect? Nutr Metab Cardiovasc Dis. 2013;23(10):905-12.
125. Ndumele CE, Coresh J, Lazo M, Hoogeveen RC, Blumenthal RS, Folsom AR, et al. Obesity, subclinical myocardial injury, and incident heart failure. JACC Heart Fail. 2014;2(6):600-7.
126. Tatsumi T, Akashi K, Keira N, Matoba S, Mano A, Shiraishi J, et al. Cytokine-induced nitric oxide inhibits mitochondrial energy production and induces myocardial dysfunction in endotoxin-treated rat hearts. J Mol Cell Cardiol. 2004;37(3):775-84.
127. Stewen P, Mervaala E, Karppanen H, Nyman T, Saijonmaa O, Tikkanen I, Fyhrquist F. Sodium load increases renal angiotensin type 1 receptors and decreases bradykinin type 2 receptors. Hypertens Res. 2003;26(7):583-9.
128. Dellefave-Castillo LM, Cirino AL, Callis TE, Esplin ED, Garcia J, Hatchell KE, et al. Assessment of the Diagnostic Yield of Combined Cardiomyopathy and Arrhythmia Genetic Testing. JAMA Cardiol. 2022;7(9):966-74.
129. Bos JM, Will ML, Gersh BJ, Kruisselbrink TM, Ommen SR, Ackerman MJ. Characterization of a phenotype-based genetic test prediction score for unrelated patients with hypertrophic cardiomyopathy. Mayo Clin Proc. 2014;89(6):727-37.
130. Murphy SL, Anderson JH, Kapplinger JD, Kruisselbrink TM, Gersh BJ, Ommen SR, et al. Evaluation of the Mayo Clinic Phenotype-Based Genotype Predictor Score in Patients with Clinically Diagnosed Hypertrophic Cardiomyopathy. J Cardiovasc Transl Res. 2016;9(2):153-61.
131. Naraen A, McKay V, Shaw M, Modi S, Fairbairn T, Somauroo J, et al. Clinical predictors of informative genetic testing in hypertrophic cardiomyopathy. Eur J Prev Cardiol. 2020;27(7):777-9.

132. Morita SX, Kusunose K, Haga A, Sata M, Hasegawa K, Raita Y, et al. Deep Learning Analysis of Echocardiographic Images to Predict Positive Genotype in Patients With Hypertrophic Cardiomyopathy. Frontiers in Cardiovascular Medicine. 2021;Volume 8 - 2021.
133. McGurk KA, Owen B, Watson WD, Nethononda RM, Cordell HJ, Farrall M, et al. Heritability of haemodynamics in the ascending aorta. Sci Rep. 2020;10(1):14356.
134. Mayosi BM, Keavney B, Kardos A, Davies CH, Ratcliffe PJ, Farrall M, Watkins H. Electrocardiographic measures of left ventricular hypertrophy show greater heritability than echocardiographic left ventricular mass. Eur Heart J. 2002;23(24):1963-71.
135. Rider OJ, Nethononda R, Petersen SE, Francis JM, Byrne JP, Leeson P, et al. Concentric left ventricular remodeling and aortic stiffness: a comparison of obesity and hypertension. Int J Cardiol. 2013;167(6):2989-94.
136. Rider OJ, Lewandowski A, Nethononda R, Petersen SE, Francis JM, Pitcher A, et al. Gender-specific differences in left ventricular remodelling in obesity: insights from cardiovascular magnetic resonance imaging. European Heart Journal. 2012;34(4):292-9.
137. Kramer CM, Appelbaum E, Desai MY, Desvigne-Nickens P, DiMarco JP, Friedrich MG, et al. Hypertrophic Cardiomyopathy Registry: The rationale and design of an international, observational study of hypertrophic cardiomyopathy. Am Heart J. 2015;170(2):223-30.
138. Gorman GS, Schaefer AM, Ng Y, Gomez N, Blakely EL, Alston CL, et al. Prevalence of nuclear and mitochondrial DNA mutations related to adult mitochondrial disease. Ann Neurol. 2015;77(5):753-9.
139. Bagnall RD, Ingles J, Dinger ME, Cowley MJ, Ross SB, Minoche AE, et al. Whole Genome Sequencing Improves Outcomes of Genetic Testing in Patients With Hypertrophic Cardiomyopathy. J Am Coll Cardiol. 2018;72(4):419-29.
140. Lopes LR, Macken WL, Preez SD, Kotwal H, Savvatis K, Sekhri N, et al. An analysis of mitochondrial variation in cardiomyopathy patients from the 100,000 genomes cohort: m.4300A>G as a cause of genetically elusive hypertrophic cardiomyopathy. Human Genomics. 2024;18(1):136.
141. Thomson KL, Ormondroyd E, Harper AR, Dent T, McGuire K, Baksi J, et al. Analysis of 51 proposed hypertrophic cardiomyopathy genes from genome sequencing data in sarcomere negative cases has negligible diagnostic yield. Genetics in Medicine. 2019;21(7):1576-84.
142. Arbelo E, Protonotarios A, Gimeno JR, Arbustini E, Barriales-Villa R, Basso C, et al. 2023 ESC Guidelines for the management of cardiomyopathies. Eur Heart J. 2023.
143. Taivassalo T, Jensen TD, Kennaway N, DiMauro S, Vissing J, Haller RG. The spectrum of exercise tolerance in mitochondrial myopathies: a study of 40 patients. Brain. 2003;126(Pt 2):413-23.
144. Gao Y, Zhang Z, Zhou S, Li G, Lou M, Zhao Z, et al. Reference values of left and right atrial volumes and phasic function based on a large sample of healthy Chinese adults: A cardiovascular magnetic resonance study. Int J Cardiol. 2022;352:180-7.
145. Truong VT, Palmer C, Wolking S, Sheets B, Young M, Ngo TNM, et al. Normal left atrial strain and strain rate using cardiac magnetic resonance feature tracking in healthy volunteers. Eur Heart J Cardiovasc Imaging. 2020;21(4):446-53.

146. Li G, Zhang Z, Gao Y, Zhu C, Zhou S, Cao L, et al. Age- and sex-specific reference values of biventricular strain and strain rate derived from a large cohort of healthy Chinese adults: a cardiovascular magnetic resonance feature tracking study. Journal of Cardiovascular Magnetic Resonance. 2022;24(1):63.
147. Dabir D, Child N, Kalra A, Rogers T, Gebker R, Jabbour A, et al. Reference values for healthy human myocardium using a T1 mapping methodology: results from the International T1 Multicenter cardiovascular magnetic resonance study. J Cardiovasc Magn Reson. 2014;16(1):69.
148. Moolman JA, Reith S, Uhl K, Bailey S, Gautel M, Jeschke B, et al. A newly created splice donor site in exon 25 of the MyBP-C gene is responsible for inherited hypertrophic cardiomyopathy with incomplete disease penetrance. Circulation. 2000;101(12):1396-402.
149. Geier C, Gehmlich K, Ehler E, Hassfeld S, Perrot A, Hayess K, et al. Beyond the sarcomere: CSRP3 mutations cause hypertrophic cardiomyopathy. Hum Mol Genet. 2008;17(18):2753-65.
150. Landstrom AP, Weisleder N, Batalden KB, Bos JM, Tester DJ, Ommen SR, et al. Mutations in JPH2-encoded junctophilin-2 associated with hypertrophic cardiomyopathy in humans. J Mol Cell Cardiol. 2007;42(6):1026-35.
151. van der Zwaag PA, van Rijsingen IA, de Ruiter R, Nannenberg EA, Groeneweg JA, Post JG, et al. Recurrent and founder mutations in the Netherlands-Phospholamban p.Arg14del mutation causes arrhythmogenic cardiomyopathy. Neth Heart J. 2013;21(6):286-93.
152. Leoni C, Blandino R, Delogu AB, De Rosa G, Onesimo R, Verusio V, et al. Genotype-cardiac phenotype correlations in a large single-center cohort of patients affected by RASopathies: Clinical implications and literature review. Am J Med Genet A. 2022;188(2):431-45.
153. Butters A, Lakdawala NK, Ingles J. Sex Differences in Hypertrophic Cardiomyopathy: Interaction With Genetics and Environment. Curr Heart Fail Rep. 2021;18(5):264-73.
154. Chong-Nguyen C, Stalens C, Goursot Y, Bougouin W, Stojkovic T, Béhin A, et al. A high prevalence of arterial hypertension in patients with mitochondrial diseases. J Inherit Metab Dis. 2020;43(3):478-85.
155. Lyon A, Ariga R, Mincholé A, Mahmod M, Ormondroyd E, Laguna P, et al. Distinct ECG Phenotypes Identified in Hypertrophic Cardiomyopathy Using Machine Learning Associate With Arrhythmic Risk Markers. Front Physiol. 2018;9:213.
156. Florian A, Ludwig A, Stubbe-Dräger B, Boentert M, Young P, Waltenberger J, et al. Characteristic cardiac phenotypes are detected by cardiovascular magnetic resonance in patients with different clinical phenotypes and genotypes of mitochondrial myopathy. J Cardiovasc Magn Reson. 2015;17(1):40.
157. Lopes LR, Murphy D, Bugiardini E, Salem R, Jager J, Futema M, et al. Iterative Reanalysis of Hypertrophic Cardiomyopathy Exome Data Reveals Causative Pathogenic Mitochondrial DNA Variants. Circ Genom Precis Med. 2021;14(3):e003388.
158. Verhaert D, Richards K, Rafael-Fortney JA, Raman SV. Cardiac involvement in patients with muscular dystrophies: magnetic resonance imaging phenotype and genotypic considerations. Circ Cardiovasc Imaging. 2011;4(1):67-76.
159. Bates MGD, Hollingsworth KG, Newman JH, Jakovljevic DG, Blamire AM, MacGowan GA, et al. Concentric hypertrophic remodelling and subendocardial

dysfunction in mitochondrial DNA point mutation carriers†. European Heart Journal - Cardiovascular Imaging. 2012;14(7):650-8.
160. Ho CY, Abbasi SA, Neilan TG, Shah RV, Chen Y, Heydari B, et al. T1 measurements identify extracellular volume expansion in hypertrophic cardiomyopathy sarcomere mutation carriers with and without left ventricular hypertrophy. Circ Cardiovasc Imaging. 2013;6(3):415-22.
161. Markousis-Mavrogenis G, Giannakopoulou A, Belegrinos A, Pons MR, Bonou M, Vartela V, et al. Cardiovascular Magnetic Resonance Imaging Patterns in Rare Cardiovascular Diseases. J Clin Med. 2022;11(21).
162. Vehof V, Büther F, Florian A, Drakos S, Chamling B, Kies P, et al. Hybrid CMR- and FDG-PET-Imaging Gives New Insights Into the Relationship of Myocardial Metabolic Activity and Fibrosis in Patients With Becker Muscular Dystrophy. Front Cardiovasc Med. 2022;9:793972.
163. Liu J, Zhao S, Yu S, Wu G, Wang D, Liu L, et al. Patterns of Replacement Fibrosis in Hypertrophic Cardiomyopathy. Radiology. 2022;302(2):298-306.
164. Fulton N, Rajiah P. Utility of magnetic resonance imaging in the evaluation of left ventricular thickening. Insights Imaging. 2017;8(2):279-93.
165. Aldrugh S, Valle JE, Parker MW, Harrington CM, Aurigemma GP. Prevalence of Left Ventricular Hypertrophy Caused by Systemic Hypertension Preceding the Development of Severe Aortic Stenosis. Am J Cardiol. 2021;150:89-94.
166. Mahrholdt H, Wagner A, Deluigi CC, Kispert E, Hager S, Meinhardt G, et al. Presentation, patterns of myocardial damage, and clinical course of viral myocarditis. Circulation. 2006;114(15):1581-90.
167. Chung H, Kim Y, Park CH, Kim JY, Min PK, Yoon YW, et al. Effect of sarcomere and mitochondria-related mutations on myocardial fibrosis in patients with hypertrophic cardiomyopathy. J Cardiovasc Magn Reson. 2021;23(1):18.
168. Weng Z, Yao J, Chan RH, He J, Yang X, Zhou Y, He Y. Prognostic Value of LGE-CMR in HCM: A Meta-Analysis. JACC Cardiovasc Imaging. 2016;9(12):1392-402.
169. Vignaux O, Dhote R, Duboc D, Blanche P, Dusser D, Weber S, Legmann P. Clinical significance of myocardial magnetic resonance abnormalities in patients with sarcoidosis: a 1-year follow-up study. Chest. 2002;122(6):1895-901.
170. Ise T, Hasegawa T, Morita Y, Yamada N, Funada A, Takahama H, et al. Extensive late gadolinium enhancement on cardiovascular magnetic resonance predicts adverse outcomes and lack of improvement in LV function after steroid therapy in cardiac sarcoidosis. Heart. 2014;100(15):1165-72.
171. Ommen SR, Mital S, Burke MA, Day SM, Deswal A, Elliott P, et al. 2020 AHA/ACC Guideline for the Diagnosis and Treatment of Patients With Hypertrophic Cardiomyopathy: Executive Summary: A Report of the American College of Cardiology/American Heart Association Joint Committee on Clinical Practice Guidelines. Circulation. 2020;142(25):e533-e57.
172. Schapira AH. Mitochondrial diseases. Lancet. 2012;379(9828):1825-34.
173. Maron BJ, Desai MY, Nishimura RA, Spirito P, Rakowski H, Towbin JA, et al. Management of Hypertrophic Cardiomyopathy: JACC State-of-the-Art Review. J Am Coll Cardiol. 2022;79(4):390-414.
174. Rowin EJ, Maron BJ, Carrick RT, Patel PP, Koethe B, Wells S, Maron MS. Outcomes in Patients With Hypertrophic Cardiomyopathy and Left Ventricular Systolic Dysfunction. J Am Coll Cardiol. 2020;75(24):3033-43.

175. Burczak DR, Newman DB, Jaffe AS, Ackerman MJ, Ommen SR, Geske JB. High-Sensitivity Cardiac Troponin T Elevation in Hypertrophic Cardiomyopathy Is Associated With Ventricular Arrhythmias. Mayo Clin Proc. 2023;98(3):410-8.
176. Moreno V, Hernández-Romero D, Vilchez JA, García-Honrubia A, Cambronero F, Casas T, et al. Serum levels of high-sensitivity troponin T: a novel marker for cardiac remodeling in hypertrophic cardiomyopathy. J Card Fail. 2010;16(12):950-6.
177. Meyers DE, Basha HI, Koenig MK. Mitochondrial cardiomyopathy: pathophysiology, diagnosis, and management. Tex Heart Inst J. 2013;40(4):385-94.
178. Kubo T, Baba Y, Hirota T, Tanioka K, Yamasaki N, Yamanaka S, et al. Differentiation of infiltrative cardiomyopathy from hypertrophic cardiomyopathy using high-sensitivity cardiac troponin T: a case-control study. BMC Cardiovasc Disord. 2015;15:53.
179. Tanislav C, Feustel A, Franzen W, Wüsten O, Schneider C, Reichenberger F, et al. Persistent increase in cardiac troponin I in Fabry disease: a case report. BMC Cardiovasc Disord. 2011;11:6.
180. Fukushima K, Nagao M, Yamamoto A, Serizawa N, Ishizaki U, Suzuki A, et al. Discrepancy between significant fibrosis and active inflammation in patients with cardiac sarcoidosis: combined and image fusion analysis of cardiac magnetic resonance and (18)F fluorodeoxyglucose positron emission tomography. Eur J Hybrid Imaging. 2019;3(1):9.
181. Aoyama R, Takano H, Kobayashi Y, Kitamura M, Asai K, Amano Y, et al. Evaluation of myocardial glucose metabolism in hypertrophic cardiomyopathy using 18F-fluorodeoxyglucose positron emission tomography. PLoS One. 2017;12(11):e0188479.
182. Kagaya Y, Ishide N, Takeyama D, Kanno Y, Yamane Y, Shirato K, et al. Differences in myocardial fluoro-18 2-deoxyglucose uptake in young versus older patients with hypertrophic cardiomyopathy. Am J Cardiol. 1992;69(3):242-6.
183. Uehara T, Ishida Y, Hayashida K, Shimonagata T, Miyake Y, Sago M, et al. Myocardial glucose metabolism in patients with hypertrophic cardiomyopathy: assessment by F-18-FDG PET study. Ann Nucl Med. 1998;12(2):95-103.
184. Dass S, Cochlin LE, Suttie JJ, Holloway CJ, Rider OJ, Carden L, et al. Exacerbation of cardiac energetic impairment during exercise in hypertrophic cardiomyopathy: a potential mechanism for diastolic dysfunction. Eur Heart J. 2015;36(24):1547-54.
185. Valkovič L, Clarke WT, Schmid AI, Raman B, Ellis J, Watkins H, et al. Measuring inorganic phosphate and intracellular pH in the healthy and hypertrophic cardiomyopathy hearts by in vivo 7T 31P-cardiovascular magnetic resonance spectroscopy. Journal of Cardiovascular Magnetic Resonance. 2019;21(1):1-11.
186. Crilley JG, Boehm EA, Blair E, Rajagopalan B, Blamire AM, Styles P, et al. Hypertrophic cardiomyopathy due to sarcomeric gene mutations is characterized by impaired energy metabolism irrespective of the degree of hypertrophy. J Am Coll Cardiol. 2003;41(10):1776-82.
187. Lodi R, Rajagopalan B, Blamire AM, Crilley JG, Styles P, Chinnery PF. Abnormal cardiac energetics in patients carrying the A3243G mtDNA mutation measured in vivo using phosphorus MR spectroscopy. Biochim Biophys Acta. 2004;1657(2-3):146-50.
188. Bates MG, Hollingsworth KG, Newman JH, Jakovljevic DG, Blamire AM, MacGowan GA, et al. Concentric hypertrophic remodelling and subendocardial

dysfunction in mitochondrial DNA point mutation carriers. Eur Heart J Cardiovasc Imaging. 2013;14(7):650-8.
189. Campbell T, Slone J, Huang T. Mitochondrial Genome Variants as a Cause of Mitochondrial Cardiomyopathy. Cells. 2022;11(18).
190. Popoiu TA, Dudek J, Maack C, Bertero E. Cardiac Involvement in Mitochondrial Disorders. Curr Heart Fail Rep. 2023;20(1):76-87.
191. Peoples JN, Saraf A, Ghazal N, Pham TT, Kwong JQ. Mitochondrial dysfunction and oxidative stress in heart disease. Exp Mol Med. 2019;51(12):1-13.
192. Mok BY, de Moraes MH, Zeng J, Bosch DE, Kotrys AV, Raguram A, et al. A bacterial cytidine deaminase toxin enables CRISPR-free mitochondrial base editing. Nature. 2020;583(7817):631-7.
193. Stanek A, Brożyna-Tkaczyk K, Zolghadri S, Cholewka A, Myśliński W. The Role of Intermittent Energy Restriction Diet on Metabolic Profile and Weight Loss among Obese Adults. Nutrients. 2022;14(7).
194. Reuter MC, Massera D, Axel L, Latson LA, Goldstein JM, Stepanovic A, Sherrid MV. Weight loss in hypertrophic cardiomyopathy: A clinical case series. Int J Cardiol Cardiovasc Risk Prev. 2023;17:200179.
195. Barron AJ, Hughes AD, Sharp A, Baksi AJ, Surendran P, Jabbour RJ, et al. Long-term antihypertensive treatment fails to improve E/e' despite regression of left ventricular mass: an Anglo-Scandinavian cardiac outcomes trial substudy. Hypertension. 2014;63(2):252-8.